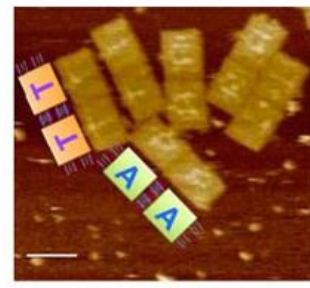
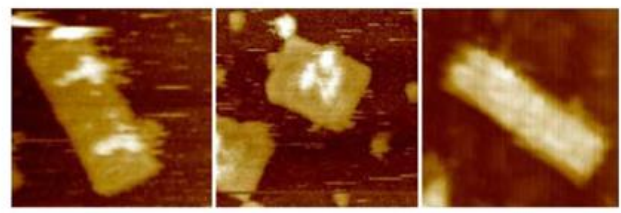
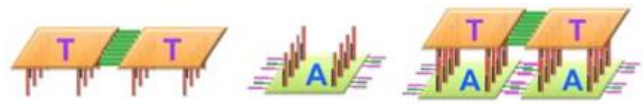
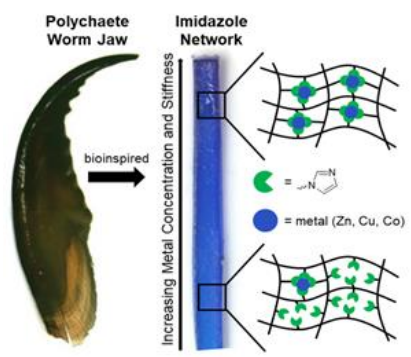
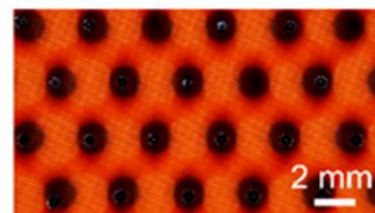
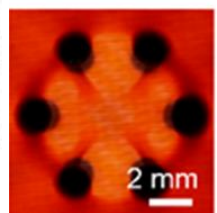
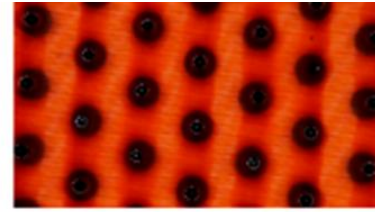
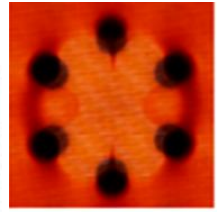
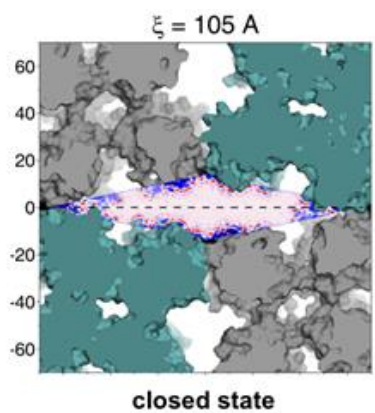
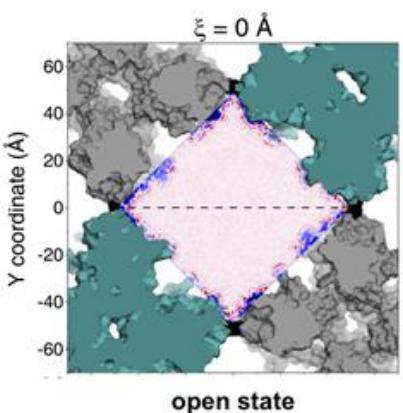
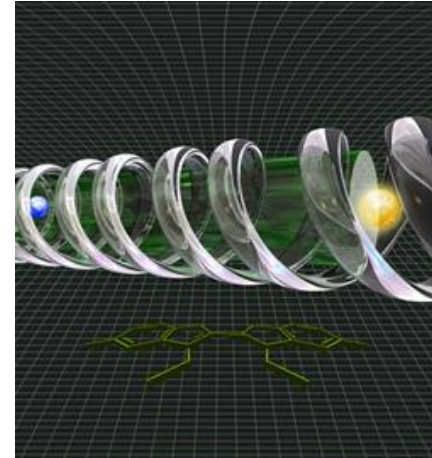
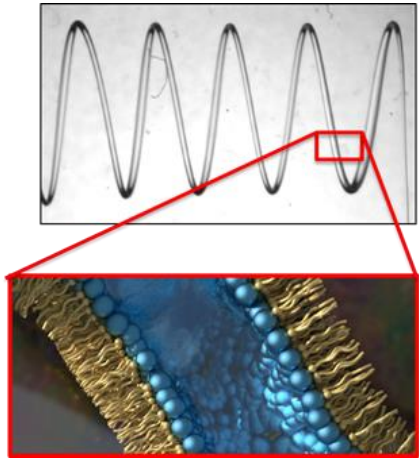
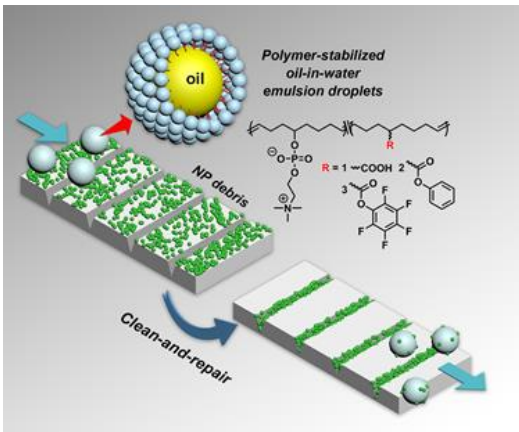


Biomolecular Materials

Principal Investigators' Meeting–2019

August 20–22, 2019

Gaithersburg Marriott Washingtonian Center, Gaithersburg, MD



On the Cover

Top Left: In a novel simultaneous clean-and-repair mechanism, nanoparticle (NP) debris, shown as green spheres, are moved to cracks by flowing oil-in-water droplets. The droplets pick up the NPs, then deposit them in the cracked regions. This process simultaneously cleans the surface and repairs damage. *Courtesy: Todd Emrick, University of Massachusetts-Amherst (Sathyan, et al., Advanced Functional Materials 29, 1805219, DOI:10.1002/adfm.201805219, 2019).*

Top Center: A helix of water printed in a silicone oil (top) where the structures are stabilized by the formation, assembly and jamming of nanoparticle surfactants (schematic, bottom). *Courtesy: Thomas Russell, Lawrence Berkeley National Laboratory (Forth, et al., Advanced Materials 1707603, DOI: 10.1002/adma.201707603, 2018)*

Top Right: Depiction of an “excitonic wire” to fabricate artificial light-harvesting systems using a new type of DNA-templated cyanine dye aggregate with strong inter-chromophore coupling mimicking the certain natural light-harvesting systems. The DNA-templated dye aggregates have been used as the molecular bridge to build up a donor-bridge-acceptor energy transfer system and the result suggests almost no energy loss through bridge and from bridge to acceptor. *Courtesy: Hao Yan, Arizona State University (Zhou, et al., J. Am. Chem. Soc., 141, 21, 8473-8481, DOI: 10.1021/jacs.9b01548, 2019)*

Middle Left: 2D water density plots show the hydration effects induced by the protein surfaces on the local solvent structure for an open lattice (left) and a closed lattice (right). Computational simulations established that the dynamic rearrangement of the square protein components is predominantly governed by reorganization of water molecules. This understanding enabled the successful redesign of the assembly pathway that enabled predictive chemical and mechanical toggling of the assembled structure between three different states with varying porosities. *Courtesy: F. Akif Tezcan, University of California, San Diego (Alberstein, et al., Nature Chemistry, 10, 732, DOI: 10.1038/s41557-018-0053-4, (2018)*

Middle Right: A responsive liquid infused in a non-smooth surface converts a simple magnetic field into a wide range of dynamic and ordered surface shapes. Shifting the position of the field relative to the textured surface (left) reconfigures the fluid surface into drastically different multiscale geometries. Each shape emerges from a unique interplay involving the fluid, texture, magnetic forces, and intricate energy conversion pathways (graded orange indicates relative height of the fluid; darkest areas are macroscale features). *Courtesy: Joanna Aizenberg, Harvard University (Ma, et al., Nature, 559, 77–82, DOI: 10.1038/s41586-018-0250-8, 2018)*

Bottom Left: A bioinspired mechanical gradient was created using metal-ligand interactions resulting in a continuous gradient material that spans over a 200-fold difference in stiffness. The material can be facilely created with a common syringe pump relying on the dynamic nature of the monodentate ligands. *Courtesy: Zhibin Guan, University of California, Irvine (Neal, et al., Angewandte Chemie International Edition 56, 15575–15579, DOI: 10.1002/anie.201707587, 2017)*

Bottom Right: New process achieves self-replication and selective control of evolving properties. Seven million copies were made in just 24 cycles that mimicked the light and temperature pattern of Earth’s days and nights. On the left above are schematics with corresponding atomic force microscopy images below. A seed of two rafts labeled “T” has protruding sticky ends (red vertical rods). At “night” during low temperatures, the sticky ends on “A” rafts reversibly assemble on the complementary ends of the “T” seed. At “sunrise,” the ultraviolet light causes the two “A” rafts to bind together. As the temperature rises during the “day,” the bound “A” offspring are released from the parent “T”. On the right, the offspring after several cycles are shown (scale bar is 100 nanometer). *Courtesy: Paul Chaikin, New York University (He, et al., Nature Materials 16, 993, DOI: 10.1038/NMAT4986, 2017)*

This document was produced under contract number DE-SC0014664 between the U.S. Department of Energy and Oak Ridge Associated Universities.

The research grants and contracts described in this document are supported by the U.S. DOE Office of Science, Office of Basic Energy Sciences, Materials Sciences and Engineering Division.

Foreword

This volume comprises the scientific content of the 2019 Biomolecular Materials Principal Investigators' Meeting sponsored by the Materials Sciences and Engineering (MSE) Division in the Office of Basic Energy Sciences (BES) of the U. S. Department of Energy (DOE). The meeting, held on August 20–22, 2019, at the Gaithersburg Marriott Washingtonian Center in Gaithersburg, Maryland, is the eighth such meeting on this topic conducted by BES. Biology offers an extraordinary source of inspiration for creating new lighter and stronger materials to improve fuel economy, materials to control transport across membranes and make separations and purification processes more efficient, energy-efficient synthesis and assembly of functional materials, and processes that can convert light, carbon dioxide, and water to fuels. The meeting's focus is on the fundamental science supported by the Biomolecular Material Core Research Area (CRA) to achieve spatial and temporal control of energy-efficient pathways for assembling materials with energy relevant capabilities based on the principles and concepts of biology. The agenda at this year's meeting is representative of many of the major scientific areas supported by this CRA to achieve this goal. This meeting will provide an opportunity to consider how this program may continue to evolve to support DOE's mission and to help MSE in assessing the state of the program, identifying new research directions and recognizing programmatic needs. It also provides participants the opportunity to see the entire research program, learn about the latest advances, develop new ideas, and forge new collaborations.

Since biology has already figured out ways in which matter, energy, entropy, and information are organized and manipulated across multiple length scales using nonequilibrium processes, the challenge for us is to understand, adapt, and improve upon them so that they will become valuable and practical under a broader range of harsher, nonbiological conditions. The major scientific challenges that drive Biomolecular Materials CRA activities directly correspond to the scientific challenges laid out in the BES reports, including Challenges at the Frontiers of Matter and Energy: Transformative Opportunities for Discovery Science and Basic Research Needs for Synthesis Science. These challenges include realizing predetermined functionality and information content approaching that of biological materials through spatial and temporal control of assembly pathways, and tunable management of interfaces and assembly defects. Other objectives are the development of predictive models to guide the creation of beyond-equilibrium matter that goes beyond what nature has achieved to advance the frontiers of energy science, and accelerating materials discovery by exploiting complex chemistries and interfacial systems. Another area of interest are new approaches to integrate emerging theoretical, computational, and in situ characterization tools to investigate spatial and temporal evolution during synthesis and assembly, and to direct synthesis with real-time adaptive control. Consequently, major programmatic thrusts are self-, directed-, and dissipative-assembly to form adaptive materials with self-regulating capabilities; resilient materials incorporating autonomous self-healing/regrowth processes; control of bioinspired synthesis to achieve targeted functionality and precise functional group positioning; and design and creation of new materials incorporating low-energy mechanisms for energy and fluid transport with programmable selectivity.

I look forward to the active participation of the attendees at this meeting and hope that the collective sharing of their ideas and new research results will bring fresh insights for the continued development of this field and its value to DOE, as has been the case at past BES principal investigators' meetings. The advice and help of Meeting Chairs Joanna Aizenberg and Aleksandr Noy in organizing this meeting are deeply appreciated. My sincere thanks go to Teresa Crockett

in MSE and Linda Severs at the Oak Ridge Institute for Science and Education (ORISE) for their outstanding work in taking care of all the logistical aspects of the meeting.

Mike Markowitz,
Program Manager, Biomolecular Materials
MSE, BES, Office of Science
U.S. Department of Energy

Table of Contents

Foreword	i
Agenda	vii
Poster Listing	xiii

Laboratory Projects

<i>Precision Synthesis and Assembly of Ionic and Liquid Crystalline Polymers</i> Juan J. de Pablo, Wei Chen, Paul Nealey, and Matthew Tirrell	3
---	---

Bioinspired Materials

Surya Mallapragada, Andrew Hillier, Marit Nilsen-Hamilton, Tanya Prozorov, Alex Travesset, David Vaknin, and Wenjie Wang	11
---	----

Design, Synthesis, and Assembly of Biomimetic Materials with Novel Functionality

Aleksandr Noy, Anthony van Burren, James J. De Yoreo, Chun-Long Chen, and Marcel Baer	17
--	----

Adaptive Interfacial Assemblies Towards Structuring Liquids

Thomas P. Russell, Paul D. Ashby, Phillip Geissler, Brett A. Helms, and Alex Zettl	21
---	----

Dynamics of Active Self-Assembled Materials

Alexey Snezhko, Andrey Sokolov, and Andreas Glatz	27
--	----

University Grant Projects

Dynamic and Complex Multi-Compartment and Internally Ordered Emulsions

Nicholas L. Abbott and Juan J. de Pablo	35
--	----

Energy Transductions in Multimodal Stimuli-Responsive Reconfigurable Systems with Information Encoding Capabilities

Joanna Aizenberg and Anna Balazs	41
---	----

Principles of De Novo Protein Nanomaterial Assembly in 1, 2 and 3 Dimensions

David Baker	47
--------------------------	----

Design and Synthesis of Structurally Tailored and Engineered Macromolecular (STEM) Gels

Anna C. Balazs, Krzysztof Matyjaszewski, and Tomasz Kowalewski	52
---	----

<i>Designing Bio-inspired, Adaptive Gels with Controllable 3D Structures</i> Anna C. Balazs	57
<i>Electrolyte-Mediated Assembly of Like-Charged Colloids</i> Michael J. Bedzyk and Sumit Kewalramani	62
<i>Morphogenesis-Inspired Assembly Mechanisms in Multi-Phase Colloidal Materials</i> Michael A. Bevan and Joelle Frechette	67
<i>Self-Assembly and Self-Replication of Novel Materials from Particles with Specific Recognition</i> Paul M. Chaikin, David Pine, Nadrian C. Seeman, and Marcus Weck	72
<i>Microtubule Based Three Dimensional Active Matter</i> Zvonimir Dogic	79
<i>Self-Assembly of Virus Particle Based Materials for Hydrogen Catalysis</i> Trevor Douglas and Masaki Uchida	83
<i>Control of Charge Transfer and Light-Driven Reactions in Nanocrystal-Enzyme Complexes</i> Gordana Dukovic	85
<i>Reactive and Functional Droplets as Bioinspired Materials for Recognition and Transport</i> Todd Emrick	90
<i>Early Formation Stages and Pathway Complexity in Functional Bio-Hybrid Nanomaterials</i> Lara A. Estroff and Ulrich Wiesner	94
<i>Programmable Dynamic Self-Assembly of DNA Nanotubes</i> Elisa Franco and Rebecca Schulman	99
<i>Bioinspired Design of Multifunctional Dynamic Materials</i> Zhibin Guan	104
<i>Autonomous Motility of Synthetic Protocells Driven by Biochemical Catalysis</i> Daniel A. Hammer, Daeyeon Lee, and Matthew C. Good	109
<i>Dissipative Assembly of Carboxylic Acid Anhydrides for Nonequilibrium Systems Chemistry</i> C. Scott Hartley	114
<i>Bioinspired Mineralizing Microenvironments Generated by Liquid-Liquid Phase Coexistence</i> Christine D. Keating	118

<i>Controlling Lattice Organization, Assembly Pathways and Defects in Self-Assembled DNA-Based Nanomaterials</i> Sanat K. Kumar and Oleg Gang	123
<i>Command of Active and Responsive Elastomers by Topological Defects and Patterns</i> Oleg D. Lavrentovich, Sergij V. Shiyanovskii, and Qi-Huo Wei	128
<i>Biomolecular Assembly Processes in the Design of Novel Functional Materials</i> Jeetain Mittal	133
<i>Calibration between Trigger and Color: Electrically Driven Neutralization of a Genetically Encoded Coulombic Switch Precisely Tunes Reflectin Assembly</i> Daniel E. Morse	139
<i>Electrostatic Driven Self-Assembly Design of Functional Nanostructures</i> Monica Olvera de la Cruz and Michael J. Bedzyk	144
<i>Active Noise to Control and Direct Self-Assembly</i> J. Palacci	149
<i>Self-Assembly and Self-Replication of Novel Materials from Particles with Specific Recognition: Self-Assembly of Colloids with Chemically Heterogeneous Surfaces</i> David J. Pine, Joonsuk Oh, Gi-Ra Yi, and Sharon Glotzer	151
<i>Nanomaterial Construction through Peptide Computational Design and Hierarchical Solution Assembly</i> Darrin J. Pochan, Christopher Kloxin, and Jeffery G. Saven	154
<i>Metal-Ions Impart Self-Assembling Functionality to Intrinsically Disordered Proteins</i> C. R. Safinya, Y. Li, and K. Ewert	157
<i>Tension- and Curvature- Controlled Fluid-Solid Domain Patterning in Single Lamellae</i> Maria M. Santore and Gregory M. Grason	162
<i>Controlling Exciton Dynamics with DNA Origami for Quantum Information Science</i> Gabriela S. Schlau-Cohen, Mark Bathe, and Adam Willard	167
<i>Resilient Hydrogels from the Nanoscale to the Macroscale</i> Rebecca Schulman	171
<i>What Are the Principles Controlling Biomimetic Heteropolymer Secondary Structure?</i> Michael Shirts	175
<i>Bio-inspired Polymer Membranes for Resilience of Electrochemical Energy Devices</i> Meredith N. Silberstein	179

<i>Synthesis of Novel Hybrid Nanostructures Employing Advanced Structural Characterization Techniques</i> Sunil K. Sinha and Atul N. Parikh	183
<i>Self-Assembly, Crystal Quality, and the Biomimetic Reconfiguration of Colloidal Structure</i> Michael J. Solomon and Sharon C. Glotzer	188
<i>Materials Exhibiting Biomimetic Carbon Fixation and Self Repair: Theory and Experiment</i> Michael S. Strano	193
<i>Protein Self-Assembly by Rational Chemical Design</i> F. Akif Tezcan	198
<i>Designing Adaptive Information Processing Materials using Nonequilibrium Forcing</i> Suriyanarayanan Vaikuntanathan	203
<i>Self-Assembly and Self-Replication of Novel Materials from Particles with Specific Recognition: The Depletion Interaction Approach</i> Marcus Weck, Paul M. Chaikin, David Pine, and Nadrian C. Seeman	205
<i>Dynamic, Adaptive, Systems and Materials: Complex, Simple, and Emergent Behaviors</i> George M. Whitesides	211
<i>Exploring Fundamental Properties of Dynamic DNA Origami –Nanoparticle Composites</i> Jessica Winter, Carlos Castro, Michael Poirier, and Ezekiel Johnston-Halperin	215
<i>DNA Nanostructure Directed Designer Excitonic Networks</i> Hao Yan, Neal Woodbury, Yan Liu, Mark Bathe, David Whitten, and Su Lin	220
Author Index	227
Participant List	231

Agenda

2019 Biomolecular Materials Principal Investigators' Meeting

Meeting Chairs: **Joanna Aizenberg** (Harvard University) and **Aleksandr Noy** (Lawrence Livermore National Laboratory)

Tuesday, August 20, 2019

7:00 – 8:00 **Breakfast** (also presentation and poster set-up. Copies of all presentations for Monday need to be given to Teresa Crockett prior to the end of the meeting on Tuesday.)

Session 1: **Liquid Phase Materials and Active Assemblies**
Chair: **Aleksandr Noy**, Lawrence Livermore National Laboratory

8:00 – 8:30 **Nicholas Abbott**, Cornell University
Dynamic and Complex Multi - Compartment and Internally Ordered Emulsions

8:30 – 8:40 *Discussion*

8:40 – 9:10 **Christine Keating**, Pennsylvania State University
Bioinspired Mineralizing Microenvironments Generated by Liquid-Liquid Phase Coexistence

9:10 – 9:20 *Discussion*

9:20 – 9:50 **Thomas Russell**, Lawrence Berkely National Laboratory
Adaptive Interfacial Assemblies towards Structuring Liquids

9:50 – 10:00 *Discussion*

10:00 – 10:30 **Break**

10:30 – 11:00 **Zvonimir Dogic**, University of California, Santa Barbara
Microtubule-Based Three Dimensional Active Matter

11:00 – 11:10 *Discussion*

11:10 – 11:40 **Joanna Aizenberg**, Harvard University
Energy Transductions in Multimodal Stimuli-Responsive Systems with Information Encoding Capabilities and Nonequilibrium Signal Processing

11:40 – 11:50 *Discussion*

- 11:50 – 12:30 **Poster Introductions (Posters 1-12)**
- 12:30 – 1:30 **Working lunch with continued discussions; BES Update by Michael Markowitz, Team Lead for Materials Discovery, Design and Synthesis; Program Updates by Michael Markowitz, Program Manager, Biomolecular Materials CRA**
- 1:30 – 3:00 **Poster Session 1 and Discussions**
- Session 2: **Liquid Phase Materials and Active Assemblies, continued**
Chair: **Michael Shirts**, University of Colorado
- 3:00 - 3:30 **Todd Emrick**, University of Massachusetts, Amherst
Reactive and Functional Droplets as Bioinspired Materials for Recognition and Transport
- 3:30 – 3:40 *Discussion*
- 3:40 – 4:10 **Michael Bevan**, Johns Hopkins University
Morphogenesis-Inspired Assembly Mechanisms in Multi-phase Colloidal Materials
- 4:10 – 4:20 *Discussion*
- 4:20 – 4:50 **Break**
- 4:50 – 5:20 **Monica Olvera de la Cruz**, Northwestern University
Electrostatic Driven Self-Assembly Design of Functional Nanostructures
- 5:20 - 5:30 *Discussion*
- 5:30 – 7:00 **Poster Session 1, continued**
- 7:00 – 8:30 **Working Dinner: General discussion on new opportunities, collaborative exchanges**

Wednesday, August 21, 2019

7:00 – 8:00 **Breakfast** (Also presentation and poster set-up. Copies of all presentations for Tuesday need to be given to Teresa Crockett prior to the end of the meeting on Wednesday.)

Session 3: **Programming Assembly Using Encoded Information**

Chair: **Lara Estroff**, Cornell University

8:00 – 8:30 **Jessica Winter**, Ohio State University
Exploring Fundamental Properties of Dynamic DNA Origami –Nanoparticle Composites

8:30 – 8:40 *Discussion*

8:40 – 9:10 **Paul Chaikin**, New York University
Self-Assembly and Self-Replication of Novel Materials from Particles with Specific Recognition

9:10 – 9:20 *Discussion*

9:20 – 9:50 **Elisa Franco**, University of California, Los Angeles and **Rebecca Schulman**, Johns Hopkins University
Programmable Dynamic Self-Assembly Of DNA Nanostructures

9:50 – 10:00 *Discussion*

10:00 – 10:25 **Break**

10:25 – 10:55 **Cyrus Saffinya**, University of California, Santa Barbara
Miniaturized Hybrid Materials Inspired by Nature

10:55 – 11:05 *Discussion*

11:05 – 11:35 **Anna Balazs**, University of Pittsburgh
Controlled Growth of STEM Gels: Towards Creating Tunable Hierarchically Structured Materials

11:35 – 11:45 *Discussion*

11:45 – 12:25 **Poster Introductions (Posters 13-24)**

12:25 – 1:25 **Working Lunch with discussions on potential new programmatic directions**

1:25 – 2:55 **Poster Session 2**

- Session 4: **Programming Assembly Using Encoded Information, continued**
Chair: **Joanna Aizenberg**, Harvard University
- 2:55 – 3:25 **James De Yoreo**, Pacific Northwest National Laboratory
Design, Synthesis, and Assembly of Biomimetic Materials with Novel Functionality
- 3:25 – 3:35 *Discussion*
- 3:35 – 4:05 **Scott Hartley**, Miami University of Ohio
Dissipative Assembly of Carboxylic Acid Anhydrides for Nonequilibrium Systems Chemistry
- 4:05 – 4:15 *Discussion*
- 4:15 – 4:40 **Break**
- 4:40 – 5:10 **David Baker**, University of Washington
Principles of De Novo Protein Nanomaterial Assembly in 1, 2 and 3 Dimensions
- 5:10 – 5:20 *Discussion*
- 5:20 – 5:50 **Oleg Lavrentovich**, Kent State University
Command of Active and Responsive Elastomers by Topological Defects and Patterns
- 5:50 – 6:00 *Discussion*
- 6:00 – 7:00 **Poster Session 2, continued**
- 7:00 – 8:30 **Working Dinner: General discussion on new opportunities, collaborative exchanges**

Thursday, August 22, 2019

- 7:00 – 8:00 **Breakfast** (Also presentation & poster set-up. Copies of all presentations for Thursday need to be given to Teresa Crockett prior to the end of the meeting.)

Session 5 **Patterns for Assembly**
Chair: **Michael Solomon**, University of Michigan

- 8:00 – 8:30 **Maria Santore**, University of Massachusetts, Amherst
Tension- and Curvature- Controlled Fluid-Solid Domain Patterning in Single Lamellae

- 8:30 – 8:40 *Discussion*
- 8:40 – 9:10 **Sunil Sinha**, University of California, San Diego
Synthesis of Novel Hybrid Nanostructures Employing Advanced Structural Characterization Techniques
- 9:10 – 9:20 *Discussion*
- 9:20 – 9:50 **Michael Bedzyk**, Northwestern University
Electrolyte-Mediated Assembly of Like-Charged Colloids
- 9:50 – 10:00 *Discussion*
- 10:00 – 10:30 Break
- 10:30 – 11:00 **Paul Nealey, Argonne National Laboratory**
Precision Synthesis and Assembly of Ionic and Liquid Crystalline Polymers
- 11:00 – 11:10 *Discussion*
- 11:10 – 11:40 **Meredith Silberstein**, Cornell University
Bio-inspired Polymer Membranes for Resilience of Electrochemical Energy Devices
- 11:40 – 11:50 *Discussion*
- 11:50 – 12:00 *Remarks, Concluding Comments*
Joanna Aizenberg and **Aleksandr Noy**, Meeting Chairs
Mike Markowitz, Program Manager, Biomolecular Materials
- 12:00 **Adjourn**

Poster List

Biomolecular Materials Principal Investigators' Meeting

Poster Presenters, Tuesday August 20

1. **Alexey Snezhko (Argonne National Laboratory):** Dynamics of Active Self-Assembled Materials
2. **Suriyanarayanan Vaikuntanathan (University of Chicago):** Designing Adaptive Information Processing Materials Using Non-equilibrium Forcing
3. **Rebecca Schulman (Johns Hopkins University):** Resilient Hydrogels from the Nanoscale to the Macroscale
4. **Michael Strano (Massachusetts Institute of Technology):** Materials Exhibiting Biomimetic Carbon Fixation and Self-Repair: Theory and Experiment: 1
5. **Michael Strano (Massachusetts Institute of Technology):** Materials Exhibiting Biomimetic Carbon Fixation and Self-Repair: Theory and Experiment: 2
6. **Dan Hammer (University of Pennsylvania):** Autonomous Motility of Synthetic Protocells Driven by Biochemical Catalysis
7. **Anna Balazs (University of Pittsburgh):** Designing Bio-Inspired, Adaptive Gels with Controllable 3D Structures
8. **Amit Nagarkar/George Whitesides (Harvard University):** DYNAMIC, Adaptive, Systems and Materials: Complex, Simple, and Emergent Behaviors
9. **Michael Solomon (University of Michigan):** Self-assembly, Crystal Quality, and the Biomimetic Reconfiguration of Colloidal Structure
10. **Zhibin Guan (University of California, Irvine):** Bioinspired Design of Multifunctional Dynamic Materials
11. **Gordana Dukovic (University of Colorado):** Control of Charge Transfer and Light-driven Reactions in Nanocrystal-Enzyme Complexes
12. **Darrin Pochan (University of Delaware):** Nanomaterial Construction through Peptide Computational Design and Hierarchical Solution Assembly
13. **Jeffrey Saven (University of Pennsylvania):** Nanomaterial Construction through Peptide Computational Design and Hierarchical Solution Assembly

Poster Presenters, Wednesday August 21

14. **Surya Mallapragada (Ames Laboratory):** Bioinspired Materials
15. **Hao Yan (Arizona State University):** Biomimetic Light Harvesting Complexes Based on Self-Assembled Dye-DNA Nanostructures
16. **Dan Morse (University of California, Santa Barbara):** Reflectin: Protein Driver of Dynamically Tunable Biophotonics; New Paradigm for Tunably Reconfigurable Materials
17. **Trevor Douglas (Indiana University):** Self-Assembly of Virus Particle Based Materials for Hydrogen Catalysis
18. **Michael Shirts (University of Colorado):** What Are the Principles Controlling Biomimetic Heteropolymer Secondary Structure?
19. **Sanat Kumar (Columbia University):** Controlling Lattice Organization, Assembly Pathways and Defects in Self-Assembled DNA-Based Nanomaterials
20. **F. Akif Tezcan (University of California, San Diego):** Protein Self-Assembly by Rational Chemical Design
21. **Jeetain Mittal (Lehigh University):** Biomolecular Assembly Processes in the Design of Novel Functional Materials
22. **David Pine (New York University):** Self-Assembly of Colloids with Chemically Heterogeneous Surfaces
23. **Marcus Weck (New York University):** Self-Assembly and Self-Replication of Novel Materials from Particles with Specific Recognition: The Depletion Interaction Approach
24. **Lara Estroff (Cornell University):** Controlling Structure Formation Pathways in Functional Bio-Hybrid Nanomaterials
25. **Aleksandr Noy (Lawrence Livermore National Laboratory):** Design, Synthesis, and Assembly of Biomimetic Materials with Novel Functionality

LABORATORY PROJECTS

PRECISION SYNTHESIS AND ASSEMBLY OF IONIC AND LIQUID CRYSTALLINE POLYMERS

Wei Chen, Juan J. de Pablo, Paul F. Nealey, Matthew Tirrell – Argonne National Laboratory

i) **Program Scope:** our FWP work has focused on three themes: i) heterocharged polymers ii) ionic transport in charged self-assembled block polymers and iii) Polymeric liquid crystals and their influence on nematic order and orientation.

ii) **Recent Progress**

Multi-Valent Hetero-Charged Polymeric Materials: Recent work has followed two distinct directions within the broad area of multi-valent, hetero-charged polymer systems: Polyelectrolyte brushes in the presence of multi-valent ions, and, interactions of polycations with nucleic acids. Each direction has yielded some surprises.

Pursuing a line of work discussed in our last report, we have developed a theoretical model for the collapse of polyelectrolyte brushes in the presence of multivalent ions, focusing on the formation of lateral inhomogeneities in the collapsed state. Polyelectrolyte brushes are important in a variety of applications, including stabilizing colloidal particles and lubricating surfaces. Many uses rely on the extension of the densely grafted polymer chains from the surface in the extended brush morphology. In the presence of multivalent ions, brushes are significantly shrunken relative to monovalent ionic solutions, which greatly affects their properties.

The nature of the shrinkage of the layers in multi-valent ions is decidedly different from the shrinkage of uncharged polymer brushes in poor solvent. Specifically, uncharged brushes shrink uniformly as solvent quality decreases. We have shown unambiguously that this is not the case with polyelectrolyte brushes in the presence of multi-valent ions. (1,2) Both theoretical considerations and data from surface forces measurements and atomic force microscopy lead to the conclusion that rather than uniform shrinkage or formation of pinned micelles, polyelectrolyte brushes in the presences of multi-valent ions form distinctive cylindrical bundles. The equilibrium brush heights predicted for these structures are of a similar magnitude to those measured experimentally. The formation of lateral structures can open new avenues for stimuli-responsive applications that rely on nanoscale pattern formation on surfaces.

Most of our early work with multi-valent interactions was done with tri-valent ions on the presumption that the effects of shrinkage and the formation of lateral inhomogeneities in the collapsed state would be stronger with tri-valents than di-valents. Our recent work on a series of di-valent ions (Langmuir) shows that this is not categorically the case. What came out of this di-valent work is evidence of marked ion specificity. Di-valent barium in solution exerts much stronger effects of brush shrinkage than calcium or magnesium; calcium is marginally stronger than magnesium. All our work so far has been done on poly(styrene sulfonate) brushes, which led us to notice a correlation between the solubility of the sulfate salts of these di-valent cations and the shrinkage. Di-valent cations that make more poorly soluble sulfate salts provoke stronger shrinkage.

Shrinkage is not the only effect on polymer brushes induced by multi-valent ions. They also cause strong adhesion between polyelectrolyte brushes. We have extracted an empirical rule from our observations of adhesion with tri-valent ions. That is, when experiments are done at fixed ionic strength produced largely by mono-valent ions, addition of tri-valent ions into the medium to the level where just 1 in 1000 (0.1%) of the ions is tri-valent, produces adhesion. There is as yet no quantitative theoretical understanding of this observation.

This observation instigated another line of investigation in the last year. Polyelectrolyte brushes have long been touted as delivering high lubricity to surfaces, but this low friction phenomenon has only been observed in media without added salt, or with added mono-valent salt. In a *Science* (3) paper last year, we confirmed our suspicions arising from our earlier observation of adhesion, namely that high friction between polyelectrolyte brushes is also induced by multi-valent ions. Friction starts at the 0.1% tri-valent level and becomes stronger as the brushes shrinkage and lateral heterogeneities develop. The *Science* paper was also the subject of a Perspective commentary in the same issue. Di-valent ions also induce higher friction with the same pattern of ion-specificity discussed above for shrinkage.

The second broad area of our work on multi-valent, hetero-charged polymer systems is our exploration of interactions of polycations with nucleic acids. Though polycations, such as polylysine, have been used

extensively and increasingly in nucleic acid delivery systems for gene therapy and other applications, there is very little understanding, or even raw data, on their structure or means of formation. We have been in good position to produce (4) this fundamental understanding. In a paper last year (4), we published the unexpected finding that, in polylysine complexes with nucleic acids, double-stranded nucleic acids form solid complexes and single-stranded nucleic acids form fluid complexes. This is true over a wide range of types of nucleic acid structures: DNA or RNA, linear or hairpin, partially complementary double strands. The principal reason, we showed, is due to the greater linear charge density of double strands. Double-stranded DNA has about four times the linear charge density of single-stranded; one factor of two comes from the two chains, the second factor of two comes from linear contraction due to double helix formation.

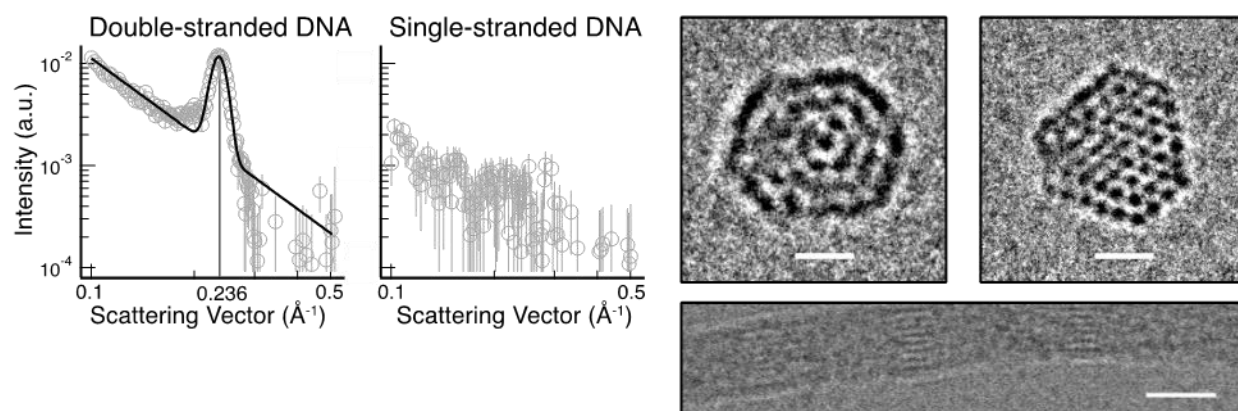


Figure 1. The peak position (0.236 \AA^{-1}) corresponds to an inter-helix spacing of 2.7 nm, close to the DNA helix size. No wide-angle peak is seen with single-stranded DNA. The scale bars are 25 nm.

Actual delivery applications generally are in the form of micelles generated by complexation of nucleic acids with block copolymers of polylysine and polyethylene glycol. In a Nano Letters paper (see Fig. 1), we examined the structures of these micellar complexes in the light of what we now know about the homopolymer complexes. We found via small-angle-x-ray scattering, that micellar complexes with single-stranded nucleic acids are spheres that are fairly uniform in size, while micellar complexes with double-stranded nucleic acids are highly extended and rod-like, with fairly uniform radii but variable lengths. This consistent difference we attribute to the fluid versus solid nature of the respective micellar cores. Further evidence of this comes from a small peak we discovered in the wide-angle-x-ray-scattering illustrated in the figure below. The peak, present in double-stranded samples, is absent in single-stranded samples. Thus, there may be some induction of crystalline or liquid crystal-like structure in the confined cores of these micelles. This may bear some connection to the liquid crystalline self-assembly work discussed in another part of this report.

Our efforts to understand the behavior of polycation/nucleic acid interactions had led us to develop a theoretical formalism capable of describing complex coacervation in the context of mixtures of flexible and semi-flexible molecules (5). Note that the persistence length of a simple polycation such as polylysine is on the order of one nm, whereas that of DNA is on the order of 50 nm. More specifically, by combining scaling approaches and the random phase approximation (RPA), we developed a theory of coacervates formed from rigid polyanions (including DNA) and flexible polycations. We find that at low stiffness of the polyanion, coacervates are isotropic liquids with two different correlation lengths, equal to the mesh sizes of the polyanion and polycation interpenetrating semidilute solutions. When the polyanion stiffness exceeds a threshold, the coacervate undergoes liquid crystalline ordering (LCO). The formation of a nematic phase is induced by anisotropic excluded volume and anisotropic Coulomb interactions between semiflexible polyanions. Our theoretical predictions of LCO within the coacervate formed from flexible and semiflexible polyelectrolytes are consistent with our experimental results and previous experimental literature reports.

Ion-Conducting Polyelectrolytes: A second major direction within our groups has sought to refine and expand the experimental electrochemical platform developed by our team to probe nanoscale ion transport phenomena near solid-solid interfaces. Briefly, this platform centers around the use of custom-fabricated interdigitated electrode arrays (IDEs) which are coated with thin polymer electrolyte films (< 200 nm). The microstructure of such films can be precisely controlled or characterized by directed self-assembly (DSA) and microscopy methods, respectively. This in turn enables us to fully describe any intrinsic ion transport phenomena present in block copolymers or other similar layered, nanostructured electrolytes.

In a recent publication, we have directly quantified the role of defects on ionic transport in nanostructured block copolymer electrolytes (BCEs) (10). We demonstrated that a single defect, such as a dislocation, anywhere in the path of an ion conducting route disconnects and precludes that pathway from contributing to the conductivity and results in an increase in the dielectric parameter of the film. When all the ion conduction pathways are blocked between electrodes, the conductivity is negligible, 4 orders of magnitude lower compared to a completely connected morphology and the dielectric parameter increases by a factor of 50 (Fig. 2). These results have profound implications for the interpretation, design, and processing of block copolymer electrolytes for applications as ion conducting membranes.

By eliminating the presence of ion blocking defects, we were able to quantify more precisely the intrinsic changes in ionic conductivity due to the presence of a mixed interface between the conductive and nonconductive blocks. By fully homogenizing the surface of IDEs, we can direct the parallel assembly of amphiphilic BCEs, and achieve a continuous single-grain structure. Comparison between the conductivities of the BCEs with the analogous homopolymer electrolytes reveals that ionic conductivity is relatively decreased in the BCE by as much as fifty percent. Moreover, the degree of these changes was found to correlate well with the degree of interfacial mixing, as quantified by mean-field theory calculations (Fig.3). These effects are analyzed using a two-layer model, which demonstrates that the PEO conductivity at the interface could be significantly reduced by the presence of only a few percent polystyrene. Finally, the fraction of inactive PEO is found to be independent of temperature, suggesting that the diminished conductivity cannot be explained only by decreased segmental dynamics nearby the domain interface.

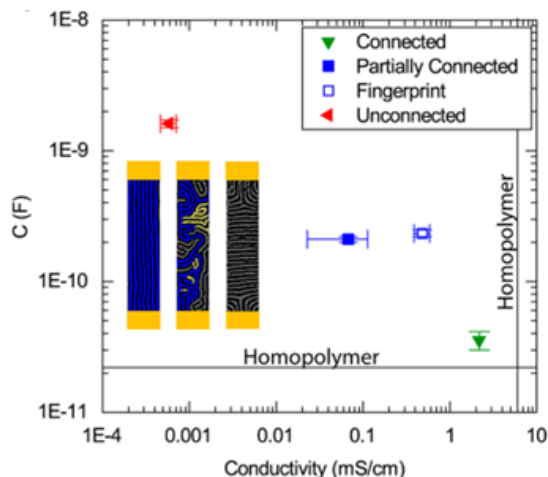


Figure 2 - Calculated C and conductivity for each BCE structure orientation. Inset shows analyzed SEM micrographs of ion conduction pathways (percolated paths labeled in blue with nonparticipating sections in yellow)

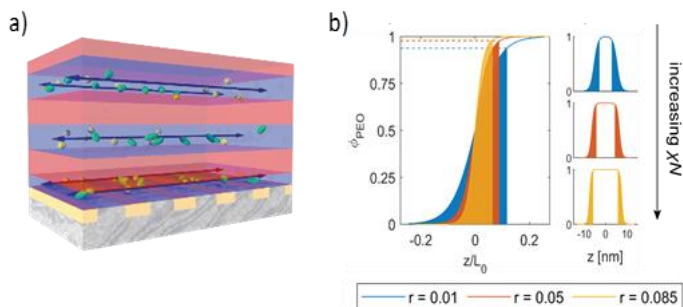


Figure 3 – Illustration of a cross-section of the BCE coated IDE and the direction of the electric field during the EIS measurement (a) and PEO concentration profiles from SCFT at different salt concentrations. Shaded regions correspond to the effective inactive interfacial region determined via electrochemical impedance spectroscopy.

The concept of interfacial ion transport can be expanded to other nanostructure-forming solid electrolyte systems, such as nanocomposite electrolytes where polymer-inorganic interfaces govern overall material properties. In a paper published earlier this year (9), we performed electrochemical measurements on thin polymer electrolyte films grafted to the inorganic SiO₂ IDE substrate. Thickness dependent conductivity measurements reveal the effects of this grafted polymer-inorganic interface

on ionic mobility. These promising results suggest that we can use the IDE platform as a means to study any number of interfaces by straightforward functionalization of the IDE surface.

Anisotropic and Liquid Crystalline Polymeric Assemblies: The third major area of focus of our team is concerned anisotropic, ordered liquids and polymeric systems. Generally speaking, the anchoring behavior of nematic liquid crystals (NLCs) confined between surfaces on the ground state without external field is of both fundamental and applied interests. To date, research has focused on the photo response of LC azobenzene polymeric systems to obtain either planar or homeotropic orientations of LCs. The broader behavior of liquid crystalline polymers (LCP) in a nematic medium has not been considered yet. Therefore, tuning the polar angle of LC molecules on solid surfaces continues to be a challenge, and more insights are needed about the polymer chain conformation as it extends into the LC medium.

At the theoretical and computational levels, our efforts to characterize liquid crystalline polymers have been accompanied by the development of new methods that allow one to combine detailed quantum mechanical calculations with classical simulations in a highly efficient manner (19,20). These methods rely extensively on machine learning and, moving forward, we will seek to expand them across a wide range of materials platforms.

To address this need, we have synthesized side-chain LC polymer brushes, poly(6-(4-methoxy-azobenzene-4'-oxy) hexyl methacrylate) (PMMAZO), bearing azobenzene mesogenic groups in the side chains attached to the polymethacrylate main chain (14). Different grafting densities of PMMAZO surfaces were fabricated by tethering different concentrations of PMMAZO solutions to Si surfaces. The out-of-plane polar angle of 5CB on the brush layer gradually changes from $\sim 0^\circ$ to $\sim 62^\circ$ by simply increasing the grafting density of the polymer brush from 0.0219 to 0.0924 chains per nm^2 , thereby leading to a highly effective way of tuning the anchoring behavior of NLCs. Surface force apparatus measurements are used to determine that 5CB is a good solvent for PMMAZO brushes, and to understand the relationship between chain conformation in 5CB and the anchoring behavior of LC molecules on the polymer brush layer.

In previous work, we used theory and evolutionary computation to design patterned PMMAZO brush surfaces to stabilize specific phases of chiral liquid crystals, including Blue-phases (BPs), which form a crystalline structure of topological defects that provides selective visible-light reflection. We managed to control the crystallographic plane of the lattice that is presented to the substrate or the interface and, in this way, we generated stable and perfectly ordered macroscopic single-crystal specimens of blue phases I and II (16). This platform also permitted further exploration of the crystal nucleation and growth process of BPs (15). In particular, the transformation between BPs, where crystal features arise in the submicron regime, was predicted to be martensitic in nature when one considers the collective behavior of the double-twist cylinders. More recently, we established that the cell thickness window necessary to form single crystals of BP II [100] on chemically patterned surfaces is between $1.5 \mu\text{m}$ and $18 \mu\text{m}$ (17). Numerical simulations also revealed that the free energy density of the BP II is lower when it is confined into a hybrid homeotropic-patterned cell, and that the influence of the pattern becomes less significant as the channel thickness increases. We have now analyzed in more detail the periodicity or width ratio range of stripe-like patterns that stabilize the formation of uniform BP I and BP II with pre-designed lattice orientation (18). Three transition regimes have been identified based on pattern parameters and periodicity: $L_s=130\text{-}170 \text{ nm}$ for single crystal of BP II (100); $L_s=180\text{-}200 \text{ nm}$ for single crystal of BP I (110); $L_s=2L_0$ or $3L_0$ with $W_p/L_s=0.5$ for monodomain BP I (110). Unveiling that how these parameters affect the equilibrated morphologies of BPs will be critical for both further improving current display and optical technologies and for expanding the spectrum of directed self-assembly of BPs for applications.

iii) Future Plans.

Our *future plans* include investigating the solvation behavior of lithium salts in polymer interfaces and how it influences the ion mobility, and exploring chemical and electrochemical reactivity of polymers with different battery components, such as lithium metal anodes and ceramic solid-state electrolytes.

In the context of liquid crystalline materials, our future plans also include (1) exploring the correlation length of the BPLC, as the effect of distance to the bulk is limited by the existence of grain boundaries (2) sculpting grain boundaries, based on the BP single crystal idea with different lattice orientations, and (3) probing the distortion and the strain release mechanism of the BP unit cell during the martensitic transformation by in-situ resonant soft X-ray scattering (RSOXS) measurements.

iv-v) Publications resulting from work supported by the DOE grant over the previous two years

- (1) "Lateral structure formation in polyelectrolyte brushes induced by multi-valent ions", B. Brettmann, P. Pincus and M. Tirrell, *Macromolecules*, **50**, 1225-1235 (2017).
- (2) "Multi-valent ions induce lateral structural inhomogeneities in polyelectrolyte brushes", J. Yu, N.E. Jackson, X. Xu, B.K. Brettmann, M. Ruths, J.J. de Pablo and M. Tirrell, *Science Advances*, **3**, Article Number: eaao1497 (2017).
- (3) "Multi-valent counterions diminish the lubricity of polyelectrolyte brushes", J. Yu, N. E. Jackson, X. Xu, Y. Morgenstern, Y. Kaufman, M. Ruths, J. J. de Pablo, M. Tirrell, *Science*, **360**, 1434–1438 (2018); Perspective commentary on this article in same addition: "More friction for polyelectrolyte brushes", M. Balluaff, *Science*, **360**, 1399-1400 (2018).
- (4) "Oligonucleotide–peptide complexes: Phase control by hybridization", J. R. Vieregg, M. Lueckheide, A. B. Marciel, L. Leon, A. J. Bologna, J. R. Rivera, M. Tirrell, *J. Am. Chem. Soc.*, **140**, 1632–1638 (2018).
- (5) "Liquid Crystalline and Isotropic Coacervates of Semiflexible Polyanions and Flexible Polycations," A. M. Romyantsev and J. J. de Pablo, *Macromolecules*, (2019) **52**, 5140-5156. DOI:doi.org/10.1021/acs.macromol.9b00797
- (6) "Structure-property relationships of oligonucleotide polyelectrolyte complex micelles", M. Lueckheide, J.R. Vieregg, A.J. Bologna, L. Leon and M. Tirrell, *Nano Letters*, **18**, 7111-7117 (2018).
- (7) "Ion-specific effects of di-valent ions on the structure of polyelectrolyte brushes", X. Xu, D. Mastropietro, M. Ruths, M. Tirrell, J. Ying, *Langmuir*, in press, 2019.
- (8) "Interrogation of Electrochemical Properties of Polymer Electrolyte Thin Films with Interdigitated Electrodes," Sharon, D.; Bennington, P.; Liu, C.; Kambe, Y.; Dong, B. X.; Burnett, V. F.; Dolejsi, M.; Grocke, G.; Patel, S. N.; Nealey, P. F.. *J. Electrochem. Soc.* 2018, **165** (16), H1028–H1039.
- (9) "Nanothin Film Conductivity Measurements Reveal Interfacial Influence on Ion Transport in Polymer Electrolytes." Dong, B. X.; Bennington, P.; Kambe, Y.; Sharon, D.; Dolejsi, M.; Strzalka, J.; Burnett, V. F.; Nealey, P. F.; Patel, S. N. *Mol. Syst. Des. Eng.* 2019, **4** (3), 597–608.
- (10) "Role of Defects in Ion Transport in Block Copolymer Electrolytes." Kambe, Y.; Arges, C. G.; Czaplowski, D. A.; Dolejsi, M.; Krishnan, S.; Stoykovich, M. P.; de Pablo, J. J.; Nealey, P. F. *Nano Lett.*, in press, 2019.
- (11) "Structure and proton conduction in sulfonated poly(ether ether ketone) semi-permeable membranes: a multi-scale computational approach," Molina, J., de Pablo, J.J.; Hernandez-Ortiz, Juan P, *Phys. Chem. Chem. Phys.*, 2019, **21**, 9362-9375.
- (12) "Influence of Homopolymer Addition in Templated Assembly of Cylindrical Block Copolymers," Doise, J.; Bezik, C.; Hori, M.; de Pablo, J.J., Gronnheid, R., 2019, *ACS Nano*, **13**, 4073-4082.
- (13) "Free energy of metal-organic framework self-assembly," Colon, Yamil J.; Guo, Ashley Z.; Antony, Lucas W.; de Pablo, J.J., *J. Chem. Phys.*, 2019, **150**, 104502.
- (14) "Engineering the Anchoring Behavior of Nematic Liquid Crystals on Solid Surface by Varying the Density of Liquid Crystalline Polymer Brush." Li X., Yanagimachi T., Bishop C., Smith C., Dolejsi

- M., Xie H., Kurihara K., Nealey P. *Soft Matter*, 2018, **14**, 7569-7577.
- (15) "Mesoscale Martensitic Transformation in Single Crystals of Topological Defects." Li X., Martinez-Gonzalez JA., Hernandez-Ortiz JP., Ramirez-Hernandez A., Zhou Y., Sadati M., Zhang R., Nealey P.F., de Pablo J. J., *PNAS*, 2017, **114**, 10011-10016.
- (16) "Directed Self-Assembly of Liquid Crystalline Blue-Phases into Ideal Single-Crystals," Martinez-Gonzalez JA. Li X, Sadati M., Zhou Y., Zhang R., Nealey PF., de Pablo J.J. *Nat. Commun.*, 2017, **8**, 15854.
- (17) "Thickness dependence of forming single crystal by liquid-crystalline blue phase on chemically patterned surface." Li, X.; Martinez-Gonzalez, JA.; de Pablo JJ.; Nealey, P. F. *Emerging Liquid Crystal Technologies XIII*, 2018, 10555, 1055514.
- (18) "Perfection in Nucleation and Growth of Blue-Phase Single Crystals: Small Free-Energy Required to Self-Assemble at Specific Lattice Orientation." Li, X.; Martinez-Gonzalez, JA.; Park, K.; Yu, C.; Zhou, Y.; de Pablo JJ.; Nealey, P. F., *ACS Appl. Mater. Interfaces*, 2019, **11**, 9487-9495.
- (19) "Recent advances in machine learning towards multiscale soft materials design," Jackson, Nicholas E.; Webb, Michael A.; de Pablo, Juan J., *Current Opinion in Chemical Engineering*, (2019), **23**, 106-114.
- (20) "Electronic structure at coarse-grained resolutions from supervised machine learning," Jackson, Nicholas E.; Bowen, Alec S.; Antony, Lucas W.; Vishwanath, V.; de Pablo, J.J., *Science Advances*, (2019), **5**, eaav1190.
- (21) "Nanocrystalline Oligo(ethylene sulfide)-b-poly(ethylene glycol) Micelles: Structure and Stability," Sevgen, Emre; Dolejsi, Moshe; Nealey, Paul F.; Hubbell, J., and de Pablo, J.J., 2018, *Macromol.*, **51**, 9538-9546.
- (22) "Structural Correlations and Percolation in Twisted Perylene Diimides Using a Simple Anisotropic Coarse-Grained Model," Bowen, Alec S.; Jackson, Nicholas E.; Reid, Daniel R.; de Pablo, J.J., *J. Chem. Theory and Comp.*, 2018, **14**, 6495-6504
- (23) "Tenfold increase in the photostability of an azobenzene guest in vapor-deposited glass mixtures," Qiu, Yue; Antony, Lucas W.; Torkelson, John M.; de Pablo, J.J., and Ediger, M.D., *J. Chem. Phys.*, 2019, **149**, 204503 .
- (24) "Defect Annihilation Pathways in Directed Assembly of Lamellar Block Copolymer Thin Films," Hur, Su-Mi; Thapar, Vikram; Ramirez-Hernandez, Abelardo; Nealey, P.F., and de Pablo J.J., *ACS Nano*, 2018, **12**, 9974-9981.
- (25) "Emergence of radial tree of bend stripes in active nematics," A. Sokolov, A. Mozafari, R. Zhang, J. de Pablo, A. Snezhko, *Physical Review X*, (2019), in press.
- (26) "Directed Self-Assembly of Colloidal Particles onto Nematic Liquid Crystalline Defects Engineered by Chemically Patterned Surfaces." Li, Xiao, Julio C. Armas-Pérez, Juan P. Hernández-Ortiz, Christopher G. Arges, Xiaoying Liu, Jose A. Martinez-Gonzalez, Leonidas E. Ocola, Camille Bishop, Helou Xie, Juan J. de Pablo, and Paul F. Nealey. *ACS nano* **11**, no. 6 (2017): 6492-6501.

- (27) "Comparing solvophobic and multivalent induced collapse in polyelectrolyte brushes." Jackson, Nicholas E., Blair K. Brettmann, Venkatram Vishwanath, Matthew Tirrell, and Juan J. de Pablo. *ACS Macro Letters* 6, no. 2 (2017): 155-160.
- (28) "A multi-chain polymer slip-spring model with fluctuating number of entanglements: Density fluctuations, confinement, and phase separation." Ramírez-Hernández, Abelardo, Brandon L. Peters, Ludwig Schneider, Marat Andreev, Jay D. Schieber, Marcus Müller, and Juan J. de Pablo. *The Journal of chemical physics* 146, no. 1 (2017): 014903.
- (29) "Structure–Property Relationships of Oligonucleotide Polyelectrolyte Complex Micelles," Michael Lueckheide, Jeffrey R. Viereg, Alex J. Bologna, Lorraine Leon, and Matthew V. Tirrell, *ACS Nano Letters*, (2018). DOI: 10.1021/acs.nanolett.8b03132
- (30) Reversible Sub-Volt Manipulation of Insulator-Metal Transition with Redox Poly (Ionic Liquids) Gating for Ultralow-Power Electronic, Chen, W.; Tirrell, M.; Zhou, H.; Zhang, L.; s, ANL-IN-18-091, 2018. – Argonne IP Disclosure.
- (31) "Chlorination of Side Chains: A Strategy for Achieving a High Open Circuit Voltage Over 1.0 V in Benzo [1, 2-b: 4, 5-b'] dithiophene-Based Non-Fullerene Solar Cells", Chao, P.; Mu, Z.; Wang, H.; Mo, D.; Chen, H.; Meng, H.; Chen, W.; He, F., *ACS Appl. Energy Mater.*, 2018, 1, 2365-2372.
- (32) "Synergistic effects of chlorination and a fully two-dimensional side-chain design on molecular energy level modulation toward non-fullerene photovoltaics", Chao, P.; Wang, H.; Mo, D.; Meng, H.; Chen, W.; He, F.; *J. Mater. Chem. A*, 2018, 6, 2942-2951. (Cover Story)
- (33) "The integrated adjustment of chlorine substitution and two-dimensional side chain of low band gap polymers in organic solar cells", Yang, Z.; Chen, H.; Wang, H.; Mo, D.; Liu, L.; Chao, P.; Zhu, Y.; Liu, C.; Chen, W.; He, F.; *Polym. Chem.*, 2018, 9, 940-947. (Cover Story)
- (34) "Generalized skew-symmetric interfacial probability distribution in reflectivity and small-angle scattering analysis", Jiang, Z.; Chen, W.; *J. Appl. Crystallogr.*, 2017, 50, 1653-1663.
- (35) Li, X.; Armas-Pérez, JC.; Hernández-Ortiz, JP. Arges, CG.; Liu, Xi.; Martinez-Gonzalez, JA.; Ocola, LE.; Bishop, C.; Xie, H.; de Pablo, JJ.; Nealey, PF. Directed Self-Assembly of Colloidal Particles onto Nematic Liquid Crystalline Defects Engineered by Chemically Patterned Surfaces. *ACS Nano*, 2017, 11(6), 6492-6501.
- (36) "Ion Conduction in Microphase-Separated Block Copolymer Electrolytes." Kambe, Y.; Arges, C. G.; Patel, S.; Stoykovich, M.; Nealey, P. F. *The Electrochemical Society Interface*, 2017, 26, 61-67.
- (37) "Interconnected Ionic Domains Enhance Conductivity in Microphase Separated Block Copolymer Electrolytes," Arges, C. G.; Kambe, Y.; Dolejsi, M.; Wu, G.; Segal-Peretz, T.; Ren, J.; Cao, C.; Kline, R. J.; Nealey, P. F. *Journal of Materials Chemistry A*, 2017, 11, 5619-5629.
- (38) "Quantitative Three-Dimensional Characterization of Block Copolymer Directed Self-Assembly on Combined Chemical and Topographical Pre-Patterned Templates." Segal-Peretz, T.; Ren, J.; Xiong, S.; Khaira, G. S.; Bowen, A.; Ocola, L. E.; Divan, R.; Doxastakis, M.; Ferrier, N. J.; de Pablo, J. J.; Nealey, P. F. *ACS Nano*, 2017, 11, 1307-1319.
- (39) "Fabrication of Nanoporous Alumina Ultra-filtration Membrane with Tunable Pore Size Using Block Copolymer Templates," Zhou, C.; Segal-Peretz, T.; Oruç, M. E.; Suh, H. S.; Wu, G.; Nealey, P. F. *Adv. Funct. Mater.* 2017, 27, 1701756.

- (40) "Intra-molecular Charge Transfer and Electron Delocalization in Non-Fullerene Organic Solar Cells", Wu, Q.; Zhao, D.; Goldey, M. B.; Filatov, A. S.; Sharapov, V.; Colón, Y. J.; Cai, Z.; Chen, W.; de Pablo, J. J.; Galli, G.; Yu, L.; *ACS Appl. Mater. Interfaces*, 2018, **10**, 10043–10052.
- (41) "Derivation of Multiple Covarying Material and Process Parameters Using Physics-Based Modeling of X-ray Data." Khaira, G.; Doxastakis, M.; Bowen, A.; Ren, J.; Suh, HS.; Segal-Peretz, T.; Chen, X.; Zhou, C.; Hannon, AF.; Ferrier, NJ.; Vishwanath, V.; Sunday, DF.; Gronheid, R.; Kline, RJ.; de Pablo, JJ.; Nealey, PF., *Macromolecules*, 2017, **50**, 7783–7793.

Bioinspired Metamaterials

PIs: Surya Mallapragada, Andrew Hillier, Marit Nilsen-Hamilton, Tanya Prozorov, Alex Traveset, David Vaknin, and Wenjie Wang, Ames Laboratory

Mailing Address: Division of Materials Sci. and Eng., Ames Laboratory, Ames, IA 50011

Program Scope

This FWP focuses on the development of new use-inspired mesoscale 2D and 3D structures that can serve as functional metamaterials and investigation of fundamental questions related to the development of controlled nanostructures and their hierarchical assemblies. Metamaterials provide an excellent example of targeting function, but the bioinspired approaches proposed here and insights gained into hierarchical self-assembly are broadly applicable beyond metamaterials. Nature abounds with examples of hierarchically assembled hybrid materials with multi-scale structures conferring unique properties and functions. This FWP uses coupled organic and biological templates to control the growth of metallic phases to form hierarchically self-assembled functional nanocomposite materials. Having previously successfully demonstrated the value of an integrated experimental approach guided by computation for synthesis of bioinspired nanocomposite materials *in vitro*, our team is now focused on using bioinspired approaches to synthesize self-assembled systems beyond those seen in living organisms. We are applying our ability to manipulate nanoscale particles into self-assembled architectures with spatial control to create “use-inspired” functional tailored metamaterials. This bottom-up approach for functional materials design aligns well with DOE’s priorities laid out in the Synthesis workshop report for the synthesis of complex nanostructures and multi-scale assemblies of potential energy relevance, and directly addresses the *DOE’s Grand Challenge*, to orchestrate atomic and electronic constituents to control material properties.

Recent Progress

We are developing bioinspired bottom-up synthesis approaches with macromolecular templates for metallization to create nanoscale structures and to enable higher-level 2D and 3D mesoscale organization and alignment. The two goals of this work are to 1) develop the underlying science to design, synthesize and characterize individual metallic nanostructures, and 2) develop approaches to assemble these individual nanostructures into 2D and 3D mesoscale superstructures. Progress towards each of these goals is summarized below.

Goal 1. Creation of individual nanostructured resonators:

Our first goal involves developing techniques for the bottom-up fabrication of individual theory-predicted nanoresonators such as split ring resonators (SRR). Theory will continue to guide experimental approaches by modeling the expected electromagnetic properties of the fabricated and metallized nanostructures, as in **Fig. 1**. We are exploring various designs and simulations for more complex new metallized DNA templates structures, contingent upon the capabilities of DNA architecture to construct the required templates for metallization. We are developing new

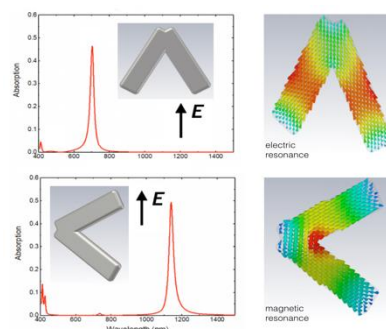


Fig. 1. Electromagnetic model for 100nm side length Origami DNA triangles with one side removed to open a gap and metallized with 5nm silver. This structure will work similar to a conventional SRR and has a magnetic resonance at about 1340nm.

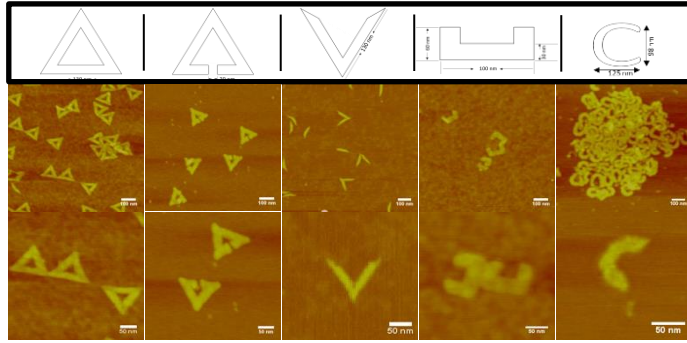


Fig. 2 DNA origami nanostructures of various shapes designed and created to serve as templates for metallization

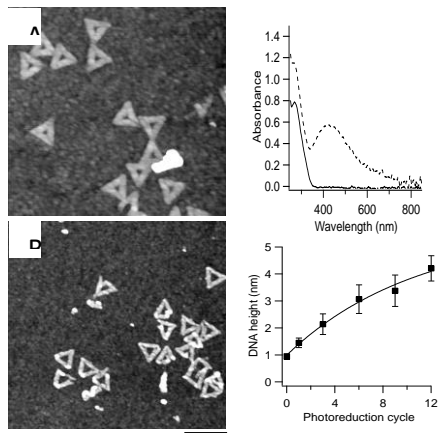


Fig. 3 AFM images of DNA origami (A) before and (B) after photoreduction. Scale = 200 nm. UV absorbance of DNA triangles before (solid) and after (dashed) metallization. DNA origami height as a function of photoreduction cycles.

numerical tools to better estimate collective response in random media and evaluate the effect of roughness on SRR response. We are numerically identifying all low-frequency resonant modes of the targeted particles and are numerically determining a database of the susceptibilities in the multipole expansion of these modes.

We are fabricating biological templates of specific shapes (**Fig. 2**) and selectively metallizing them to create particle plasmon resonances with the desired

electromagnetic response. Nucleic acids (NAs) have proved to be useful structural scaffolds for producing many 2D and 3D structures. We are creating split-ring resonators using DNA templates for metallization. The gap is an essential component of a SRR. We have devised DNA templates to create these nanostructures for metallization. We prepared circles with diameters of 135 nm by cutting and ligating portions of a double stranded DNA. V's were made using a combination of DNA origami and S1 nuclease to remove unused regions of the m13 DNA scaffold to create nanostructures with a "split". We are also designing structures with dimensions in the range of 130-200 nm using DNA origami, which are close to the ideal SRR and large enough to be visualized for the homogeneity of metal deposition. Currently designs being optimized, create C and U configurations for metallization, as shown in **Fig. 2**.

We have focused on metal NPs and metal coatings on DNA origami using solution-based processing methods. We have

primarily exploited a two-step synthesis procedure: (1) metal seeding and (2) metal growth. Metal seeding is achieved by electrostatic interactions between the negatively charged DNA with positively charged metal ions or NPs. The metal seeding step creates DNA templates decorated with small metal particles, followed by metal coating via electroless deposition (ELD). An alternative strategy for creating metal seeds directly on DNA templates involves a photochemical metal reduction process. High silver concentrations can produce significant homogeneous silver nucleation. Example results for metallization of a triangular DNA template are shown in **Fig. 3**, where the silver seed formation can be monitored via optical absorbance and the metal thickness can be controlled by the number of photoreduction cycles utilized. We have also developed TEM liquid-cell based imaging methods to investigate the mechanism of metallization and showed that we can achieve a high density of metal seeds on the DNA origami surfaces. Increasing metal thickness is achieved by several routes, including additional photochemical silver reduction steps or using one of several different ELD solutions, depending upon the metal of interest. We have successfully coated both silver and gold onto the seeded DNA templates. Silver photoreduction

coating results in a fully covered template with a thickness of ~3-4 nm depending on the number of cycles involved (**Fig. 3**). Simulations of these origami triangles with different thicknesses of silver metallization provide insights into predicted functional properties of these structures.

Goal 2: Self-assembled mesoscale 2D and 3D nanostructures: As an initial step to exploring mesoscale assembly of these nanostructures created in Goal 1, we have focused on developing techniques to assemble Au nanoparticles (NPs), and more recently, Au nanorods (NRs) with the aim of using these techniques for nanostructure assembly, using the desired nanostructures created in Goal 1. The NRs provide model nanostructures for assembly of asymmetric and larger nanostructures compared to assembly of NPs. To guide experiments, we are performing simulations and designing analytical models to describe and understand the effective sheet and bulk response of the metasurfaces and metamaterial films. Mesoscale structures are being

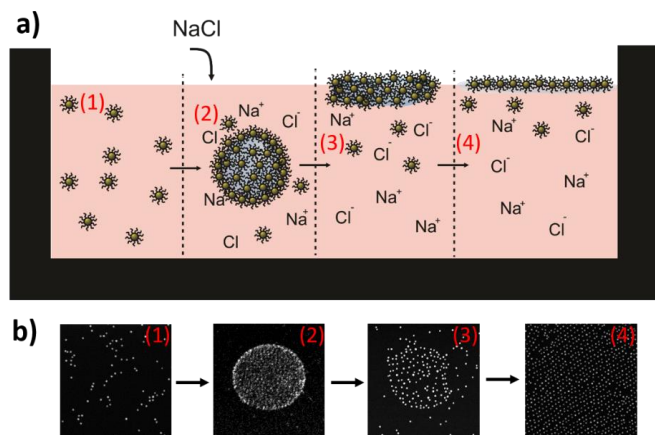


Fig. 4 a) Proposed mechanism of the phase separation of pNIPAM-Au nanoparticles in the presence of NaCl. At low salt concentrations, mobile, globular Au-pNIPAM aggregates form. Au-pNIPAM nanoparticles decorate the microdroplets of water with lower NaCl concentration. As the NaCl concentration increases, Au-PNIPAM-decorated droplets move to the water/air interface, and form the 2D lattice. **(b)** Representative STEM images highlighting each step of the proposed mechanism.

fabricated through self-assembly using two parallel strategies. The first strategy involves functionalizing the metal nanostructures with synthetic block copolymer 3D templates that *assemble functionalized NPs and NRs* into 2D and 3D materials with long-range order by changing pH, temperature, salt concentration or by interpolymer complexation. These assembly approaches are being extended to involve nanostructured components such as *SRR, created in Goal 1, self-assembled into 2D and 3D mesoscale structures* at high densities to create metamaterials and metasurfaces. The second approach involves the assembly of these nanostructured components using biomolecules. The two strategies can provide different realizations for the materials proposed and involve different

levels of complexity of components and self-assembly.

We have investigated AuNP self-assembly in the presence of dithiol ligands, and have showed short-range fcc structure with various dithiol oligomers, suggesting a robust and straight forward route to achieving simple and stable superstructures. We have shown that functionalization of AuNPs with synthetic polymers such as poly(ethylene glycol) (PEG), poly(acrylic acid) (PAA) or poly(N-isopropyl acrylamide) (PNIPAAM), followed by changing salt concentration, pH and/or temperature, can lead to long-range order in 2D at the air-liquid interface and long-range ordering under certain conditions in 3D. We have used grazing incidence X-ray scattering (GISAXS) and small angle X-ray scattering (SAXS) to investigate 2D and 3D ordering respectively. We have coupled these studies with transmission electron microscopy studies, including use of liquid cell TEM to visualize these assemblies (**Fig. 4**). Using DNA hybridization as inspiration, we have developed a strategy of interpolymer complexation (IPC) to create long-

range assemblies of AuNPs using a combination of PEG and PAA. High quality fcc single-crystals are formed in solution by assembly of AuNPs functionalized with PEO and PAA. While the initial assembly is driven by hydrogen bonding, our results, coupled with theory, suggest that van der Waals forces maintain the self-assembled long-range structure (**Fig. 5**), which is retained even

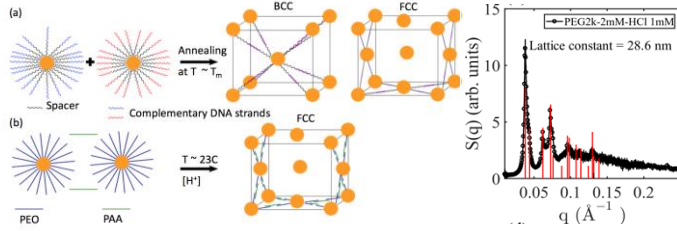


Fig. 5. (a) Nanoparticle assembly by hybridization by of complementary DNA strands (b) Assembly using interpolymer complexation of PEO and PAA. All nearest neighbor connections for fcc are not shown for the purpose of clarity (c) SAXS data for PEO-PAA system showing fcc structure

when the structure is removed from aqueous solution. This is in contrast to 3D mesoscale assemblies created using DNA hybridization. Therefore, our new approach to creating mesoscale assemblies using IPC can provide a reliable and robust method to create stable mesoscale assemblies with long-range order. Our initial results with NR assembly indicate that IPC between PEG and PAA can also lead to short range assemblies of NRs.

We are studying defect tolerance and the effect of disorder in predominantly ordered planar arrangements of the fabricated nano-resonators as they would occur on a functional metasurface (**Fig. 6**). Two types of disorder are being taken into account: (a) variation and uncertainty in the geometric properties of the individual particles, e.g., size variations, changes in metallization thickness and coverage, defect in the metallization; and (b) variations in the phase coherence in the scattering from spatial distributed particles and, in particular, changes to the resonant modes from near-field interaction of neighboring particles mediated by local evanescent fields and brought about by randomization of the near-field coupling between neighboring nanoresonant NPs because of shape, and positional disorder.

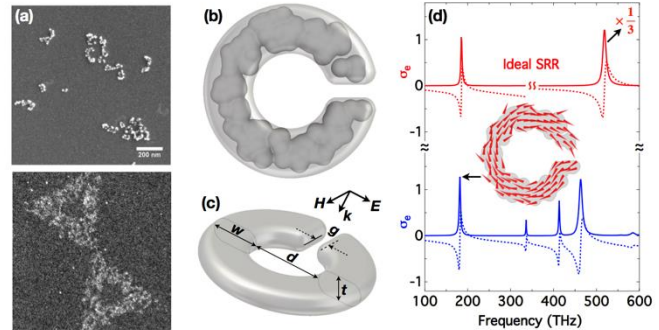


Fig. 6. Resembling self-assembled DNA origami metamaterials elements via accumulation of random spheres for surfaces roughness. (a) Example SEM images of “rough” DNA-based structures seeded with metal NPs. (b) Example of rough SRR constructed with 120 spheres of radius 8 to 9 nm inside the profile of an ideal SRR (c) schematic of SRR unit under excitation with indicated polarization (d) comparison of retrieved sheet electric conductivity for ideal SRR and the example rough SRR. The inset shows circulating current distribution at 182 THz, corresponding to the electrically-induced magnetic mode.

Future Plans

In our future work, we will take advantage of the methods we have developed to assemble AuNPs to assemble the SRR nanostructures that we have created. We will study the optical response of individual metallized DNA templates to determine the impact of various system parameters on optical resonance. Once large-scale assemblies of metallized nanostructures are created, we will perform FTIR measurements of the transmission and reflection spectra of these films for both polarizations. These data will allow us to determine effective electric and magnetic sheet conductivities of the formed metasurfaces. Results will be compared to numerical simulations of the theoretical structure of the ordered assemblies.

Publications (Aug 2017-Aug 2019)

- 1) Londono-Calderon, A., Hossen, M.M., Palo, P.E., Bendickson, L., Nilsen-Hamilton, M., Hillier, A.C., Vergara, S., and Prozorov, T., “Imaging of Unstained DNA Origami Triangles with Electron Microscopy”, *Small Methods* (2019), *under review*.
- 2) Nayak, S., Horst N., Zhang, H., Wang, W., Mallapragada, S.K., Travesset, A., and Vaknin, D., “Interpolymer Complexation as a Strategy for Nanoparticle Assembly and Crystallization”, *J. Phys. Chem. C*, **123**, 836 (2019).
- 3) Nayak, S., Fieg, M., Wang, W., Bu, W., Mallapragada, S., and Vaknin, D., “Effect of (Poly) electrolytes on the Interfacial Assembly of Poly (ethylene glycol)-Functionalized Gold Nanoparticles.”, *Langmuir*, **35**, pp.2251-2260 (2019).
- 4) Londono-Calderon, A., Nayak, S., Mosher, C. L., Mallapragada, S.K., and Prozorov, T., “New Approach to Electron Microscopy Imaging of Gel Nanocomposites *in situ*”, *Micron*, **120**, 104-112 (2019).
- 5) Bhattarai, N., Prozorov, T., “Direct Observation of Early Stages of Growth of Multilayered DNA-templated Au-Pd-Au Core-Shell Nanoparticles in Liquid Phase”, *Frontiers in Bioengineering and Biotechnology*, section Nanobiotechnology, (2019), DOI: 10.3389/fbioe.2019.00019.
- 6) Nayak, S., Horst, N., Zhang, H., Wang, W., Mallapragada, S., Travesset, A., and Vaknin, D., “Ordered networks of gold nanoparticles cross-linked by dithiol-oligomers”, *Particle & Particle Systems Characterization*, **35**, 1800097 (2018).
- 7) Hossen, M. M.; Bendickson, L.; Palo, P.; Yao, Z.; Nilsen-Hamilton, M.; Hillier, A. C., Creating Metamaterial Building Blocks with Directed Photochemical Metallization of Silver onto DNA Origami Templates. *Nanotechnology*, **29**, 355605 (2018).
- 8) Vaknin, D., Wang, W., Islam, F., Zhang, H., “Polyethylene-Glycol-Mediated Self-Assembly of Magnetite Nanoparticles at the Liquid/Vapor Interface.” *Advanced Materials Interfaces*, **5**, 1701149 (2018).
- 9) Wang, W., Lawrence, J.J., Bu, W., Zhang, H., and Vaknin, D., “Two-Dimensional Crystallization of Poly(N-isopropylacrylamide)-Capped Gold Nanoparticles.” *Langmuir*, **34**, 8374-8378 (2018).
- 10) Londono-Calderon, A., Bendickson, L., Palo, P.E., Nilsen-Hamilton, M., Mallapragada, S., and Prozorov, T. “*In-Situ* Nucleation, Growth and Evolution of Au Nanoparticles during Metallization of DNA Origami Visualized with HAADF-STEM”, *Microsc. Microanal.* **24** (Suppl 1), 282 (2018), <https://doi.org/10.1017/S1431927618001903> (this paper received 2018 M&M Postdoctoral Scholar Award).
- 11) Waltmann, T., Waltmann, C., Horst, N., and Travesset, A., “Many Body Effects and Icosahedral Order in Superlattice Self-Assembly”, *J. American Chemical Society*, **140**, 8236 (2018).
- 12) Ren, S., Sun, Y., Zhang, F., Travesset, A., Wang, C.-Z., and Ho, K.-M. “Calculation of critical nucleation rates by the persistent embryo method: Application to quasi hard sphere models”, *Soft Matter*, **14**, 9185 (2018).
- 13) Yang, Y., Zhang, F., Wang, C.-Z., Ho, K.-M., and Travesset, A., “Implementation of Metal-friendly EAM/FS-type Semi-empirical Potentials in HOOMD blue: mGPU-accelerated Molecular Dynamics Software.” *J. Comp. Phys.* **359**, 352 (2018).

- 14) Waltmann, C., Horst, N., and Travesset, A., “Potential of mean force for two nanocrystals: Core geometry and size, hydrocarbon unsaturation, and universality with respect to the force field”, *J. Chem. Phys.* **149**, 034109 (2018).
- 15) Rodriguez-Navarro, A.B., McCormack, H.H., Fleming, R. H., Alvarez-Lloret, P., Romero-Pastor, J., Dominguez-Gasca, N., Prozorov, T., Dunn, I. C., “Influence of physical activity on tibial bone material properties in laying hens”, *J. Struct. Biol.* **201**, 36-45 (2018).
- 16) Wang, W., Zhang, H., Mallapragada, S., Travesset, A., and Vaknin, D., “Ionic depletion at the crystalline Gibbs layer of PEG-capped gold nanoparticles at aqueous surfaces”, *Phys. Rev. Materials*, **1**, 076002 (2017).
- 17) Zhang, H., Wang, W., Mallapragada, S., Travesset, A. and Vaknin, D. “Ion Specific Interfacial Crystallization of Polymer-Grafted Nanoparticles”, *Journal of Phys. Chem. C*, **121**, 15424 (2017).
- 18) Woehl, T.J., Prozorov, T., “Future prospects in liquid cell EM of biomaterials” in *Liquid Cell Electron Microscopy*, Ed. F. Ross, Cambridge University Press, New York, NY, 476 – 500 (2017), ISBN: 9781-107-11657-3.
- 19) Prozorov, T., Almeida, T. P., Kovats, A., Dunin-Borkowski, R. E., “Off-axis electron holography of bacterial cells and magnetic nanoparticles in liquid”, *J. R. Soc. Interface Mater.* **14**, 20170464 (2017).
- 20) Waltmann, C., Horst, N., and Travesset, A., “Capping Ligand Vortices as `Atomic Orbitals` in Nanocrystal Self-Assembly”, *ACS Nano*, **11**, 11273 (2017).
- 21) Zhang, H., Nayak, S., Wang, W., Mallapragada, S., Vaknin, D., “Interfacial Self-Assembly of Polyelectrolyte-Capped Gold Nanoparticles”, *Langmuir*, **33**, pp. 12227-12234 (2017).
- 22) Travesset, A., “Topological structure prediction in binary nanoparticle superlattices”, *Soft Matter*, **13**, 147 (2017)
- 23) Zhang, H., Wang, W., Akinc, M., Mallapragada, S., Travesset, A. and Vaknin, D., “Assembling and Ordering Polymer Grafted Nanoparticles in three dimensions”, *Nanoscale*, **9**, 8710 (2017).
- 24) Zhang, H., Wang, W., Mallapragada, S., Travesset, A., and Vaknin, D., “Macroscopic and Tunable nanoparticle superlattices”, *Nanoscale*, **9**, 164 (2017).

Design, Synthesis, and Assembly of Biomimetic Materials with Novel Functionality

Aleksandr Noy, Anthony van Burren (LLNL), James J. De Yoreo, Chun-Long Chen, Marcel Baer (PNNL)

Program Scope

The overarching goal of this project is to develop synthetic self-assembling systems that mimic the hierarchical nature of biological membranes and carry out high-level functions based on a predictive understanding of both assembly and function. In particular, we seek to create fully synthetic self-assembling biomimetic structures that mimic the environment, versatility, and functionality of cell membranes based on a predictive understanding of: (a) the link between macromolecular sequence and organization, (b) controls on assembly and ordering, (c) incorporation of functional units with a focus on artificial carbon nanotube porins (CNTPs), and (d) mechanisms of fast and selective transport through these materials. Our approach integrates synthesis of defined sequence peptoid polymers, in situ atomic-level characterization of molecular structure and interactions, assembly dynamics and interfacial structure, molecular simulations of structure and assembly, and measurements of ionic and molecular transport through tailored carbon nanotube porin channels. Taken together, these advances build a foundation for design of functional materials based on an understanding of the link between sequence, assembly, and function to result in a new generation of biomimetic membranes with rationally-tunable pore size and chemical selectivity for applications in a wide range of energy systems.

Recent Progress

Component development for a synthetic membrane system: Water and ion transport in 0.8 nm CNTPs (*Science*, 2017, *Faraday Disc.* 2018). We have synthesized CNTPs with diameters of 1.5 nm (wCNTP) and 0.8 nm (nCNTP). Both nCNTPs and wCNTPs supported fast water transport (Fig. 1) with nCNTP water permeability an order of magnitude higher than that of wCNTPs, indicating that strong molecular confinement of water molecules in narrow pores provided the critical ingredient for fast transport. nCNT permeability exceeded that of biological water channel, aquaporin-1 (AQP1). We also found that removal of negative charge at the nCNTP entrance (either by pH change or by functionalization) increased water permeability. We also established that nCNTPs are highly specific cation channels with permselectivity close to 1 even at seawater level salinities.

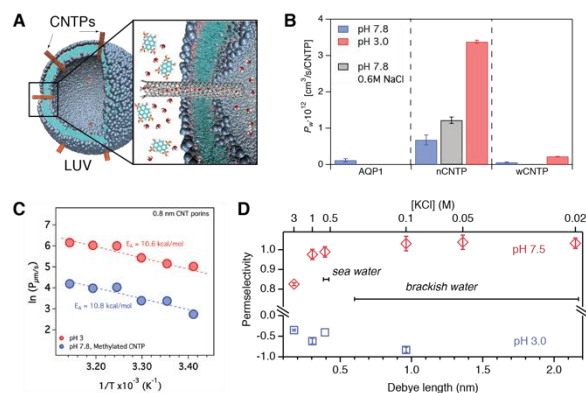


Figure 1. Water and ion transport in CNTPs. (A) Schematics of the osmotic transport measurement. (B). Water permeability of CNTPs at different pH. Gray bar shows water permeability at seawater-level NaCl draw. (C) Activation energies for unmodified CNTPs at pH3 and for methylamide-functionalized CNTPs at pH 7.5. (D) Ion transport permselectivity of CNTPs.

Component development for synthetic membrane systems: Folding membrane-mimetic 2D nanomaterials into single-walled nanotubes (*Nature Comm.* 2018, *Angew. Chem.* 2019). We recently changed the chemistry of hydrophobic sidechains from (N₄cipe)₆ residues to six N-[(4-bromophenyl)methyl]glycines (Nbp_m)₆ and assembled the resulting lipid-like peptoids into highly-designable, stiff and dynamic single-walled peptoid nanotubes (SW-PNTs) (Fig. 2). XRD and TEM data show that PNTs assembled from Nce₆Nbp_m₆ are highly crystalline and exhibit a wall thickness of 3.1 ± 0.1 nm (Fig.

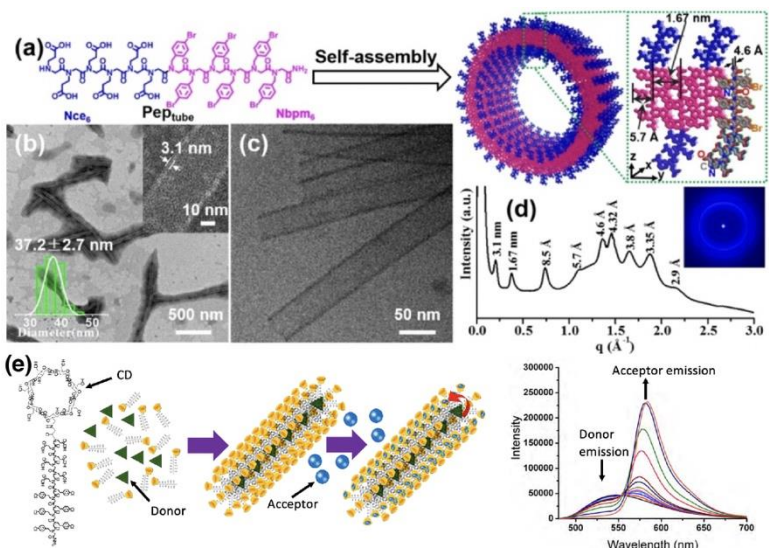


Figure 2. (a) Structure of Pept_{tube} and the scheme showing its assembly nanotubes. (b) TEM image of peptoid nanotubes showing the tube wall thickness of 3.1 nm and diameter of 37.2 ± 2.7 nm. (c) Cryo-TEM image of peptoid nanotubes. (d) XRD spectrum of peptoid nanotubes. (e) 1D peptoid micelles with cyclodextrin cages and an example of an efficient FRET obtained in these compounds with donor and acceptor molecules in the micelle interior and exterior, respectively

2b,d), similar to the thickness of our previously-reported 2D nanomembranes assembled from (N₄cipe)₆ peptoids. TEM studies showed that amphiphilic peptoids self-assembled into highly uniform nanotubes through a unique “rolling-up and closure of nanosheet” mechanism. By tuning the number of Nbp_m residues and their functionalization, we tuned PNTs wall thickness, diameter and stiffness and showed that these structures can be used for water decontamination. Peptoid platform also enabled us to introduce a wide range of functional groups, such as fluorescent dye and β-cyclodextrin (CD) within PNTs, demonstrating their various applications, such as water decontamination. For example, we appended CD groups to the hydrophilic end (Figure 2e) and co-assembled the peptoids with donor chromophores. We then incubated the resulting peptoid assemblies with acceptor chromophores to enable Förster resonance energy transfer (FRET). This FRET-active system exhibited an energy transfer efficiency in water of as much as 61%, which is a high level of performance when compared to other synthetic aqueous FRET-active systems. Thus, the hierarchical nature of these peptoid assemblies enabled us to mimic natural light harvesting systems.

Molecular simulations of peptoid assembly, membranes, tubes and CNTPs in peptoid membranes. We refined the dihedral parameterization of our earlier all-atom force field based on high level DFT in combination with extensive free-energy sampling with semi-empirical methods. Subsequent simulations of small peptoids reveal nonstandard, random-coil conformations, high degree of flexibility and large loss of entropy near model surfaces. We also used classical MD to study the effect of both ion type and concentration on the oligomerization of NH₂-(Nce-Ncp)₆-H and NH₂-(CH₂)₆-(Nce-Ncp)₆-H peptoids. Simulations show that ions largely affect association of

peptoids through the formation of salt bridges, but a different mechanism mediated by the hydrophobic $\text{NH}_2\text{-(CH}_2\text{)}_6$ tail. Simulations of peptoid membranes with embedded CNTPs show that, in contrast to lipid membranes, CNTPs reside in the membrane in an untilted configuration. Differences in water structure and dynamics above the membrane's hydrophilic and hydrophobic ridges are found.

Developing a fully synthetic membrane system: CNTPs in block-copolymer bilayers.

As an intermediate step towards a fully tunable synthetic membrane system we demonstrated insertion of CNTPs into block co-polymer PB-PEO bilayer membrane. CNTPs maintained their highly efficient permeability characteristics in polymersome membranes. We showed that wCNTP channels can be used to deliver small molecules to the interior of polymersomes (Figure 3a). CNTPs also acted as versatile membrane connectors for different vesicles to enable efficient communication between vesicular compartments (Figure 3b).

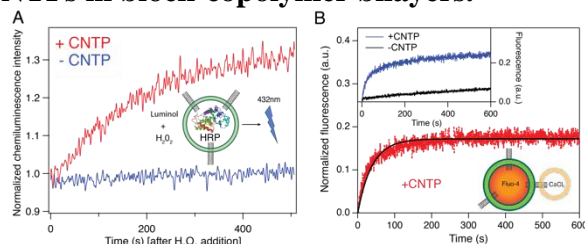


Figure 3. Molecular transport in CNTP/block-copolymer membranes. (A) Chemiluminescence time traces obtained for CNTP/polymersomes sequestering HRP enzyme after addition of luminol and H_2O_2 to the solution. (B) Ca^{2+} transport between CNTP-docked vesicles.

Probing atomic layer structure of CNTPs in block copolymer layers. In-situ SAXS/WAXS and molecular dynamics simulations indicated that CNTP presence has an effect on block copolymer-lipid mixed vesicles morphology. The in-situ SAXS/WAXS experiments suggest that the CNTs enhance the hydrophobic density by enhancing the liquid crystalline interactions of the polybutadiene and dioleoyl groups. Time resolved SAXS experiments indicated that the peptoid molecules first assemble into an amorphous structure prior to crystallization, with the first observable peaks being associated with the aromatic interactions. Indeed, crystallization kinetics increase dramatically with the halide that is functionalized on the aromatic group in the peptoid in the order $\text{I} > \text{Br} \geq \text{Cl}$. Analysis of data from co-crystallized CNTP-peptoid experiments is ongoing.

Future Plans

Our future plans center on continuing to characterize assembly process, atomic level structure, and transport properties of CNTP/peptoid membranes and using these systems to understand and manipulate the interfacial water structure and mechanisms for highly-efficient transport and molecular selectivity.

Publications

R.H. Tunuguntla, R.Y. Henley, Y.-C. Yao, T.A. Pham, Wanunu M., A. Noy (2017) *Enhanced water permeability and tunable ion selectivity in subnanometer carbon nanotube porins*. **Science** 357, (6353) 792-796 (2017).

- R.H. Tunuguntla, A.Y. Hu, Y. Zhang, A. Noy *Impact of PEG additives and pore rim functionalization on water transport through sub-1-nm carbon nanotube porins*, **Faraday Disc.**, v. 209, 359 – 369 (2018).
- J.R. Sanborn, X. Chen, Y.-C. Yao, J. A. Hammons, R.H. Tunuguntla, Y. Zhang, C. Newcomb, J. Soltis, J.J. De Yoreo, A. Van Buuren, A.N. Parikh, A. Noy *Carbon Nanotube Porins in Amphiphilic Block-Copolymers as Fully-Synthetic Mimics of Biological Membranes* **Adv. Mater.**, v.30(51) p.1803355 (2018) Frontispiece Cover.
- Jiao, F.; Wu, X.; Jian, T.; Zhang, S.; Jin, H.; He, P.; Chen, C.-L.; DeYoreo, J. J. Hierarchical Assembly of Peptoid-Based Cylindrical Micelles Exhibiting Efficient Resonance Energy Transfer in Aqueous Solution. **Angew. Chem., Int. Ed.**, <https://doi.org/10.1002/anie.201904598> (2019).
- Jin, H.; Jian, T.; Ding, Y.-H.; Chen, Y.; Mu, P.; Wang, L.; Chen, C. L. Solid-phase synthesis of three-armed star-shaped peptoids and their hierarchical self-assembly. **Biopolymer**, 110, e23258, (2019).
- B. Stel, I. Gunkel, X. Gu, B. Rad, T. P. Russell, J.J. De Yoreo, M. Lingenfelder, “Contrasting chemistry of block copolymer films control the dynamics of protein self-assembly at the nanoscale” **ACS Nano**, 13, 4018-4027 (2019).
- Yan F., Liu L., Walsh T. R., Gong Y., El-Khoury P. Z., Zhang Y., Zhu Z., De Yoreo J. J., Engelhard M. H., Zhang X., and Chen C. L. (2018) Controlled synthesis of highly-branched plasmonic gold nanoparticles through peptoid engineering. **Nature Comm.** 9, (1) Article ID# 2327 (2018).
- O’Callahan, B. T.; Crampton, K. T.; Novikova, I. V.; Jian, T.; Chen, C. L.; Evans, J. E.; Baschke, M. B.; El-Khoury, P. Z.; Lea, A. S. Imaging nanoscale heterogeneity in ultrathin biomimetic and biological crystals. **J. Phys. Chem. C**, 122, 24891-24895, (2018).
- Merrill N. A., Yan F., Jin H., Mu P., Chen C. L., Knecht M. R. Tunable assembly of biomimetic peptoids as templates to control nanostructure catalytic activity. **Nanoscale** 10, (26) 12445-12452, (2018).
- Jin H., Ding Y. H., Wang M., Song Y., Liao Z., Newcomb C. J., Wu X., Tang X. Q., Li Z., Lin Y., Yan F., Jian T., Mu P., and Chen C. L. Designable and dynamic single-walled stiff nanotubes assembled from sequence-defined peptoids. **Nature Comm.** 9, (1) 270, (2018).
- Chen, C. L., Peptoid-based membrane-mimetic two dimensional nanomaterials. Proc. **SPIE** 10639, Micro- and Nanotechnology Sensors, Systems, and Applications X, 106390X, 1 – 10.
- Song, Y.; Wang, M.; Li, S.; Jin, H.; Cai, X.; Du, D.; Li, H.; Chen, C. L.; Lin, Y. Efficient cytosolic delivery using crystalline nanoparticles assembled from fluorinated peptoids. **Small**, 14, 1803544, (2018).
- B. Stel, F. Cometto, B. Rad, **J. J. De Yoreo** and M. Lingenfelder, “Dynamically resolved self-assembly of S-layer proteins on solid surfaces” **Chem. Comm.**, 54, 10264-10267,(2018).
- A. Prakash, M.D. Baer, C.J. Mundy, J. Pfaendtner Peptoid Backbone *Flexibility Dictates Its Interaction with Water and Surfaces: A Molecular Dynamics Investigation* **Biomacromolecules**, 193, 1006-1015 (2018).
- J.K. Denton, P.J. Kelleher, M.A. Johnson, M.D. Baer, S.M. Kathmann, C.J. Mundy, B.A. Wellen Rudd, H.C. Allen, T. H. Choi, K.D. Jordan *Molecular-level origin of the carboxylate head group response to divalent metal ion complexation at the air–water interface* **Proc. Natl. Acad. Sci. USA**, doi.org/10.1073/pnas.1818600116 (2019).

Adaptive Interfacial Assemblies Towards Structuring Liquids

Thomas P. Russell, Materials Sciences Division, Lawrence Berkeley National Laboratory

Paul D. Ashby, Molecular foundry, Lawrence Berkeley National Laboratory

Phillip Geissler, Chemistry Department, University of California Berkeley

Brett A. Helms, Molecular foundry, Lawrence Berkeley National Laboratory

Alex Zettl, Physics Department, University of California Berkeley

Program Scope

Materials are usually codified as solids or liquids based on their structural stability, dynamic response and rheological properties. Producing materials that spans from the liquid to solid state with dynamic responsiveness and that address many challenges posed to next-generation energy technologies, ranging from batteries to thermoelectrics, to storage and separations media, have been elusive. In this field work proposal (FWP) –*Adaptive Interfacial Assemblies Towards Structuring Liquids*– we advance a new concept in materials to meet these challenges based on the interfacial formation, assembly and jamming of nanoparticle surfactants (NPSs) to shape liquids (1). We hypothesize that if we learn to manipulate the interfacial packing of the NPSs using external triggers, a new class of materials will emerge that combines the desirable characteristics of fluids—rapid transport of energy carriers (e.g. electrons or protons), conformability to arbitrary shapes, and controlled dissipation of mechanical energy—with the structural stability of a solid. This new class of material has the hierarchical characteristics of a structured solid that span from the nanoscopic to macroscopic and the dynamic characteristics of liquids with dynamics over a broad range of time scales, making them mesoscale (2) in both space and time. Revolutionary design strategies will emerge to direct mechanical, electrical or optical energy flow and energy conversion, for example chemical to mechanical. To realize the potential of these adaptive structured liquids, fundamental challenges in NPS chemistries, their assemblies and dynamics must be met to structure liquids and affect controlled changes in the assemblies, both locally and globally.

Three objectives of this FWP are:

- **Understanding the Basic Principles of Structuring of Liquids:** We hypothesize that if we can experimentally characterize and theoretically understand the static structure and dynamics of NPS assemblies, we will be able to tailor the spatial distribution and response of two immiscible liquids, enabling the design of reconfigurable, energy relevant systems.
- **Structured Liquids That Adapt and Respond:** If we can tailor the functionality of NPSs, we will be able to design responsiveness into the mesoscale structuring of the liquids by controlling the binding strength of the NPSs to the interface and their interactions within the plane of the interface.
- **Mesoscale Assemblies: Fundamentals and Function:** If we can tailor the interfacial assembly of NPSs, we will be able to translate response on the nanoscopic level to the macroscopic level, producing hierarchical assemblies where function can be achieved across multiple length scales.

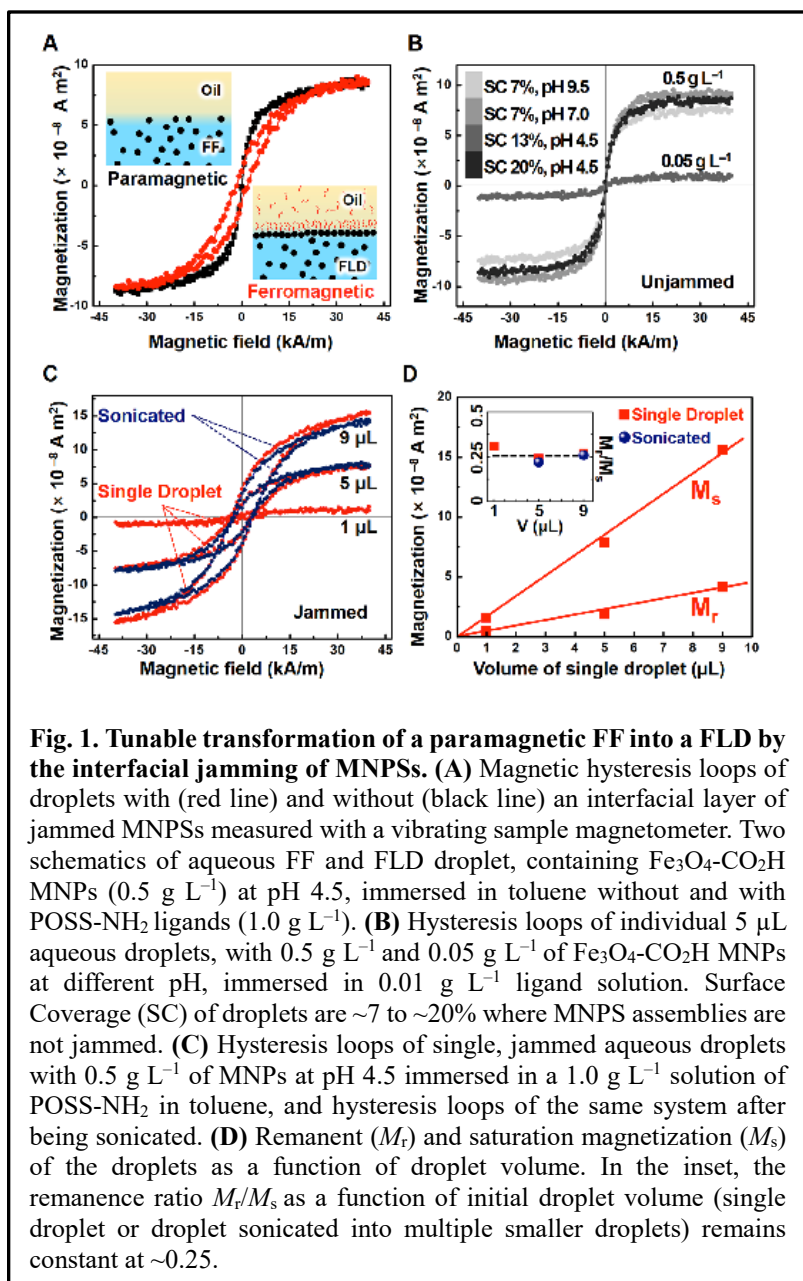
The challenges in understanding the non-equilibrium structure of materials, in designing chemistries to evoke specific responses, and in developing experimental tools to characterize disordered assemblies over multiple length scales are many and complex. This FWP integrates expertise in **synthesis, theory, characterization** with continuous feedback loop between the investigators to meet this challenge.

Recent Progress

Ferromagnetic Liquids

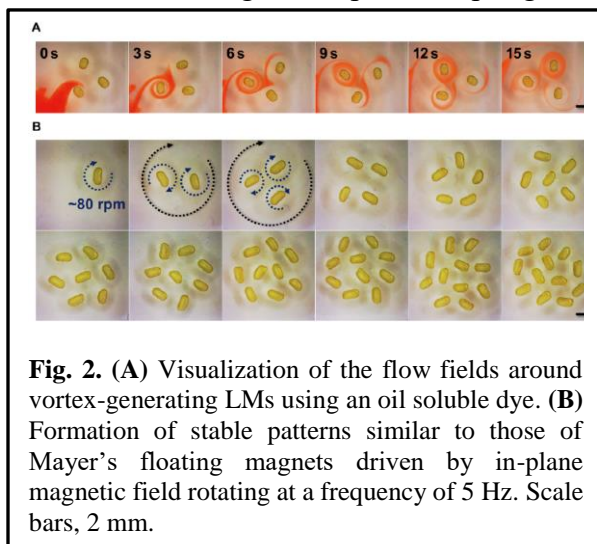
Magnetic materials are primarily thought to be condensed matter, i.e. solids, susceptible to external stimuli, such as magnetic field or geometrical constraints, and widely used in our daily life. Ferrofluids (FFs), dispersions of magnetic nanoparticles in carrier fluids, are paramagnetic liquids that only magnetize in the presence of an external magnetic field. FFs rapidly lose magnetization when the field is removed. While FFs exhibit interesting liquid and magnetic properties, and the loss of magnetization has limited their applications. We show a route to reversibly transform FFs into ferromagnets by the formation, assembly, and jamming of a monolayer of magnetic nanoparticle-surfactants (MNPSs) at a liquid-liquid interface. This new type of magnetic ferromagnetic liquid droplets, exhibits a finite coercivity and remanent magnetization at room temperature, yet, retains characteristics of liquids.

Magnetic hysteresis loops of $\text{Fe}_3\text{O}_4\text{-CO}_2\text{H}$ ferrofluid droplets (Figure 1A), measured by a vibrating sample magnetometer, show a saturation magnetization (M_s) that depends on the total number of MNPs in the droplets, as well as a vanishing coercive field (H_c) and remanent magnetization (M_r). By adding POSS-NH₂ ligands to the toluene, MNP-surfactants form at the interface. Increasing



the concentration of the MNPs in the droplet or decreasing pH, increases the coverage of the interface by MNP-surfactants, reducing the interfacial tension. With sufficiently surface coverage, the MNP-surfactants jam and the ferrofluid droplet transforms into a ferromagnetic liquid droplet. The magnetic hysteresis loops of identical ferrofluid droplets with and without the jammed interfacial assemblies of MNP-surfactants are shown in Figure 1A. For both, M_s is the same, since the total number of MNPs is identical, but $M_r \sim 1.89 \times 10^{-8} \text{ A m}^2$ and $H_c \sim 7.2 \text{ kA m}^{-1}$ for the ferromagnetic liquid droplet, demonstrating their ferromagnetic character. The jammed, interfacial assemblies of the MNP-surfactants are disordered and have a mechanical rigidity that suppresses thermal fluctuations characteristic of isolated MNPs. The jammed MNPs no longer freely rotate. The spatial separation between adjacent MNP-surfactants is $< 5 \text{ nm}$ which, combined with the orientation of the dipole magnetization within the MNPs, enhances the thermal stability of the magnetization and transforms the droplet surface into a ferromagnetic layer, similar to a fixed assembly of MNPs (3, 4). When the field is removed, the moment of the ferromagnetic liquid droplet remains until the droplet is exposed to a field exceeding the switching field, whereupon the MNP-surfactant assembly unjams (M_r and H_c vanish), allowing the liquid to be reshaped and re-magnetized. Reshaping the droplet by other external fields or reducing the binding energy of the MNP-surfactants will also unjam the MNP-surfactants, providing further routes to control the magnetization. This ability to manipulate the magnetization further distinguishes ferromagnetic liquid droplets from ferrofluids and common ferromagnetic materials.

If the MNP-surfactant assembly is not jammed, no hysteresis is observed (Figure 1B). In Figure 1B variations in M_s arise from differences in the total number of MNPs in each droplet. With full MNP-surfactant coverage, e.g. single droplets of $[\text{Fe}_3\text{O}_4\text{-CO}_2\text{H MNPs}] = 0.5 \text{ g L}^{-1}$ at pH 4.5 in toluene containing $[\text{POSS-NH}_2] = 1.0 \text{ g L}^{-1}$, the interfacial assembly jams and a typical ferromagnetic hysteresis loop is seen (Figure 1C). Hysteresis loops were measured for single droplets with different volumes, and the same droplets sonicated into numerous smaller droplets. This preserves the total volume (summed over all droplets) of the MNP dispersions, but increases the surface-to-volume ratio (S/V) by two orders of magnitude M_s and M_r scale linearly with the total volume (total number of MNPs), while H_c remains constant (Figure 1C). Quite surprisingly, for a given total volume, M_r is independent of S/V with largely varying droplet sizes. The mean separation distance between the dispersed MNPs is $\sim 350 \text{ nm}$, too large for dipolar coupling. For comparison, 100-nm diameter, 10-nm thick nanodiscs with much larger saturation magnetizations are completely uncorrelated when the separation distance is $> 60 \text{ nm}$ (5). The MNPs dispersed in the droplet freely diffuse, yet a strong coupling and correlation of the dispersed MNPs to those jammed at the interface is evident, and the liquid droplets behave like solid magnets. Furthermore, the ratio of M_r/M_s for the ferromagnetic liquid droplets is 0.25, independent of droplet volume, which is the same as that for frozen ferrofluids at 4.5 K and fixed assemblies of Fe_3O_4 MNPs (6-8). Consequently, ferromagnetic liquid droplets have a similar energy barrier to overcome during magnetization reversal as their



frozen/solid counterparts. Therefore, ferromagnetic liquid droplets have the magnetic properties of a solid.

Once magnetized, the ultra-soft liquid magnet retains a finite permanent magnetic dipole, enabling the non-contact manipulation, include translational and processional motions, by external fields. Cylindrical ferromagnetic liquid droplets, buoyant in the surrounding liquid, respond to a rotating permanent magnet, by rotating at an increasing angular velocity that asymptotes to a size-dependent maximum velocity (Figure 2). Magnetized ferromagnetic liquid droplets can be separated out in both static and rotating magnetic fields. Assemblies of multiple ferromagnetic liquid droplets form switchable, dynamic self-organized patterns, similar to those of Mayer's floating magnets. The ability to shape and manipulate ferromagnetic liquid droplets opens possibilities for magnetically-actuated liquid sensors, all-liquid magnetic data storage and magnetically-driven 3D-printed robotic systems.

Future Plans

In joint publications we have documented progress in realizing our goals, yet, fundamental questions remain on NPS assemblies, their dynamics and responsiveness. We will develop dynamic covalent bonding chemistries, experimentally and theoretically characterize the kinetics and dynamics of NPS formation assembly and response, demonstrate transport of energy carriers, introduce active materials to generate systems with directed evolutionary structural changes, and delve deeper into the recently discovered, remarkable changes in the magnetic characteristics of the assemblies due to jamming. We will capitalize on recent developments in optical, electron microscopic and x-ray imaging to gain unprecedented insight into jamming and vitrification, and long-standing challenge in materials science.

Our plans are to build on the original objectives of the Program:

1. **Understanding the Basic Principles of Structuring of Liquids:** We hypothesize that if we can experimentally characterize and theoretically understand the static structure and dynamics of NPS assemblies, we will be able to tailor the spatial distribution and response of two immiscible liquids, enabling the design of reconfigurable, energy relevant systems.
2. **Structured Liquids That Adapt and Respond:** If we can tailor the functionality of NPSs, we will be able to design responsiveness into the mesoscale structuring of the liquids by controlling the binding strength of the NPSs to the interface and their interactions within the plane of the interface.
3. **Mesoscale Assemblies: Fundamentals and Function:** If we can tailor the interfacial assembly of NPSs, we will be able to translate response on the nanoscopic level to the macroscopic level, producing hierarchical assemblies where function can be achieved across multiple length scales.

The challenges in understanding the non-equilibrium structure of materials, in designing chemistries to evoke specific responses, and in developing experimental tools to characterize disordered assemblies over multiple length scales are many and complex.

References

1. M. Cui, T. Emrick and T.P. Russell, Stabilizing Liquid Drops in Nonequilibrium Shapes by the Interfacial Jamming of Nanoparticles, *Science* 342, no. 6157 (2013): 460–463. doi:10.1126/science.1242852
2. J. Hemminger, J., G. Crabtree. J. Sarrao, From Quanta to the Continuum: Opportunities for Mesoscale Science (2012):
3. A. H. Lu, E. L. Salabas, F. Schuth, Magnetic nanoparticles: synthesis, protection, functionalization, and application. *Angew. Chem.* **46**, 1222-1244 (2007).
4. J. J. Benkoski *et al.*, Field induced formation of mesoscopic polymer chains from functional ferromagnetic colloids. *J. Am. Chem. Soc.* **129**, 6291-6297 (2007)
5. R. Streubel, N. Kent, S. Dhuey, A. Scholl, S. Kevan, P. Fischer, Spatial and temporal correlations of XY macro spins. *Nano. Lett.* **18**, 7428-7434 (2018).
6. E. C. Stoner, E. P. Wohlfarth, A mechanism of magnetic hysteresis in heterogeneous alloys. *Philos. Trans. Roy. Soc. London. Ser A, Math. Phys. Sci.* **240**, 599-642 (1948).
7. W. Luo, S. R. Nagel, T. F. Rosenbaum, R. E. Rosensweig, Dipole interactions with random anisotropy in a frozen ferrofluid. *Phys. Rev. Lett.* **67**, 2721-2724 (1991).
8. G. F. Goya, T. S. Berquó, F. C. Fonseca, M. P. Morales, Static and dynamic magnetic properties of spherical magnetite nanoparticles. *J. Appl. Phys.* **94**, 3520-3528 (2003).

Publications

1. C. Huang, J. Forth, W. Wang, K. Hong, G.S. Smith, B. A. Helms, and T. P. Russell, “Bicontinuous structured liquids with sub-micrometre domains using nanoparticle surfactants”, *Nature Nanotechnology* (2017) DOI:10.1038/nnano.2017.182
2. J. Forth, X. Liu, J. Hasnain, A. Toor, K. Miszta, S. Shi, P. L. Geissler, T., Emrick, B. A. Helms, T. P. Russell, “Reconfigurable Printed Liquids”, *Adv. Mater.* 2018, 30, 1707603. DOI: 10.1002/adma.201707603
3. C. Huang, Y. Chai, Y. Jiang, J. Forth, P. D. Ashby, M. M. L. Arras, K. Hong, G. S. Smith, P. Yin, T. P. Russell, “The Interfacial Assembly of Polyoxometalate Nanoparticle Surfactants”, *Nano Lett.* 2018, 18, 2525-2529. DOI: 10.1021/acs.nanolett.8b00208
4. A. Toor, S. Lamb, B. Helms, T. P. Russell, “Reconfigurable Microfluidic Droplets Stabilized by Nanoparticle Surfactants”, *ACS Nano* 2018, 12, 2365-2372. DOI: 10.1021/acsnano.7b07635
5. Z. Zhang, Y. Jiang, C. Huang, Y. Chai, E. Goldfine, F. Liu, W. Feng, J. Forth, T. E. Williams, P. D. Ashby, T. P. Russell and B. A. Helms, “Guiding kinetic trajectories between jammed and unjammed states in 2D colloidal nanocrystal-polymer assemblies with zwitterionic ligands”, *Sci. Adv.* 2018, 4 : eaap8045 DOI: 10.1126/sciadv.aap8045
6. M. Cui, C. Miesch, I. Kosif, H. Nie, P. Kim, H. Kim, T. Emrick, T. P. Russell, “Transition in Dynamics as Nanoparticles Jam at the Liquid/Liquid Interface”, *Nano Lett.* 2017, 17, 6855-6862. DOI: 10.1021/acs.nanolett.7b03159
7. S. Shi, T. P. Russell, “Nanoparticle Assembly at Liquid–Liquid Interfaces: From the Nanoscale to Mesoscale”, *Adv. Mater.* 2018 1800714 DOI: 10.1002/adma.201800714
8. S. Shi, X. Liu, Y. Li, X. Wu, D. Wang, J. Forth, T. P. Russell, “Liquid Letters”, *Adv. Mater.* 2018, 30, 1705800 DOI: 10.1002/adma.201705800

9. R. Li, Y. Chai, Y. Jiang, P. D. Ashby, A. Toor, T. P. Russell, “Carboxylated Fullerene at the Oil/Water Interface”, *ACS Appl. Mater. Interfaces* 2017, 9, 34389–34395 DOI: 10.1021/acsami.7b07154
10. Y. Li, X. Liu, Z. Zhang, S. Zhao, G. Tian, J. Zheng, D. Wang, S. Shi, T. P. Russell, “Adaptive Structured Pickering Emulsions and Porous Materials Based on Cellulose Nanocrystal Surfactants”, *Angew. Chem. Int. Ed.* 2018, 57, 13560–13564. DOI: 10.1002/ange.201808888
11. W. Feng, Y. Chai, J. Forth, P.D. Ashby, T.P.Russell, B.A. Helms, “Harnessing Liquid-in-Liquid Printing and Micropatterned Substrates to Fabricate 3-Dimensional All-Liquid Fluidic Devices”, *Nat. Comm.*, 2019, 10, 1095. DOI:10.1038/s41467-019-09042-y
12. J. Forth, P. Y. Kim, G. Xie, X. Liu, B. A. Helms, T. P. Russell, “Building Reconfigurable Devices Using Complex Liquid–Fluid Interfaces”, *Adv. Mater.* 2019, 1806370. DOI: 10.1002/adma.201806370

Dynamics of Active Self-Assembled Materials

PI: Alexey Snezhko, Co-Investigators: Andrey Sokolov, Andreas Glatz

**Materials Science Division, Argonne National Laboratory, 9700 South Cass Avenue,
Argonne, IL 60439**

Program Scope

Self-assembly, a natural tendency of simple building blocks to organize into complex architectures, is a unique opportunity for materials science. The in-depth understanding of self-assembly paves the way for the design of tailored smart materials for emerging energy technologies, such as materials that can self-heal, regulate porosity, strength, water or air resistance, viscosity, or conductivity. Developing understanding and control of self-assembled out of equilibrium materials pose a significant challenge since they are intrinsically complex, with often-hierarchical organization occurring on many nested length and time scales.

The program is focused on the fundamental aspects of out-of-equilibrium dynamics and self-assembly of bio-inspired materials. The main research direction focuses on the design of novel active materials that can arise from a fundamental understanding of dynamic self-assembly and organization in colloids far from equilibrium. We explore two highly complementary systems: driven colloids energized by external fields, and suspensions of active swimmers. The main difference between these systems is the way energy is injected: driven colloids are externally energized whereas microscopic swimmers are self-propelled. The major challenges are: understanding fundamental mechanisms that lead to collective behavior from the interactions between unitary building blocks and designing new active self-assembled materials with tunable structural and transport properties.

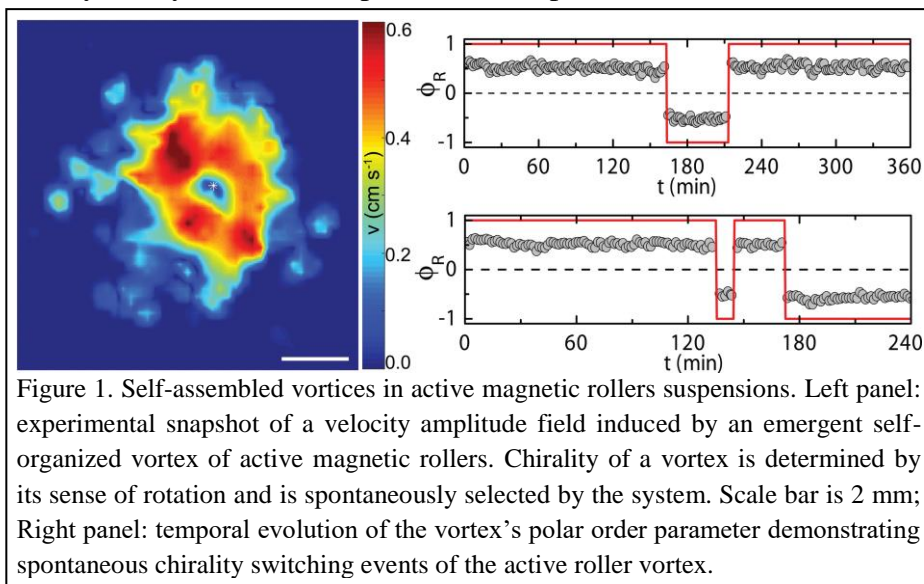
In the past two years our program yielded discoveries of active turbulent states in ensembles of spinners emerging as a result of spontaneous symmetry breaking of clock/counterclockwise rotations of self-assembled particle chains, new unconfined vortex states with spontaneously changing chiralities in systems of active ferromagnetic rollers, novel methods of manipulation and control of transport and self-organization in active suspensions of swimmers by a surface patterning. All of these structures and phenomena are generally not available through thermodynamics and accessible only out of equilibrium. For all these systems we have developed theoretical understanding leading to a better control of the emergent self-assembled structures and dynamics. In the next three years we will explore new approaches to synthesis and discovery of novel self-assembled active materials stemming from recent advances of our program: functional tunable colloidal structures and transport based on actively spinning units (Quincke and magnetic rollers), dynamic patterns in active nematic materials realized by suspensions of active swimmers in liquid crystals.

The program synergistically integrates experiment and simulations, and focuses on the fundamental issues at the forefront of contemporary materials science.

Recent Progress

Manipulation of emergent vortices in swarms of magnetic rollers. Microscopic particles energized by an external energy injection exhibit a plethora of fascinating collective phenomena, yet mechanisms of control and manipulation of active phases often remain lacking. We discovered the emergence of unconfined macroscopic vortices in a system of ferromagnetic rollers energized by a vertical alternating magnetic field and elucidated the complex nature of magnetic roller-vortex interactions with inert scatterers. The magnetic rollers and subsequent self-assembled vortices emerge as a result of a spontaneous symmetry breaking of the rotational chiral symmetry (clockwise or counter-clockwise) experienced by a magnetic particle in a uniaxial alternating magnetic field and phase synchronization between rollers in a certain range of the magnetic field parameters. The results demonstrate that active vortex patterns do not always require geometrical confinement for their observation and stem from the interplay between self-propulsion and particle alignment interactions. While the direction of the vortex rotation is randomly selected by the system from experiment to experiment, we discovered that

the roller vortex can spontaneously change its chirality state, see Figure 1. Our work also demonstrates that active self-organized vortices have an ability to move across the surface. We reveal the capability of certain non-active particles to efficiently pin an active roller vortex and manipulate its



dynamics. Building on our findings, we demonstrated the potential of magnetic active roller vortices to successfully cage and transport inert particles at the microscale. The ability to manipulate active colloidal structures is crucial for the development of directed transport at the micro-scale and progress of self-assembled micro-robotics. The work provides new insight into fundamental aspects of collective dynamics in active roller materials and yields new tools for particle manipulation at the microscale.

Self-organized active vortex lattices by design. A suspension of micro-swimmers is possibly the simplest realization of active matter, i.e. a class of systems transducing stored energy into mechanical motion. Collective swimming of hydrodynamically interacting bacteria resembles turbulent flow. We revealed that this seemingly chaotic motion could be efficiently rectified by a geometrical confinement. We demonstrated a successful self-organization of a concentrated suspension of motile bacteria *Bacillus subtilis* constrained by two-dimensional periodic arrays of

microscopic vertical pillars (see Figure 2). We discovered that bacteria self-organized into a lattice of hydrodynamically bound vortices with a long-range anti-ferromagnetic order controlled by the pillars' spacing. The patterns attain their highest stability and nearly perfect order for the pillar spacing comparable with an intrinsic vortex size of an unconstrained bacterial turbulence. We demonstrated that the emergent antiferromagnetic order could be further manipulated and turned into a ferromagnetic state by introducing chiral pillars. Our study provides an insight into self-organization of concentrated bacterial suspension under seemingly insignificant geometrical constraints: a periodic array

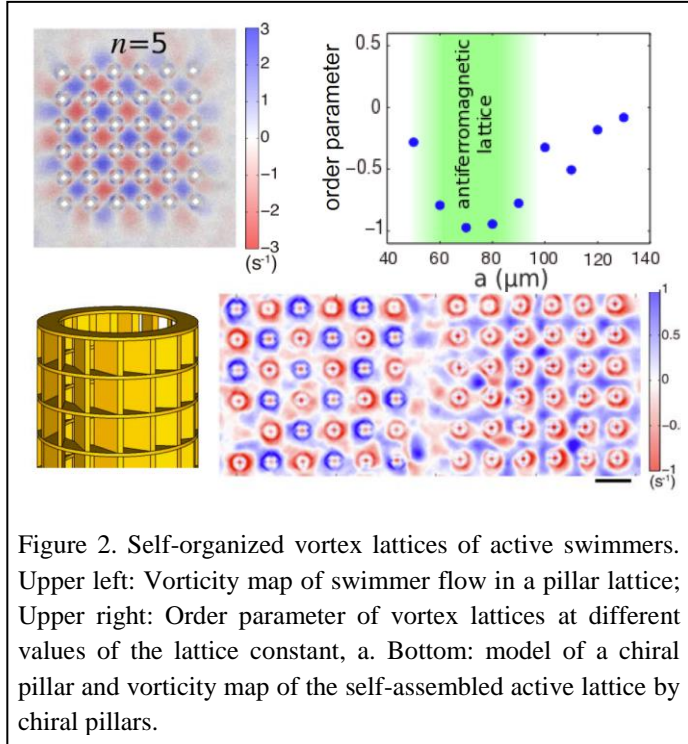


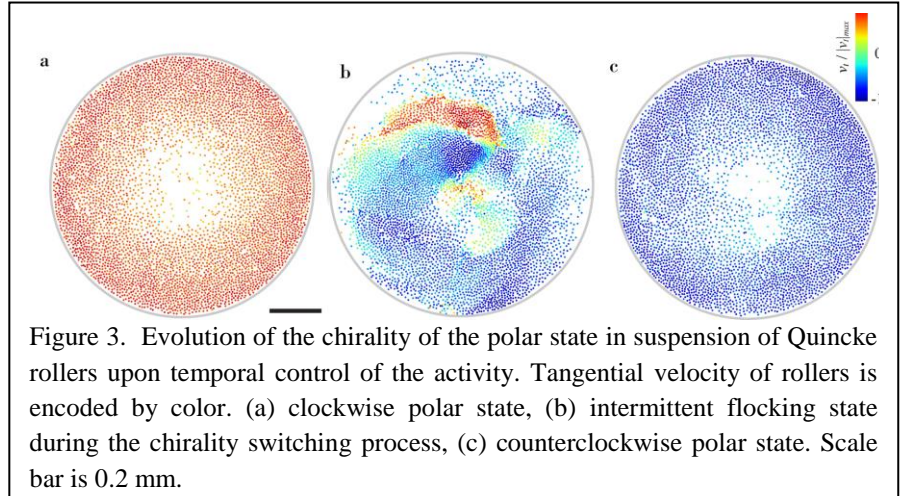
Figure 2. Self-organized vortex lattices of active swimmers. Upper left: Vorticity map of swimmer flow in a pillar lattice; Upper right: Order parameter of vortex lattices at different values of the lattice constant, a . Bottom: model of a chiral pillar and vorticity map of the self-assembled active lattice by chiral pillars.

of tiny pillars, taking only 3–5% of total suspension volume, drastically alters chaotic bacterial swimming pattern and turns it into a periodic vortex array. Our work provides novel strategies for minimally invasive control of active matter that may be applicable to other experimental systems exhibiting vortex formation under geometrical confinement. Self-organization of bacteria in nearly perfect vortex lattices can be also used as a tool for more efficient energy extraction by an array of gears driven by swimmers.

Future Plans

Control of chiral states and memory effects in populations of active colloidal rollers. This research direction is stemming from our successful study of dynamic self-assembly of magnetic colloidal rollers. Chiral active liquids composed of spinning individual units represent a new class of active materials where both energy and angular momentum is injected at the microscopic level. Spontaneous emergence of particle flocks and global polar states are prime examples of remarkable collective dynamics and self-organization recently observed in active chiral liquids. Formation of globally correlated polar states in such systems proceeds through an emergence of a macroscopic steadily rotating vortex that spontaneously selects a clockwise or counterclockwise global chiral state. Our preliminary studies in a system of electric field driven Quincke rollers reveal that active chiral liquids in a collective vortex state exhibit memory and the subsequent formation of the polar states with certain chirality could be manipulated by means of temporal control of the activity. We demonstrated recently in experiments a controlled sequence of the emergent chirality states in an ensemble of active rollers. We envision comprehensive studies, both experimental and computational, of complex dynamics of chiral

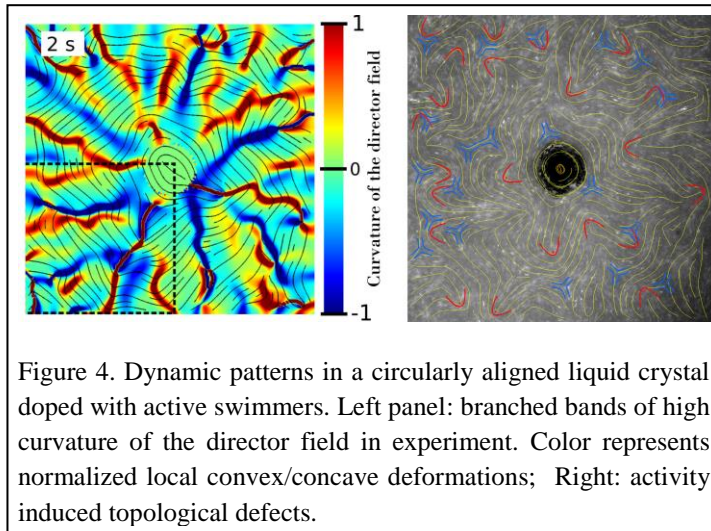
states in a system of Quincke and magnetic rollers. The primary goals of the research are: (i) understanding how the information about the chiral state of the colloidal ensemble is encoded in the active system; (ii) exploration of design concepts of various active tunable chiral phases for



use in directed transport at the microscale. This research will provide new fundamental insights into mechanisms of the spontaneous formation of the collective polar states in active roller materials and provide means of control of the corresponding chiral states. We expect that with chirality of the emergent collective states controlled on demand, active chiral liquids will offer new possibilities for flow manipulation, transport and mixing at the microscale.

Emergent dynamic patterns in active liquid crystals.

Active nematic matter is a new class of non-equilibrium systems that combine mechanical properties of liquid crystals with motility introduced on a microscopic level. To develop efficient control over active nematic materials the intricate interplay between activity and liquid crystallinity has to be tackled. We plan to explore in detail onset of dynamic patterns and flows in active liquid crystalline materials governed by



the interplay of activity, elasticity and geometry. We envision that these materials will have unique mechanical and transport properties. Our preliminary findings obtained in circularly aligned liquid crystal doped with micro-swimmers revealed novel dynamic patterns comprised of branched bend stripes of high curvature of the liquid crystal's director field (Fig. 4) and accompanied by self-induced hydrodynamic flows that can be potentially manipulated by

the design of the material. Dynamic patterns go together with activity induced topological defects. We plan to investigate the role of the defects and induced hydrodynamic flows on the transport properties of active nematics. We anticipate that these reconfigurable active composite materials will provide us with new tools for control and manipulation of microscopic transport and liquid crystallinity.

Publications

1. G. Kokot, A. Vilfan, A. Glatz, A. Snezhko, “Diffusive ferromagnetic roller gas”, *Soft Matter* **15**, 3612 (2019)
2. Y. Wang, S. Canic, G. Kokot, A. Snezhko, I. Aranson, “Quantifying hydrodynamic collective states of magnetic colloidal spinners and rollers”, *Physical Review Fluids* **4**, 013701 (2019)
3. G. Kokot, A. Snezhko, “Manipulation of emergent vortices in swarms of magnetic rollers”, *Nature Communications* **9**, 2344 (2018)
4. D. Nishiguchi, I. Aranson, A. Snezhko, A. Sokolov, “Engineering bacterial vortex lattice via direct laser lithography”, *Nature Communications* **9**, 4486 (2018)
5. M. Genkin, A. Sokolov, I. Aranson, “Spontaneous topological charging of tactoids in a living nematic”, *New Journal of Physics* **20**, 043027 (2018)
6. G. Kokot, S. Das, R. G. Winkler, G. Gompper, I. Aranson, and A. Snezhko, “Active turbulence in a gas of self-assembled spinners”, *Proceedings of the National Academy of Sciences* **114**, 12870 (2017)
7. Y-L Wang, X. Ma, J. Xu, Zhi-Li Xiao, A. Snezhko, R. Divan, L. Ocola, J. Pearson, B. Janko, W. Kwok, “Switchable geometric frustration in an artificial-spin-ice/superconductor hetero-system”, *Nature Nanotechnology* **13**, 560 (2018)
8. F. Peruani, I. Aranson, “Cold Active Motion: How Time-Independent Disorder Affects the Motion of Self-Propelled Agents”, *Physical Review Letters* **120**, 238101 (2018)
9. A. Sokolov, L.D. Rubio, J.F. Brady, I. Aranson, “Instability of expanding bacterial droplets”, *Nature communications* **9**, 1322 (2018)
10. M. Smylie, H. Claus, W.-K. Kwok, E. Loudon, M. Eskildsen, A. Sefat, R. Zhong, J. Schneeloch, G. Gu, E. Bokari, P. Niraula, A. Kayani, C. Dewhurst, A. Snezhko, U. Welp, “Superconductivity, pairing symmetry, and disorder in the doped topological insulator $\text{Sn}_{1-x}\text{Sn}_x\text{Te}$ for $x \geq 0.10$ ”, *Physical Review B* **97**, 024511 (2018)
11. M. Michalska, F. Gambacorta, R. Divan, I. Aranson, A. Sokolov, P. Noirot, P. D. Laible, “Tuning antimicrobial properties of biomimetic nanopatterned surfaces”, *Nanoscale* **10**, 6639 (2018)
12. M. Mizuhara, L. Berlyand, I. Aranson, “Minimal model of directed cell motility on patterned substrates”, *Physical Review E* **96**, 052408 (2017)

13. S. Zhou, O. Tovkach, D. Golovaty, A. Sokolov, I. Aranson, O. D. Lavrentovich. "Dynamic states of swimming bacteria in a nematic liquid crystal cell with homeotropic alignment" , *New Journal of Physics* **19**, 055006 (2017)
14. M. Smylie, K. Willa, H. Claus, A. Snezhko, I. Martin, W.-K. Kwok, Y. Qiu, Y. S. Hor, E. Bokari, P. Niraula, A. Kayani, V. Mishra, and U. Welp, "Robust odd-parity superconductivity in the doped topological insulator $\text{NbxBi}_2\text{Se}_3$ ", *Physical Review B* **96**, 115145 (2017)
15. G. Kokot, G. Kolmakov, I. Aranson, A. Snezhko, "Dynamic self-assembly and self-organized transport of magnetic micro-swimmers", *Scientific Reports (Nature)* **7**, 14726 (2017)

***UNIVERSITY
GRANT
PROJECTS***

Dynamic and Complex Multi-Compartment and Internally Ordered Emulsions

Nicholas L. Abbott, Cornell University (Principal Investigator) and Juan J. de Pablo, University of Chicago (Co-Investigator)

Program Scope

Biological systems rely on a hierarchy of dynamic, complex and reconfigurable compartments to carry out functions essential for life. This hierarchical organization serves as an amplifier that allows highly localized, molecular events to propagate into the mesoscale, and enables functions essential for life, such as energy storage and transduction, to be carried out. Biological systems typically achieve these functions via non-equilibrium processes, with structure and dynamics that arise from dissipative processes involving an interplay of advective and diffusive transport processes. We are pursuing a program of research in which we seek to recreate such principles using *structured oils* – oils that have nematic and smectic organization of the type found in biological membranes – and coexisting aqueous and organic isotropic phases with the goal of achieving functions closer to the sophistication of living systems. We are elucidating new hierarchical design strategies that heavily leverage phase coexistence, interfacial ordering, and interfacial energy gradients to realize equilibrium and non-equilibrium, dynamic mesoscale phenomena using micrometer-sized liquid crystal (LC) droplets containing multiple compartments. Specifically, this project is unmasking how equilibrium and dynamical phenomena emerge from hierarchical organization in asymmetric, reconfigurable, thermotropic LC assemblies. We are advancing new hierarchical designs and dissipative processes in complex soft matter systems reminiscent of a range of phenomena seen in living biological systems

Recent Progress

Our recent progress has focused on elucidation of the structure and properties of multi-compartment LC systems, including droplets formed by coexisting aqueous/fluorocarbon/hydrogenated phases, with particular effort devoted to understanding phase behavior and interfacial ordering. We have also emphasized elucidation of the role that symmetry breaking plays in non-equilibrium states of droplets.

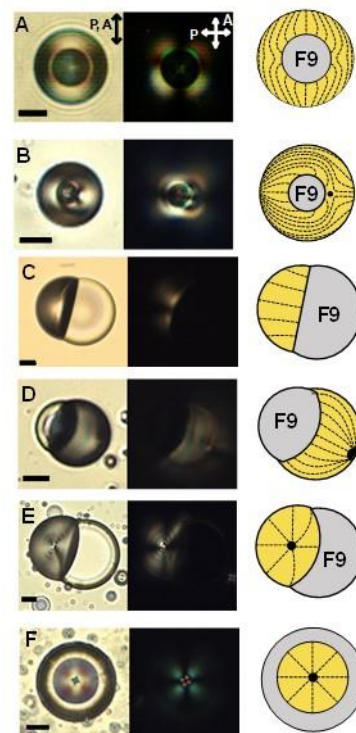


Fig. 1 Micrographs (left: parallel polars; middle: crossed polars) and schematic illustrations (right) show surfactant-dependent morphology of F9-5CB droplet emulsions dispersed in (A,B) glycerol and in the aqueous phases of (C) 2 mM SDS, (D) 1 mM PFOA and (E,F) 2 mM PFOA, respectively. Scale bars, 10 μm .

One of the key challenges that we have addressed is elucidation of the temperature and composition-dependent phase behavior of mixtures of LCs and perfluorocarbon oils, as needed to guide the design of complex multi-compartment emulsions. Two specific experimental systems have been studied as representative platforms. First, we investigated the phase behavior of mixtures of the aromatic fluorocarbon oil perfluorobenzene (FB) and hydrogenated cyanobiphenyl and terphenyl mesogens (E7). We discovered that FB and E7 exhibit coexisting nematic and isotropic phases over a temperature range that is far broader than previously identified for coexisting isotropic-nematic two phase systems. This

discovery has enabled precise and continuous control over the morphologies of complex emulsions, as described below. The underlying role of electrostatic interactions between fluorinated and hydrogenated aromatics in the phase behavior was identified. Second, we examined the phase behavior of perfluorononane (F9) and nematic 4-cyano-4'-pentylbiphenyl (5CB). In contrast to FB, 5CB and other hydrogenated LCs investigated were immiscible with F9 (at all temperatures leading to nematic ordering).

A second set of accomplishments have involved elucidation of the orientational ordering of LCs at aqueous and perfluorocarbon interfaces present in multicompartiment emulsions. We compared experimental observations of the morphology of complex emulsion droplets (Fig. 1) to simulations performed using a Landau-de Gennes (LdG) free energy to identify the interfacial ordering. We found that conical anchoring conditions at aqueous interfaces in these systems led to exotic LC defect structures, including structures called “elastic hexadecapoles” (Fig. 2). When combined, these integrated efforts have defined new and previously unanticipated

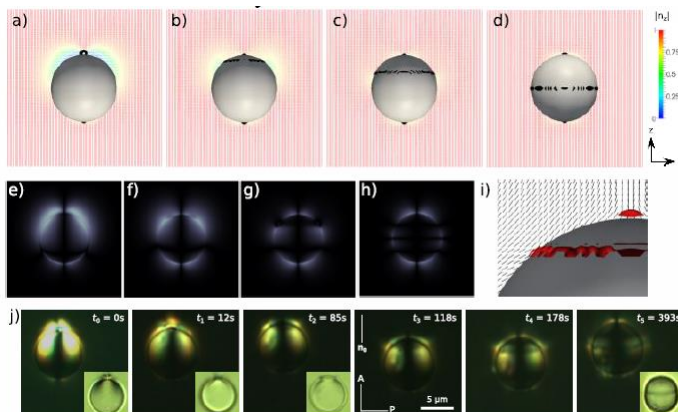


Fig. 2 a-d) A temporal sequence of relaxing configurations (initial condition $\theta_e = 60^\circ$; equilibrium condition $\theta_e = 45^\circ$). The director field is colored by its projection onto the z-axis, and the defects are shown in black (isosurface for $S = 0.6$). e-h) Corresponding simulated polarized light textures. i) Director field near the defect ring in b). The director field is shown in black and the defects are shown in red (isosurface for $S = 0.6$). j) Sequence of experimental images showing the transition from a dipolar to a hexadecapolar structure (crossed polarizers). The first texture is overexposed to enhance the visibility of a boojum defect. Insets show corresponding textures taken between parallel polarizers. The size of the bottom side of the inset image is $9.5 \mu\text{m}$.

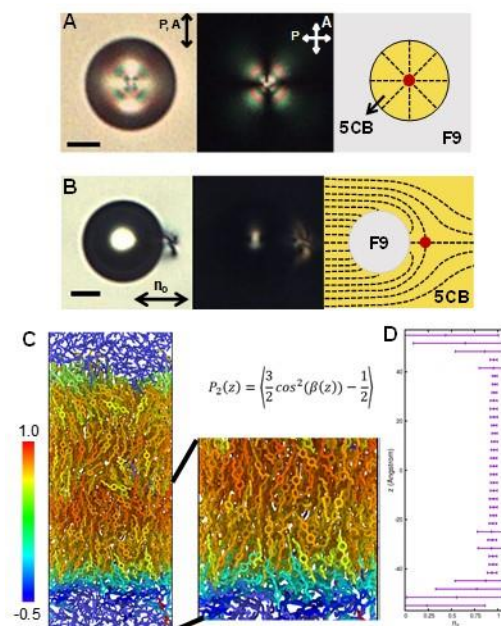


Fig. 3 Micrographs of (A) a 5CB drop in F9, (B) an F9 drop in 5CB. (C) Numerical simulations of molecular orientation and (D) nematic ordering of 5CB molecules at F9 interface. Scale bars, $10 \mu\text{m}$.

approaches for design of complex LC emulsions via control of LC tilt angle. We also made the observation that nematic phases of 5CB assume a perpendicular orientation at interfaces to isotropic F9 phases (Fig. 3). This result contrasts to other nematic interfaces to immiscible isotropic liquids (e.g., water and glycerol), where nematic 5CB orients parallel to the interface. Additional experimentation, including interfacial tension measurements, and atomistic simulations yielded molecular-level insight into the origins of the interfacial ordering, identifying, in particular, the role of F9 in disrupting the antiparallel orientations of 5CB mesogens in the nematic phase near the interface. Overall, these results provide new insights into the molecular-level interfacial organization of LCs that can be exploited for rational design of responsive multi-compartment emulsions at and beyond equilibrium.

We leveraged the above-described understanding of the phase behavior of FB-E7 mixtures and ordering at interfaces to prepare complex emulsions with coexisting nematic and isotropic domains. The partial miscibility of FB and E7 yielded emulsion droplets with nematic and isotropic domain morphologies that changed continuously with increasing temperature (Fig. 4). These observations also yielded the finding that topological defects are absent. We performed additional numerical simulations of the director profiles via the Landau-de Gennes (LdG) continuum model, simulated the corresponding optical micrographs, and then compared the simulated light micrographs to our experimental observations. This comparison identified the nematic-isotropic FB interface to be characterized by very weak surface anchoring energies.

Our observations have demonstrated that use of isotropic perfluorocarbons along with perfluorocarbon and hydrocarbon surfactants enables access to a wide range of emulsion droplet morphologies, including morphologies with nematic shells, nematic cores or Janus-type structures with distinct chemical faces (Fig. 1). These morphologies arise in part because of preferential adsorption of fluorocarbon and

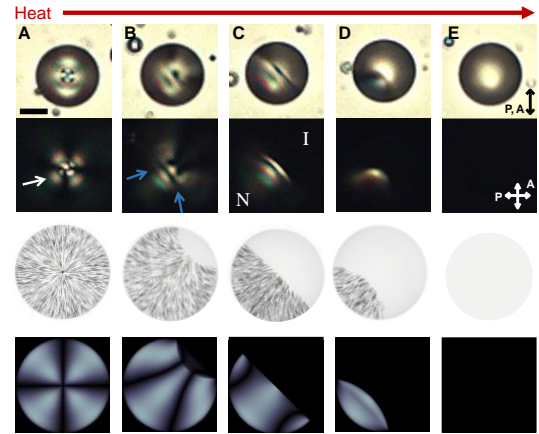


Fig. 4 Thermal reconfiguration of droplet comprised of FB-E7 mixture. Polarized light micrographs (row 1 & 2), simulated director profiles (row 3) and polarized light textures (row 4) of droplets of FB-E7 dispersed in aqueous 1 mM SDS solutions, upon heating across the N-I coexistence region at (A) 35.0 °C, (nematic), (B) 45.0 °C, (C) 46.0 °C, (D) 47.0 °C, and (E) 47.5 °C (isotropic), respectively. Scale bar, 10 μm .

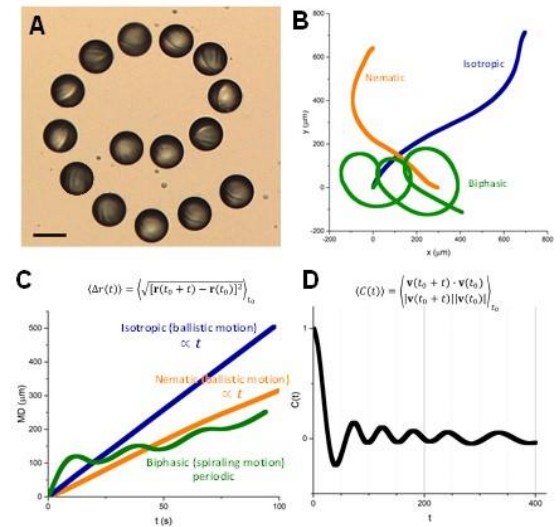


Fig. 5 (A) Time-lapse micrographs of a two-phase (Janus droplet) exhibiting a spiral trajectory. (B) Trajectories of Janus droplets and (C) mean displacement of Janus droplet and single-phase droplets. (D) Auto correlation of velocity of a Janus droplet. Scale bar, 50 μm

hydrocarbon surfactants on the perfluorocarbon and hydrocarbon rich interfaces, respectively, of the emulsion droplets.

Whereas the investigations described above largely address systems at equilibrium (or in metastable states), more recently, we have moved to explore how the broken symmetries of complex multicompartiment LC droplets behave under conditions that lie beyond equilibrium. We have discovered that control of the internal morphology of complex LC emulsion droplets (based on hydrocarbon-perfluorocarbon partial miscibility, as described above) can lead to emergent dynamic organizations of the droplets at much large scales when driven beyond equilibrium. We dispersed FB-E7 droplets into surfactant solutions with concentrations higher than their critical micelle concentration, triggering processes of solubilization, generation of interfacial tension gradients (Marangoni phenomena) and swimming behaviors of the multiphase emulsion droplets. Our experimental observations revealed that biphasic droplets comprised of an isotropic and nematic compartment exhibited a range of unusual dynamical behaviors, including a “spiraling” behavior. Under the same conditions, single-phase nematic or isotropic droplets showed ballistic motion (Fig. 5). We also observed that the spontaneous motion of the droplets, which is generated by interfacial tension gradients, can feedback into changes in the internal morphology of the coexisting nematic and isotropic compartments (Fig. 6).

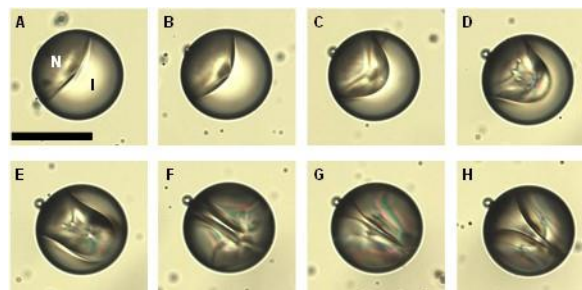


Fig. 6 (A-H) Micrographs showing reorganization of internal morphology of a two-phase nematic-isotropic droplet during spontaneous motion driven by gradients in surfactant concentration. Scale bar, 100 μm .

Future Plans

Our future studies will include studies of multiphase droplets with chiral nematic (e.g., cholesteric) and other complex LC phase domains, including blue phases (BPs). In preliminary experiments with BPs, when the mixture was dispersed into an aqueous surfactant solution, we observed spontaneous droplet motion arising from the interfacial tension gradients. Our future studies will explore how the dynamic motion and internal organization of BPs are coupled. Here we envisage the chiral nature of the BP phase to potentially lead to a number of interesting effects, including internal and surface flows (connected to Marangoni stresses) that will be chiral in nature, and thus lead to chiral droplet trajectories. In our preliminary studies, we also observed BP droplets to undergo phase transitions from BP to cholesteric phase during solubilization (Fig. 7). Interestingly, the phase transition appeared to start at the center of the BP droplet even though the solubilization processes occur at the outer surface.

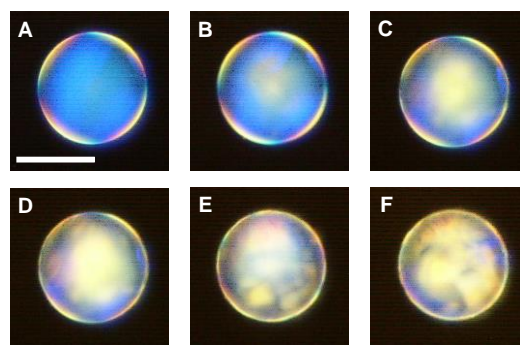


Fig. 7 Micrographs of phase transition from LC blue phase to cholesteric phase within a droplet dispersed in a concentrated cationic surfactant solution (A to F correspond to images obtained as a function of time). Scale bar, 50 μm .

Publications

Wang, X., Zhou, Y., Kim, Y.-K., Betancur, V.P., Delalande, L., Tsuei, M., Yang, Y., de Pablo, J. J., Abbott, N.L., Confined Nematic Ordering in Reconfigurable Multicompartment Emulsion Drops Formed by Hydrogenated Mesogens and Isotropic Perfluorocarbons, to be submitted.

Pérez Lemus, G., Wang, X., Kim, Y. K., Tsuei, M., Yang, Y., Abbott, N.L., de Pablo, J. J., Molecular Structure of Canonical Liquid Crystal at Fluorocarbon Interfaces, to be submitted.

Wang, X., Zhang, R., Mozaffari, A., Kim, Y. K., Tsuei, M., Yang, Y., de Pablo, J. J., Abbott, N.L., Dynamic Motion of Janus Droplets with Nematic Compartments, to be submitted.

Yang, Y., Betancur, V.P., Kim, Y.-K, Wang, X., Tsuei, M, de Pablo, J.J., Abbott, N. L., Blue Phase Liquid Crystals in Nanoemulsions, to be submitted.

V. Palacio--Betancur, J. C. Armas-Perez, S. Villada-Gil, N. L. Abbott, Juan P. Hernandez-Ortiz J. de Pablo, Manipulation of Blue Phases via Geometrical Frustration, **2019**, submitted.

M. Sadati, J. A. Martinez-Gonzalez, Ye Zhou, N. Taheri Qazvini, V. Palacio Betancur, K. Kurtenbach, X. Li, E. Bukusoglu, R. Zhang, J. P. Hernandez-Ortiz, N. L. Abbott, and J. J. de Pablo, A Chiral Liquid Crystal Kaleidoscope Created by Deformable Confinement, **2019**, submitted.

Fuster, H.A., Wang, X., Wang, X., Bukusoglu, E., Spagnolie, S.E., and Abbott, N.L., Programming van der Waals Interactions with Complex Symmetries into Colloids using Liquid Crystallinity, **2019**, submitted.

Kim, Y.-K., Noh, J., Nayani, K., and Abbott, N.L., Soft Matter from Liquid Crystals at and Beyond Equilibrium, **2019**, submitted.

Bedolla Pantoja, M.A., Yang, Y. and Abbott, N.L., Toluene-Induced phase transitions in blue phase liquid crystals. *Liquid Crystals*, **2019**, 1-12.

Zhou, Y., Senyuk, B., Zhang, R., Smalyukh, I.I. and de Pablo, J.J., Degenerate conic anchoring and colloidal elastic dipole-hexadecapole transformations. *Nature Communications*, **2019**, 10, 1000.

Wang, X., Zhou, Y., Kim, Y.-K., Tsuei, M., Yang, Y., de Pablo, J.J. and Abbott, N.L., Thermally reconfigurable Janus droplets with nematic liquid crystalline and isotropic perfluorocarbon oil compartments. *Soft matter*, **2019**, 15, 2580-2590.

Cheng, K.C., Bedolla-Pantoja, M.A., Kim, Y.K., Gregory, J.V., Xie, F., de France, A., Hussal, C., Sun, K., Abbott, N.L. and Lahann, J., Templated nanofiber synthesis via chemical vapor polymerization into liquid crystalline films. *Science*, **2018**, 362, 804-808.

Sleczkowski, P., Zhou, Y., Iamsaard, S., de Pablo, J.J., Katsonis, N. and Lacaze, E., Light-activated helical inversion in cholesteric liquid crystal microdroplets. *Proceedings of the National Academy of Sciences*, **2018**, 115, 4334-4339.

Ramezani-Dakhel, H., Sadati, M., Zhang, R., Rahimi, M., Kurtenbach, K., Roux, B. and de Pablo, J.J., Water Flux Induced Reorientation of Liquid Crystals. *ACS Central Science*, **2017**, 3, 1345-1349.

Bukusoglu, E., Martinez-Gonzalez, J.A., Wang, X., Zhou, Y., de Pablo, J.J. and Abbott, N.L., Strain-induced alignment and phase behavior of blue phase liquid crystals confined to thin films. *Soft Matter*, **2017**, 13(47), 8999-9006.

Armas-Pérez, J.C., Li, X., Martínez-González, J.A., Smith, C., Hernández-Ortiz, J.P., Nealey, P.F. and de Pablo, J.J., Sharp Morphological Transitions from Nanoscale Mixed-Anchoring Patterns in Confined Nematic Liquid Crystals. *Langmuir*, **2017**, 33, 12516-12524.

Wang, X., Zhou, Y., Kim, Y.K., Miller, D.S., Zhang, R., Martinez-Gonzalez, J.A., Bukusoglu, E., Zhang, B., Brown, T.M., de Pablo, J.J. and Abbott, N.L., Patterned surface anchoring of nematic droplets at miscible liquid-liquid interfaces. *Soft Matter*, **2017**, 13, 5714-5723.

Energy Transductions in Multimodal Stimuli-Responsive Reconfigurable Systems with Information Encoding Capabilities

PI: Joanna Aizenberg, Wyss Institute for Biologically Inspired Engineering at Harvard University

Co-PI: Anna C. Balazs, University of Pittsburgh

Program Scope

We have proposed to create responsive and dynamically adaptive artificial systems that utilize chemo-mechanical energy transduction to “*recognize*”, “*store*”, and “*communicate*” information about the local environment. These capabilities are enabled through our use of arrays of stimuli-responsive, high-aspect-ratio microstructures. These microstructures form the core of integrated, complex systems that can sense changes in the local environment and respond by reversibly expanding, contracting, bending and tilting, and thus, exhibiting detectable outputs that can be readily read out. The central feature of the proposed systems is their capacity to “*encode*” and store information about the first stimulus and, through a cascade of energy transductions, to *respond in more than an “on-off” mode* to complex, non-equilibrium downstream stimuli. Primary stimuli of a chemical or physical nature allow one to access different types of information encoding and energy transduction in our hybrid systems, while the nature, magnitude, directionality, and onset rates of downstream stimuli produce differentially patterned, clearly distinguishable responses.

The active elements of the proposed designs are either *stimuli-responsive hydrogels* or *liquid crystalline elastomers*. These two systems can encode, in a precise spatiotemporal fashion, environmental stimuli such as pH, temperature, electromagnetic field, light and others. The modularity of the proposed designs is expected to produce types of energy transductions that have not been available in previous “on-off” systems that relied on the equilibration with the environment in their action. We expect the generated knowledge about the parameter space in these novel systems to be useful in other bioinspired biomolecular systems, including those with *built-in self-regulating and autonomic capabilities*. We also anticipate that these bioinspired chemo-mechanical systems, in addition to being extremely interesting from the fundamental science perspective, might prove useful in designing *next-generation sensors, actuators, optical elements, and highly-efficient information storage devices*.

We first chose liquid crystalline elastomer (LCE) to *demonstrate proof-of-concept* energy transductions and information encoding capabilities. The anisotropic mechanical responses of LCE with respect to the external field-controlled LC direction form the basis of designing active microstructures. As shown in Fig. 1b, in nematic phase, the interaction among LC functional groups stretches the polymer chains along the direction of the LCs (so-called director), whereas

this strain can be released upon heating the system until the transition into isotropic phase takes place (corresponding to the temperature above T_{n-i}). As a result, a *unidirectional contraction of the elastomer* along the director can be achieved. When cooling the system back until the transition into nematic phase takes place (temperature below T_{n-i}), the LC constraints recover, and the *elastomer deforms back to its original size*. Thus, the anisotropic nature of LCE transmits the molecular configurations controlled by external fields (e.g. electric or magnetic field) into microscopic deformation behaviors.

Recent Progress

To test the anisotropic response of *temperature-responsive LCEs*, we synthesized a microstructure using the monomer shown in Fig. 1a. Upon heating, the microstructure showed (with respect to the initial sizes) approximate 40% contraction and 20% expansion parallel and perpendicular to the direction of the applied magnetic field during a nematic-isotropic phase transition (Fig.1b).

As we proposed, the magnetic field is sensed by

the LC monomers inside the microstructures, that are “locked” in corresponding molecular configuration by the subsequent polymerization. This configuration can be, in turn, read out by temperature as different types of deformations of microstructures enabled by

anisotropic mechanical responses of LCE, *as predicted by finite element simulations* (Fig. 1c). By controlling the magnetic field in arbitrary uniaxial directions in 3D, various molecular alignments can be obtained, and so-induced *deformation behaviors match the results shown in*

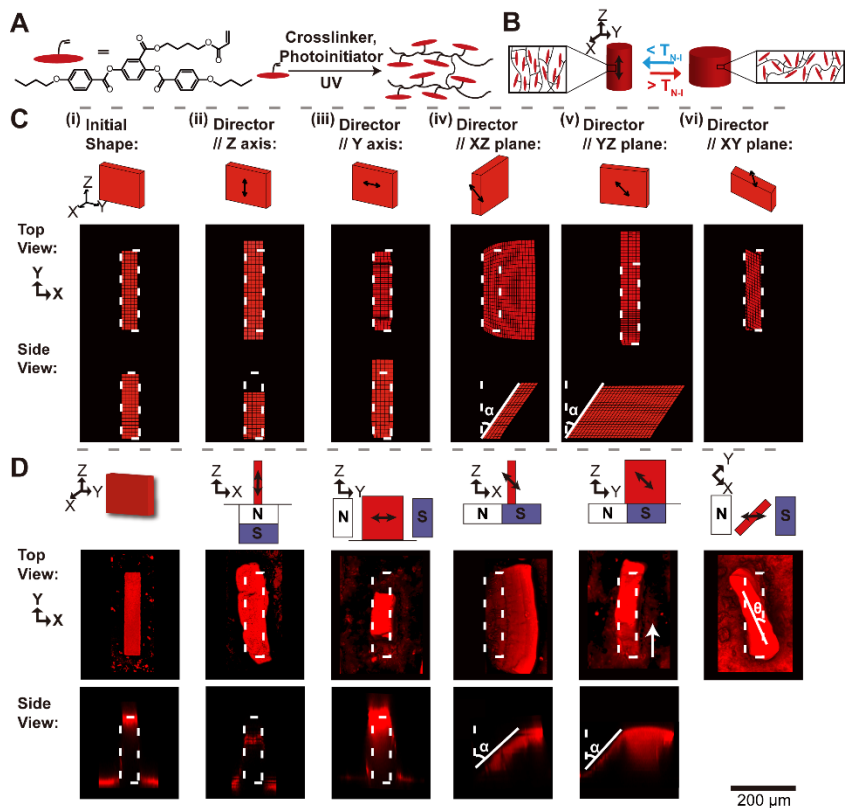


Figure 1 Thermal-responsive LCE microplates with different internal molecular configurations. **a**, Molecular structure of reactive LC monomer and the polymerization process to form an LCE. **b**, Schematic illustration of the LCE that undergoes anisotropic deformation during the phase transition when the director is oriented along the structure. **c**, Finite element simulation results, showing the initial shape (i) and the types of deformation that will originate from the director orientation along the Z-axis (ii), along the Y-axis (iii), in the X-Z plane (iv), in the Y-Z plane (v), and in the X-Y plane (vi). White dashed lines indicate the original shape of the microplate. **d**, Top: schematics of designed, 3D magnetic fields and the corresponding director orientations. Double-headed black arrows represent the director. Bottom: fluorescence confocal micrographs of the thermal-responsive deformation of the corresponding synthesized LCE microplates. White dashed outlines indicate the original shape of the LCE microplate.

simulations. As shown in Fig. 1d, a palette of actuations, including *uniaxial shrinkage*, *out-of-plane tilting*, *mechanically unfavored in-plane tilting*, and *twisting* can be realized. This thermally responsive transformation of the microstructures into a pre-designed shape, demonstrates the potential of using microscopic deformation to read out molecular configuration predetermined in the first exposure to the magnetic field.

Building upon this deformable microstructural platform, we have demonstrated its potential applications in: (i) *controlled adhesion* by programming the correlative movements of LCE microstructural array (Fig. 2a); (ii) *information encryption* at a larger scale, where different molecular configurations were encoded in separate regions to show an ‘H’ pattern upon heating to the isotropic phase (Fig. 2b).

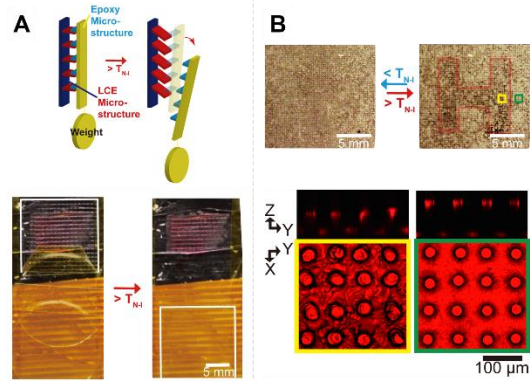


Figure 2 | Potential applications of LCE microstructure arrays. **a**, Controlled adhesive system enabled by correlative movement of LCE microstructures. **b**, Information encryption based on two-step polymerization.

In addition to temperature, we *incorporated light-responsiveness* to the LCE microstructures, to enable another mode of actuation, namely self-regulated deformations. By including photosensitive azobenzene-based crosslinkers, we can activate the deformation of the LCE

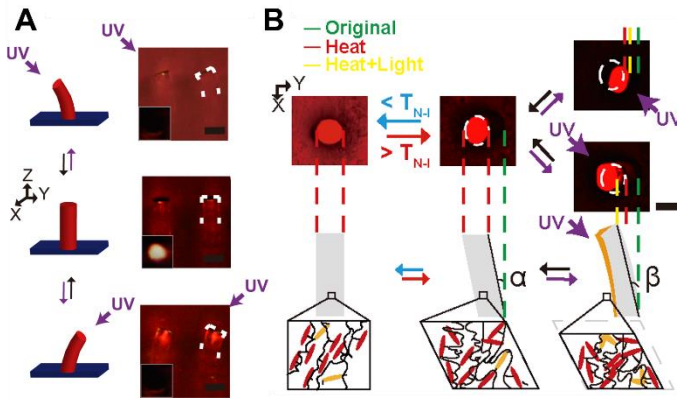


Figure 3 | UV-induced deformation of LCE microstructures. **a**, Molecular structure of photoresponsive dopant. **b**, Schematic illustration of the mechanism of photo-induced bending of LCE microposts. **c**, Dynamic bending of LCE microposts towards the position of incoming UV light.

microstructures by illumination using UV light. Due to the limited penetration depth of UV light, LCE microstructures will generate a bimorph structure depending on the direction of incoming UV. As a result, we demonstrate in Fig. 3a that the microstructures can manipulate its response to consistently bend towards the position of the UV source, a signature of self-regulation which senses and responds to the changing external stimulus continuously. This light-responsive self-regulated deformation can be readily implemented to previously described thermal-responsive pre-determined deformation to realize multi-responsive deformable

materials. As shown in Fig. 3b, we can selectively introduce pre-determined or self-regulated deformation mode by intentionally exposing the LCE system to heat, light or both stimuli. After coating the microstructures’ tips with metal thin film, these LCE pillars exhibited *self-regulated*

reflection. These results suggest the possibility to utilize this deformable platform as a light following substrate for highly efficient solar energy capture device or an antenna.

Besides microscopic deformations demonstrated above, we recently discovered another LCE chemical system which can show non-monotonic deformation behaviors. As illustrated in Fig. 4, with the continuous heating of the system, LCE microstructures showed first shrinkage and then expansion along the LC director. We believe this counterintuitive deformation behavior can further expand the already rich deformation palette of LCEs, and find applications in synthetic homeostatic materials.

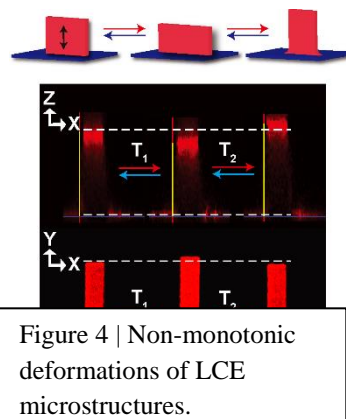


Figure 4 | Non-monotonic deformations of LCE microstructures.

Future Plans

To better understand the deformation behaviors realized in the reported LCE platform, detailed computer simulations will be performed. They will help explain the coupling between the LC mesogens and polymer chains, and how it affects the micro/macroscale thermal responsive deformation behaviors. We will further experimentally expand non-monotonic behaviors of LCE to include out-of-plane tilting, in-plane tilting and twisting demonstrated earlier in monotonic fashion. Moreover, to practically utilize these actuation behaviors, we will explore the possibility to achieve fast (within seconds), non-contact actuation of these LCE microstructural platforms by exploiting photothermal effect. We plan to further explore applications of these responsive and dynamically adaptive artificial systems. In addition to the LCE-based systems, the ones based on stimuli-responsive hydrogels with chemomechanical energy-transducing capabilities will be explored, with the general goal of uncovering and exploiting bioinspired non-equilibrium transformations with information-encoding capabilities.

References

1. Ohm, C., Brehmer, M., Zentel, R., *Advanced Materials* 22, 3366-3387 (2010).
2. White, T. J., Broer, D. J., *Nature Materials* 14, 1087-1098 (2015).
3. Buguin, A., Li, M., Silberzan, P., Ladoux, B., Keller, P., *Journal of the American Chemical Society* 128, 1088-1089 (2006).
4. Ware, T. H., McConney, M. E., Wie, J. J., Tondiglia, V. P., White, T. J., *Science* 347, 982-984 (2015).
5. Palagi, S., Mark, A. G., Reigh, S. Y., Melde, K., Qiu, T., Zeng, H., Parmeggiani, C., Martella, D., Sanchez-Castillo, A., Kapernaum, N., Giesselmann, F., Wiersma, D. S., Lauga, E., Fischer, P., *Nature Materials* 15, 647-654 (2016).
6. Yu, Y., Nakano, M., Ikeda, T., *Nature* 425, 145 (2003).

Publications

1. Yao, Y. X.; Waters, J. T.; Shneidman, A. V.; Cui, J. X.; Wang, X. G.; Mandsberg, N. K.; Li, S. C.; Balazs, A. C.; Aizenberg, J. Multiresponsive polymeric microstructures with encoded predetermined and self-regulated deformability. *Proceedings of the National Academy of Sciences of the United States of America* **2018**, *115*, 12950-12955.
2. Wang, W. D.; Timonen, J. V. I.; Carlson, A.; Drotlef, D. M.; Zhang, C. T.; Kolle, S.; Grinthal, A.; Wong, T. S.; Hatton, B.; Kang, S. H.; Kennedy, S.; Chi, J.; Blough, R. T.; Sitti, M.; Mahadevan, L.; Aizenberg, J. Multifunctional ferrofluid-infused surfaces with reconfigurable multiscale topography. *Nature* **2018**, *559*, 77-82.
3. Aizenberg, M.; Okeyoshi, K.; Aizenberg, J. Inverting the Swelling Trends in Modular Self-Oscillating Gels Crosslinked by Redox-Active Metal Bipyridine Complexes. *Advanced Functional Materials* **2018**, *28*, 27 1704205
4. Daniel, D.; Yao, X.; Aizenberg, J. Stable Liquid Jets Bouncing off Soft Gels. *Physical Review Letters* **2018**, *120*, 2, 028006
5. Hou, X.; Li, J. Y.; Tesler, A. B.; Yao, Y. X.; Wang, M.; Min, L. L.; Sheng, Z. Z.; Aizenberg, J. Dynamic air/liquid pockets for guiding microscale flow. *Nature Communications* **2018**, *9*, 733
6. Oh, I.; Keplinger, C.; Cui, J. X.; Chen, J. H.; Whitesides, G. M.; Aizenberg, J.; Hu, Y. H. Dynamically Actuated Liquid-Infused Poroelastic Film with Precise Control over Droplet Dynamics. *Advanced Functional Materials* **2018**, *28*, 39, 1802632
7. Wu, F.; Chen, S. Y.; Chen, B. Y.; Wang, M.; Min, L. L.; Alvarenga, J.; Ju, J.; Khademhosseini, A.; Yao, Y. X.; Zhang, Y. S.; Aizenberg, J.; Hou, X. Bioinspired Universal Flexible Elastomer-Based Microchannels. *Small* **2018**, *14*, 18, 1702170
8. Hu, Y. H.; Kim, P.; Aizenberg, J. Harnessing structural instability and material instability in the hydrogel-actuated integrated responsive structures (HAIRS). *Extreme Mechanics Letters* **2017**, *13*, 84-90.
9. Sutton, A.; Shirman, T.; Timonen, J. V. I.; England, G. T.; Kim, P.; Kolle, M.; Ferrante, T.; Zarzar, L. D.; Strong, E.; Aizenberg, J. Photothermally triggered actuation of hybrid materials as a new platform for in vitro cell manipulation. *Nature Communications* **2017**, *8*, 14700.
10. Korevaar, P., Kaplan, C.N., Grinthal, A., Rust, R. M., Aizenberg, J. Non-equilibrium signal integration in hydrogels, *Submitted*.

11. Waters, J. T., Li, S., Yao, Y., Lerch, M. M., Aizenberg, M., Aizenberg, J., Balazs, A. C. Twist again: dynamically and reversibly controllable chirality in liquid crystalline elastomer microposts, *Submitted*.
12. Aizenberg, J., Yao, Y., Wang, X., et al. Liquid crystalline elastomers with tunable deformation monotonicity, *In preparation*.

Principles of De Novo Protein Nanomaterial Assembly in 1, 2 and 3 Dimensions

David Baker, University of Washington

Program Scope

We are exploring the *de novo* design of multi-component protein nanomaterials that self-assemble into 1D (fiber), 2D (array), or 3D (crystal) architectures. We have designed, with near atomic accuracy, 1D helical filaments with a wide range of diameters that assemble both *in vivo* and *in vitro* into precisely ordered micron scale fibers. We have designed, again with atomic level accuracy, 2D hexagonal arrays that assemble rapidly upon mixing the two designed protein components. The arrays span multiple microns and are robust to fusion of a wide range of functional groups enabling the precise arraying in 2D of multiple functionalities. We have extended these approaches to design of protein-inorganic hybrid materials. We have shown that lattice-matched interfaces between proteins and inorganic crystal interfaces can be designed with Rosetta, and that these interfaces promote the assembly of liquid crystal-like monolayers that amplify subtle asymmetry in muscovite mica in millimeter-scale co-alignment of proteins along one mica lattice direction. Incorporation of designed end to end interactions between the designed proteins leads to formation of unbounded 1D fibers on mica, and incorporation of designed trimeric interactions directs formation of highly ordered hexagonal arrays on the mineral surface.

Recent Progress

We have created a general computational approach to designing self-assembling helical filaments from monomeric proteins and used this approach to design proteins that assemble into micrometer-scale filaments with a wide range of geometries *in vivo* and *in vitro*. Cryo-electron microscopy structures of six designs are close to the computational design models. The filament building blocks are idealized repeat proteins, and thus the diameter of the filaments can be systematically tuned by varying the number of repeat units. The assembly and disassembly of the filaments can be controlled by engineered anchor and capping units built from monomers lacking

one of the interaction surfaces. The ability to generate dynamic, highly ordered structures that span micrometers from protein monomers opens up possibilities for the

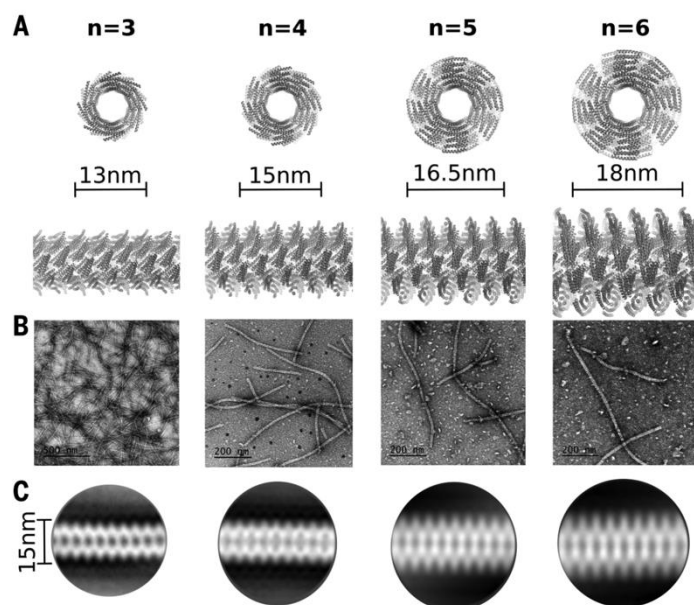


Fig. 1. Modular tuning of fiber diameter. DHF58 filament variants with different numbers of repeats were characterized by EM. (A) Cross sections and side views of computational models based on the four-repeat cryo-EM structure. The number of repeats (n) is shown at the top. (B) Negative stain electron micrographs. (C) 2D-class averages.

fabrication of new multiscale metamaterials.

Unbounded materials that assemble following mixing of two or more protein components are rare in nature and an outstanding challenge for computational protein design. We have computationally designed a nearly crystalline p6 two-dimensional material built from D2 and D3 protein building blocks individually soluble at mM concentrations which assembles upon mixing the two components at nM concentrations. Micrometer scale hexagonal arrays nearly identical to the design model are formed in cells when the two components are co-expressed, and *in vitro* when the two components are mixed. Confocal microscopy and atomic force microscopy at the micron and nanometer scale reveals preferred assembly pathways and robust self-healing of lattice defects, and complex patterns can be generated *in vitro* by incorporating differentially modified components at different stages of assembly on target substrates of choice. With the incorporation of Notch and Tie-2 receptor ligands, the designed arrays bind and assemble at the plasma membrane of mammalian cells, where they cause rapid clustering of the receptors, drive signaling through the Angiopoietin pathway, block endocytosis and trigger localized remodeling of the actin cytoskeleton. The robustness and controllability of assembly go far beyond any natural 2D protein material, and as a variety of protein domains can be fused to either or both building blocks without disrupting assembly, the material enables new approaches in areas ranging from induction of cell polarity to wound healing to 3D printing.

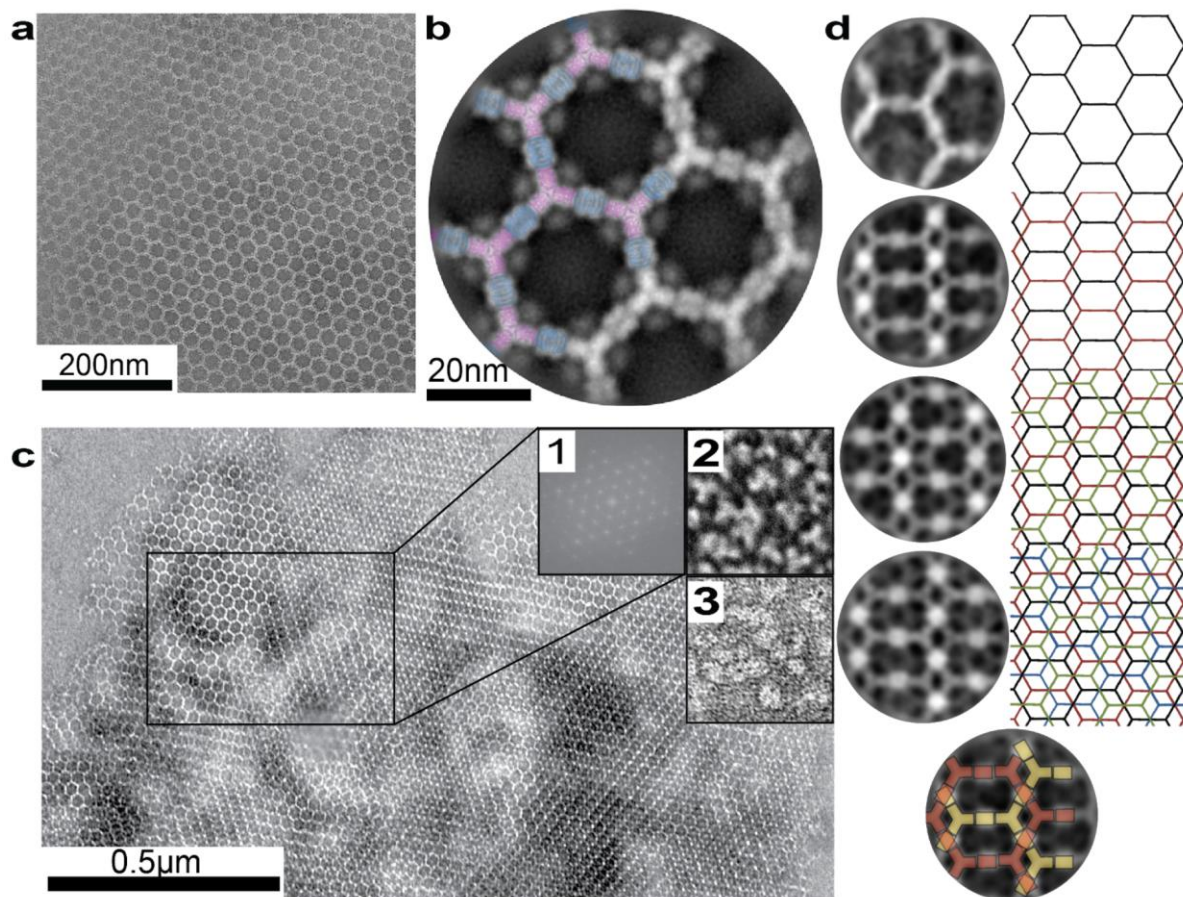


Figure 2. EM characterization of *in vitro* assembled material. a) Negative stain TEM of a single **AGFP+B** array. b) average of (a) (gray) overlaid on the computational model (**A** in magenta and **B** in green). GFP density is

evident near the **A** N-term. c) Negative stain TEM of an array spanning multiple microns. Insets: 1) FFT of a selected region (blue rectangle), 2) **A** alone, 3) **B** alone. d) Vertical projections (left column) of stacked arrays and corresponding inferred lattice packing arrangements (right column). In all cases, half of **B** of one array (red) is positioned exactly above half of **B** of the other array (yellow) with their vertical rotation axes coincident and rotated 60° perpendicular to the plane (bottom panel).

The ability of proteins and other macromolecules to interact with inorganic surfaces is essential to biological function. The proteins involved in these interactions are highly charged and often rich in carboxylic acid side chains, but the structures of most protein–inorganic interfaces are unknown. We explored the possibility of systematically designing structured protein–mineral interfaces, guided by the example of ice-binding proteins, which present arrays of threonine residues (matched to the ice lattice) that order clathrate waters into an ice-like structure. We designed proteins displaying arrays of up to 54 carboxylate residues geometrically matched to the potassium ion (K^+) sublattice on muscovite mica (001). At low K^+ concentration, individual molecules bind independently to mica in the designed orientations, whereas at high K^+ concentration, the designs form two-dimensional liquid crystal phases, which accentuate the inherent structural bias in the muscovite lattice to produce protein arrays ordered over tens of millimeters. Incorporation of designed protein–protein interactions preserving the match between the proteins and the K^+ lattice led to extended self-assembled structures on mica: designed end-to-end interactions produced micrometer-long single-protein-diameter wires and a designed trimeric interface yielded extensive honeycomb arrays. The nearest-neighbor distances in these hexagonal arrays could be set digitally between 7.5 and 15.9 nanometers with 2.1-nanometre selectivity by changing the number of repeat units in the monomer. These results demonstrate that protein–inorganic lattice interactions can be systematically programmed and set the stage for designing protein–inorganic hybrid materials.

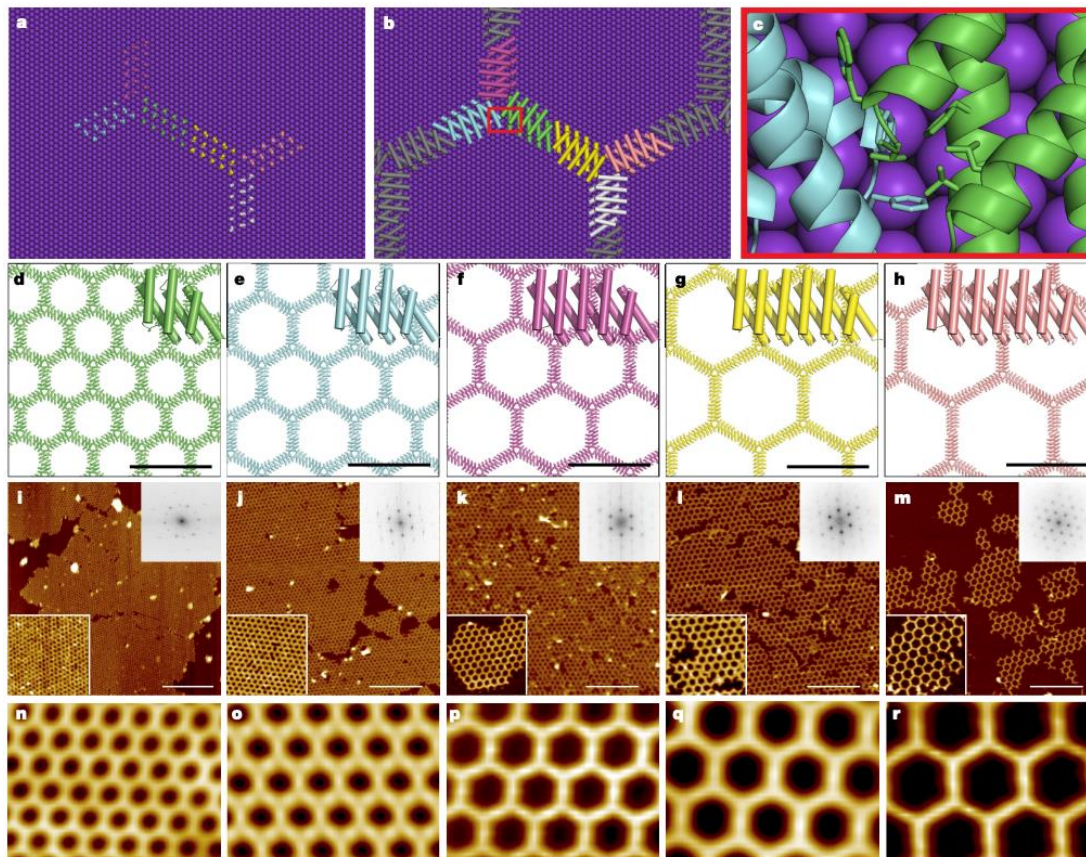


Fig. 3 Protein–protein interactions drive formation of the tunable hexagonal lattice. a–c, Hexagonal lattice design concept. a, Latticematching side chains from six molecules of DHR10-mica5-H in the honeycomb lattice. b, DHR10-mica5-H proteins containing the side chains shown in a. c, Magnification of the red square in b showing packing of hydrophobic side chains at the designed trimer interface. d–h, Computational models of DHR10-micaX-H hexagonal arrays for 3, 4, 5, 6 and 7 repeat units. Insets at top right corners show one monomer with different numbers of repeat units. The scale bars are 20 nm. i–m, AFM images of DHR10-micaX-H lattices with X = 3, 4, 5, 6 and 7 repeat units. The scale bars are 200 nm. Insets are higher-magnification views (200 nm × 200 nm; lower left corner) and Fourier transforms (upper right corner). n–r, Averaged images of i–m. The field of view is 80 nm by 60 nm. The concentrations of DHR10-micaX-H with 3, 4, 5, 6 and 7 repeat units are 0.76 μM , 0.62 μM , 0.225 μM , 0.044 μM and 0.017 μM , respectively. The buffer is 20 mM Tris-HCl and 3 M KCl.

Future Plans

We have recently developed a second generation of environmentally responsive fibers that assemble and disassemble rapidly in response to changes in solution conditions. We are in the process of characterizing these designs and drafting a manuscript for publication.

Publications

Shen, H. et al. De novo design of self-assembling helical protein filaments. *Science*. 392, 705-709. (2018)

Pyles, H. et al. Controlling protein assembly on inorganic crystals through designed protein interfaces. *Nature*. 571, 251-256 (2019)

Ben-Sasson, A. et al. Design of a two-component co-assembling two-dimensional protein material
Manuscript in preparation

Design and Synthesis of Structurally Tailored and Engineered Macromolecular (STEM) Gels

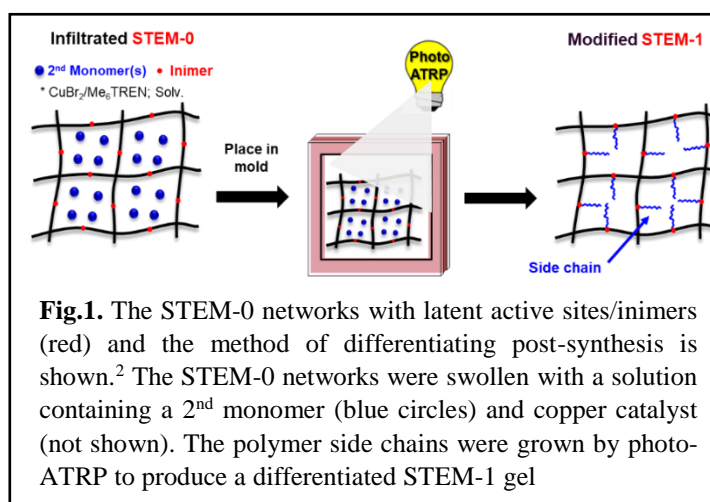
PI: Anna C. Balazs (Univ. of Pittsburgh); Co-PI: Krzysztof Matyjaszewski (Carnegie Mellon University) and Tomasz Kowalewski (Carnegie Mellon University)

Program Scope

Polymer gels that undergo structural reconfigurations and shape-changes in response to temperature, pH, or light provide ideal materials for actuators, drug release agents, biomimetic systems, and scaffolds for tissue engineering. To increase and tailor the functionality of such responsive networks, we developed our “Structurally Tailored and Engineered Macromolecular (STEM)” gels. Building on this foundational work, we established new routes for the additive *molecular manufacturing* of complex, dynamically tunable soft materials. The use of spatially selective controlled polymerizations affords an unprecedented level of control over supramolecular architecture, providing new, fundamental insights between the structure and properties of soft materials that approach the complexity of biological systems. Indeed, the proposed work is inspired by biological materials that seamlessly integrate multiple components into one construct, enabling the system to exhibit remarkably complex and adaptive behavior. Owing to the “living” nature of controlled radical polymerizations used as the keystone synthetic tool for these materials, some STEM gels display attributes of living biological materials, e.g., by conceptually mimicking the growth of new tissue or emergence of new functions.

Recent Progress

We are addressing the significant challenge of designing artificial materials that mimic the elasticity of biological materials and simultaneously maintain their durability. Gels swollen in solvent are promising candidates for addressing this challenge because their elastic and shear moduli are comparable to biological tissues. This similarity in moduli, however, often leads to mechanical embrittlement when the gels are used in important applications. Moreover, the solvent can evaporate or leach into the environment. To tackle these limitations, we developed an additive manufacturing approach, involving STEM gels with dangling polymer side chains that are covalently attached to the network (**Figure 1**).¹⁻⁴ The side chains replace the solvent, like diluent permanently tethered to the network



We synthesized STEM gels containing latent active sites (called inimers) available for post-synthesis modification (**Figure 1**). The polymer side chains can subsequently be grown from the inimers. Inspired by biological stem cells, the STEM gels initially exist in an

undifferentiated state; new properties and functionalities can be introduced by careful selection and addition of polymer side chains. The STEM gels were synthesized using orthogonal polymerization techniques. The undifferentiated or STEM-0 gels were synthesized by reversible addition-fragmentation chain transfer (RAFT) polymerization containing an atom transfer radical polymerization (ATRP) inimer. Taking advantage of the gel's swelling properties, a second monomer and ATRP catalyst were infiltrated into the gel. Then, dangling polymer side chains were grown from the network by photo-induced ATRP (UV or blue light). This approach permits spatiotemporal control over the resulting material. For example, undifferentiated STEM-0 gels were modified to a single material that is amphiphilic or combines hard/soft properties.

This approach was further used to synthesize “super-soft” gels.² These STEM-1 gels were created by growing soft poly(n-butyl acrylate) (PBA) side chains from the network. PBA was chosen because of its low glass transition temperature (T_g) of -50°C . In this way, above the gel's T_g , the PBA side chains effectively plasticize the network and behave as a permanent “solvent.” These STEM-1 gels were extremely soft with Young's moduli between 42-590 kPa, depending on sample composition.

One limitation of PBA, however, is its high tackiness and adhesive properties, which make it challenging to work with these materials. We addressed this issue by selecting a semi-fluorinated polymer, poly(octafluoropentyl acrylate) (POFPA).³ It has T_g of -35°C , making it comparable to PBA in terms of network plasticization. In addition, the fluorine atoms lower the gel's surface energy (much like Teflon®) to make soft, non-tacky materials.

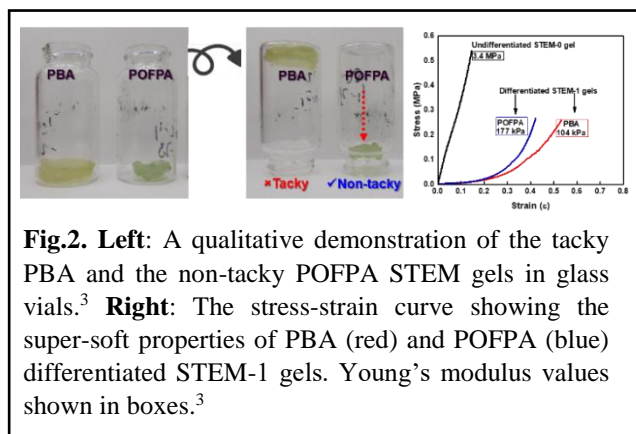


Fig.2. Left: A qualitative demonstration of the tacky PBA and the non-tacky POFPA STEM gels in glass vials.³ **Right:** The stress-strain curve showing the super-soft properties of PBA (red) and POFPA (blue) differentiated STEM-1 gels. Young's modulus values shown in boxes.³

To study the effect of varying the length of the side chains n_{sc} on the mechanical properties of the STEM gels, we model the compressive deformation of STEM-0 gels and STEM-1 gels using dissipative particle dynamics (DPD) simulations for different values of n_{sc} .² We observed that the stress for a specific value of strain decreased with an increase in n_{sc} , indicating that the side chains soften the networks for STEM-1 gels. There was a maximum saturation value of n_{sc} , beyond which the stress-strain curves of the different STEM-1 gels overlap with each other.

The cause of such a softening and saturation in the stress values was explained through the results of the DPD simulations for STEM-1 gels with varying chain lengths n_{sc} . The true stress against $F(\varepsilon)$, where $F(\varepsilon) = (1 - 1/\lambda)e^{A(\lambda-1/\lambda)}$, $\lambda = 1 - \varepsilon$, and ε is the strain is shown in **Figure 3A**. This plot shows a linear fit to the data and the slope of the line yields the modulus E . Note the decrease in the slope of the fitted lines up to $n_{sc} = 36$, showing the softening effect as sidechains with increasing lengths are added. For $n_{sc} = 36, 48$, the lines overlap, showing the saturation effect. The E values for systems with different chain lengths and plot the product of the normalized modulus and normalized volume $\bar{E}\bar{V}$ against the normalized volume \bar{V} are shown

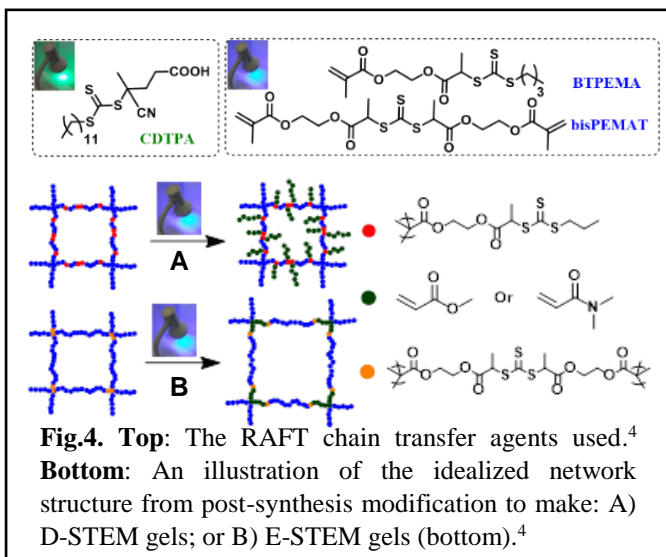
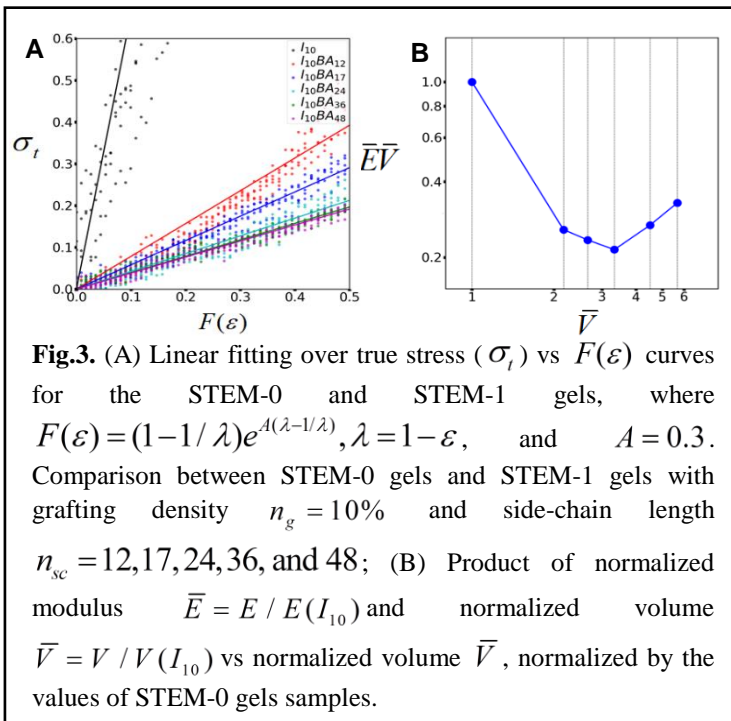
in **Figure 3B**). This plot provides significant insight into the cause of softening as chain length is increased, as well as the saturation effect observed beyond a critical length (here $n_{sc} = 36$).

In **Figure 3B**, a monotonic decrease in $\bar{E}\bar{V}$ up to the volume ~ 3.5 is seen, corresponding to side-chain length $n_{sc} = 12, 17,$ and 24 , domain 1.

Beyond this value, an increase in $\bar{E}\bar{V}$ is represented by domain 2. Domain 1 is dominated by the backbone networks, and can explain the softness of the sample through the addition of the sidechains. From the classical theory of rubber elasticity $EV \propto NkT$, where N equals the number of chemical crosslinks plus the number of entangled physical crosslinks. Hence, the observed decrease in $\bar{E}\bar{V}$ is related to a decrease in N after the addition of sidechains. The decrease in N is due to the spreading out of the backbone chains after adding sidechains and the reduced backbone-backbone contacts. Domain 2 is dominated by the sidechains, and this can explain the saturation in the residual modulus. Here N equals half of the number of backbone-sidechain chemical crosslinks plus the number of entangled sidechain-sidechain physical crosslinks. The half-factor is due to the chemical crosslink being a part of the backbone as well as the sidechain. The slope of the curve equals 1, which implies $\bar{E}\bar{V}$ is proportional to volume \bar{V} ((**Figure 3B**)). Thus, the number density N/V is constant, which explains the saturation seen in **Figure 3A**.

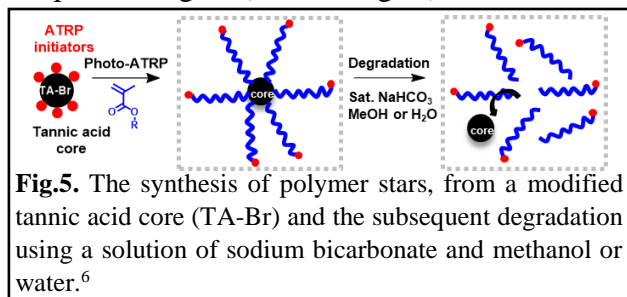
When the post-synthesis additive modifications were performed by photo-ATRP, it was necessary to introduce a copper catalyst into the gels. To use a metal-free approach, and to use visible light, we developed a new approach using a combination of RAFT chain transfer agents and dual visible light wavelengths.^{4,5} In the first step, a STEM-0 gel was synthesized under green light. In the second step, another monomer was infiltrated and polymerized under blue light. RAFT chain transfer agent, CDTPA, that absorbs green light and initiates polymerization was selected (**Figure 4**). Then a RAFT inimer, BTPEMA, and a RAFT crosslinker, bisPEMAT, that absorb blue light, but are completely inert under green light were synthesized (**Figure 4**).

When the post-synthesis additive modifications were performed by photo-ATRP, it was necessary to introduce a copper catalyst into the gels. To use a metal-free approach, and to use visible light, we developed a new approach using a combination of RAFT chain transfer agents and dual visible light wavelengths.^{4,5} In the first step, a STEM-0 gel was synthesized under green light. In the second step, another monomer was infiltrated and polymerized under blue light. RAFT chain transfer agent, CDTPA, that absorbs green light and initiates polymerization was selected (**Figure 4**). Then a RAFT inimer, BTPEMA, and a RAFT crosslinker, bisPEMAT, that absorb blue light, but are completely inert under green light were synthesized (**Figure 4**).



When using BTPEMA, a dangling side chain architecture was formed (D-STEM gels) (**Figure 4**). The bisPEMAT allowed for the synthesis of expandable gels (E-STEM gels) with increased molecular weight between the crosslinks (**Figure 4**).

We are also creating malleable materials that exhibit self-healing, stimuli-responsive shape changing, and degradable materials. Such materials will help reduce plastic environmental pollution and waste accumulation. In our synthetic efforts, a natural product, tannic acid was modified to be used as a polymer star core (**Figure 5**).⁶ Tannic acid is found in teas and is generally recognized as safe by the US FDA. The tannic acid was modified with ATRP initiator sites. Then polymer star arms were grown from the core using biocompatible ethylene glycol. Working toward subtractive manufacturing, it was demonstrated that the tannic acid polymer stars can be degraded under mild basic conditions. In addition, cytotoxicity assays were performed on the stars and corresponding degraded polymers and were found to be nontoxic at the concentrations tested. Such degradable stars will be incorporated into STEM gels and then degraded under basic conditions.



Future Plans

(i) “Subtractive manufacturing” thrust, in which we have demonstrated spatially selective removal of the material through local degradation of polymer chains will be expanded to develop materials that will “self-degrade” in response to specific triggers. This will be accomplished through the incorporation of labile (degradable) linkages throughout the entire network to facilitate global and/or local degradation. Envisioned ways to control the specific triggering of the degradation process will involve strategic incorporation of degradation-driving (photo)catalysts within the network or through photobase generation. (ii) The incorporation of catalysts will be extended to the use of stem gels as soft, highly permeable catalyst supports, which will act as hybrids between heterogeneous and homogeneous catalysts. Of particular interest will be the exploration of the extent to which the local dynamics of gel microenvironments will enhance the catalytic activity and turnover of a variety of catalysts. One of the first targets in these studies will be Ir^{III} based photocatalysts, renowned for their efficiency in photocatalytic water splitting. (iii) Work centered on “super-soft” materials, in which the materials behave as “never drying” gels owing to the presence of highly mobile secondary chains mimicking the presence of a solvent, will be continued to develop stimulus responsive materials through the incorporation of polymer chains exhibiting the property of lower critical solution temperature (LCST). “Classical” LCST polymers are comprised of a combination of hydrophilic (e.g. oligo(ethylene oxide), OEO) and hydrophobic moieties. One of the particularly exciting extensions of this theme will be the development of materials with a high content of hydrophilic moieties, which will effectively act as solvating “water cluster mimics”. Thus, the soft STEM gels swollen in water (i.e., initial hydrogels) will retain softness even after water evaporation due to their intrinsic low T_g properties. Also, they will be designed to generate hydrophobic “skin” to better retain water. It is envisioned that these materials will eventually act as “persistent” highly water retentive hydrogels, with bioinspired applications, such as extracellular matrix mimics, artificial cartilage matrices, cell culture supports or plant growth supports (artificial soil).

Publications supported by DOE grant (These are also the references for the above sections.)

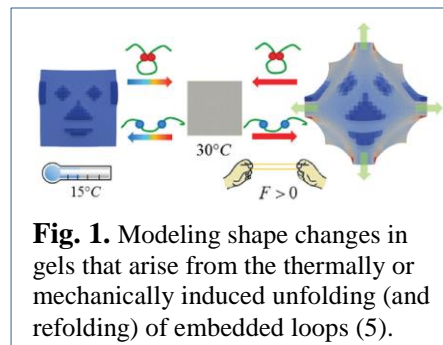
- (1) Cuthbert, J.; Beziau, A.; Gottlieb, E.; Fu, L.; Yuan, R.; Balazs, A. C.; Kowalewski, T.; Matyjaszewski, K., Transformable Materials: Structurally Tailored and Engineered Macromolecular (STEM) Gels by Controlled Radical Polymerization, *Macromolecules* 2018, 51, 3808-3817.
- (2) Cuthbert, J.; Zhang, T.; Biswas, S.; Olszewski, M.; Shanmugam, S.; Fu, T.; Gottlieb, E.; Kowalewski, T.; Balazs, A. C.; Matyjaszewski, K., Structurally Tailored and Engineered Macromolecular (STEM) Gels as Soft Elastomers and Hard/Soft Interfaces, *Macromolecules* 2018, 51, 9184-9191.
- (3) Cuthbert, J.; Martinez, M. R.; Sun, M.; Flum, J.; Li, L.; Olszewski, M.; Wang, Z.; Kowalewski, T.; Matyjaszewski, K., Non-Tacky Fluorinated and Elastomeric STEM Networks, *Macromolecular Rapid Communications* 2019, 40, 1800876.
- (4) Shanmugam, S.; Cuthbert, J.; Flum, J.; Fantin, M.; Boyer, C.; Kowalewski, T.; Matyjaszewski, K., Transformation of gels via catalyst-free selective RAFT photoactivation, *Polym. Chem.* 2019, 10, 2477-2483.
- (5) Shanmugam, S.; Cuthbert, J.; Kowalewski, T.; Boyer, C.; Matyjaszewski, K., Catalyst-Free Selective Photoactivation of RAFT Polymerization: A Facile Route for Preparation of Comblike and Bottlebrush Polymers, *Macromolecules* 2018, 51, 7776-7784.
- (6) Cuthbert, J.; Yerneni, S. S.; Sun, M.; Fu, T.; Matyjaszewski, K., Degradable Polymer Stars Based on Tannic Acid Cores by ATRP, *Polymers* 2019, 11, 752.
- (7) Shanmugam, S.; Matyjaszewski, K., Reversible Deactivation Radical Polymerization: State-of-the-Art in 2017, *ACS Symposium Ser.* 2018, 1284, 1-39.
- (8) Matyjaszewski, K., *Advanced Materials by Atom Transfer Radical Polymerization*, *Adv. Mater.* 2018, 30, 1706441.
- (9) Zeng, Z.; Wen, M.; Ye, G.; Huo, X.; Wu, F.; Wang, Z.; Yan, J.; Matyjaszewski, K.; Lu, Y.; Chen, J., Controlled Architecture of Hybrid Polymer Nanocapsules with Tunable Morphologies by Manipulating Surface-Initiated ARGET ATRP from Hydrothermally Modified Polydopamine, *Chem. Mater.* 2017, 29, 10212-10219.
- (10) Beziau, A.; Fortney, A.; Fu, L.; Nishiura, C.; Wang, H.; Cuthbert, J.; Gottlieb, E.; Balazs, A. C.; Kowalewski, T.; Matyjaszewski, K., Photoactivated Structurally Tailored and Engineered Macromolecular (STEM) gels as precursors for materials with spatially differentiated mechanical properties, *Polymer* 2017, 126, 224-230.
- (11) Matyjaszewski, K., *Polymer Chemistry: Current Status and Perspective*, *Chemistry International* 2017, 39, 7-11.

Designing Bio-inspired, Adaptive Gels with Controllable 3D Structures

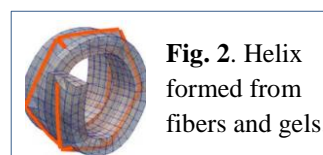
PI: Anna C. Balazs, University of Pittsburgh, Pittsburgh, PA 15261

Program Scope

Using theory and simulation, we introduce biologically inspired motifs into gels to design materials that exhibit complex collective behavior in response to external stimuli (1-9). In this way, we can facilitate the fabrication of environmentally adaptive sensors and actuators whose functionality can be “programmed” and “reprogrammed” without chemical modification to the material, but simply with the application of heat and/or light. We focus on two ubiquitous structural motifs in biology—loops and fibers—(see **Figs. 1 and 2**) that both play a crucial role in enabling the dynamic, beneficial structural changes in living organisms. Namely, the loops in biomolecules (DNA and proteins) give these molecules the necessary flexibility to perform functions that affect behavior across a range of length scales. The fibers in soft tissue (or bone in muscle) provide a level of stiffness that improves the mechanical performance of the system. Inspired by the utility of these biological motifs, we incorporate these structural elements into thermo-responsive gels and thereby introduce new dynamic behavior and functionality into the system.



The common feature of these loop- and fiber-containing gels is that the application of heat leads to the novel forms of three-dimensional (3D) self-organization, spontaneously transforming uniform structures into functional shapes or converting 2D layers into 3D forms. Moreover, the transformations are reversible, allowing one sample of material to provide useful service in different environments. Overall, these studies allow us to address challenges of importance to the DOE Biomolecular Materials program: mastering spatial and temporal control of hierarchical architectures and non-equilibrium systems.

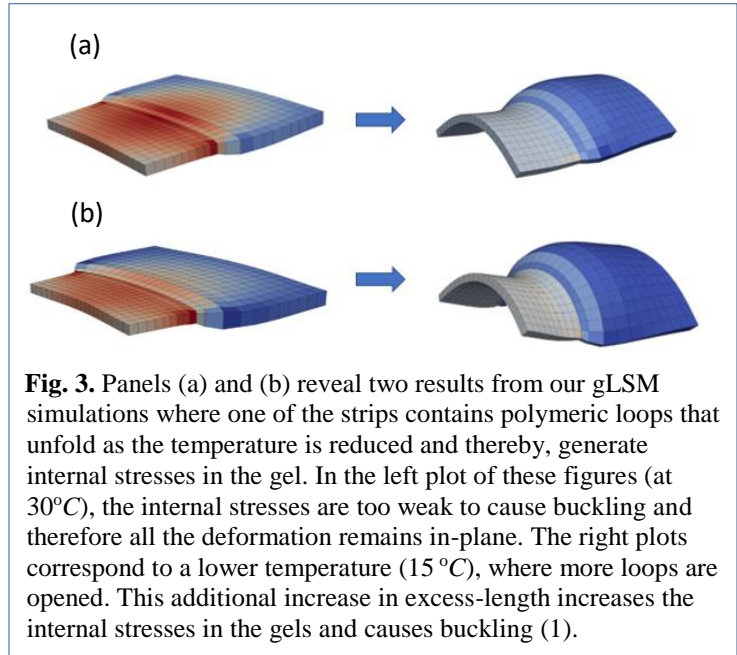


Recent Progress

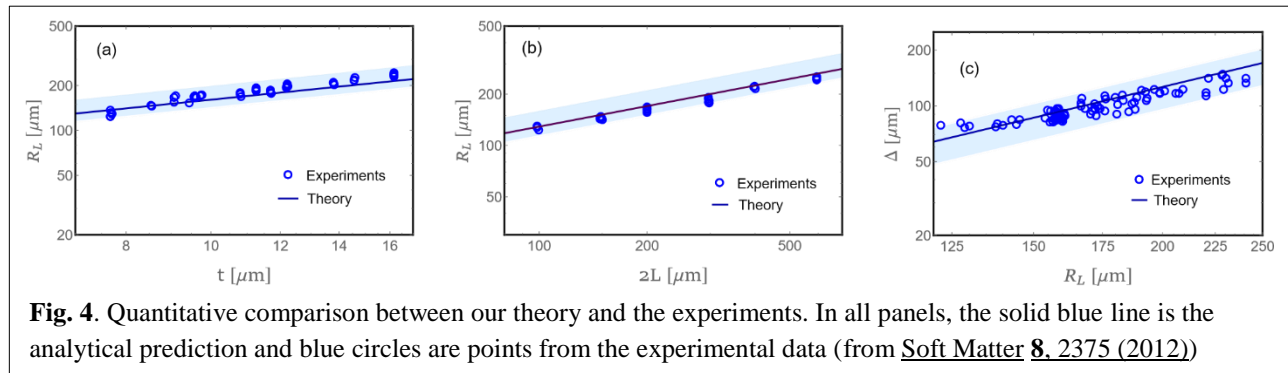
A. Shape Transitions in Bi-strip Gels with Differential Degrees of Swelling

We utilized our model for loop-containing networks (5) to mimic the process of morphogenesis in biological systems (1). Morphogenesis is the process by which biological organisms develop their shape. The growth of biological tissue involves the addition of mass to an evolving structure; if the structure is formed from an elastic material, the growth commonly drives a two-dimensional (2D) shape to transition into a three-dimensional (3D) configuration. In particular, the addition of mass to the 2D architecture introduces in-plane strains that can only be relaxed by the materials’ reconfiguration into a 3D morphology. To gain insight into physicochemical factors that can affect the transition of 2D layers into 3D structures and the

subsequent elastic relaxation within the material, researchers have focused on morphological transitions that can be induced in hydrogels. Notably, polymeric hydrogels can mimic the mechanical behavior of biological tissues and have been used extensively as tissue replacements. Moreover, while biological growth processes are in general time-dependent, such as cell division or accretion of surfaces, in many cases the time-scales for the subsequent elastic relaxations are much faster than these dynamical evolutions. Therefore, at least to leading order, non-stationary effects can often be neglected. Hence, the understanding of 2D-to-3D shape changes in hydrogels of finite, fixed size can yield significant insight into shape changes within biological tissue.



We derived an analytical model (1) that allows us to quantitatively predict the features of 2D-to-3D shape changes in polymer gels that encompass different degrees of swelling within the material and thus, can model different regions of growth within the sample. Such gels can be realized, for example, by introducing variations in the cross-link density within the network or polymerizing the chains to be relatively longer in one area of the sample than another. Focusing on a bi-strip gel that swells into a “bi-roll” (**Fig. 3**), we determined the radii and amplitudes within a given roll, and the length of the transition layer between the two rolls.



The predictions from our model agree *quantitatively* with available experimental data (J. Kim, J. A. Hanna, R. C. Hayward, and C. D. Santangelo, *Soft Matter* **8**, 2375 (2012)). In particular, in Fig. 9 we plot the analytical predictions against the experimental data. Since the experimental radius $R_{K=0}$ is not equivalent to R_L we added a shaded area around the theoretical curve. This shaded area corresponds to the regime between the minimum and maximum radii of a predicted 3D shape. While in **Fig. 4a**, the radius R_L is plotted as a function of the thickness, t , in **Fig. 4b** it is plotted as a function of the total length, $2L$. In the third plot, **Fig. 4c**, we compare the

theoretical transition layer and its experimental counterpart, Δ_{exp} . As can be seen, we obtain excellent agreement with the experimental measurements.

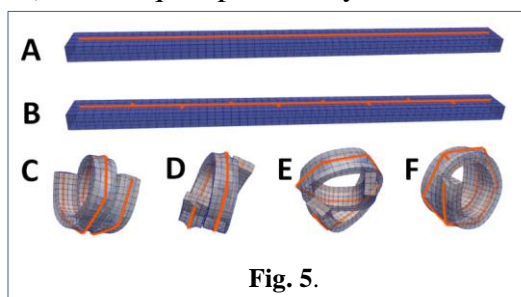
In addition, we carried out numerical simulations that account for the complete non-linear behavior of the gel, and show good agreement between the analytical predictions and the numerical results (1). Models that provide quantitative predictions on the final morphology in such heterogeneously swelling hydrogels are useful not only for understanding growth patterns in biology, but also for establishing how to accurately tailor the structure of gels to meet the requirements of various technological application. This paper was chosen as an *Editors Choice*.

Building on this model, we examined the behavior of inclusions in plates and derived an analytical model that predicts the 2D-to-3D shape transitions in the system (2). Furthermore, we extended the theory to describe shape transitions in polymeric gels, and compared the results with numerical simulations that account for the complete elastodynamic behavior of the gels. The agreement between the theory and these simulations indicates that our results are observable experimentally. Notably, our findings can provide guidelines for analyzing more complicated systems that encompass interactions between several buckled inclusions.

B. Forming Chiral Structures with Controllable Chirality Using Gel-fiber Composites

Using our gel lattice spring model (gLSM), we showed that the incorporation of fibers on the surface of long, thin gels (7) leads to the formation of helical structures with controlled chirality (8). We focused on thermo-responsive gels, which exhibit a lower critical solubility temperature (LCST) and thus shrink when heated above a certain temperature. The stiff fibers are attached to the surface of a gel and inhibit the nearby network from undergoing the heat-induced collapse. Away from the fibers, however, the network can readily shrink in response to the increased temperature. This competition between the constrained and unconstrained regions of the heated gel regulates the structural evolution and final geometry of the sample (7).

To determine how the arrangement of the fibers controls the bending and curvature of thin films, we arranged nine adjacent fibers on the top surface of the sample shown in **Fig. 5A**. The systems are initially equilibrated at $T = 20\text{ }^{\circ}\text{C}$, where the sample forms a flat bar; the systems are then heated and re-equilibrated at $T = 32\text{ }^{\circ}\text{C}$. The samples bend into either a helical structure (**Fig. 5C-D**) or a knot-like structure (**Fig. 5E**) with equal probability. The helical structures display opposite chirality with equal probability (**Fig. 5C-D**). In other words, the final structure is unstable because the system displays mirror symmetry about the central, vertical plane. If, however, short fibers are introduced in an alternating pattern perpendicular the long, central fiber (**Fig. 5B**), the mirror symmetry is broken and the heated samples always bend into a helical structure with controlled chirality (**Fig. 5F**).



C. Designing Self-reinforcing Gels

Biological systems display a variety of mechanisms to mitigate the effects of an applied force, and even harness the force to perform a useful function. The exposure of cryptic binding sites is a prime example of an adaptive, biological response to mechanical force that ultimately

produces the beneficial effect of strengthening of the biomaterial. Incorporated into a polymer network, cryptic sites could provide a number of distinct advantages, which are best illustrated by referring to schematic in **Fig. 6**. The green polymer network contains loops that are held together by a “cryptic bond”, which is formed between the blue cryptic sites. The application of force breaks the cryptic bonds and frees the “hidden length” that was stored in the loops. As is typical in polymer gels, the network in **Fig. 6** also contains dangling chains that branch off the main framework. These dangling chains encompass reactive end groups, which are marked in yellow within the figure. Similar to the wasted loops, the unbound dangling ends do not contribute to optimizing the material’s mechanical performance. If, however, the reactive ends bind to the exposed cryptic sites, they could form “struts” that stiffen the gel. This mechano-responsive stiffening would allow the material to resist further deformation (up to some critical level) and thus, extend the functionality of the gel. In other words, the introduction of the mechano-responsive cryptic sites provides a means of improving the materials’ mechanical properties in the presence of an applied force.

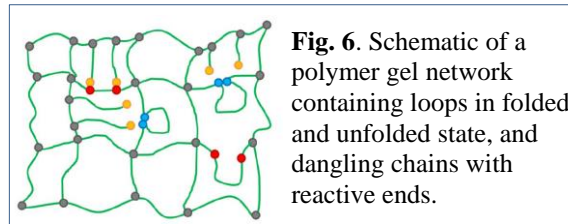


Fig. 6. Schematic of a polymer gel network containing loops in folded and unfolded state, and dangling chains with reactive ends.

We extended our gLM model (5) to obtain **Fig. 7**, which contrasts cases where the ends on the dangling chains are reactive and can bind to the cryptic sites on the unfolded loops (binding curve in red) versus the case where the dangling ends are not reactive and do not bind to the exposed cryptic sites (no binding curve in green) (9). The fact that the red curve lies below the green one indicates that the binding inhibits the effect of the applied force; that is, the struts prevent the stretching and swelling of the LCST gel as the temperature is lowered. Notably, above $T > T_c$, the red curve lies above the green curve because for this choice of parameters, the force is sufficiently strong to unfold all the loops even above T_c where the LCST gel de-swells and the exposed sites are bound to the dangling chains.

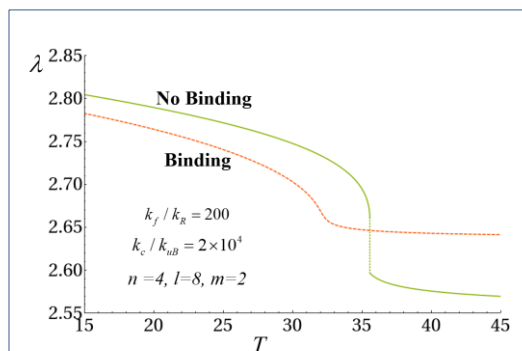


Fig. 7. Lateral extension of the gel (along the direction of force) λ as a function of temperature and under the effect of a tensile force (for the set of parameters indicated in the curve).

Future Plans

Our model for the 2D-to-3D transitions of a single inclusion within an elastic sheet (2) will be extended to analyze a number of inclusions that are arranged in different geometries to determine factors that regulate the final structure formation. We will also extend our studies of gel-fiber composites (7) to determine factors that control the evolution and structure formation of materials encompassing multiple interacting helices (8). We will augment our models of self-reinforcing gels (9) to determine the system’s response to force ramps, where the applied force is incremented with time, and thereby analyze the dynamics of bond formation and rupture in the systems under different loading cycles of applied force. These studies will provide additional guidelines for creating dynamically responsive self-reinforcing gels.

Publications supported by DOE grant (These are also the references for the above sections.)

1. Oshri, O., Biswas, S., Balazs, A.C., “Modeling the formation of double rolls from heterogeneously patterned gels”, *Physical Review E*, 99 (2019) 033003.
2. Oshri, Oz, Biswas, S., and Balazs, A.C., “Modeling the behavior of inclusions in circular plates undergoing 2D-to-3D shape changes”, *PRE*, submitted.
3. Oshri, O., Liu, Y., Aizenberg, J., Balazs, A.C. “On the delamination of a thin sheet from a soft adhesive Winkler substrate”, *PRE*, 97 (2018) 062803 (13 pages).
4. Xiong, Y., Dayal, P., Balazs, A.C., and Kuksenok, O. “Phase transitions and pattern formation in chemo-responsive gels and composites”, *Israel Journal of Chemistry*, 58 (2018) 693-705.
5. Biswas, S., Vashin, V.V. and Balazs, A.C., “Patterning with Loops” to Dynamically Reconfigure Polymer Gels, *Soft Matter*, 14 (2018) 3361 - 3371.
6. Kuksenok, O., Singh, A. and Balazs, A. C. “Designing Polymer Gels and Composites that Undergo Bio-inspired Phototactic Reconfiguration and Motion”, *Bioinspiration and Biomimetics*, 13 (2018) 035004.
7. Zhang, T., Yashin, V.V., and Balazs, A.C., “Fibers on the Surface of Thermo-responsive Gels Induce 3D Shape Changes”, *Soft Matter*, 14 (2018) 1822-1832.
8. Zhang, T., Yashin, V.V., and Balazs, A.C., “Forming Helical Composites with Controllable Chirality from Fiber-decorated Gels”, *in preparation*.
9. Biswas, S., Vashin, V.V. and Balazs, A.C, “Self-stiffening in Thermo-mechanically Responsive Gels”, *in preparation*.

Electrolyte-mediated assembly of like-charged colloids

Michael J. Bedzyk (PI), Northwestern University and Sumit Kewalramani (co-PI), Northwestern University.

Program Scope

The project aims are to understand how electrolytes, consisting of mono- and di-valent ions, affect interactions between like-charged biomolecular nano-constructs, and to utilize the electrolyte-mediated interactions for controlling reactions and assembly at the nanoscale. The project focus is:

- (1) *Ionic distribution surrounding charged nanoparticles.* The distributions of ions surrounding charged nanoparticles are studied under conditions pertinent to nanoparticle assembly and reactions.
- (2) *Nanoparticle association in electrolyte solutions.* Electrolyte-mediated interactions are utilized to (a) create ordered assemblies of charged nanoparticles and (b) control reactions between like-charged, but dissimilar nanoparticles for systematically modifying the structure and function of these reacting particles.
- (3) *Nanoparticle interactions in highly saline solutions.* The strength and range of the electrostatic interparticle interactions are studied in a salt concentration regime where classical DLVO theory is expected to break down.

The primary experimental tool in our studies is *in situ* X-ray scattering. All the experiments thus far have used DNA-coated nanoparticles as models for highly charged biomacromolecules. The experiments are coupled with theoretical calculations from the Olvera de la Cruz group at NU.

Recent Progress

Counterion distribution surrounding DNA-functionalized proteins

Proteins densely functionalized with DNA (Prot-DNA, eg. Fig. 1A) are an emerging class of highly charged bio-constructs that retain the enzymatic functionality of the protein core and exhibit advantageous characteristics due to DNA [1]. Many of the characteristics of Prot-DNA, and other nanoparticles with dense DNA coatings, have been hypothesized to critically depend on the distribution of counterions surrounding these particles [2-3]. We use anomalous small angle X-ray scattering (ASAXS) in conjunction with DFT calculations to deduce the counterion distribution surrounding Prot-DNA [4]. As a first step, we studied the case of Prot-DNA in a low salt concentration solution (50 mM RbCl), where the inter-Prot-DNA interactions can be neglected. We note that the protein cores are advantageous for ASAXS, which requires highly charged particles with relatively low electron density. Both these factors enhance the relative contribution of the counterions to the overall scattering. In fact, extracting counterion distribution by ASAXS is not feasible for electron rich metal cores coated with DNA [5].

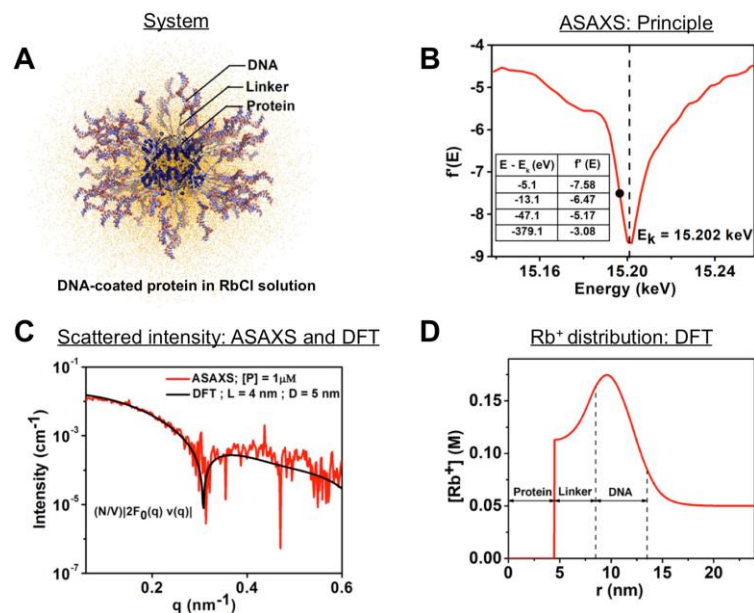


Fig. 1 (A) Schematic for the DNA-functionalized Cg catalase (Prot-DNA). The catalase protein ($\sim 9 \times 9 \times 7.5$ nm³) was functionalized with 40 single-stranded DNA that were 18 bases long. The Prot-DNA were dispersed in 50 mM RbCl at 1 or 4 μM concentration. (B) The reduction in the scattering power of Rb^+ counterion for X-ray energies near the Rb^+ K absorption edge. This sharp reduction leads to subtle X-ray energy dependent changes to the scattering profile from Prot-DNA-counterion system. (C) Analysis of SAXS intensities measured at four different X-ray energies (inset, 1B) yields a cross-term profile (red). Also shown is the best-fit (black), which is based on the counterion distribution in (D).

interactions are expected to induce Prot-DNA assembly into crystalline lattices [6].

Enzymatic degradation of DNA

As an example of electrolyte-mediated reaction at the nanoscale, we studied the deoxyribonuclease I (DNase I)-mediated degradation of DNA tethered to a protein core (Fig. 2A). DNase-I is an endonuclease in mammalian and human tissues [7-8]. It catalyzes the direct nucleophilic attack of the phosphorus atom on the DNA backbone by a water hydroxyl, resulting in the cleavage of the P-O 3' bond and the formation of 5' phosphate terminated nucleotides [9]. DNase I-mediated DNA degradation requires the presence of divalent cations, such as Mg^{2+} and Ca^{2+} , which stabilize DNase I conformation [9,10], and allow association between like-charged DNA and DNase I [10]. We used time-dependent small angle X-ray scattering (SAXS) to deduce the changes in the Prot-DNA structure during the DNase I mediated DNA degradation and to extract the kinetic parameters for this reaction. Molecular dynamics (MD) simulations elucidated the distribution of mono- and di-valent cations surrounding Prot-DNA in a prototypical reaction condition that was used in SAXS measurements.

The key findings from ASAXS-DFT are:

- (1) Rb^+ residing within the DNA shell compensate $\sim 90\%$ of the DNA charge. The Rb^+ distribution extends beyond the DNA shell by ~ 1.3 nm, consistent with Debye-Huckel theory for 50 mM RbCl. The Rb^+ distribution profile that best describes the measured ASAXS effect (Fig. 1C) is shown in Fig. 1D.
- (2) The length L of the linker used to covalently attach the DNA to the protein core, and the length of the DNA (here, 18 base long single stranded (ss)-DNA) were found to be $L = 4 \pm 0.5$ nm and $D = 5 \pm 0.6$ nm. Overall, ASAXS reveals submolecular features of Prot-DNA and the distribution of counterions surrounding these particles with 1 nm resolution.

The success of our ASAXS-DFT approach paves the way for future studies on the counterion distribution in the high-salt concentration regime, where electrolyte-mediated

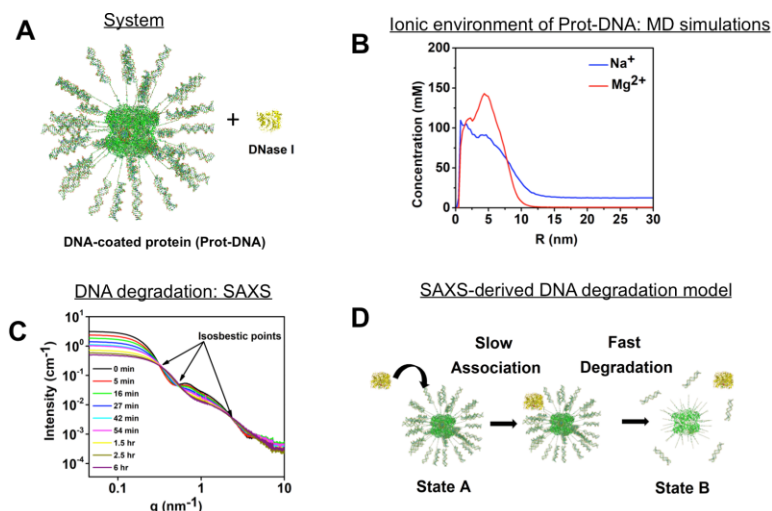


Fig. 2 (A) Schematic for a Prot-DNA depicting a Cg catalase core (~ 9 nm x 9 nm x 7.5 nm) covalently linked with 40 double stranded (ds)-DNA. Also shown is DNase I (~ 4.6 nm x 4.2 nm x 3.4 nm), drawn to scale. For reactions, Prot-DNA and DNase I were dispersed in a buffer containing 10 mM Tris. HCl, 0.5 mM CaCl₂ and 2.5 mM MgCl₂. (B) MD simulations-derived, angular averaged distribution profiles for mono- and di-valent cations surrounding the Prot-DNA as a function of distance from the protein surface. For simplicity in simulations, all mono- and di-valent cations are treated as Na⁺ and Mg²⁺, respectively. (C) Time-dependent SAXS from 4 μM Prot-DNA, 167 nM DNase I reaction mixture. The nodes (isosbestic points) in the intensity profiles imply a two state system with time-dependent populations of pristine and fully degraded Prot-DNA. (D). Schematic of the SAXS –derived reaction pathway.

The key results from the combined SAXS-MD study are:

- (1) The counterionic cloud surrounding the Prot-DNA consists of 1.09× more divalent cations than monovalent cations (Fig. 2B) even though the solution had a 4.8× abundance of monovalent cations, in the prototypical solution conditions used. This large number of divalent counterions supports the catalytic function of DNase I.
- (2) At any given time in the reaction, the ensemble of Prot-DNA can be described as a linear combination of pristine Prot-DNA and Prot-DNA that are sans the DNA. This two state system implies that once a DNase I attaches to a Prot-DNA, it rapidly degrades all the DNA on the Prot-DNA such that no intermediate states are observable (Figs. 2C-D).

- (3) The rate constant for the DNA degradation is ~ 5 orders of magnitude higher than that for DNase I-DNA association: $k_{ass} = (2.0 \pm 0.6) \times 10^{-6} \text{ nM}^{-1} \text{ s}^{-1}$ and $k_{deg} = 0.21 \pm 0.04 \text{ s}^{-1}$.

The approach presented here lays groundwork for label-free analysis of biological catalytic reactions.

Future Plans

First, we will extend ASAXS studies on ionic distributions to more complex scenarios where the solution will contain mixtures of mono- and di-valent cations. These ASAXS studies will be combined with time-dependent SAXS studies on DNase I-mediated DNA degradation to correlate the local ionic cloud structure with the kinetics of the enzymatic reaction. Second, we will use SAXS and ultra-SAXS (USAXS) to extract the interparticle correlations in highly saline solutions. These experiments will provide insights into interparticle interactions in a regime where the classical DLVO theory is no longer valid. Furthermore, these experiments will test recent intriguing surface force measurements [11-12], which show that in the high salt concentration

regime (1-10 M), the electrostatic screening length rapidly increases with salt concentration. Such an effect has not yet been observed in a bulk system, such as colloids in solution.

References

1. Brodin, J. D.; Auyeung, E.; Mirkin, C. A. DNA-mediated engineering of multicomponent enzyme crystals. *Proc. Natl. Acad. Sci. U. S. A.*, **112**, 4564–4569 (2015).
2. Seferos, D. S.; Prigodich, A. E.; Giljohann, D. A.; Patel, P. C.; Mirkin, C. A. Polyvalent DNA nanoparticle conjugates stabilize nucleic acids. *Nano Lett.* **9**, 308–311 (2009).
3. Jin, R.; Wu, G.; Li, Z.; Mirkin, C. A.; Schatz, G. C. What Controls the Melting Properties of DNA-Linked Gold Nanoparticle Assemblies? *J. Am. Chem. Soc.* **125**, 1643–1654 (2003).
4. Krishnamoorthy, K.; Hoffman, K.; Kewalramani, S.; Brodin, J. D.; Moreau, L. M.; Mirkin, C. A.; Olvera de la Cruz, M.; Bedzyk, M. J. Defining the Structure of a Protein Nucleic Acid Conjugate and its Counterionic Cloud, *ACS Cent. Sci.* **4**, 378-386 (2018).
5. Kewalramani, S.; Zwanikken, J. W.; Macfarlane, R. J.; Leung, C.-Y.; Olvera de la Cruz, M.; Bedzyk, M. J. Counterion Distribution Surrounding Spherical Nucleic Acid-Au Nanoparticle Conjugates Probed by X-ray Scattering, *ACS Nano* **7**, 11301-11309 (2013).
6. Kewalramani, S.; Guerrero-Garcia, G. I.; Moreau, L. M.; Zwanikken, J. W.; Mirkin, C. A.; Olvera de la Cruz, M.; Bedzyk, M. J. Electrolyte-Mediated Assembly of Charged Nanoparticles. *ACS. Cent. Sci.* **2**, 219-224 (2016).
7. Lacks, S. A. Deoxyribonuclease I in Mammalian Tissues. Specificity of Inhibition by Actin. *J. Biol. Chem.* **256**, 2644-2648 (1981).
8. Shiokawa, D; Tanuma, S-I. Characterization of human DNase I family endonucleases and activation of DNase γ during apoptosis. *Biochemistry* **40**, 143-152 (2001).
9. Suck, D.; Oefner, C., Structure of DNase I at 2.0 Å resolution suggests a mechanism for binding to and cutting DNA. *Nature* **321**, 620-625 (1986).
10. Guérault, M.; Picot, D.; Abi-Ghanem, J.; Hartmann, B.; Baaden, M., How Cations Can Assist DNase I in DNA Binding and Hydrolysis. *PLoS Computational Biology* **2010**, *6* (11), e1001000.
11. Perez-Martinez, C. S.; Smith, A. M.; Perkin, S. Underscreening in Concentrated Electrolytes. *Faraday Discussions* **199**, 239-259 (2017).
12. Perez-Martinez, C. S.; Smith, A. M.; Perkin, S. Scaling Analysis of the Screening Length in Concentrated Electrolytes. *Phys. Rev. Lett.* **119**, 026002 (2017).

Publications

1. Krishnamoorthy, K.; Hoffman, K.; Kewalramani, S.; Brodin, J. D.; Moreau, L. M.; Mirkin, C. A.; Olvera de la Cruz, M.; Bedzyk, M. J. Defining the Structure of a Protein Nucleic Acid Conjugate and its Counterionic Cloud, *ACS Cent. Sci.* **4**, 378-386 (2018).
2. Moreau, L. M.; Jones, M. R.; Roth, E. W.; Wu, J.; Kewalramani, S.; O'Brien, M. N.; Chen, B.-R.; Mirkin, C. A. and Bedzyk, M. J. The Role of Trace Ag in the Synthesis of Au Nanorods, *Nanoscale*, **11**, 11744-11754 (2019).

3. Krishnamoorthy, K.; Kewalramani, S.; Ehlen, A.; Moreau, L. M.; Mirkin, C. A.; Olvera de la Cruz, M.; Bedzyk, M. J. Enzymatic Degradation of DNA Probed by In-Situ X-ray Scattering, *ACS Nano*, *Under Revision* (2019).

Morphogenesis-Inspired Assembly Mechanisms in Multi-Phase Colloidal Materials

Michael A Bevan, Johns Hopkins University (Principal Investigator) and Joelle Frechette, Johns Hopkins University (Co-Investigator)

Program Scope

Nature employs morphogenesis to create and remodel spatial distributions of multi-scale cellular tissue architectures with complex functions. However, it has been difficult using synthetic materials to mimic the structures, properties, and development of tissues in living systems. This project aims to design multi-phase colloidal assembly processes to obtain hierarchically structured materials with exceptional emergent properties that are inspired by morphogenic processes and unique biological structures. Our approach investigates how multiple length scales can be accessed by serial and parallel combinations of nano- and micro- colloidal assembly on drops, which can be polymerized and undergo subsequent assembly and patterning (as protein, cellular, extracellular matrix analogs). We employ external fields to provide spatiotemporal feedback control of particle positions, orientations, and local assembly as part of assisting transport processes and non-equilibrium kinetic pathways that avoid arrested states and yield high structural fidelity across length scales (as a biological feedback loop analog). Implementing this approach requires developing new fundamental insights into coupling out-of-equilibrium colloidal assembly within individual droplets with larger scale transport and adhesion of droplets, which involves complex interactions and dynamics determined by conservative and dissipative forces operating over disparate length- and time- scales.

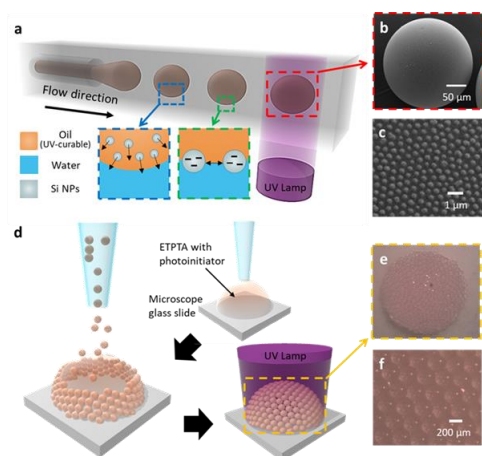


Fig. 1. Fluid-based multiphase colloidal assembly to create a hierarchical structure inspired by mosquito compound eyes. a, Schematic of experimental setup for microlens fabrication. b,c, SEM images of a UV-cured microsphere with nanoscale surface topography (b) and hexagonal arrangement of silica nanoparticles (300 nm) on microsphere surface (c). d, Assembly of microlenses into compound lens. e,f, Images of microsphere-decorated dome (convex-planar shape) (e) and hexagonally close-

Recent Progress

We first investigated assembly of spherical particles and drops inspired by the mosquito eye (Fig. 1), which is a truly hierarchical multiscale and multifunctional ordered structure. Nanoscale features are present on the ommatidium (nanonipples, ~ 100 nm) to provide antifogging and antireflective properties, whereas the microscale dimension of an individual ommatidium ($26 \mu\text{m}$) provides a nearly infinite depth of field without focusing elements. The hemispherical arrangement of the ommatidia forms the compound eye ($500 \mu\text{m}$) and provides a large field of view. The

hierarchical structure and curvature of the mosquito compound eye is challenging to produce because of the presence of multiple curved length scales. We developed a liquid process based on the assembly of liquid droplets to naturally introduce the necessary curvature and deformability that alleviate fabrication challenges. Our building blocks are droplets stabilized by nanoparticles. The droplets act as microlenses and are assembled onto a larger sessile droplet to form compound lenses or liquid marbles. We then rely on the mobility of liquid marbles under shear to create arrays of compound lenses. Finally, we polymerize the lenses to arrest the assembled structure and form a mechanically robust hierarchical material.

External vibration prior to polymerization converts the deposited compound lens into liquid marbles (Fig. 2a-b), which can be used to create patterns. The liquid marbles are mobile and readily roll without leaving residue on a solid.

We deposit and arrest marbles

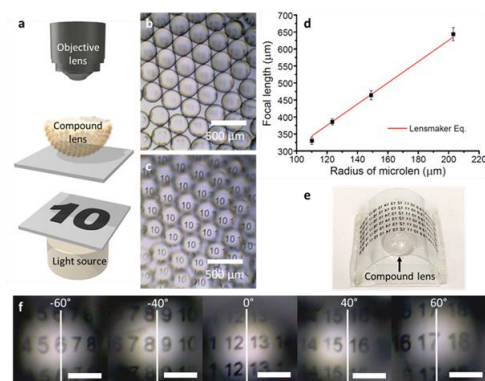


Fig. 3. Optical properties of compound lenses. a, Setup to determine the focal length of individual compound convex-planar lens. b,c, Image using a 4× objective focused on the vertex of a small group of microlenses (125 μm radius) that are part of an individual compound lens (b), number projected by the microlenses focused on focal point (c). d, Agreement with lensmaker equation for focal length vs. microlens radii. e, Set-up for field of view measurements on hemi-cylindrical sheet for inverse concave-convex lens. f, Output images projected by the micro-compound lenses at different viewing angles by tilting the microscope stage.

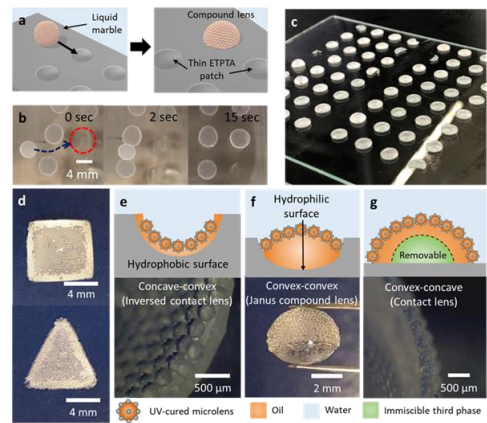


Fig. 2. Reconfigurable assembly of compound lenses. a, Process to prepare multiple compound lenses on patterned surfaces. b, Deposition of compound eye liquid marble onto circular patches. c, Polymerized compound lens arrays (8×8). d, Images showing shape control of deposited compound lens through patterning patches. e-g, Cross-sectional (e,g) and side (f) views of alternate lens types via interfacial properties.

at pre-defined locations to create arrays (Fig. 2c). Importantly, control over interfacial interactions allow us to keep microlenses as monolayers at the oil-water interface, and a microparticle-stabilized liquid marble does not coalesce if it contacts other marbles (Fig. 2b,d). We further show that through manipulation of surface chemistry, topography, or introduction of immiscible third-phase fluid, the same general process can create very different lens types (Fig. 2e-g). We created a novel “Janus compound lens” where the input image captured by the microlens array is magnified by the rear conventional convex lens. We can create microlenses with different radii (25-250 μm) by manipulating the flow rates of the inner (oil) and outer (aqueous) phases.

The hexagonally-close packed microlens array (Fig. 3 a,b) projects multiple identical images with nearly infinite depth of field (Fig. 3c). We find in our material that the overall viewing angle is 149° (Fig. 3f), with evenly spaced and undistorted images. To function in humid environments, nanonipples on ommatidia surfaces render

mosquito eyes naturally anti-fogging. Similarly, the silica nanoparticles on the surface of the microlens provide anti-fogging properties. For the superhydrophilic lens, the anti-fogging properties are due to spreading of condensed water droplets on the compound lens to produce a thin continuous water film. Once the film forms, no further fogging occurs. When the compound lens is superhydrophobic anti-fogging properties are due to collection of water droplets in the interstices between the microlenses. Without silica nanoparticles, microscale water droplets grow on the microlens and distort the image.

To understand how to introduce anisotropic particles into/onto patterned drops and to quantify their phase behavior, microstructures, and assembly dynamics, new algorithms have been developed to analyze particle coordinates from experiments and simulations. An algorithm to calculate near neighbors via a novel tessellation scheme is depicted in Fig. 4. Fig. 4 also shows representative cases of particles with four and six neighbors determined via tessellation, which are used to compute novel local 4-fold and 6-fold bond orientational order parameters, ψ^s_4 and ψ^s_6 , based on stretch coordinates along each particle's principal axes. These novel local order parameters are used to determine the phase behavior for computer simulations of hard super-ellipses in two-dimensions, which provide a basis to analyze microscopy results for super-ellipses in electric fields. The new parameters naturally determine local order for every single particle which allows them to characterize defects, local microstructures, and non-equilibrium dynamics in addition to phase behavior.

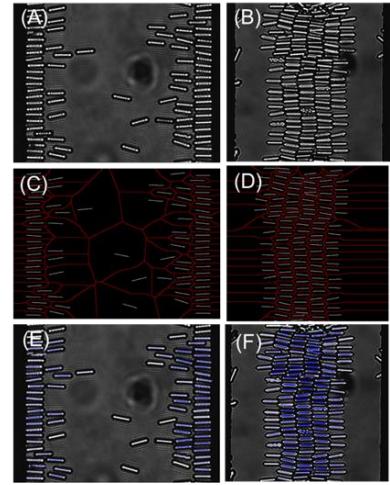


Fig. 4. Electric field amplitude and frequency-dependent assembly of super-ellipsoidal particles in non-uniform fields at (A) 100kHz, 0.5Vpp; (B) 15MHz, 1.0Vpp. (C,D) Tessellation of images in A, B to compute neighbors for order parameters calculations. (E,F) Particles colored according to C_6 , which is connectivity parameter that combines coordination number and stretched six-fold order.

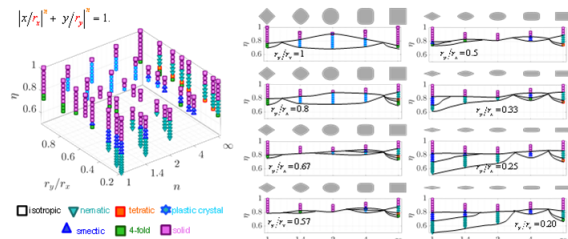


Fig. 5. Phase diagram of hard super-ellipses vs. shape parameter, n , aspect ratio, r_y/r_x , and area fraction, η . (left) 3D phase diagram provides a comprehensive conceptual diagram for broad range of shapes encompassing disks, ellipses, squares, rectangles, etc., and continuum of many other shapes. (right) Constant aspect ratio cross sections of 3D phase diagram show systematically how shape parameter, n , or roundedness of corners produces non-monotonic trends in phase behavior for fixed aspect ratios.

By performing simulations of different particle shapes described by the super-ellipse equation (Fig. 5), a

comprehensive phase diagram has been prepared for the two dimensional phase behavior of hard super-ellipses vs. the shape parameter, n , aspect ratio, r_y/r_x , and area fraction, η (Fig. 5). Cross-sectional planes at different aspect ratios with rendered particle shapes show more clearly the phase behavior for a broad range of particle shapes captured in the overall plot. Figs. 4,5 together show

the capability of the new parameters, ψ^s_4 and ψ^s_6 , to quantify the local symmetry and phases for a broad range of different anisotropic particle shapes. In addition to identifying microstructures corresponding to thermodynamic phases, such parameters will also be used as reaction coordinates to quantify assembly dynamics and as sensors for feedback control using machine learning methods.

These analysis tools were then applied to experiments of electric field mediated interactions, structure, and assembly of super-ellipse particles experiencing induced dipolar interactions. Experiments demonstrate frequency-dependent assembly of anisotropic polymer (SU-8 photoresist) particles in non-uniform AC electric fields (Fig. 6). To understand how pair potentials are connected to microstructures and phase behavior, integrated experiments and models were developed to investigate how anisotropic particles produce different configurations as a function of applied field parameters. Fig. 6 shows experiments (A-E) at 5MHz vs. voltage, which are compared to simulations (K-O) at identical conditions. Increasing field amplitude increases positional and orientational order, changing particles from a fluid to a nematic phase. Inverse analyses to obtain potentials that capture experimental results can be visualized through matching radial and angular distribution functions. More work is needed to refine the dipolar energy landscape based on deviations in the first coordination shell in high density crystalline phases (F).

Future Plans

Future plans will integrate our understanding of colloidal assembly using external fields with our ability to manipulate droplet assembly and patterning to control simultaneously colloidal assembly within multiple droplets. We will first work on controlling colloidal assembly within a single droplet, and then extend the process to multiple droplets on arrays. One important direction will investigate droplets armored with non-spherical particles where the particles are organized in a fashion that leads to anisotropic optical properties. In general, we plan to move to more complex target structures by systematically introducing increasingly complex anisotropic shape elements and patterning into particle, drop, and substrate components of hierarchical structures. By introducing additional degrees of freedom, such processes are anticipated to require external fields to enable feedback control over the interactions, dynamics, and assembly of anisotropic particles within and on patterned drops of varying shape. This approach should achieve the overall project goal of morphogenesis inspired multi-phase colloidal assembly of biomimetic structures.

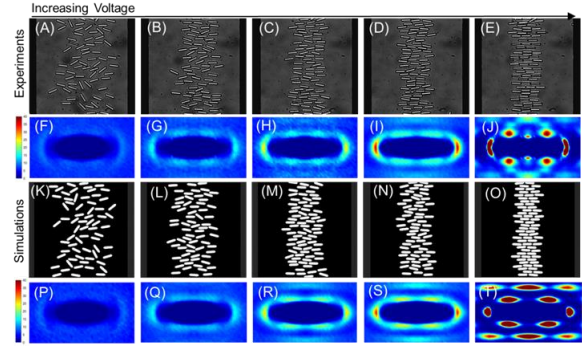


Fig. 6. Microstructure of SU8 super-ellipsoids in non-uniform electric fields (same electrode configuration as Fig. 4) as a function of electric field amplitude at a fixed frequency of 5MHz. (A-E) Optical microscopy experiment images for field amplitudes corresponding to applied voltages of (left-to-right) 0.4V, 0.7V, 1.0V, 1.3V, and 4V. (F-J) Pair correlation functions, $g(r, \theta)$, constructed from particle coordinates in microscopy images. NVT Monte Carlo simulation (K-O) renderings and (P-T) $g(r, \theta)$ based on interactions potentials described in more detail in analysis in Fig. 6.

Publications

“Multifunctional Liquid Marble Compound Lenses,” Donglee Shin, Tianxu Huang, Denise Neibloom, Michael A. Bevan and Joelle Frechette, submitted for publication, 2019.

“Hard Superellipse Phase Behavior & Microstructures,” Isaac Torres-Diaz and Michael A. Bevan, in preparation for publication, 2019.

“Electric Field Mediated Interactions and Assembly of Superellipse Colloids” Rachel Stein, Isaac Torres-Diaz and Michael A. Bevan, in preparation for publication, 2019.

“Spatially Varying Phase Behavior on Multi-Dimensional Energy Landscapes” Jianli Zhang, Junyan Yang and Michael A. Bevan, in preparation for publication, 2019.

“Feedback Controlled Colloidal Assembly on Morphing Energy Landscapes” Jianli Zhang, Yuanxing Zhang and Michael A. Bevan, in preparation for publication, 2019.

Self-Assembly and Self-Replication of Novel Materials from Particles with Specific Recognition.

Paul M. Chaikin, David Pine, Dept. of Physics, New York University.

Nadrian C. Seeman, Marcus Weck, Dept. of Chemistry, New York University.

Program Scope

This program seeks to extend the use of specific DNA recognition and hybridization from the nanoscale to the micro scale. We have exhibited self-replication of DNA origami motifs in one and two dimensions and have recently extended the replication procedure to three dimensions and also shown mutation, selection and competition. We have shown that DNA functionalization allows programmed colloidal assembly and architecture of arbitrary design. A current goal is DNA assisted self-assembly and activation of colloidal micro-machines.

Recent Progress

Spatial Positioning of Single-Walled Carbon Nanotubes. Single-wall carbon nanotubes (SWCNTs) offer many potential advantages for the construction of nanoelectronics and photonic devices. One of the key problems that prevents their convenient utility is the inability to organize them in specific directions at specific points. Here, we report a method to derivatize one end of a SWCNT, and demonstrate that two SWCNTs can be precisely located on a DNA origami construct. The idea behind the method is that a solubilizing DNA single strand is likely to have its 5' end near the reactive end of the SWCNT. If this end contains an amino group, it can react covalently with the SWCNT. The other solubilizing DNA molecules can be replaced by another sequence, and the covalent strand can be used to place that end

precisely. Examples of the types of results that can be obtained by this methodology are shown in Figure 1. Each panel shows a schematic and AFM images.

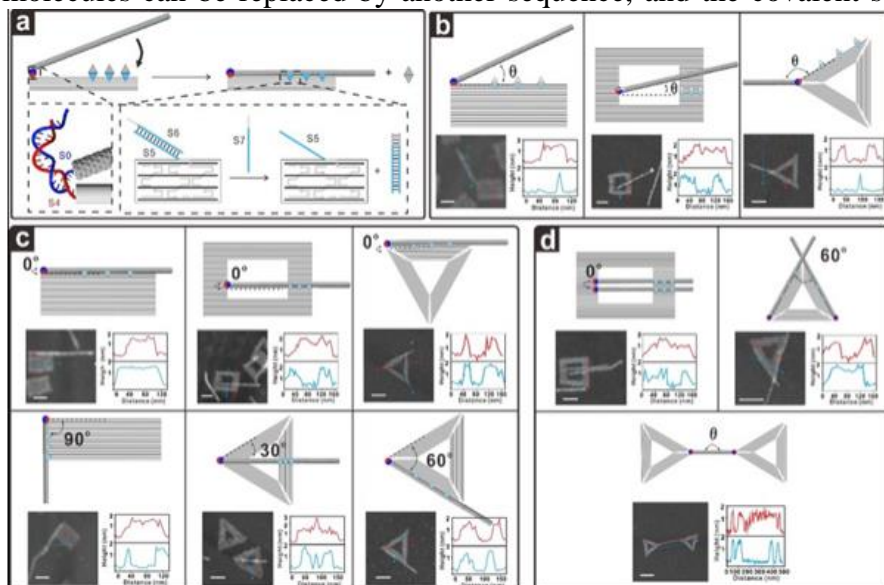


Fig. 1. a). Scheme for placement of DNA end functionalized SWCNTs onto DNA origami templates. b). One-point linkage between SWCNTs and DNA origami templates. c). Control of one SWCNT's orientation on DNA origami templates. d). Control of two SWCNTs' orientation on the DNA origami.

Mutation and selection. Evolution requires mutation. In order to direct the evolution of new materials mutation is a key ingredient. We developed a simple dimer system which allows mutation and different growth rates for the original and mutated dimers. Our monomer tiles have vertical sticky ends that bind and unbind with temperature and horizontal ends that when properly paired can be permanently crosslinked by illuminating with UV. For usual self-

replication and competition we only allow A to vertically bind to A, B to B, C to C, and D to D. Starting with AB seeds and A,B,C,D monomers the result is exponential growth of AB with no other species. We now change the sticky ends so that A binds to A 68% of the time and A binds to C 32% of the time. Similarly for B-B and B-D, C-C and C-A, and D-D and D-B, Fig. 2.

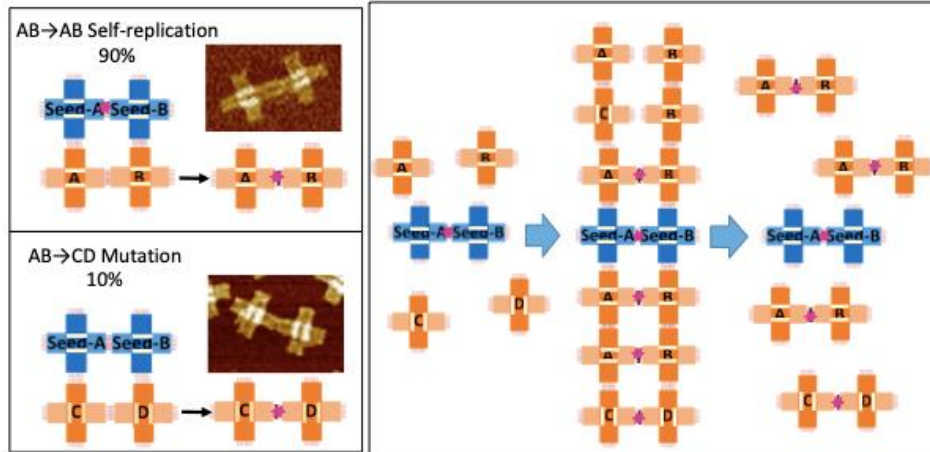
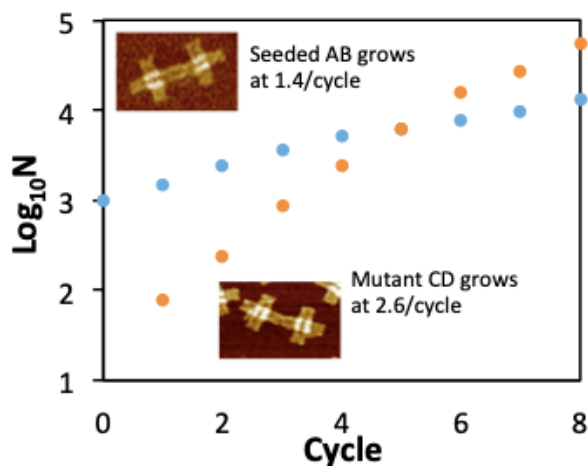


Fig. 2. Left - we adjust the vertical binding sequences such that AB (=,=) binds AB 90% of the time and CD (||,||) 10% of the time. Likewise CD binds to CD 90% and to AB 10%. Right- Our usual “litter” self-replication - cooling a seed dimer can bind monomers vertically in a ladder. The rungs are crosslinked by UV exposure and heating releases the daughter

dimers. Starting with only AB dimer seeds the ladder can now have mistakes. The UV rung crosslinking only binds AB and CD not CB. The offspring can have CD mutants.

We set the system so that AB replicates at a rate of 1.4/cycle while CD replicates at 2.6/cycle. But we only put in AB seeds, Fig. 3. At cycle 0 there are only AB dimers and no CD dimers. $N = 1000 \times (\text{number of dimers}) / (\text{number of seed dimers})$. After cycle 1 $N_{AB} \sim 1400$ and $N_{CD} \sim 100$. The slope of the curve reflects the faster growth rate of CD over AB. By 6 cycles the population



of CD dimers is greater than that of the original AB seeded species.

Fig. 3. We start with two species AB dimers and CD dimers which replicate at different rates by templating. We then make the template recognition imperfect so that an AB has a 10% probability of templating CD (and vice versa). We seed the system only with AB dimers. Initially C and D only exist as nonreplicating pieces. After a generation there are some CD dimers. The crosstalk between species continues but the faster growth rate of CD allows it to take over the system in ~ 6 generations. The mutation creating a CD dimer has led to a new dominant self-replicating species.

Self-replication in two and three dimensions. Previously we demonstrated replication of 1D and 2D motifs, DNA origami tiles joined at their horizontal edges, by templating on their vertical edges or surfaces. Direct 3D templating would require going to the fourth dimension. Instead we have developed two schemes that involve the folding of 2D structures to make them 3D. 1) we unfold a 3D structure, template in 3D on the parent surfaces and then refold. 2) We use the edges of a 3D structure and then fold the monomers in such a way that they can be permanently crosslinked into the 3D structure and then released. A simple 3D structure is a cube corner as can be made by joining the closest edges of the B and C crosstiles in the orange parent of Fig. 4. The

cube corner, Fig. 5, can be replicated by releasing these edges to make the flat 2D structure, replicating it as in figure 1 and then refolding both the parent and daughters to make two cube corner structures.

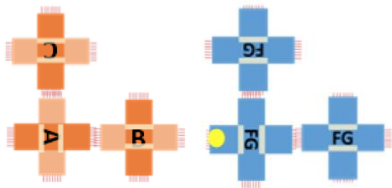


Fig. 4. Schematic of two dimensional self replication by templating the blue monomers to the surface of the parent (using complementary ssDNA), then permanently crosslinking the blue monomers at their common edges (using DNA modified with UV activated ^{CNV}K pseudo bases) and releasing from the parent (by heating).

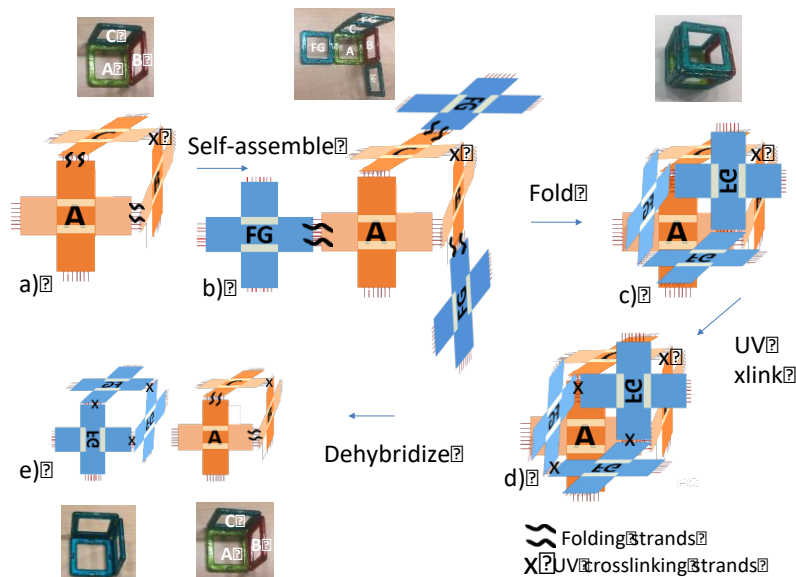


Fig. 5. Self replication cycle for 3D cube corners. a) A cube corner “parent” made by folding (\approx strands) and crosslinking (x strands) 3 DNA origami crossstiles. b) Daughter tiles are assembled by reversible hybridization of DNA on specific edges of the parent. c) folding strands close the cube bringing edges of the daughter tiles together. d) the daughter edges are hybridized and then permanently UV crosslinked. e) Parent and daughters are separated by heating.

The direct 3D-3D replication is shown in Fig. 5. Here we start with a cube corner as in Fig. 5a upper left as the parent or seed. (A magnetic square toy shows the orientation of the cube corner faces.) Next generation monomer tiles are DNA functionalized to assemble on specific edges of the parent as flaps on hinges. There is some probability that they can reach and bind with the other flaps to complete the cube but this is not efficient. We add additional DNA single strands on the parent and daughter tiles that hybridize to fold the flaps inward to finish the cube corners. The daughter tiles are now in a position to be hybridized and after annealing UV light is applied to permanently crosslink the daughters in a complementary cube corner. Heating releases the cube corners, replicating and doubling the number of cube corners with each cycle, Fig. 6.

DNA powered micro machines. Although there have been several DNA motors previously produced, they typically work on a scale of nanometers and hours. We engineer devices that work on the colloidal or cellular scale (microns) at fractions of a second. Our basic design is a

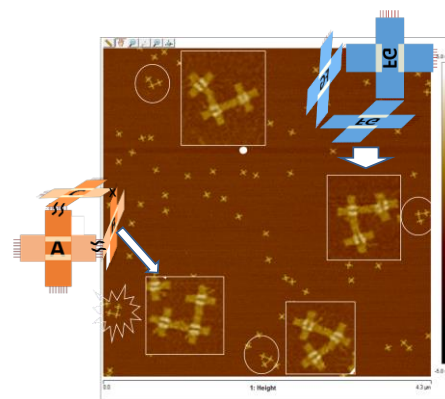


Fig. 6. AFM images indicate the parent (orange) and daughter (blue) trimers formed by the cube corner technique. Parents are identified by all “=” signs being aligned. Daughters have a mismatch. The 3D cube corner is most often ruptured by the strong forces flattening the origami on the Mica surface. But on the bottom we see an unbroken daughter though still flattened. Cross-tiles are 100nm x 100nm

The direct 3D-3D replication

flexible hinge between stiff rods spanned by complementary DNA single strands which can bind to close the hinge, Fig. 7. The geometry dictates a mechanical advantage of ~ 30 . Our accordion device consists of 9 hinges, the first rod attached to a substrate and the last to a colloid which can be pulled with a laser tweezer to an extension of ~ 4 microns. Pulling unzips the DNA in the

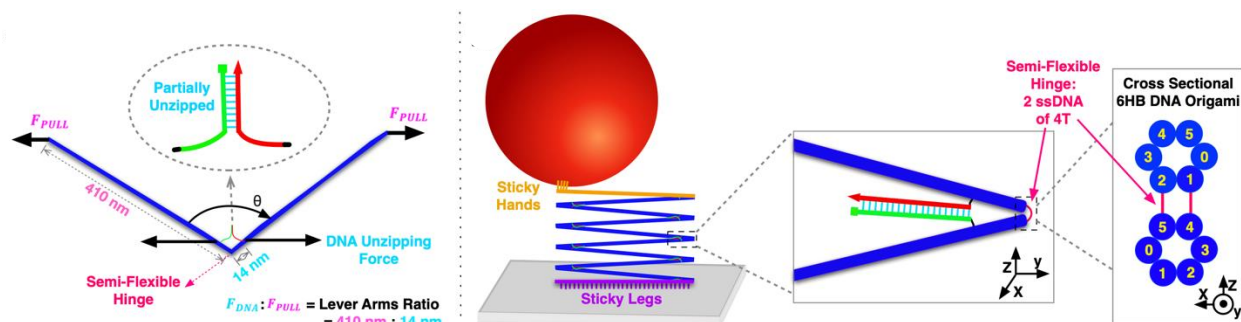


Fig. 7. Center -Accordion structure with 9 DNA hinges and working distance ± 4 microns. Right- Two rods (6Helix bundles) hinged by ssDNA and coupled with complementary ssDNA provides a lever arm (left) advantage of ~ 30 amplifying the 30nm scale DNA unzipping to micron scale.

hinges and stores energy. Releasing the colloidal particle the DNA zips up, recovering the stored energy in $< \frac{1}{2}$ second and moving the colloid at speeds > 10 microns/sec. A force-extension measurement, Fig. 8., on the accordion structure with and without complementary DNA near the hinges shows that the energy stored in the DNA unzipping and recovered is $436k_B T$ compared to the $468k_B T$ calculated hybridization energy for the DNA sequences used.

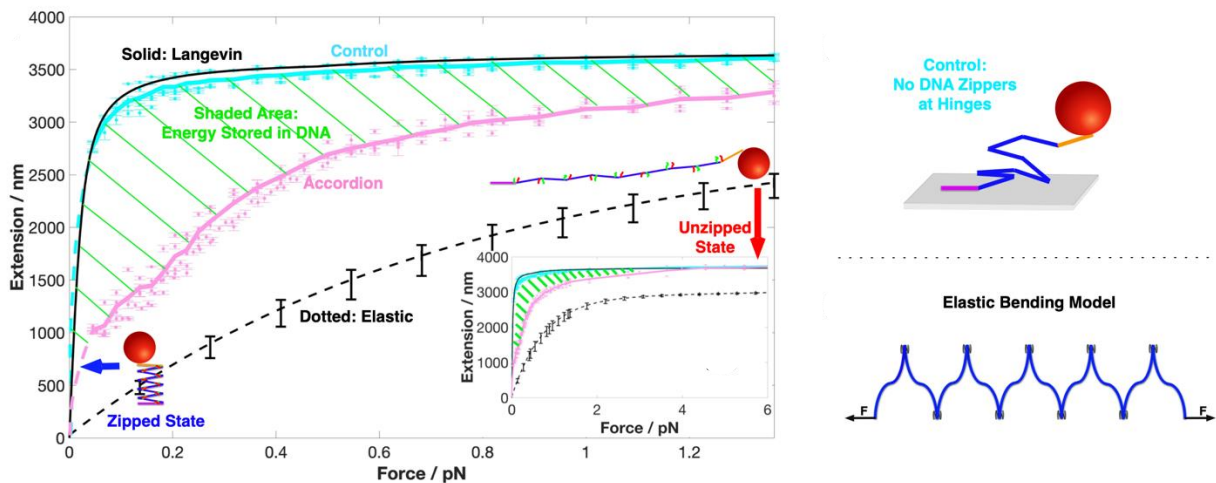


Fig. 8. Force-extension curve for our 9 hinge accordion structure (pink). Control (cyan) is without complementary DNA strands near hinges. Langevin (black) is calculation for freely jointed rods. Elastic (dotted) calculation is if the DNA hinges remained zipped, hybridized. The energy stored in DNA unzipping is the shaded area.

Future Plans

- Replication of more complex 2 and 3 dimensional structures
- Further mutation, selection and competition experiments
- Directed evolution of materials and devices
- DNA micro-machines, pumps, motile and swimming systems using DNA heat engines with local heating as “fuel”

Publications 2017-2019

1. Wang, Xiao, Ruojie Sha, Martin Kristiansen, Carina Hernandez, Yudong Hao, Chengde Mao, James W. Canary, and Nadrian C. Seeman. "An Organic Semiconductor Organized into 3D DNA Arrays by "Bottom-up" Rational Design." *Angewandte Chemie International Edition* 56, no. 23 (2017): 6445-6448.
2. Zion, Matan Yah Ben, Xiaojin He, Corinna C. Maass, Ruojie Sha, Nadrian C. Seeman, and Paul M. Chaikin. "Self-assembled three-dimensional chiral colloidal architecture." *Science* 358, no. 6363 (2017): 633-636.
3. Zheng, Xiaolong, Mingzhu Liu, Mingxin He, David J. Pine, and Marcus Weck. "Shape-Shifting Patchy Particles." *Angewandte Chemie* 129, no. 20 (2017): 5599-5603.
4. Hao, Yudong, Martin Kristiansen, Ruojie Sha, Jens J. Birktoft, Carina Hernandez, Chengde Mao, and Nadrian C. Seeman. "A device that operates within a self-assembled 3D DNA crystal." *Nature chemistry* 9, no. 8 (2017): 824.
5. He, Xiaojin, Ruojie Sha, Rebecca Zhuo, Yongli Mi, Paul M. Chaikin, and Nadrian C. Seeman. "Exponential growth and selection in self-replicating materials from DNA origami rafts." *Nature materials* 16, no. 10 (2017): 993.
6. Zhang, Yin, Angus McMullen, Lea-Laetitia Pontani, Xiaojin He, Ruojie Sha, Nadrian C. Seeman, Jasna Brujic, and Paul M. Chaikin. "Sequential self-assembly of DNA functionalized droplets." *Nature communications* 8, no. 1 (2017): 21.
7. Seeman, Nadrian C., Ruojie Sha, Jens Birktoft, Jianping Zheng, Wenyan Liu, Tong Wang, and Chengde Mao. "Designed 3D DNA crystals." In *3D DNA Nanostructure*, pp. 3-10. Humana Press, New York, NY, 2017.
8. Hernandez, Carina, Jens J. Birktoft, Yoel P. Ohayon, Arun Richard Chandrasekaran, Hatem Abdallah, Ruojie Sha, Vivian Stojanoff, Chengde Mao, and Nadrian C. Seeman. "Self-assembly of 3D DNA crystals containing a torsionally stressed component." *Cell chemical biology* 24, no. 11 (2017): 1401-1406.
9. Conn, Fiona W., Michael Alexander Jong, Andre Tan, Robert Tseng, Eunice Park, Yoel P. Ohayon, Ruojie Sha, Chengde Mao, and Nadrian C. Seeman. "Time lapse microscopy of temperature control during self-assembly of 3D DNA crystals." *Journal of Crystal Growth* 476 (2017): 1-5.
10. Ellis-Monaghan, Joanna A., Greta Pangborn, Nadrian C. Seeman, Sam Blakeley, Conor Disher, Mary Falcigno, Brianna Healy, Ada Morse, Bharti Singh, and Melissa Westland. "Design tools for reporter strands and DNA origami scaffold strands." *Theoretical Computer Science* 671 (2017): 69-78.
11. Conn, Fiona W., Michael Alexander Jong, Andre Tan, Robert Tseng, Eunice Park, Yoel P. Ohayon, Ruojie Sha, Chengde Mao, and Nadrian C. Seeman. "Time lapse microscopy of temperature control during self-assembly of 3D DNA crystals." *Journal of Crystal Growth* 476 (2017): 1-5.

12. Elacqua, Elizabeth, Xiaolong Zheng, Cicely Shillingford, Mingzhu Liu, and Marcus Weck. "Molecular Recognition in the Colloidal World." *Accounts of chemical research* 50, no. 11 (2017): 2756-2766.
13. Zhao, Yue, Ruojie Sha, Yudong Hao, Carina Hernandez, Xinshuai Zhao, David Rusling, Jens J. Birktoft et al. "Self-Assembled Three-Dimensional Deoxyribonucleic Acid (DNA) Crystals." *Foundations of Crystallography* 74 (2018): a253.
14. Zhang, Yin, Xiaojin He, Rebecca Zhuo, Ruojie Sha, Jasna Brujic, Nadrian C. Seeman, and Paul M. Chaikin. "Multivalent, multiflavored droplets by design." *Proceedings of the National Academy of Sciences* 115, no. 37 (2018): 9086-9091.
15. Wang, Xiao, Chen Li, Dong Niu, Ruojie Sha, Nadrian C. Seeman, and James W. Canary. "Construction of a DNA Origami Based Molecular Electro-optical Modulator." *Nano letters* 18, no. 3 (2018): 2112-2115.
16. Zhao, Jiemin, Yue Zhao, Zhe Li, Yong Wang, Ruojie Sha, Nadrian C. Seeman, and Chengde Mao. "Modulating Self-Assembly of DNA Crystals with Rationally Designed Agents." *Angewandte Chemie International Edition* 57, no. 50 (2018): 16529-16532.
17. Liu, Mingzhu, Xiaolong Zheng, Fangyuan Dong, Michael D. Ward, and Marcus Weck. "Reversible Morphology Switching of Colloidal Particles." *Chemistry of Materials* 30, no. 19 (2018): 6903-6907.
18. Wang, Xing, Arun Richard Chandrasekaran, Zhiyong Shen, Yoel P. Ohayon, Tong Wang, Megan E. Kizer, Ruojie Sha et al. "Paranemic crossover DNA: There and back again." *Chemical reviews* 119, no. 10 (2018): 6273-6289.
19. Lee, Saerom, Jeong Hoon Yoon, In-Seong Jo, Joon Suk Oh, David J. Pine, Tae Soup Shim, and Gi-Ra Yi. "DNA-functionalized 100 nm polymer nanoparticles from block copolymer micelles." *Langmuir* 34, no. 37 (2018): 11042-11048.
20. Moon, Jeongbin, In-Seong Jo, Etienne Ducrot, Joon Suk Oh, David J. Pine, and Gi-Ra Yi. "DNA-Coated Microspheres and Their Colloidal Superstructures." *Macromolecular Research* 26, no. 12 (2018): 1085-1094.
21. Gao, Xiang, Matthew Gethers, Si-ping Han, William A. Goddard III, Ruojie Sha, Richard P. Cunningham, and Nadrian C. Seeman. "The PX motif of DNA binds specifically to Escherichia coli DNA polymerase I." *Biochemistry* 58, no. 6 (2018): 575-581.
22. Zhuo, Rebecca, Feng Zhou, Xiaojin He, Ruojie Sha, Nadrian C. Seeman, and Paul M. Chaikin. "Litters of self-replicating origami cross-tiles." *Proceedings of the National Academy of Sciences* 116, no. 6 (2019): 1952-1957.
23. Pei, Hao, Ruojie Sha, Xiwei Wang, Ming Zheng, Chunhai Fan, James W. Canary, and Nadrian C. Seeman. "Organizing End-Site-Specific SWCNTs in Specific Loci Using DNA." *Journal of the American Chemical Society* (2019).
24. Ohayon, Y., Hernandez, C., Chandrasekaran, A.R., Wang, X., Abdallah, H., Jong, M.A., Mohsen, M., Sha, R., Birktoft, J.J., Lukeman, P.S. and Chaikin, P.M., Stephen L. Ginell, Chengde Mao, and Nadrian C. Seeman. Designing Higher Resolution Self-Assembled 3D

DNA Crystals via Strand Terminus Modifications. *ACS Nano*. DOI:
10.1021/acsnano.9b02430 (2019)

Microtubule based three dimensional active matter

Principle Investigator: Zvonimir Dogic, Department of Physics, University of California at Santa Barbara, Santa Barbara, CA 93106.

Program Scope:

Active matter is an assembly of microscopic objects, each consuming energy to generate continuous dynamics. Interactions between such animate units lead to emergent properties that are strikingly different from those found in conventional materials assembled from inanimate passive objects. The field of active matter aims to develop a theoretical framework that robustly predicts the emergence of large-scale dynamical behaviors, given elemental units of known structure and interactions. The paucity of motile elements that robustly operate in higher dimensions led to the situation where there are relatively few studies of three-dimensional active matter, especially when compared to the rapid advances being made with 2D systems. However, studies of 3D active matter are important from both fundamental and applied perspectives. From a fundamental perspective diverse physical properties of equilibrium materials are highly dependent on the system dimensionality. From a practical perspective, active matter provides a versatile platform for the engineering of macroscale autonomous motion that is collectively powered by nanoscale molecular machines. It is likely that many applications will require materials that robustly operate in three dimensions. These arguments advocate for experimentally realizing 3D model systems of active matter and elucidating that structural and dynamical properties. While continuing quantitative studies of already established 2D experimental systems, over the past two years we have made significant progress of extending our model systems of microtubule based active matter to three dimensions and characterizing their structure and dynamics. We described the most important advances below.

Recent Progress:

Mechanics of composite microtubule bundles: At the most basic level all of the active matter materials studied in this project are driven by motor driven extensile microtubule bundles that are held together by weak depletion attractions. Of particular importance is the motor driven buckling and fraying of such bundles. We have developed a novel optical tweezers based method to assemble bundles with known structure and quantitatively study their buckling and fraying in response to an imposed external stress. Measurements of the applied force as a function of compression strain reveals that the composite bundles fray above a critical strain. Decreasing strain leads to filament rebundling, but this occurs at a very different magnitude of imposed strain. We have measured the resulting adhesion hysteresis and how it depends on the relevant microscopic parameters (Fig. 1). We have also developed a method of self-consistently coarse-graining the discrete theoretical description to test our experimental findings for which continuum description is more appropriate.

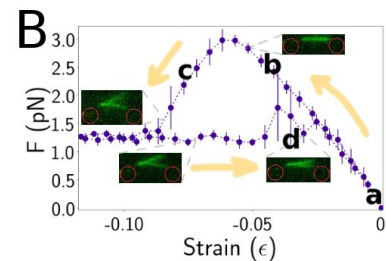


Fig. 1: Plotting applied force as a function of strain reveals adhesion hysteresis of fraying microtubule bundles.

Dynamics of confined 2D active nematics: In bulk, 2D active nematics exhibit chaotic dynamics that is driven by unbinding and annihilation of point-like topological defects. We studied how

hard-wall boundaries transform the chaotic dynamics of a bulk system into regular circular flows. We quantified the behavior of the confined active nematics over multiple regimes. Our experiments revealed two distinct phenomena that are not described by the existing theories. First, experiments revealed

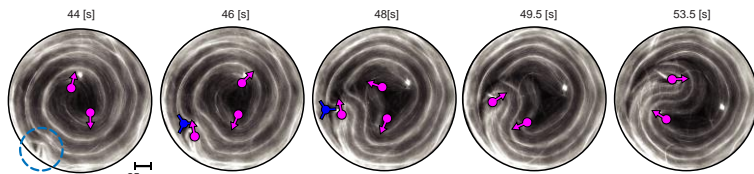


Fig. 2: Confined 2D active nematics exhibit robust doubly period dynamics consisting on boundary induced defect nucleation and inwards propagation that is superimposed on the circular flows.

existence of a doubly-periodic spatiotemporal pattern, whereas theory predicts a singly-periodic circulation (Fig. 2). Second, experiments showed that the transition from circular flows to turbulence occurs in two distinct steps as a function of confinements size. In a first step, we observed proliferation of topological defects that coexist with circular flows. In a subsequent step there is complete loss of coherence and transition to bulk-like turbulence. In contrast, theory predicts that both the onset of defect proliferation and loss of coherence occur at the same confinement strength. Based on the analysis of the evolving director field of confined active nematics, we suggested ways in which to improve the current theories of active nematics. More broadly, the dynamics of confined active nematics we studied is evocative of the phenomena observed in living organisms, which frequently exhibit robust self-organized patterns on lengthscales and timescales that are significantly larger than those of the biochemical constituents. Understanding the organizing principles that drive the dynamics of confined active nematics might reveal general strategies for rationally engineering adaptable and reconfigurable biomimetic materials.

Quantifying the instability of 3D extensile fluids: Theoretical predictions that aligned extensile rod-like agents are inherently unstable is a foundational result that underlies much of the rich phenomenology of the active nematic liquid crystals. Over the past year we have undertaken efforts to systematically study the onset and growth of such instabilities and how they depends on both the material properties of the active nematics and the confinement geometry (Fig. 3). Specifically, using an initial state consisting of flow aligned microtubule bundles

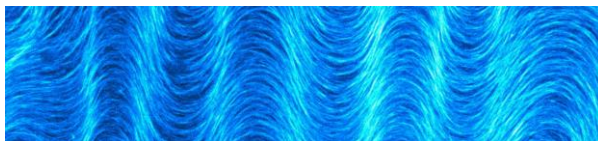


Fig. 3. Shear aligned extensile microtubule bundles exhibit instability whose wavelength and growth rate are determined by the three dimensional confining geometries.

we have developed a unique method of measuring the wavelength and the growth rate of the instability. Extensive experiments demonstrated that the characteristics of the instability, including the wavelength and its growth rate, are not intrinsic to the material under consideration but are largely determined by the hydrodynamic interactions that are imposed by the boundary conditions.

Statistical properties of 2D active nematics: We studied the dynamics of a tunable 2D active nematic liquid crystal composed of microtubules and kinesin motors confined to an oil–water interface. In this system kinesin motors continuously inject mechanical energy into the system through ATP hydrolysis, powering the relative microscopic sliding of adjacent microtubules. This in turn generates macroscale autonomous flows and chaotic dynamics. We used particle image velocimetry to quantify two-dimensional flows of such active nematics and extract their statistical properties. In agreement with the

hydrodynamic theory, we found that the vortex areas of chaotic flows are exponentially distributed, which allowed us to extract the characteristic system length scale. We determined the dependence of the resulting active nematic length scale on the ATP concentration, which is the experimental knob that tunes the magnitude of the active stress. Our data raise important questions regarding the possible mappings between the experimentally controlled ATP concentration and the active stresses that are the input of existing theoretical models. Our work suggest a quantitative mapping that is rooted in the Michaelis–Menten kinetics that governs the microscopic stepping motion of individual kinesin motors.

Development of model systems of 3D active fluids: Our original work demonstrated robust assembly of microtubule based active fluids that are powered by kinesin molecular motors. Over the past few years we have improved on the initial formulation of isotropic active fluids in several important ways. First, by switching to the non-processive kinesin motors we significantly increased the temporal stability of the active dynamics. Second, by using a different linking strategy to create kinesin clusters we have extended the duration of active dynamics from several hours to several days (Fig. 4). Third, by replacing broadly acting depletant agents with a specific microtubule cross-linker that still allows for interfilament sliding, we have created systems that are miscible with passive soft materials, such as, polymer gels or colloidal liquid crystals. Using these features we have developed a new model system of 3D active nematics with a number of unique desirable features that will allow for characterization of their spatial structure and temporal dynamics with unprecedented detail.

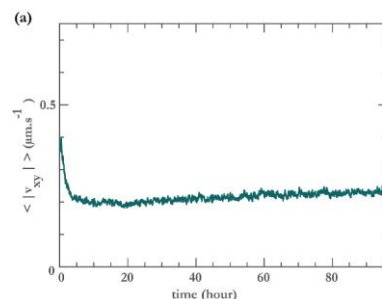


Fig. 4: SNAP-linked kinesin active gels exhibit steady state dynamics on timescales of hundred allows allowing for acquisition of highly quantitative data.

Structure and dynamics of 3D active nematics: In 2D active nematics, the continual injection of energy by the energy consuming self-propelled anisotropic constituents destabilizes large-scale uniform alignment, leading to chaotic turbulent-like state in which pairs of motile point-like defects are continually created and destroyed. Such universal dynamics can be described by coarse-grained theoretical model and is observed in remarkably diverse 2D systems of varying scales and complexities, ranging from shaken granular rods and motile living cells. In two-dimensions motile topological defects are necessarily point-like. How dynamics of active nematics generalizes to 3D materials remains poorly understood. Several obstacles have hindered progress in this direction. First, many of the existing model systems of two-dimensional active nematics are not easily generalized to higher dimensions. Second, characterizing dynamics of three dimensional materials requires full structural and dynamical characterization of topological defects on macroscopic length scales, an experimental feat that has not been accomplished for equilibrium materials.

We have assembled 3D active nematics that are comprised of uniform mixture of extensile microtubule bundles and passive colloidal rods in a nematic phase. At high enough microtubule concentrations the extensile bundles generate active stresses that are transmitted on the passive liquid crystal, generating steady state turbulent like dynamics. By relying on the advances in light sheet imaging we have been able to directly visualize the structure of the 3D nematic field on

millimeter scales with a single filament resolution, and follow the temporal evolution of such a field. Such data has shown that topologically neutral disclination loops are the lowest energy excitations of 3D active nematics. Furthermore, detailed analysis of the director field revealed that the system dynamics is dominated by a family of loops interpolating between two emblematic geometries: the *wedge-twist* and *pure-twist* loops. In steady state the density of loops is constant. Tracking loop dynamics allowed us to identify dominant mechanisms of loop creation and annihilation, as well as recombination event by which loops merge and split from a background percolating network of disclination lines (Fig. 5).

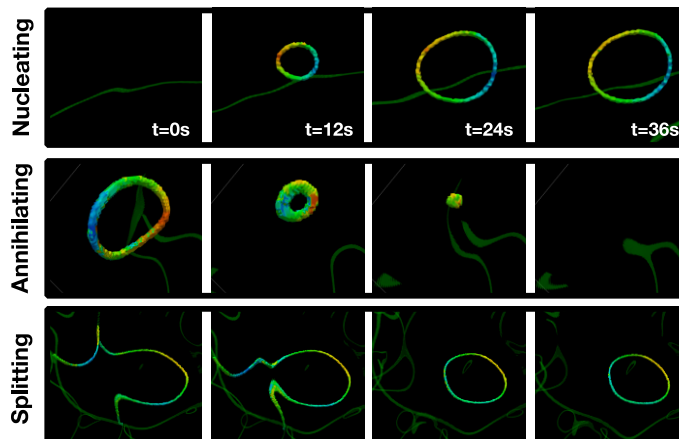


Fig. 5. Dynamics of nucleation and self-annihilation of topologically neutral disclination loops in 3D active nematics. Third row show recombination of a disclination loop with a background network that spans the sample.

Future Plans: The development of composite 3D active nematics is opening up many new exciting experimental opportunities. In one significant direction we are studying the dynamics of 3D active nematics confined in various geometries. Of particular importance is to develop methods of homeotropic anchoring in order to explore how activity induces a transition of a point-like topologically charged hedgehog defect into an extended disclination loop. In a complementary direction we are studying how defects arise from initially aligned 3D active nematics, and how this depends on the confinement size. To characterize the properties of the constituent extensible bundles we are currently extending our optical tweezer techniques to measure the rate at which kinesin motors generate filament sliding and the force that is exerted by such sliding microtubules.

Publications which acknowledge full or partial DOE support:

1. "Self-organized dynamics and the transition to turbulence of confined active nematics" Achini Opathalage, Michael M. Norton, Michael P. N. Juniper, Blake Langeslay, S. Ali Aghvami, Seth Fraden, and Zvonimir Dogic, *Proc. Nat. Acad. Sci.* **116** 4788-4797 (2019)
2. "Statistical Properties of Autonomous Flows in 2D Active Nematics" Linnea M Lemma, Stephen J Decamp, Zhihong You, Luca Giomi, Zvonimir Dogic, *Soft Matter*, **15**, 3264-3272 (2019).
3. "Microtubules soften due to cross-sectional flattening" Edvin Memet, Feodor Hilitski, Margaret A. Morris, Walter J. Schwenger, Zvonimir Dogic, and L. Mahadevan, *eLife*, 34695 (2018).
4. "Active matter at the interface between materials science and cell biology" Daniel Needleman and Zvonimir Dogic, *Nature Reviews Materials* **2**, Article number: 17048 (2017).

Self-Assembly of Virus Particle Based Materials for Hydrogen Catalysis

Trevor Douglas (PI) Department of Chemistry, Indiana University

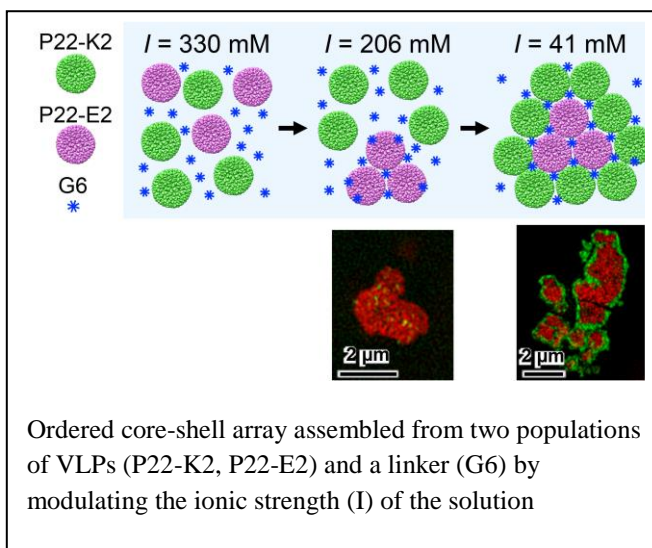
Masaki Uchida (Co-I), Department of Chemistry, Fresno State University

Program Scope

The overall goal of this project is to design and assemble materials, over multiple lengthscales, that incorporate active catalysts. We will design and refine strategies for using the P22 as a nanoscale building block for controlling the higher order assembly of multiple capsids to form hierarchically ordered 3-D superlattice arrays. These directed assembly approaches will be combined to create active P22-based materials that are capable of undertaking complex catalytic reactions.

Recent Progress

We have demonstrated the bio-inspired modular construction of materials with three levels of hierarchy using virus-like particles (VLPs). The first level of hierarchy is the formation of catalytically active VLPs through directed enzyme encapsulation concurrent with VLP assembly. This was achieved by exploiting a capsid formation process involving two types of subunit proteins, coat proteins (CPs) and scaffolding proteins (SPs). Cargo proteins such as enzymes can be directed inside of VLPs through genetic fusion with SP. The second level of hierarchy is the assembly of these VLP building blocks into ordered three-dimensional arrays. This was achieved through electrostatic interaction between negatively charged VLPs and positively charged linker molecules. Ordered VLP arrays with face-centered cubic (FCC) lattices were formed at an optimal solution ionic strength at which proper balance between attractive and repulsive interaction between the building blocks was realized. We demonstrated that an array, constructed from two populations of enzyme packaged VLPs, exhibited a coupled two-step catalytic conversion for isobutanol synthesis from alpha-ketoisovalerate via



isobutyraldehyde. Assembly conditions can be finely tuned by manipulating the surface charge of VLPs. This leads to implementation of the third level of hierarchy into the arrays. Two populations of VLPs were selectively assembled with spatial control over each population within the array resulting in construction of a core-shell array with an FCC structure (Fig 1).

Future Plans

We recently adopted a course-grain computational method to model the higher order assembly of these VLPs. Effective feedback between computational model and experimental verification can lead to the design of hierarchically organized VLP arrays with desired functionalities in a predictable manner and allow us to explore a wide parameter space (ionic strength, VLP surface charge, dendrimer to VLP ratio) which will inform future experiments.

Design and assembly of materials that are catalytically responsive to changes in external environment (pH, ionic strength).

Co-encapsulation of partner enzymes for hydrogen production (cytB and cytB reductase together with the [NiFe] hydrogenase Hyd-1).

Publications

- William M. Aumiller Jr., Masaki Uchida, Trevor Douglas “Protein cage assembly across multiple length scales” *Chem. Soc. Rev.* (2018) 47, 3433-3469. DOI: 10.1039/C7CS00818J
- William M. Aumiller Jr., Masaki Uchida, Daniel W. Biner, Heini M. Miettinen, Byeongdu Lee, and Trevor Douglas “Stimuli Responsive Hierarchical Assembly of P22 Virus-Like Particles” *Chem. Mater.* (2018), 30, 2262–2273. DOI: 10.1021/acs.chemmater.7b04964
- Kimberly McCoy, Masaki Uchida, Byeongdu Lee, Trevor Douglas “Templated Assembly of a Functional Ordered Protein Macromolecular Framework from P22 Virus - Like Particles” *ACS Nano* (2018), 12, 3541-3550. DOI: 10.1021/acsnano.8b00528
- Masaki Uchida, Kimberly McCoy, Masafumi Fukuto, Lin Yang, Hideyuki Yoshimura, Heini M. Miettinen, Ben LaFrance, Dustin Patterson, Benjamin Schwarz, Jonathan A. Karty, Peter E. Prevelige Jr., Byeongdu Lee, Trevor Douglas “Modular self-assembly of protein cage superlattices for multistep catalysis and material regeneration” *ACS Nano* (2018), 12, 942-953. DOI: 10.1021/acsnano.7b06049
- Ekaterina Selivanovitch, Trevor Douglas “Virus capsid assembly across different length scales inspire the development of virus-based biomaterials” *Current Opinion in Virology* (2019) 36, 38-46. DOI: 10.1016/j.coviro.2019.02.010
- Nicholas E. Brunk, Masaki Uchida, Byeongdu Lee, Masafumi Fukuto, Lin Yang, Trevor Douglas, and Vikram Jadhao “Dendrimer-mediated Assembly of Virus-like Particles into Arrays via Electrostatic Control” *ACS Appl. Bio Mater.* 2019252192-2201. DOI: 10.1021/acsabm.9b00166

Control of charge transfer and light-driven reactions in nanocrystal-enzyme complexes

Gordana Dukovic, University of Colorado Boulder

Program Scope

The overarching long-term goal of this project is to understand how the remarkable light-harvesting properties of semiconductor nanocrystals could be synergistically combined with the outstanding properties of redox enzymes that catalyze complex and useful reactions to enable efficient solar photochemistry. This approach is inspired by photosynthesis, where light absorption is coupled to catalysis via electron transfer steps. Specifically, this project is focused on how the structural properties of semiconductor nanocrystals govern their interactions with natural enzymes, the electron pathways involved, and the final chemistry at the enzyme active site. We aim to provide design principles for synthetically tailoring these optimal light absorbers and integrating them with enzymatic catalysts in a way that minimizes energy-wasting processes. Furthermore, we aim to understand and control the excited state properties of nanocrystals to enhance their photochemistry.

Recent Progress

1. Elucidating and controlling electron transfer from CdS nanorods to hydrogenase for photochemical H₂ generation

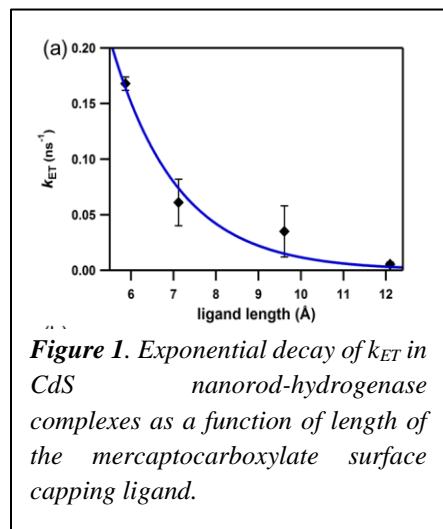
For several years, we have been working on understanding and controlling electron transfer (ET) from Cd-chalcogenide nanocrystals, such as CdS nanorods, and [FeFe] Hydrogenase I from *Clostridium acetobutylicum* and elucidating the relationship between this ET and the overall photochemical activity.^{1,2,3,4,5,6} This work is in collaboration with the group of Paul King at the National Renewable Energy Laboratory. In prior reporting periods, we have measured ET kinetics with transient absorption (TA) spectroscopy, developed a kinetic model to extract rate constants for this process, found that the competition between ET and electron-hole recombination in the nanocrystal is the main factor that determines H₂ production efficiency, and found that the rate constant for ET depends on the ligands capping the nanocrystal surface.^{2,3,5} In the last two years, we have continued to improve our understanding and control of this process. The following are two key accomplishments of the last 2 years in this area.

A method for calculating quantum efficiency of charge transfer competing against non-exponential processes and its application to the nanocrystal-hydrogenase system.

Photoexcited charge transfer from semiconductor nanocrystals to charge acceptors is a key step for photon energy conversion in semiconductor nanocrystal-based light-harvesting systems. Charge transfer competes against relaxation processes within the nanocrystals, and this competition determines the quantum efficiency of charge transfer. The quantum efficiency is a critical design element in photochemistry, but in nanocrystal-acceptor systems its extraction from experimental data is complicated by sample heterogeneity and intrinsically non-exponential

excited-state decay pathways. We systematically explored these complexities using TA spectroscopy over a broad range of timescales to probe ET from CdS nanorods to hydrogenase. To analyze the experimental data, we built a model that quantifies the quantum efficiency of charge transfer in the face of competing, potentially non-exponential, relaxation processes. Our approach can be applied to calculate the efficiency of charge or energy transfer in any donor–acceptor system that exhibits non-exponential donor decay and any ensemble distribution in the number of acceptors provided that donor relaxation and charge transfer can be described as independent, parallel decay pathways. We applied this analysis to our experimental system and unveiled the connections between particle morphology and quantum efficiency. The approach

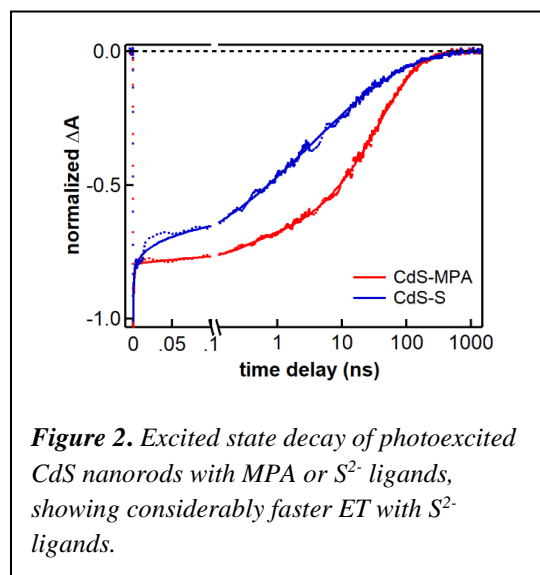
developed here is straightforward to implement and should be applicable to a wide range of systems. This work was published this year.⁶



Fast ET with ultra-short surface-capping ligands in CdS-hydrogenase. The binding interaction between CdS nanorods and hydrogenase is electrostatic in nature, with negatively charged 3-mercaptopropionic acid (MPA) ligands on the nanocrystal surface binding to the positively charged patch on the enzyme, which is the docking site of the natural electron donor, ferredoxin. The MPA ligands therefore form the interface between the two components and it is natural to expect them to play an important role in determining the value of k_{ET} . We measured the value of k_{ET} , as well as the H_2

quantum yield, as a function of the length of the aliphatic chain of the mercaptocarboxylate ligands and found an exponential decay behavior (**Figure 1**) that suggests that the ligand serves as a tunneling barrier for the electron. This work was published in 2018.⁵ This result suggests

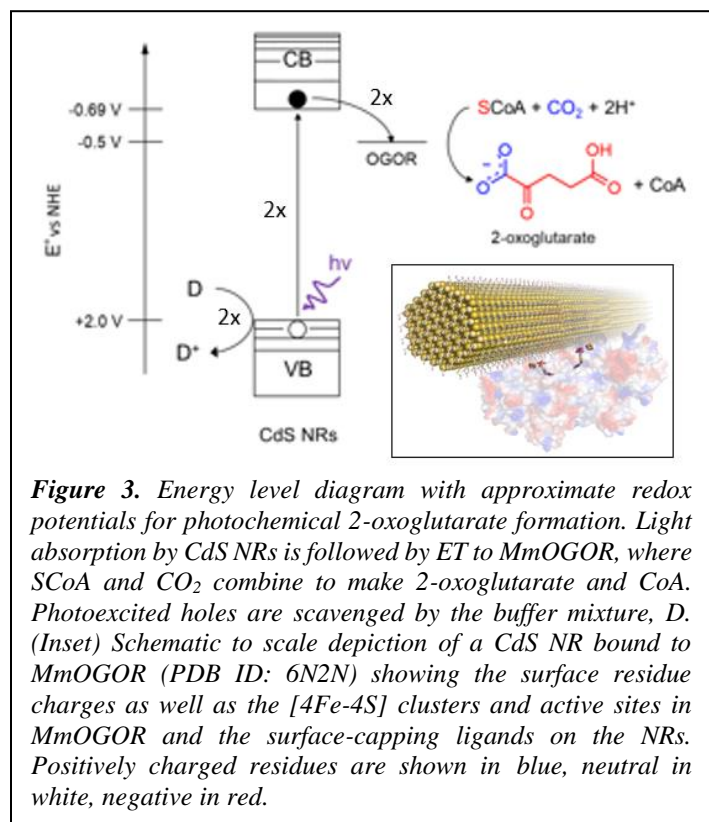
that the value of k_{ET} can be manipulated over a wide range by careful selection of surface capping ligands.



Using photoexcited nanocrystals to drive enzyme catalysis allows for the possibility of delivering multiple electrons at the same time, allowing us to perhaps observe new behavior or mechanisms in enzymatic catalysis. To enable the simultaneous transfer of multiple electrons, the ET must be competitive with Auger recombination which occurs on the timescale of approximately 100 ps. We demonstrated with CdS-hydrogenase that we can achieve sufficiently fast ET rates by switching the nanocrystal surface ligands from our usual mercaptopropionate (MPA) to the ultra-short single

atom ligand S^{2-} , which greatly reduces the tunneling barrier for ET from the nanocrystal to the enzyme. Measurements of ET rate constants obtained by TA spectroscopy for CdS-hydrogenase systems for CdS nanorods with MPA versus those with S^{2-} surface ligands showed ET time constants of ~ 16 ns and ~ 43 ps, respectively—indicating that with S^{2-} ligands, ET could compete with Auger recombination for multiple simultaneous ETs to the enzyme (**Figure 2**). This work is being prepared for publication.

2. Light-driven carbon-carbon bond formation via CO_2 reduction catalyzed by complexes of CdS nanorods and a 2-oxoacid oxidoreductase

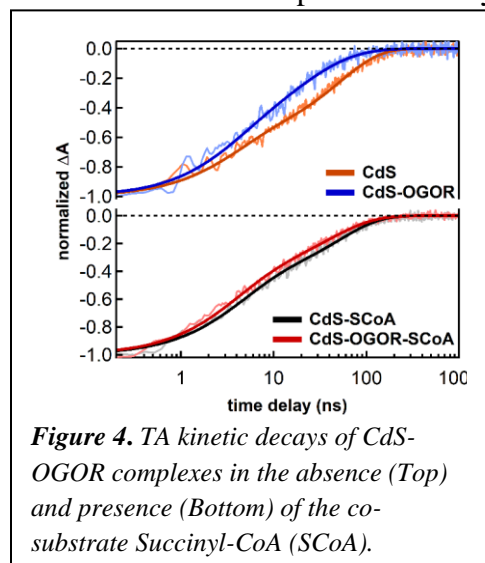


Redox enzymes are capable of catalyzing a vast array of useful reactions, but they require redox partners that donate or accept electrons. Semiconductor nanocrystals provide a mechanism to convert absorbed photon energy into redox equivalents for enzyme catalysis. In collaboration with the group of Sean Elliott at Boston University, we recently described a system for photochemical carbon-carbon bond formation to make 2-oxoglutarate by coupling CO_2 with a succinyl group. Photoexcited electrons from CdS nanorods transfer to 2-oxoglutarate:ferredoxin oxidoreductase from *Magnetococcus marinus* MC-1 (MmOGOR), which catalyzes a carbon-carbon bond formation reaction (**Figure 3**).⁷ We thereby decouple MmOGOR from its native role in the reductive tricarboxylic acid cycle and drive it directly with light. We examine the

dependence of 2-oxoglutarate formation on a variety of factors and, using ultrafast transient absorption spectroscopy, elucidate the critical role of electron transfer (ET) from CdS NRs to MmOGOR. We find that the efficiency of this ET depends strongly on whether the succinyl coenzyme A (SCoA) co-substrate is bound at the MmOGOR active site (**Figure 4**). We hypothesize that the conformational changes due to SCoA binding impact the CdS NR-MmOGOR interaction in a manner that decreases ET efficiency compared to the enzyme with no co-substrate bound.⁸ Our work reveals new structural considerations for the nano-bio interfaces involved in light-driven enzyme catalysis and points to the competing factors of enzyme catalysis and ET efficiency that may arise when complex enzyme reactions are driven by artificial light absorbers. This work has been submitted for publication.

3. Hole dynamics in nanocrystals

Following photoexcitation and ET to an enzyme, the nanocrystal ground state is restored by a sacrificial hole scavenger. Our understanding of hole transfer behavior is much less developed than the understanding of the electron dynamics. This is partially because photoexcited holes in CdS and related nanocrystals rapidly and efficiently trap to the nanocrystal surface so that the relevant hole state for photochemistry is trapped, rather than valence band occupation. These



trapped holes are harder to study spectroscopically than conduction band electrons and their dynamics are consequently harder to elucidate. Work supported by this grant has contributed to our understanding of trapped hole dynamics in nanocrystals. In 2016, we reported that trapped holes are mobile on CdS nanocrystal surfaces,⁹ undergoing random walk diffusion on surfaces. In 2018, we reported similar behavior for CdSe.¹⁰ Finally, this year we reported a study of temperature-dependence of this trapped hole diffusion process and found that it follows Marcus-type charge transfer behavior near room temperature, but at lower temperatures semiclassical methods are needed to describe hole dynamics.

Future Plans

Our work continues in all three areas outlined above. In the nanocrystal-hydrogenase system, our next aim is to develop a comprehensive understanding of the overall multi-step catalytic cycle that leads to H₂ production. In our work on nanocrystal-MmOGOR system, our goal is to control the dynamic interaction between the nanocrystals and the enzyme during the catalytic cycle via modification of nanocrystal structure and surface chemistry. Finally, regarding the dynamics of photoexcited holes, we are working to elucidate kinetics of hole scavenging that is interent in the nanocrystal-enzyme photochemistry.

References

- (1) *J. Am. Chem. Soc.* **2012**, *134*, 5627-5636.
- (2) *J. Am. Chem. Soc.* **2014**, *136*, 4316-4324.
- (3) *Phys. Chem. Chem. Phys.* **2015**, *17*, 5538-5542.
- (4) *J. Am. Chem. Soc.* **2017**, *139* (37), 12879-12882.
- (5) *J. Phys. Chem. C* **2018**, *122* (1), 741-750.
- (6) *J. Phys. Chem. C* **2019**, *123*, 1, 886-896.
- (7) **2019**. Submitted.
- (8) *Joule*. **2019**, *3*(2), 595-611.
- (9) *Nat. Chem.* **2016**, *8*, 1061-1066.

(10) *J. Phys. Chem. C* **2018**, 122, 29, 16974-16982.

Publications in the last 2 years supported by this award

- M. W. Ratzloff, M. B. Wilker, D. W. Mulder, C. E. Lubner, H. Hamby, K. A. Brown, G. Dukovic, P. W. King. "Activation Thermodynamics and H/D Kinetic Isotope Effect of the Hox to Hred Transition in [FeFe]-Hydrogenase." *J. Am. Chem. Soc.* **2017**, 139, 12879-12882.
- M. B. Wilker, J. K. Utterback, S. Greene, K. A. Brown, D. W. Mulder, P. W. King, G. Dukovic. "Role of Surface-Capping Ligands in Photoexcited Electron Transfer between CdS Nanorods and [FeFe] Hydrogenase and the Subsequent H₂ Generation." *J. Phys. Chem. C* **2018**, 122 (1), 741-750.
- J. K. Utterback, H. Hamby, O. M. Pearce, J. D. Eaves, G. Dukovic. "Trapped-Hole Diffusion in Photoexcited CdSe Nanorods." *J. Phys. Chem. C* **2018**, 122, 29, 16974-16982.
- J. K. Utterback, M. B. Wilker, D. W. Mulder, P. W. King, J. D. Eaves, G. Dukovic, "Quantum Efficiency of Charge Transfer Competing against Nonexponential Processes: The Case of Electron Transfer from CdS Nanorods to Hydrogenase," *J. Phys. Chem. C* **2019**, 123(1), 886–896.
- J. K. Utterback, J. L. Ruzicka, H. Hamby, J. D. Eaves, G. Dukovic. "Temperature-Dependent Transient Absorption Spectroscopy Elucidates Trapped-Hole Dynamics in CdS and CdSe Nanorods," *J. Phys. Chem. Lett.* **2019**, 10(11), 2782-2787.
- J. K. Utterback, J. L. Ruzicka, H. Keller, L. M. Pellows, G. Dukovic. "Charge Transfer Between Semiconductor Nanocrystals and Redox Enzymes." *Annu. Rev. Phys. Chem.* **2019**. *Invited*.
- H. Hamby, B. L. K. E. Shinopoulos, H. Keller, S. J. Elliott, G. Dukovic. **2019**. *Submitted*.

Reactive and Functional Droplets as Bioinspired Materials for Recognition and Transport

Principal Investigator: Todd Emrick, University of Massachusetts Amherst, 120 Governors Drive, Amherst MA 01003

Phone: 413-577-1613

Email: tsemrick@mail.pse.umass.edu

Program Scope. The scope of this program stems from Nature's sophisticated biomolecular and cellular interactions, which inspire our pursuit of novel, innovative designer materials and efficient processes with advanced capabilities. For example, biological cell signaling and recruiting pathways associated with wound healing, and response to infection and disease, trigger repair mechanisms that emerge from complex biochemical responses.^{1,2} Such systems are instructive for understanding how to build and implement bio-inspired synthetic materials, such as self-healing or delivery systems, for any of a variety of materials targets. However, there are major challenges associated with achieving synthetic designs that effectively mimic complex biological processes and are readily accessible synthetically. This research program designs novel synthetic polymers and studies their interfacial interactions in conjunction with surfaces and nano/mesoscale materials, with specific emphasis on smart, functional droplets that engage in biologically inspired processes. Our program objectives involve building a functional polymer platform as surfactant encapsulating layers for "smart droplets" which then participate in new types of materials recognition, transportation, and delivery. Our functional polymer designs, inspired by or borrowed from Nature, simultaneously impart desirable droplet-stabilizing properties and recognition elements into smart droplet systems.

Recent Progress

Simultaneous "clean-and-repair" of surfaces using smart droplets. Our recent progress showed that polymer-stabilized droplets can enable materials recognition and transportation in a *one-step process of clean-and-repair*. For example, droplets were prepared using trichlorobenzene (TCB) as the oil phase, selecting amphiphilic copolymers with pendent phosphorylcholine (PC) groups as the droplet stabilizers owing to their favorable surfactant properties and fouling resistance. Examples of PC-copolymers prepared for these experiments are shown in **Figure 1** and include **PC-COOH** (prepared with carboxylate-substituted comonomers), **PC-PE** (prepared with phenyl ester (PE)-substituted comonomers), and **PC-PFPE** (prepared with pentafluorophenyl ester (PFPE)-substituted comonomers). The polymers were prepared by ring-opening metathesis polymerization (ROMP) of the corresponding cyclooctene monomer precursors, while characterization by pendant drop tensiometry confirmed their appreciable surfactant properties. The interfacial tension of the TCB/water interface was reduced by adding these polymers (2 mg/mL) to water from 37 mN/m for pure water to the following: 4 mN/m for **PC-COOH**, 10 mN/m for **PC-PE**, and 8 mN/m for **PC-PFPE**. In a typical experiment, emulsion droplets were generated by agitating water (~15 mL) with the polymer (~30 mg) and oil (~1 mL). Droplets produced in this manner ranged from ~50-200 μm in

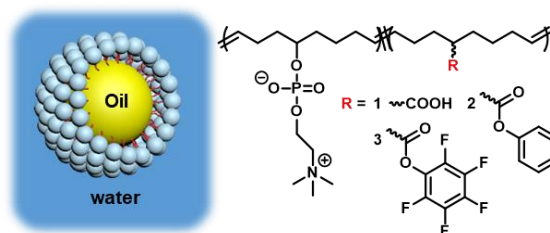


Fig. 1. Oil-in-water emulsion droplets stabilized by polymers containing zwitterionic "head groups" and reactive functionality: **PC-COOH** (1, R = COOH), **PC-PE** (2, R = phenyl ester), or **PC-PFPE** (3, R = pentafluorophenyl ester).

diameter, as determined by optical microscopy. Clean-and-repair experiments were conducted by driving droplet circulation across a cracked polymer substrate *via* a peristaltic pump, with typical crack dimensions of 1-2 μm width and 6-8 μm depth. As shown in **Figure 2**, the clean-and-repair process proceeds as follows: 1) the droplets encounter nanoparticles (NPs, ~ 40 nm diameter SiO_2) on the undamaged portions of the substrate; 2) the droplets pickup the NPs and effectively clean them from the substrate; and 3) the droplets release NPs into the cracked regions as a repair mechanism. The substrate shown in **Figure 2a** was stretched to generate cracks, followed by NP deposition, with the bright fluorescence arising from the NPs on the surface and the dark cracked regions showing a relative absence of NPs. The results of clean-and-repair experiments, performed with droplets stabilized by **PC-COOH**, are shown in **Figures 2b** and **2d**. After 300 pulsed intervals, each interval consisting of five seconds of flow and thirty seconds of rest, the fluorescence intensity on the undamaged surface was significantly weaker (nearly non-existent) than observed at the outset of the experiment, while the fluorescence in the cracked regions became prominent (**Figure 2b**). SEM imaging performed after the clean-and-repair experiments indicated accumulation of fluorescent material in the damaged regions, as seen in **Figure 2d**, while the cracks prior to the clean-and-repair experiment were empty (**Figure 2c**). Since the droplets initially introduced into the flow cell contained neither NPs nor any other fluorescent material, the material accumulated in the cracked regions arises from effective NP “relocation” from the undamaged areas into the damaged regions. To our knowledge, these results represent the first experimental example of this type of NP transportation, resulting in a new, simple, and non-invasive strategy to achieve autonomous materials healing, which in principle can be accomplished using the debris originating from a damage event.

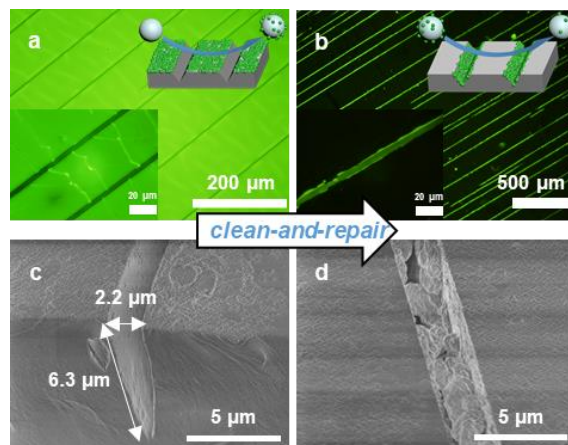


Fig. 2. Fluorescence microscope images of NP-coated substrate before (a) and after (b) clean-and-repair; c) representative SEM image of a cracked portion of the substrate before clean-and-repair; d) cracked substrate after clean-and-repair showing filler material in the crack.

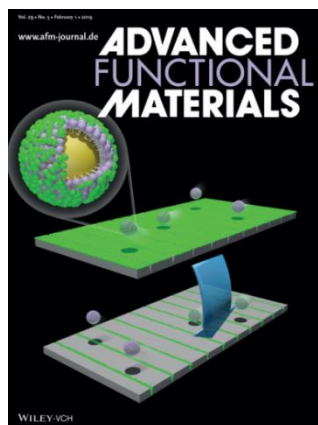


Fig. 3. Illustration of simultaneous “clean-and-repair” experiments.

The critical role of functional droplets in this clean-and-repair technique was confirmed in control experiments using water only in the flow cell, or aqueous polymer solutions (*i.e.*, no droplets). In each case, little-to-no NP pickup occurred, thus leaving little opportunity for NP relocation to the cracks. These results demonstrate that NP pickup and drop off requires chemical and interfacial interactions associated with droplet-to-surface contact, with the friction between the droplets and crack walls potentially contributing to NP drop off. Adjusting the functional groups on the polymer in turn modulates droplet-to-NP binding affinity, and thus the efficiency of NP pickup. Our manuscript on this aspect of the program was published in *Advanced Functional Materials* in 2019 (**Figure 3**) and highlighted in a *Nanowerk* spotlight article (Feb 19 2019).

New designer polymers for preparing reactive droplets. We are preparing novel polymers with pendant groups consisting of sulfothetin (ST) zwitterions, which are notably rare examples of zwitterions containing sulfur as the cationic component (nearly all zwitterions have ammonium cations). Our previous research demonstrated that droplets stabilized by homopolymers of ST-substituted polystyrene are self-adhesive (*i.e.*, tend towards droplet-to-droplet aggregation),³ making them unsuitable for the types of experiments associated with this program. Nonetheless, compelling aspects of this new class of zwitterions include their inherent reactivity, which is notably absent in conventional zwitterions, and thus we seek to prepare new forms of ST-containing polymers that can be employed in droplet/NP transportation processes. Along these lines, as shown in **Figure 4**, we are synthesizing novel ST-containing polymers using reversible addition-fragmentation chain-transfer (RAFT) polymerization (yielding **polymer 1**) and ring-opening metathesis polymerization (ROMP) (yielding **polymer 2**). The surfactancy of these polymers was confirmed qualitatively by droplet formation *via* agitating oil and aqueous polymer solutions, and will be probed quantitatively by pendant drop tensiometry. We have shown that **polymer 1**-coated droplets successfully pick up both thiol and amine-functionalized NPs, where the NPs localize to the fluid-fluid interface (**Figure 4b**); moreover, these droplets are able to capture proteins (*e.g.*, bovine serum albumin) which contain only a few amine or thiol groups (**Figure 4c**). After the pickup experiment, z-axis scanning of the droplets *via* confocal microscopy confirmed NP localization to the fluid-fluid interface. Importantly, we find that decreasing the ST content in the polymers, by copolymerization with other (non-ST) monomers, alleviates the strong inter-droplet interactions and problematic self-adhesion, while retaining the inherent reactivity of the ST group.

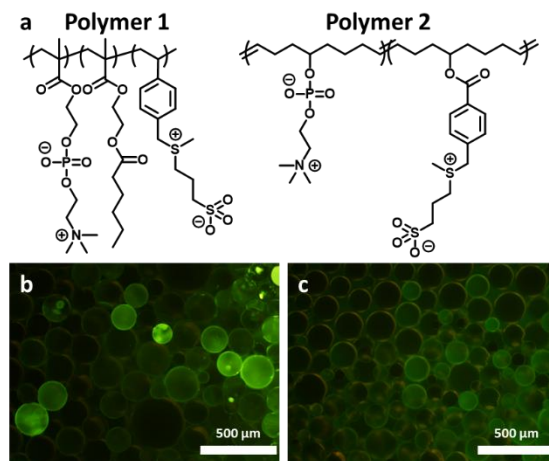


Fig. 4. (a) Structures of ST-containing polymers; (b) and (c) fluorescence microscope images of polymer 1-stabilized droplets picking up amine- and thiol-functionalized NPs, respectively.

Decorating Droplets with Mesoscale Objects. Thus far we have focused on droplet interactions with spherical (or roughly spherical) nano- and sub-micron particles. In this part of the program, we examine methods to study droplet attachment to non-spherical objects, inspired by the interactions of cell membranes with virus particles and studies of spider silk in fluids.⁴ As a first step in adapting such processes to synthetic materials, we are utilizing polymer-based ‘ribbons’, prepared by evaporative deposition of polymer solutions, that produce mesoscale structures of well-controlled aspect ratio. Success in this part of the program will realize structures in which specific portions of the ribbons attach to the fluid-fluid interface of the droplets, *i.e.*, with minimal disruption of the interface, to afford a large increase in droplet reach and the ability of droplets to probe surfaces and capture objects.

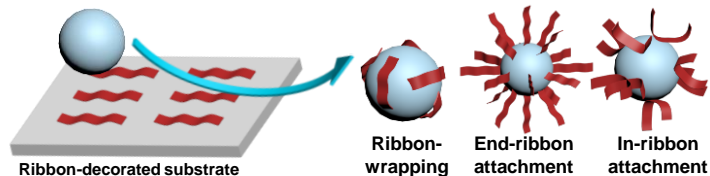


Fig 5. Idealized schematic of potential outcomes of droplet-ribbon attachment, including droplet wrapping and localized interactions by adsorption to the fluid-fluid interface.

Figure 6 shows preliminary results from experiments that represent a first step in achieving such

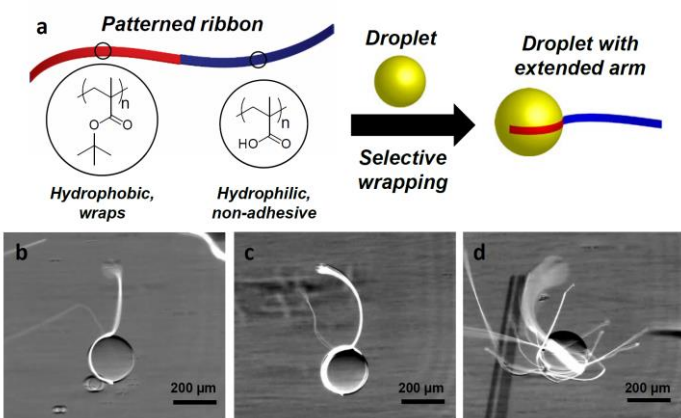


Fig. 6. (a) Illustration of a diblock polymer ribbon interacting with a liquid droplet; (b-d) fluorescence microscope images droplet-ribbon assemblies, giving one, two, and many ribbons per droplet.

droplet-ribbon assemblies, by manipulation of functional droplets with chemically patterned mesoscale ribbons. In this example, a t-boc-substituted polymer ribbon was subjected to photolithographic deprotection, through a mask, affording ribbons with hydrophilic (carboxylate) and hydrophobic (t-boc ester) portions. Bringing one or more of these ribbons into contact with oil droplets affords structures in which the hydrophobic portion of the ribbon wraps the droplet and the hydrophilic portion extends from the droplet. This gives ribbon-

decorated droplets with one or multiple extended “arms”, which we envisage using to capture reagents, probe substrates, and produce well-defined multidroplet structures.

Future Plans. Plans going forward include: 1) probing in greater depth the mechanisms of NP pickup and drop off, through building a library of polymers and NPs, and adopting high speed microscopy techniques to visualize the process as it occurs; 2) optimizing the chemistry of inherently reactive zwitterions, such as the ST groups described above, as well as functional versions of phosphorylcholines and choline phosphates; and 3) building a new platform of designer droplets, in which mesoscale objects, such as polymer ribbons, adhere to and reach from the fluid-fluid interface.

References

1. G. Gabbiani, *J. Pathol.* **2003**, *200* (4), 500. DOI: 10.1002/path.1427.
2. R. S. Kirsner, W. H. Eaglstein, *Dermatol. Clin.* **1993**, *11* (4), 629. PMID: 8222347.
3. C. F. Santa Chalarca, T. Emrick, *J. Polym. Sci. A Polym. Chem.* **2017**, *55* (1), 83. DOI: 10.1002/pola.28359.
4. H. Elettro, S. Neukirch, F. Vollrath, A. Antkowiak, *Proc. Natl. Acad. Sci. U. S. A.* **2016**, *113* (22), 6143. DOI: 10.1073/pnas.1602451113.

Publications

1. Sathyan, A.; Yang, Z.; Bai, Y.; Kim, H.; Crosby, A. J.; Emrick, T. Simultaneous “clean-and-repair” of surfaces using smart droplets. *Adv. Funct. Mater.* **2019**, *29*, 1805219. DOI: 10.1002/adfm.201970026.
2. Barber, D.; Yang, Z.; Sathyan, A.; Crosby, A. J.; Emrick, T. Ribbon-decorated droplets, manuscript in preparation.

EARLY FORMATION STAGES AND PATHWAY COMPLEXITY IN FUNCTIONAL BIO-HYBRID NANOMATERIALS

PI: Lara A. Estroff; Co-PI: Ulrich Wiesner

Department of Materials Science and Engineering, Cornell University, Ithaca, NY 14853

Program Scope

The focus of this program is on elucidating pathway complexity in interface-driven formation processes of organic-inorganic nanocomposites. We are pursuing two synthetic thrusts and a complementary *in situ* characterization thrust. The two materials systems are chosen to address the role of organic assemblies (System 1) and functionalized, nanopatterned substrates (System 2) in directing the organization of inorganic clusters/particles (amorphous and crystalline) into higher order structures. In System 1 we are investigating silica-based organic-inorganic hybrid structures. In System 2 we are developing a versatile platform based upon click-chemistry functionalization of specific blocks of thin films of synthetic block copolymers. These patterned substrates can then be used to study the nucleation and growth of inorganic materials. Finally, in a characterization thrust we are applying *in situ* fluid cell atomic force microscopy (AFM) to track interfacial nucleation and growth processes on the nanostructured BCP films with high spatial and temporal resolution. Understanding and controlling formation pathways and organic-inorganic interfaces in hybrid nanomaterials has the potential to be broadly applicable to a range of amorphous and crystalline inorganic materials. Results are therefore expected to provide general guidelines and methodologies for the controlled synthesis of hybrid nanomaterials with increasing complexity, offering enormous scientific and technological promise, in areas ranging from energy conversion and storage to catalysis to sensing.

Recent Progress

We have worked on projects originally proposed as well as new directions based on recent developments and discoveries. Specifically, we have evaluated the role of different synthesis parameters in determining the mesoporous nanostructure of never-before seen periodically structured ultrathin 2-D silica superlattices. In parallel, we have focused on applying our understanding of silica nanoparticle formation pathways to develop a new class of materials referred to as amorphous quantum nanomaterials. Such materials enable new functionalities, including optical super-resolution microscopy (SRM), which we have demonstrated on biological samples as well as block copolymer (BCP) mesostructures. We have also emphasized exploring the self-assembly mechanisms of large grains on BCP mesostructures, in an effort to further inform our ability to design templates for inorganic nucleation and growth.

2-D Mesoporous Superlattices of Silica Cages. Since early reports on directed silica self-assembly, cage-type mesoporous silica has been the subject of extensive research efforts for a variety of applications including catalysis, energy, and nanomedicine. Fundamental understanding of how order emerges from a single cage

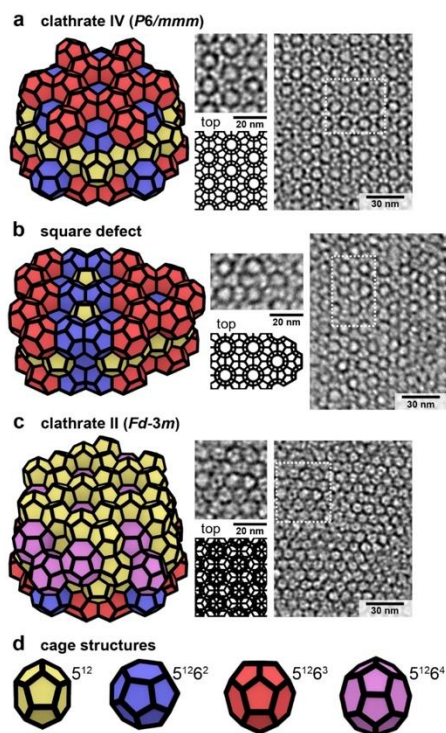


Fig. 1: Some of the silica cage based mesoporous superlattices observed.

to a 3-D superstructure, however, remains limited. We assembled mesoporous silica at an interface between two immiscible liquids under conditions that favor silica nanocage formation (1). Careful variation of synthesis conditions allowed cage assembly into 2-D superlattices with controlled number of layers (Fig. 1). Orientational correlations between cages increased with increasing layer number, suggesting that 3-D crystallographic registry emerges from the concerted co-assembly of organic and inorganic components. Borrowing ideas from 2-D electronic materials, we further demonstrated scalable synthetic approaches to mesoporous silica heterostacks with property profiles inaccessible to date.

Amorphous Quantum Nanomaterials and Super-Resolution Imaging of BCPs.

A second set of accomplishments relates to the development of amorphous quantum nanomaterials (2). By borrowing ideas from single molecule spectroscopy, we isolated single delocalized π -electron dye systems in relatively rigid ultrasmall (<10 nm dia.)

amorphous silica nanoparticles (Fig. 2). We demonstrated that chemically tuning the local amorphous silica environment around the dye over a range of compositions enables exquisite control over dye quantum behavior, leading to efficient probes for photodynamic therapy (PDT) and stochastic optical reconstruction microscopy (STORM). Resulting hybrid nanoproboscopes (e.g. srC' dots) have a versatile surface chemistry that allow interfacing with a variety of materials.

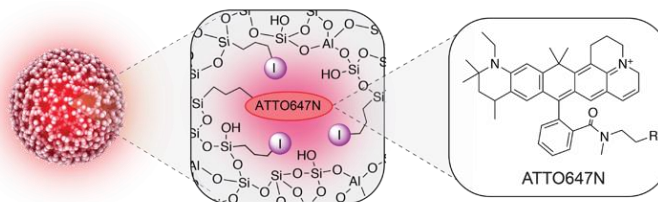


Fig. 2. Amorphous silica nanoparticle, with encapsulated delocalized π -electron dye system (ATTO647N) and silica compositional modifications that tune the quantum photophysical dye behavior under illumination (Ref. 2).

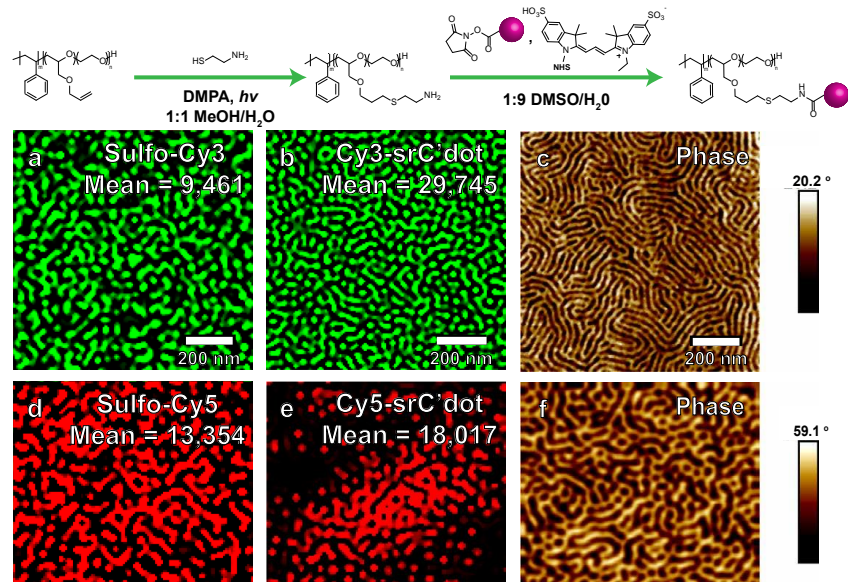


Fig. 3. NHS ester-amine click reaction scheme (top) used to attach fluorescent probes to PS-*b*-P(AGE-*co*-EO) thin film surfaces. Below: Representative STORM images of BCP surfaces: sulfo-Cy3(-) dye (a), Cy3-srC' dots (b), sulfo-Cy5(-) dye (d), and Cy5-srC' dots (e) Representative AFM phase images of unfunctionalized PS-*b*-P(AGE-*co*-EO) thin film surfaces (c, f).

In a first effort of cross-fertilization between Systems 1 and 2, we applied our newly developed srC' dots (Fig. 2) to our block-copolymer (BCP) based reactive thin film surfaces in order to perform super-resolution optical microscopy on the resulting BCP-nanoparticle hybrid materials (Fig. 3). As previously demonstrated, polystyrene-*block*-poly[(allyl glycidyl ether)-*co*-(ethylene oxide)] (PS-*b*-P(AGE-*co*-EO)) films can serve as chemically and dimensionally varying patterns that can undergo thiol-ene, NHS ester-amine, and alkyne-azide “click” surface chemistries (Fig. 3). We use

this click chemistry to covalently attach srC' dots to the hydrophilic blocks of the BCP thin films, enabling selective block staining and optical visualization. The enhanced brightness of the particle

probes offers distinct advantages over conventional dye labeling and provides a versatile method for optical imaging in the far field of materials surface nanostructures.

Preparation of Macroscopic BCP-Based Gyroidal Mesoscale Single Crystals. During our

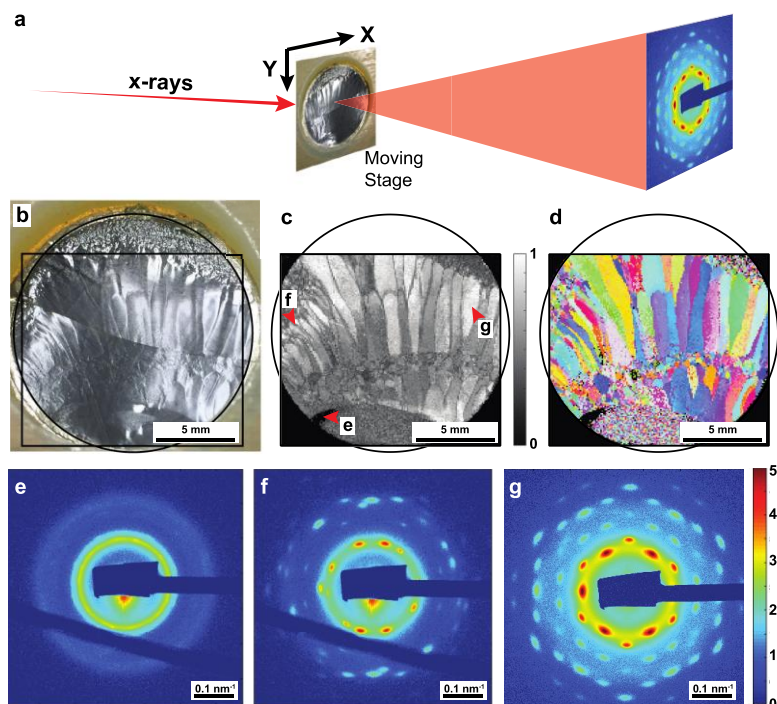


Fig. 4. (a) Small angle x-ray scattering (SAXS) set-up and analysis for a BCP nanocomposite. (b) Photo of mounted sample. (c) A map of the fraction of identified Bragg reflections accounted for by calculated diffraction patterns. (d) Orientation map where colors denote gyroid orientation relative to lab horizontal x-axis in (a). (e–g) Representative SAXS patterns from locations indicated in (c): polycrystalline (e), multi-(three) crystalline (f), and single crystal (g) areas. Diagonal bars across bottom are shadows from photodiode wire.

development of BCP templates for inorganic crystal growth (5), we serendipitously discovered a route to large single crystals of BCPs, BCP-inorganic precursor composites, and resulting mesoporous BCP directed inorganic materials with bicontinuous cubic gyroid structure. Such bulk macroscopic gyroidal single crystals with mesoscale periodicity have stayed elusive, but are needed to establish fundamental structure–property correlations for materials ordered at this lengthscale (10–100 nm). We developed a solvent evaporation-induced assembly method that provides access to large (mm to cm sized) single crystal mesostructures in thick (>100 μm) films (Fig. 4).⁽⁶⁾ After in-depth crystallographic characterization of single-crystal BCP-preceramic nanocomposite films, the structures were converted into mesoporous

ceramic monoliths, with retention of the macroscopic order. The method resulted in macroscopic bulk single crystals of multiple BCP systems, suggesting that it is broadly applicable to BCP materials assembled by solvent evaporation.

Fluid Cell AFM to Observe Hydrated BCP Structures. A long term goal of this work is to use fluid cell AFM to directly image the nucleation and growth of inorganic structures on the BCP templates. In tackling this problem, we realized that first we needed to characterize the hydrated morphology of the BCP thin films. Such characterization is also important for proper interpretation of the STORM images (Fig. 3) since these images are obtained in total internal reflection fluorescence (TIRF) mode using water. With the help of fluid-cell AFM, we can directly image how the BCP nanostructures change as a function of solution conditions (Fig. 5), and detect that there are changes in the height and width of BCP cylinders in air versus in water. We are currently investigating this swelling behavior as a function of organic functional groups covalently linked to the hydrophilic block of the BCPs. In the coming year, we will study this phenomenon further while simultaneously using fluid cell AFM to monitor inorganic crystal growth on the functionalized PS-*b*-P(AGE-*co*-EO) films.

Overall, the results described demonstrate important progress towards both our synthetic and characterization goals. Specifically, our work on 2-D silica superstructures elucidates the fundamental question, we believe for the very first time, of how in self-assembled mesoporous silica materials, 3-D order emerges on the way from a single cage to 2-D, highly confined, single layer superstructures, all the way to the bulk. In the case of individual silica nanoparticle growth, we established the new class of amorphous quantum nanomaterials, *e.g.* useful as super-resolution microscopy probes for thin film BCP nanostructures. By understanding block copolymer self-assembly, we have developed a route to grow macroscopic (mesoporous) gyroidal single-crystals. This will enable researchers, for the very first time for these cubic structures, to establish structure-property correlations in an angle-dependent way, critical for materials like BCP directed optical metamaterials or superconductors. Finally, successful results of imaging BCP thin films in a fluid cell under fully hydrated conditions will now enable *in-situ* studies of BCP nanostructure directed inorganic crystal growth.

Future Plans

For Synthesis System 1, future studies will focus on developing 3-dimensional (3D) printing methods using silica cage-like structures. This will provide access to materials in which the structure is controlled over multiple length scales, from the molecular assembly of the silica cages at the local scale all the way to the controlled shape of 3D printed macroscopic objects. For Synthesis System 2, we will continue to assess how the growth of inorganic materials/crystals on the block copolymer templates changes as a function of surface chemistry and topology, *e.g.*, looking at changes in crystallographic orientation, nanostructure, and selectivity for different oxides. We will also change the mesostructure of the polymer thin films by changing the composition of the parent block copolymer. Other plans include identifying more crystalline materials, such as zeolites, that can be templated using the BCP thin films, and using “click chemistries” to attach peptides to the surfaces to further diversify the available surface chemistries. In parallel with Synthesis System 2, we are characterizing how the template morphologies change upon hydration in solution. We will correlate the hydrated film structures to the observed inorganic crystallization patterns. We are also developing a fluid cell AFM method to study ZnO nucleation on the BCP polymer templates to understand where the first mineral begins to deposit, and how these formation pathways change as a function of interface chemistry.

References. 1) Auber, T., Ma, K., Tan, K.W., Wiesner, U., **2019**, *submitted*. 2) Kohle, F.F.E., Hinckley, J.A., Li, S.Y., Dhawan, N., Katt, W.P., Erstling, J.A., Werner-Zwanziger, U., Zwanziger, J. Cerione, R.A., Wiesner, U.B., *Adv. Mater.*, **2019**, *31*, 1806993. 3) Hinckley, J.A., Chapman, D.V., Hedderick, K.R., Oleske, K.W., Estroff, L.A., Wiesner, U.B., **2019**, *submitted*. 4) Oleske, K.W., Barteau, K.P., Turker, M.Z., Beaucage, P.A., Estroff, L.A., Wiesner, U., *Macromolecules*, **2017**, *50*, 542-549. 5) Oleske, K.W., Barteau, K.P., Beaucage, P.A., Asenath-Smith, E., Weisner, U., Estroff, L.A. *Cryst. Grow. Des.*, **2017**, *17*, 5775-5782. 6) Susca, E., Beaucage, P., Thedford, R.P., Singer, A., Gruner, S.M., Estroff, L.A., Wiesner, U. *Adv. Mater.*, **2019**, *in revision*.

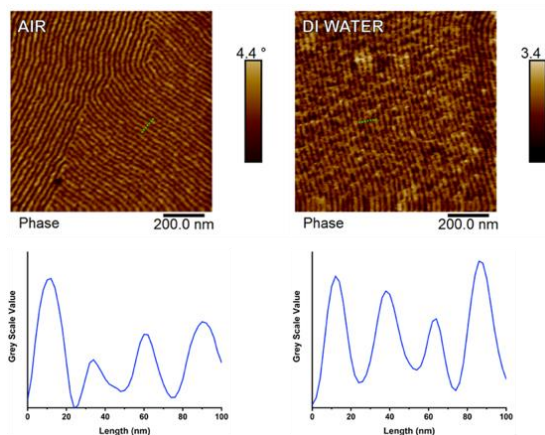


Fig. 5. Fluid cell AFM images of a PS-*b*-P(AGE-*co*-EO) film in air and in water. The domain spacing increased from 26.8 nm \pm 4.5 nm to 28.5 nm \pm 5.1 nm in DI water.

Publications Supported by BES 2017-2019

- 1) Oleske, K.W., Barteau, K.P., Turker, M.Z., Beaucage, P.A., Estroff, L.A., Wiesner, U., “Block Copolymer Directed Nanostructured Surfaces as Templates for Confined Surface Reactions”, *Macromolecules*, **2017**, *50*, 542-549.
- 2) Sun, Y.; Ma, K.; Kao, T.; Spoth, K. A.; Sai, H.; Zhang, D.; Kourkoutis, L. F.; Elser, V.; Wiesner, U., “Single particle growth trajectories of mesoporous silica nanoparticles with dodecagonal tiling.” *Nature Commun.* **2017**, *8*, Article number: 252.
- 3) Oleske, K.W., Barteau, K.P., Beaucage, P.A., Asenath-Smith, E., Weisner, U., Estroff, L.A. “Nanopatterning of Crystalline Transition Metal Oxides by Surface Templated Nucleation on Block-Copolymer Mesostructures” *Cryst. Grow. Des.*, **2017**, *17*, 5775-5782.
- 4) Kao, T., Kohle, F., Ma, K., Aubert, T., Andrievsky, A., Wiesner, U. “Fluorescent Silica Nanoparticles with Well-Separated Intensity Distributions from Batch Reactions.” *Nano Letters*, **2018**, *18*, 1305-1310.
- 5) Kohle, F.F.E., Hinckley, J.A., Li, S.Y., Dhawan, N., Katt, W.P., Erstling, J.A., Werner-Zwanziger, U., Zwanziger, J. Cerione, R.A., Wiesner, U.B. “Amorphous Quantum Nanomaterials”, *Adv. Mater.*, **2019**, *31*, 1806993.
- 6) Kohle, F.F.E., Hinckley, J.A., Wiesner, U.B. “Dye Encapsulation in Fluorescent Core-Shell Silica Nanoparticles as Probed by Fluorescence Correlation Spectroscopy”, *J. Phys. Chem. C.*, **2019**, *123*, 9813-9823.
- 7) Susca, E., Beaucage, P., Thedford, R.P., Singer, A., Gruner, S.M., Estroff, L.A., Wiesner, U. “Preparation of Macroscopic Block Copolymer-Based Gyroidal Mesoscale Single Crystals by Solvent Evaporation” *Adv. Mater.*, **2019**, *in revision*.
- 8) Goldman, A.R., Palin, D., Estroff, L.A. “Single-Crystal Composites: To Incorporate or Not To Incorporate That is the Question”, *Materials Horizons*, **2019**, *in revision*.
- 9) Auber, T., Ma, K., Tan, K.W., Wiesner, U. “Two-dimensional Mesoporous Superlattices of Silica Cages”, **2019**, *submitted*.
- 10) Hinckley, J.A., Chapman, D.V., Hedderick, K.R., Oleske, K.W., Estroff, L.A., Wiesner, U.B. “Quantitative Comparison of Dye and Ultrasmall Fluorescent Silica Core-Shell Nanoparticle Probes for Optical Super-Resolution Imaging of Block Copolymer Thin Film Surfaces”, **2019**, *submitted*.

Programmable Dynamic Self-Assembly of DNA Nanostructures

Elisa Franco, University of California Los Angeles and Rebecca Schulman, Johns Hopkins University

Program Scope

The synthesis of novel materials with self-regulation properties akin to those of biological cells is a central challenge in biomolecular materials research. In biological systems, behaviors such as growth, division, and self-repair emerge because molecular self-assembly processes are coupled to and directed by signal transduction and gene expression networks. The goal of this project is to construct synthetic materials where, analogously, adaptive, dynamic responses within materials are achieved by coordinating synthetic self-assembly processes with synthetic molecular circuits and control systems, and by controlling the flow of energy during self-assembly.

We are creating modular, programmable biosystems composed of nucleic acid nanostructures and signal processing systems. The simplicity and modularity of Watson-Crick hybridization by DNA and RNA is key to their development and the precise control that can be achieved. Having developed a toolkit where assembly and disassembly of nucleic acid structures can be directed by nucleic acid circuits that can in turn take different chemical stimuli, our current goal is to build more complex architectures and structures that can undergo complex, multistage reorganization through the direction of molecular circuits that orchestrate the assembly and disassembly of multiple types of components in multiple temporal stages. We are developing mechanisms to allow materials to exhibit sustained dynamical behaviors and show how molecular circuits can orchestrate complex adaptive responses including self-repair and motility.

The biological inspiration for the materials in this study is the cytoskeleton, in which a small set of one-dimensional fibers assembled from a small set of monomers are organized into a variety of different structures such as spindles, sarcomeres, cilia or filopodia by molecules that branch, crosslink, stabilize or destabilize the fibers and in turn the genetic circuits that control the spatiotemporal abundance and activity of these molecular components^{Ref1}. We are studying DAE-E DNA tile nanotubes as a model fiber^{Ref2} and dynamic genelet^{Ref3} and strand-displacement nucleic acid circuits^{Ref4} which can be coupled to self-assembly using short nucleic acid message strands.

Recent Progress

Integrated chemical circuits for directing DNA self-assembly. Cells can orchestrate behaviors, such as differentiation and adaptation using genetic regulatory networks (GRNs). *In vitro* GRN analogs could autonomously direct synthetic materials to exhibit some of the sophisticated behaviors of living systems. *In vitro* transcriptional circuits composed of short synthetic genelets that are transcribed by viral RNA polymerases and that utilize only nucleic acids to regulate genelet expression, are straightforward to program and implement and could in principle achieve control over chemistry as complex as that seen in living cells. However, only small genelet networks with simple functionalities have been developed.

We have shown how such larger, more powerful synthetic GRNs can be constructed by systematically integrating multiple genelet modules into larger, multifunctional networks, including a multistable network with inducible, temporal control of switching (Figure 1) and a

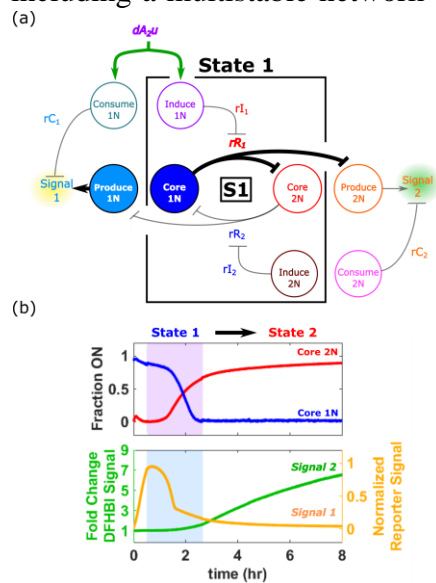


Figure 1: (a), A genelet network that regulates mutually exclusive expression of downstream signals. (b) Network operation during a state change.

pulse generator. We have developed design rules for constructing scalable genelet circuits and used predictive kinetic models to guide network design and implementation.

Hierarchical assembly of DNA nanotube architectures. A key potential opportunity in programming dynamic self-assembly processes with DNA is the ability to organize how structures self-organize in different hierarchical fashions. However, to control these processes, models of hierarchical self-assembly are needed. We have developed accurate models of DNA nanotube end-to-end joining (manuscript in review), and developed a model for hierarchical self-assembly consistent with experiments. Surprisingly, we found that the rates of DNA nanotube end-to-end joining are independent of nanotube length. This observation also explained observed dynamics of DNA nanotubes into larger networks (Figure 2). Because the coordination number of nanotube seeds, which connect nanotubes and the spacing of binding sites can be systematically varied by design, this system allows the

assembly of a wide variety of networks and characterization of the assembly mechanisms that lead to different types of material architectures at length scales of tens to hundreds of microns. Using our kinetic model of network assembly, we have identified the ratio of inter-network vs intra-network joining events as a key parameter that controls whether networks develop into “open-branching” topologies or “closed-loop” topologies.

Enzyme driven assembly and disassembly of DNA-RNA nanotubes. We demonstrated a strategy to control DNA nanotube self-assembly by activating and deactivating tiles via RNA molecules embedded in the nanostructure. We optimized tiles so that one sticky-end strand is an RNA molecule as shown in Fig. 3, left. In the absence of the RNA sticky end (green molecule in the figure), tiles are inert and cannot assemble. Upon addition or transcription of RNA trigger strand, tiles become active and assembly proceeds at speed consistent with previous measurements on all-DNA tiles^{Ref2}. Addition of RNase H to the transcription mix results in degradation of the RNA trigger strand bound to DNA, and nanotubes disassemble on a time-scale that depends on the

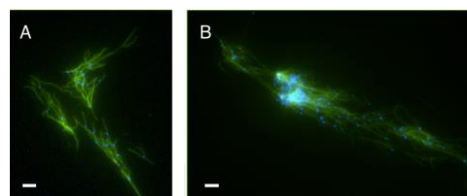


Figure 2: DNA nanotube networks have a range of topologies. Seeds labeled with Atto488 (blue), nanotubes with Cy3 (green) (A) A highly branched dendritic network topology. (B) An elongated network with many internal cycles. Scale bars 5 μm .

concentration of RNase H. Because RNAP is initially faster than degradation, we observed a transient pulse in nanotube mean length (Fig. 3, right). We also developed two simple programs to control nanotube assembly. We used a “timer” genetic circuit, where a template produces a RNA aptamer that inhibits T7 RNA polymerase. The concentration of T7 aptamer determines how quickly transcription is turned off. As soon as the transcription rate is reduced, RNase H degradation dominates causing nanotube disassembly. Finally, we used an inducible artificial transcriptional genelet to produce the RNA trigger; this circuit is fully compatible with the genelets characterized by the Schulman lab.

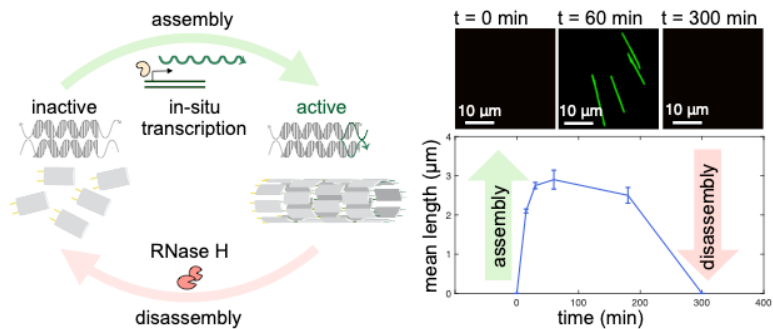


Figure 3: Enzyme driven control of assembly and disassembly of DNA-RNA nanotubes. Left: DNA tiles are unable to self-assemble if one of their sticky ends is missing; by producing the missing sticky end via in situ transcription, assembly of DNA-RNA hybrid nanotubes proceeds; degradation of the RNA sticky end by RNase H induces nanotube disassembly. Right: by calibrating the enzyme concentration, and thus the speed of RNA production and degradation, we nanotubes can be produced transiently in the sample, with controllable duration of the transient.

Future Plans

In the current funding cycle (06/15/2019-), we will design chemical systems with controlled influx of high-energy precursors, fuel components, or enzymes and removal of waste product. We will develop biochemical reaction systems and hierarchical forms of material organization that allow for control over the release of biochemical energy in different forms and the management of waste products. We will then explore how the implementation of these systems can lead to qualitative advances in the design of DNA-based and DNA-directed dynamic, multi-component materials to achieve complex chemomechanical behaviors.

References

1. D. A. Fletcher and R. D. Mullins. Cell mechanics and the cytoskeleton. *Nature*, 463:485–492, 2010.
2. P.W.K. Rothmund, A. Ekani-Nkodo, N. Papadakis, A.Kumar, D. K. Fygenzona and E. Winfree. Design and Characterization of Programmable DNA Nanotubes. *J. Am. Chem. Soc.* 126(50):16344–16353, 2004.
3. J. Kim and E. Winfree. Synthetic in vitro transcriptional oscillators. *Mol. Sys. Bio.* 7:465, 2011.
4. D. Y. Zhang and G. Seelig. Dynamic DNA nanotechnology using strand displacement reactions. *Nat. Chem.*, 3:103--113, 2011.

Publications

1. Schaffter SW, Schulman R. Building *in vitro* transcriptional regulatory networks by successively integrating multiple functional modules. *Nature Chemistry*. Accepted for publication.
2. D. Scalise and R. Schulman*. "Control of Matter at the Molecular Scale with DNA Circuits." *Annual Review of Biomedical Engineering*, June 2019. DOI: 10.1146/annurev-bioeng-060418-052357.
3. J. Zenk, M. Billups, R. Schulman. "Optimizing Component-Component Interaction Energies in the Self-Assembly of Finite, Multicomponent Structures" *ACS Omega*, accepted. *
4. L.N. Green, H.K.K. Subramanian, V. Mardanlou, J. Kim, R.F. Hariadi and E. Franco. "Autonomous dynamic control of DNA nanostructure self-assembly". *Nature chemistry*, 2019.
5. Agarwal, S., & Franco, E. Enzyme-Driven Assembly and Disassembly of Hybrid DNA–RNA Nanotubes. *Journal of the American Chemical Society*, 2019.
6. S. W. Schaffter, L. Green, J. Schneider, H. Subramanian, R. Schulman and E. Franco. "T7 polymerase transcribes and induces melting of DNA nanostructures". *Nucleic Acids Research*, 46 (10): 5332-5343, 2018. doi: 10.1093/nar/gky283.
7. M.A. Klocke, J. Garamella, H.K.K. Subramanian, V. Noireaux and E. Franco. "Engineering DNA nanotubes for resilience in the cytoplasmic environment". *Synthetic Biology* 3(1): ysy001, 2018. DOI: 10.1093/synbio/ysy001.
8. D. Agrawal, R. Jiang, S. Reinhart, A. M. Mohammed, T. Jorgenson and R. Schulman. "Terminating DNA Tile Assembly with Nanostructured Caps." *ACS Nano*, 11 (10): 9770-9779, 2017 [13.942]. DOI:10.1021/acsnano.7b02256.
9. A. Mohammed, J. Zenk, P. Šulc and R. Schulman*. "Self-assembling DNA nanotubes to connect molecular landmarks." *Nature Nanotechnology*, 12: 312-316, 2017. doi:10.1038/nnano.2016.277.*
10. L.N. Green, A. Amodio, H.K.K. Subramanian, F. Ricci and E. Franco. "pH-driven reversible self-assembly of micron-scale DNA scaffolds". *Nano Letters* 17(12):7283-8, 2017. DOI: 10.1021/acs.nanolett.7b02787
11. T. Jorgenson, A. Mohammed, D. Agrawal and R. Schulman. "Self-Assembly of Hierarchical DNA Nanotube Architectures with Well-Defined Geometries." *ACS Nano* 17 (2): 1927-1936, 2017. doi:10.1021/acsnano.6b08008.
12. A. Mohammed, A. Chisenhall, D. Schiffels, L. Velazquez, D. Fyngson, R. Schulman. "Self-assembly of precisely defined DNA nanotube superstructures using DNA origami seeds." *Nanoscale* 9 (2): 522-526, 2017. doi: 10.1039/C6NR06983E.*
13. V. Mardanlou, K.C. Yaghoubi, L.N. Green, H.K.K. Subramanian, R.F. Hariadi, J. Kim and E. Franco. "A coarse-grained model captures the temporal evolution of DNA nanotube length distributions". *Natural Computing* 17(1):183-99, 2017. DOI:10.1007/s11047-017-9657-7
14. C. Cuba Samaniego and E. Franco. An ultrasensitive biomolecular network for robust feedback control. *IFAC-PapersOnLine* 50(1): 10950-10956, 2017. DOI: 10.1016/j.ifacol.2017.08.2466

15. J.M. Stewart, H.K.K. Subramanian and E. Franco, “Self-assembly of multi stranded RNA motifs into lattices and tubular structures”. *Nucleic Acids Research* 45(9):5449-57, 2017. DOI: 10.1093/nar/gkx063
16. J. Lloyd, C.H. Tran, K. Wadhvani, C. Cuba Samaniego, H.K.K. Subramanian and E. Franco. “Dynamic control of aptamer–ligand activity using strand displacement reactions”. *ACS Synthetic Biology* 7(1):30-7, 2017. DOI: 10.1021/acssynbio.7b00277

Program Title: Bioinspired Design of Multifunctional Dynamic Materials

Principle Investigator: Zhibin Guan, Ph.D.

Mailing Address: 1102 Natural Sciences II, Irvine, CA 92697

Email: zguan@uci.edu

Program Scope

The objective of this project is to investigate new strategies for designing multifunctional dynamic materials for potential energy relevant applications. Through evolution, biological systems have developed multifunctional materials possessing superior properties in terms of multifunctionality, adaptability, stimuli-responsiveness, self-healing ability, malleability, and recyclability. Inspired by Nature, this project focuses on developing new strategies for introducing such dynamic properties into synthetic materials. Several major advances have been made in the last two years toward the design of strong malleable polymers as well as active, dissipative self-assembled materials. Specifically, (1) we developed for the first time a boroxine-based polymer network as malleable and recyclable thermosets; (2) we discovered a new silyl ether metathesis reaction and applied it as a general dynamic covalent chemistry for the design of malleable thermosets (vitrimers); and (3) we developed the first redox chemical-fueled dissipative self-assembly of active materials. Such dynamic materials may find important applications in energy production, environmental impact, energy security, and energy saving.

Recent Progress

1. First Boroxine-based Malleable and Recyclable Thermosets

Traditional cross-linked polymers (i.e., thermosets) have excellent mechanical properties, creep resistance and dimensional stability, and chemical/solvent resistance. However, a critical limitation of thermosets is that they cannot be reshaped, reprocessed, or recycled by heat or with solvent. In contrast, thermoplastic polymers can be reshaped and reprocessed, but they normally have lower mechanical strength, lower structural stability at elevated temperature, and poorer chemical/solvent resistances. One of our recent efforts is to develop new strategies to combine the excellent attributes of both thermoplastics and thermosets.

In one successful approach, we employed boroxine as dynamic crosslinks to construct a novel type of thermoset material that is strong, highly malleable, and recyclable (*J. Am. Chem. Soc.* **2018**, *140*, 6217-6220). The network is synthesized by simple dehydration and generally applicable to any boronic acid monomers. The new thermoset exhibits unusual mechanical behavior. While showing high Young's modulus (559 MPa) and tensile strength (17.8 MPa), it is highly malleable and exhibits vitrimer properties. The bulk malleability of the boroxine thermoset was corroborated with the dynamic exchange of small molecule boroxines observed with variable temperature ¹H NMR experiments. Finally, the new thermoset was found to be not only reprocessible, but also fully recyclable back to the monomer. The strikingly high malleability of our boroxine thermoset is reminiscent of the high adaptability of a commodity material, silly putty. However, a major difference is that our thermoset is strong (Young's modulus > 0.5 GPa, and tensile strength > 17 MPa) while silly putty is soft and elastomeric. With a combination of unusual properties (strong, highly malleable, and recyclable) and a multitude of tunable variables (monomer structure, comonomer, plasticizer), we envision our boroxine

thermoset to be a platform for the development of a range of new dynamic materials. The ACS Chemical & Engineering News highlighted this work for its potential impact on environmental sustainability (<https://cen.acs.org/materials/polymers/Stiff-yet-supple-plastic-reshaped/96/i23>). In the end of last year, this work was selected Research of the Year 2018 by the Chemical & Engineering News (<https://cen.acs.org/analytical-chemistry/CENs-Year-Chemistry-2018/96/i49>).

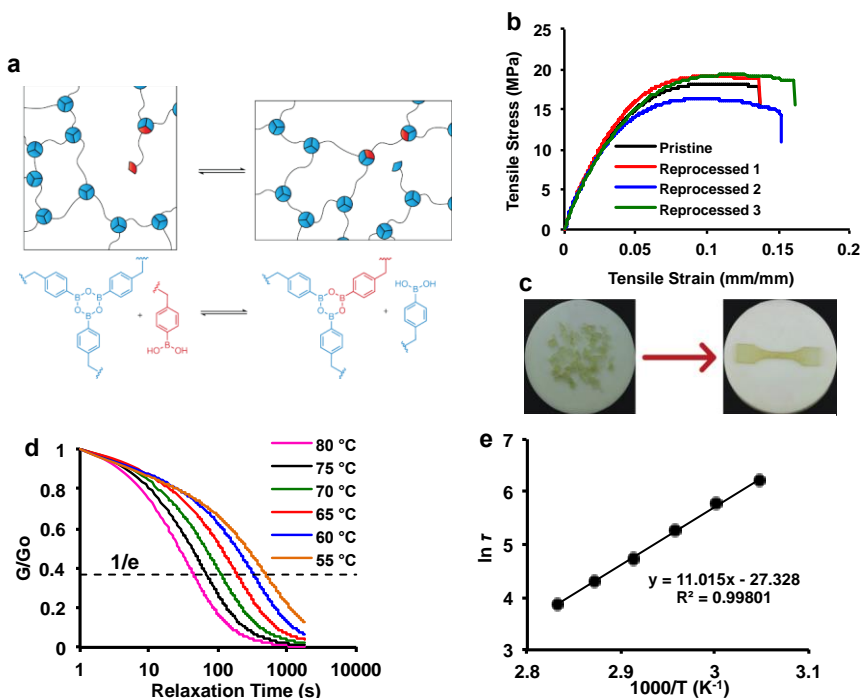


Figure 1. Boroxine-based malleable and recyclable thermosets. **a:** Design concept for vitrimers based on dynamic boroxine exchange; **b-c:** Reprocessability of the boroxine thermoset; **d:** Stress relaxation tests at various temperatures for the boroxine dynamic networks; **e:** Fragility plot with linear fit. From this fit the activation energy is calculated to be 79.5 kcal/mol.

2. Discovery of Silyl Ether Metathesis and Its Application for Vitriimer Design

In another recent study, we aim to develop a universal strategy for introducing plasticity, reprocessability and recyclability to thermosets. To achieve this goal, we must first develop a dynamic covalent chemistry that is robust and generally applicable. The dynamic covalent chemistries used in the reported vitriimer systems are either thermally and/or oxidatively unstable, or only suitable for a narrow range of polymers. To address these key issues, we have recently demonstrated silyl ether as a superior dynamic covalent motif for vitriimer design because of its high chemical and thermal stability, easy accessibility, and general applicability.

In our first-generation silyl ether-based vitriimer design, we used silyl ether exchange with free hydroxyls to introduce the malleability (*J. Am. Chem. Soc.* **2017**, *139*, 14881–14884). For general applications, the presence of free hydroxyls is undesirable because of their relatively low functional group tolerance (e.g., transesterification with polyacrylates) and potential side reactions (e.g., dehydration, oxidation). In searching for more robust dynamic covalent chemistries, we recently discovered silyl ether metathesis reaction (Fig. 2b). Silyl ethers are thermodynamically very stable and tolerant to most functional groups. Direct metathesis between silyl ethers avoids the need of free hydroxyls, which is highly desirable for dynamic polymer designs (*Manuscript submitted 2019*).

In small molecule model studies, we observed that silyl ether motifs directly exchange under anhydrous conditions catalyzed by a Brønsted or Lewis acid catalyst (Fig. 2a). For initial vitrimer demonstration, a commodity polymer, poly(ethylene-co-vinyl alcohol) (PEOH), was silylated with trimethyl silyl (TMS) groups followed by cross-linking with a bis-silyl ether crosslinker via silyl ether metathesis. The resulting thermoset showed excellent thermal stability and mechanical properties while maintaining malleability/reprocessability at elevated temperatures. This work demonstrates silyl ether metathesis reaction as a new, robust dynamic covalent chemistry to introduce plasticity, reprocessability and recyclability to thermosets. To the best of our knowledge, this represents the most thermally stable vitrimers reported. Given the fact that silyl ethers can be readily prepared by silylation of polymers carrying hydroxyl groups, copolymerization of monomers having silyl ether groups, or radical grafting with a silyl ether-containing a silyl ether motif, we envision this new dynamic covalent chemistry can be generalized for various vitrimer synthesis and studies are currently underway toward this direction.

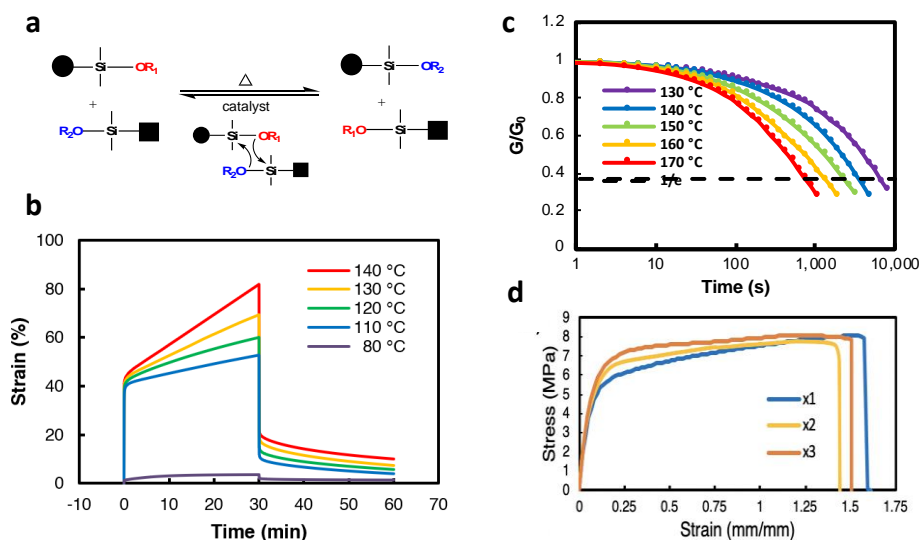


Figure 2. Silyl ether metathesis for vitrimer design. **a:** Discovery of silyl ether metathesis as a new dynamic covalent chemistry; **b:** Creep test shows the silyl ether vitrimer show good creep resistance at temperatures below its T_m while maintaining malleability above its T_m ; **c:** Stress relaxation at elevated temperature further demonstrates the malleability of the silyl ether vitrimers; **d:** Reprocessability of the silyl ether vitrimers.

3. Redox Chemical-fueled Dissipative Self-assembly of Active Materials

In a new study, we aim to develop a redox chemical-fueled dissipative self-assembly of active materials closely mimicking biological active assemblies such as microtubule system. Dissipative self-assembly is an out-of-equilibrium process in which consumption of a chemical fuel drives self-assembly of materials. In living organisms, transient self-assembly of actin networks and microtubules fueled by ATP and GTP is at the heart of a variety of cellular processes, including cellular transport, cell motility, proliferation, and morphogenesis. Such dissipative assembly processes in nature have inspired the design of synthetic active self-assembled systems driven by chemical fuels.

Synthetic dissipative assembly systems developed thus far are generally incompatible with living organisms because of the use of relatively toxic fuels and harsh conditions. To

address this issue, we recently developed a transient, out-of-equilibrium self-assembly system solely fueled by mild redox reactions. We use redox chemical reactions to simultaneously create and destroy a disulfide-based hydrogelator, leading to transient, dynamic behavior (*Manuscript submitted 2019*). By closely regulating reaction kinetics and reagent composition, macroscopic properties of the active materials are fine-tuned. Confocal fluorescence microscopy observed simultaneous active assembly and disassembly of fibers in the redox solution. Most excitingly, we recently succeeded in proof-of-concept experiments that such dissipative active assembly can be achieved with electrical redox process. As electronic signals are the default mode of transmitting information in synthetic devices, active materials that can transduce biological and electronic signals will be key to bridging living systems with devices such as for implantable power sources, wearable sensors, and therapeutic and prosthetic implants.

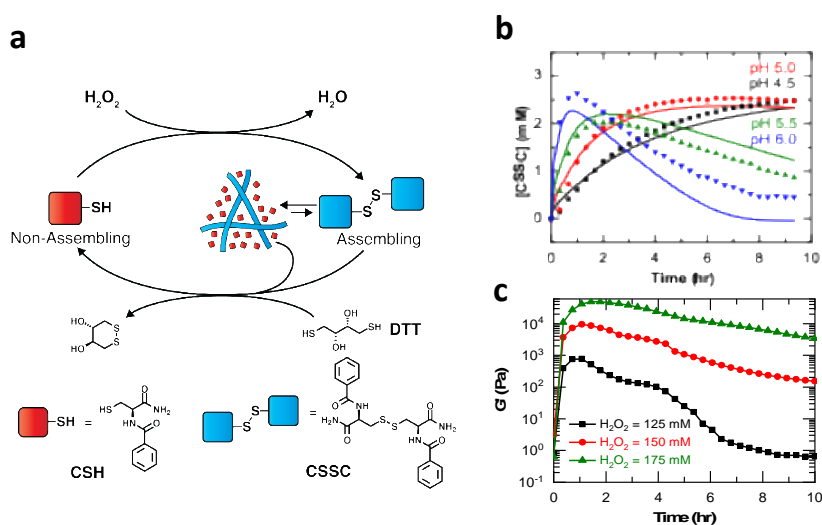


Figure 3. Redox fueled dissipative active assembly. **a:** Concept scheme for the redox chemical-fueled dissipative self-assembly of active materials; **b:** Kinetic profiles of [CSSC] for the full active system at different pH; **c:** Rheology of active assembling hydrogels at pH 5.5 with varying H_2O_2 concentrations.

Future Plans

(1) Further Investigation of Dynamic Materials Based on Dynamic B-O and Si-O Bonds

We will continue exploring the thermodynamically strong, while kinetically dynamic B-O and Si-O bonds for malleable materials design. We will generalize our designs by incorporating these dynamic covalent motifs into various polymer systems. Our goal is to develop a universal strategy for making reprocessable, recyclable, strong thermoset materials.

(2) Investigation of electrical signal triggered dissipative self-assembly of active materials

We are excited with our recent success in using redox chemical, and especially the electrical redox-fueled dissipative self-assembly of active materials. We will further our investigation of using electrical signals to provide spatio-temporal controls to active materials systems.

Publications in year 2017-2019 (which acknowledge DOE support):

1. Ogden, W.; Guan, Z. "Redox Chemical-fueled Dissipative Self-assembly of Active Materials", *Manuscript submitted, 2019*.

2. Tretbar, C. A.; Neal, J. A.; Guan, Z. “Direct Silyl Ether Metathesis for Robust and Thermally Stable Vitrimers”, *Manuscript submitted*, **2019**.
3. Muradyan, H.; Mozhdehid, D.; Guan, Z. “Self-healing Magnetic Nanocomposites from Commodity Monomers via Graft-from Approach”, *Manuscript submitted*, **2019**.
4. Li, C.; Tan, J.; Guan, Z.; Zhang, Q. “A Three-Armed Polymer with Tunable Self-Assembly and Self-Healing Properties Based on Benzene-1,3,5-tricarboxamide and Metal–Ligand Interactions” *Macromol. Rapid Comm.* **2019**, 1800909.
5. Ogden, W.; Guan, Z. “Recyclable, Strong, and Highly Malleable Thermosets Based on Boroxine Networks” *J. Am. Chem. Soc.* **2018**, *140*, 6217–6220.
 - Highlighted by ACS Chemical & Engineering News:
<https://cen.acs.org/materials/polymers/Stiff-yet-supple-plastic-reshaped/96/i23>
 - Selected as *Research of the Year 2018* by the Chemical & Engineering News:
<https://cen.acs.org/analytical-chemistry/CENs-Year-Chemistry-2018/96/i49>
6. “Silyl Ether as a Robust and Thermally Stable Dynamic Covalent Motif for Malleable Polymer Design” Nishimura, Y.; Chung, J.; Guan, Z. *J. Am. Chem. Soc.* **2017**, *139*, 14881–14884.
7. Neal, J. A.; Oldenhuis, N. J.; Novitsky, A. L.; Samson, E. M.; Thrift, W. J.; Ragan, R.; and Guan, Z. “Large Continuous Mechanical Gradient Formation via Metal-Ligand Interactions” *Angew. Chem.* **2017**, *56*, 15575-15579.

AUTONOMOUS MOTILITY OF SYNTHETIC PROTOCELLS DRIVEN BY BIOCHEMICAL CATALYSIS

Daniel A. Hammer^{1,2}, Daeyeon Lee¹, Matthew C. Good³

Departments of ¹Chemical and Biomolecular Engineering, ²Bioengineering & ³Cell and Developmental Biology, University of Pennsylvania, Philadelphia, PA 19104.

Program Scope

Our goal is to mimic cellular function through the assembly of molecular components into synthetic cells, or protocells. By assembling cell-like structures that mimic the organization and size of a natural cell but which incorporate novel components and respond to synthetic triggers, we can extend their capabilities beyond what is currently achievable in biology. The scope of this project is to construct protocells that display autonomous motility driven primarily by a novel mode of force generation: intra-protocell enzymatic activity. We will leverage our recently discovered platform for organelle self-assembly to convert chemical and optical stimuli into autonomous motion from within the protocell.

Aim 1. Random and Directional Motility of Single Protocells. We will quantify the dynamics of single protocell motion, and then examine whether additional enzymes stimulate protocell motility. We will measure the directional motility of protocells using gradients of substrates.

Aim 2. Collective Motion of Protocell Ensembles. Using both motile and non-motile capsules, we will determine the effects of interparticle hydrodynamic coupling or adhesion on the collective motion of ensembles of particles.

Aim 3. Organelle-based control of force-generation. We will use membraneless organelles built from self-assembling proteins to control protocell motility. The control system will be composed of elements including light and small molecule activated enzymatic activity, which regulates organelle assembly and cargo release. This will enable us to colocalize multi-component enzymatic cascades and logically control protocell motility using single inputs.

Recent Progress

Aim 1. Construction of a motile protocell. Cell motility requires the conversion of chemical to mechanical energy. Our goal has to been to create motile particles that are adherent to a surface, akin to how real biological cells crawl over surfaces through the sequential dynamics of extension, adhesion breaking and adhesion reformation. We have demonstrated autonomous motion in adhesive polymer-based protocells by incorporating and harnessing the energy production of an enzymatic reaction. The conceptual idea comes from the demonstration that enzymatic turnover can generate a propulsive force (Dey and Sen, 2017). We sought to harness enzymatic force by encapsulate enzymes adherent polymer vesicles to generate motion.

We prepared 5% biotinylated polymer vesicles from poly(ethylene oxide)-b-poly(butadiene) (PEO-PBD) that encapsulate catalase, an enzyme which converts hydrogen peroxide to water and oxygen, and adhered these vesicles weakly to avidin-coated surfaces. The adhesivity was modulated by varying the density of avidin which we stamped on substrates by microcontact printing. Upon addition of hydrogen peroxide, which diffuses across the membrane, catalase activity generates a differential impulsive force that enables the breakage and reformation of biotin-avidin bonds, leading to diffusive vesicle motion resembling random motility. The restricted motion of the

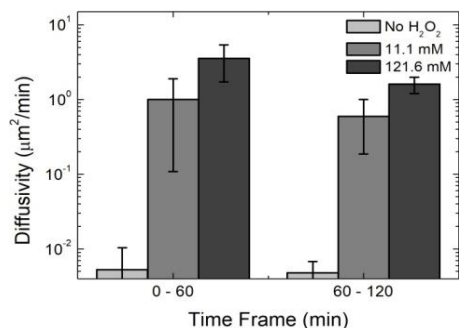


Figure 2. In a uniform field of H₂O₂, the motion of the protocells was diffusive and increased with the concentration of H₂O₂. This semi-log plot indicates a significant increase with H₂O₂ concentration, and no motion in the absence of fuel.

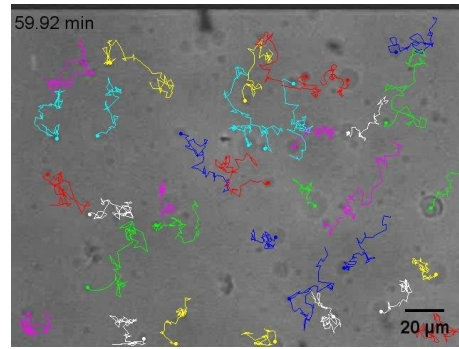


Figure 1. Representative trajectories of motile biotinylated protocells after 60 minutes of motility on an avidin coated surface at concentration of 121 mM H₂O₂.

protocells on a substrate requires breaking and reforming biotin-avidin bonds. Representative trajectories of a population of vesicles is shown in **Figure 1**. Plots of the mean squared displacement as function of time after the addition of hydrogen peroxide show that the vesicles are moving randomly, with a correlation coefficient of 1. As illustrated in **Figure 2**, the diffusivity increases with the concentration of hydrogen peroxide, indicating greater concentration of fuel leads to faster motion. Also, over time, the depletion of fuel causes the vesicles to stop moving, which can be rectified by reintroducing fuel to the protocells. Thus, we have made a protocellular mimetic of a motile cell; the paper has appeared (Jang et al., 2018).

We have preliminary evidence that in a gradient of H₂O₂, vesicles will move toward a higher concentration of H₂O₂. A gradient chamber was made by inserting a point source of H₂O₂, and the gradient of H₂O₂ is established over time, corroborated by simulations (**Figure 3**). The motion of vesicles in a gradient of H₂O₂ was compared with and without adhesion. In the absence of adhesion, vesicles moved avidly toward the point source (Fig 3C), whereas with the adhesion of adhesion, the friction led to a reduction of velocity, while the motion was still directed (Fig 3D).

Aim 3. Assembly of membraneless organelles from proteins.

Phase separation of intrinsically disordered proteins (IDPs) underlies the formation of membraneless organelles. These protein compartments represent a compelling target for bio-inspired materials engineering; specifically in this project, we aim to assemble or manipulate enzymatic activity from these droplets. We used the intrinsically disordered, arginine/glycine-rich RGG domain from the P granule protein LAF-1 to generate synthetic membraneless organelles that demonstrate controllable phase separation and cargo recruitment (**Figure 4**). The foundational hypothesis was that

multimers of RGG will more robustly phase separate than monomers, providing a handle for engineering phase separation. First, we demonstrated enzymatically triggered droplet assembly and disassembly, using propitiously inserted protease cleavable domains to alter valency and

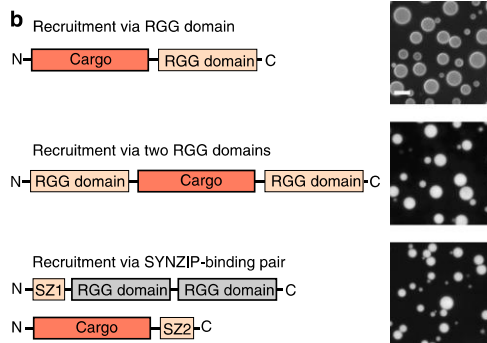
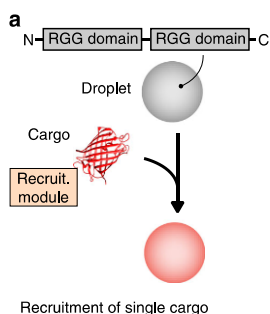


Figure 4. (A) Schematic of cargo recruitment into RGG-RGG liquid droplets. (B) Three strategies for recruitment of model cargo, RFP, normally excluded from RGG-RGG droplets: (i) recruitment via a single RGG domain, (ii) recruitment via two RGG domains, and (iii) recruitment via a high-affinity SYNZIP (SZ1-SZ2) binding pair, in which SZ1 is attached to RGG-RGG and its binding partner SZ2 is attached to RFP.

multiple schemes for controlled release of these cargos using proteases (**Figure 4**). This included connecting the cargo to one or two RGG domains, or linking the cargo to the droplets using SYNZIP protein motifs. The programmable assembly of enzymatic cargo into these droplets using

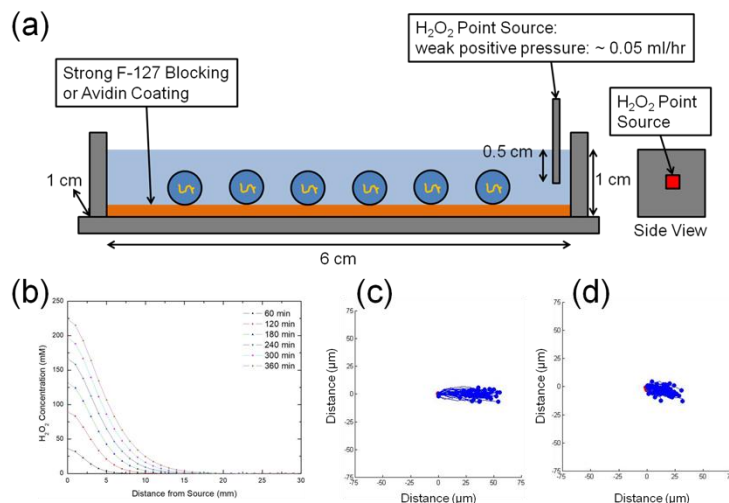


Figure 3. (a) H_2O_2 point source is connected to the reservoir of 10 wt. % H_2O_2 . (b) The gradient of H_2O_2 is calculated as a function of time and distance by the finite difference method. (c) Polymersomes on a non-adhesive pluronic F-127 surface show strong directionality. (d) Polymersome motion on an adhesive surface ($0.1 \mu\text{g}/\text{cm}^2$ avidin coating) show directional motion that is inhibited by adhesive friction.

miscibility. For example, insertion of a protease cleavable domain between two units of RGG and addition of protease led to droplet dissolution. This established a material platform that can undergo reversible phase separation which can be logically gated.

Then, we devised strategies to control the composition of droplets by selectively recruiting cargo molecules via protein interaction motifs, and demonstrated

these strategies gives us a versatile platform for generating functional membraneless organelles (Schuster et al., 2018).

In an intergroup BES collaboration between Hammer, Good and Mittal (Lehigh University), we have been determining the sequence-level features responsible for IDP phase separation, important knowledge for manipulating phase behavior with temperature as well as making multiple, communicating organelles. Based on a predictive coarse-grained (CG) model of IDPs (Mittal), we identified a critical region of RGG (amino acids 21-30) whose deletion eliminates phase separation (**Figure 5**). Finally, Mittal computationally identified those with large charge separation. Experimentally, we found these sequences would have dramatically enhanced propensity to phase separate compared to wild-type RGG (RGG Shuffle, Fig. 5). The results of this paper are in preparation (Schuster et al., 2019).

We developed a strategy for inducing or eliminating the formation of membraneless organelles using light by inserting the recently discovered, recombinantly encoded photocleavable (PhoCl) domain (Zhang et al., 2017), which is irreversibly cleaved at 405 nm. We have used light to control both the dissolution (by making RGG-PhoCl-RGG) and the formation (by making Maltose Binding Protein-PhoCL-RGG-RGG and cleaving the MBP which inhibits phase separation) of membraneless organelles. The work will facilitate the optogenetic control of droplet formation, enzymatic activity, and protocell motility. A paper is in preparation (Reed et al., 2019).

Future Plans

Aim 1. We are examining whether other enzymes drive motility. We are specifically focusing on urease (which catalyzes the conversion of urea to methanol and ammonia) and amylase (which converts starches into simple sugars). **Aim 2.** Using catalase driven capsule motility, we are developing experiments for the collective behavior of capsules. To achieve this task most elegantly, we are assembling populations of uniform populations of functionalized and nonfunctionalized capsules using microfluidics. **Aim 3.** We are using RGG membraneless organelles to assemble enzymatic activity, using either split enzymes, in which the N-terminus of the protein is linked to one RGG and the C-terminus is linked to another (such as luciferase), or in which we link enzymes to organelles using SynZip motifs (using catalase and urease).

References: Jang, W., ... D.A. Hammer, (2018) Small **14**; 1801715; Schuster, B. S., ... M. Good, and D.A. Hammer, (2018), Nature Communications **9**, No. 2985; Schuster, B. S., ... D.A. Hammer, M.C. Good and J.Mittal, (2019) in preparation, PNAS; Dey, K.K., and A. Sen. (2017) ...JACS **139**: 7666-7676; Reed, E.H., ... M.C. Good, and D.A. Hammer, (2019), in preparation, PNAS; Zhang, W....R.E. Campbell (2017) Nature Methods **14**:391-394.

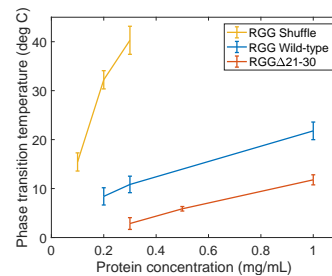


Figure 5. Protein phase behavior can be rationally tuned. Phase transition temperature for wild-type RGG domain vs. shuffled version (with large separation of charged amino acids) and vs. RGG domain with amino acids 21-30 deleted. Protein phase transition temperature is plotted vs. protein concentration.

Publications

Woo-Sik Jang, Hyun Ji Kim, Chen Gao, Daeyeon Lee, D.A. Hammer, (2018) “Enzymatically powered surface-associated self-motile protocells,” Small 14; 1801715; doi:10.1002/smll.201801715.

Schuster, Benjamin S., Ranganath Parthasarathy, Craig N. Jahnke, Ellen H. Reed, Matthew Good, and D.A. Hammer, (2018), “Controllable protein phase separation and modular recruitment to form responsive, membraneless organelles,” (2018) Nature Communications 9, No. 2985 (2018); doi: 10.1038/s41467-018-05403-1.

Schuster, Benjamin S., Gregory Dignon, Daniel A. Hammer, Matthew C. Good and Jeetain Mittal, (2019), “Sequence Perturbations to an Intrinsically Disordered Protein Induce Drastic Changes to Phase Separation,” in preparation for submission, PNAS.

Reed, Ellen H., Benjamin Schuster, Matthew C. Good, and Daniel A. Hammer, (2019), “Light responsive membraneless organelles from recombinant proteins,” in preparation for submission, PNAS.

Dissipative Assembly of Carboxylic Acid Anhydrides for Nonequilibrium Systems Chemistry

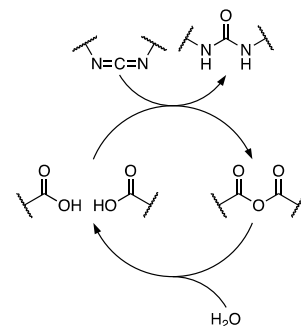
C. Scott Hartley, Department of Chemistry & Biochemistry, Miami University

Program Scope

The use of chemical fuels (e.g., ATP) is ubiquitous in biology. The consumption of energy enables temporally controlled, responsive behavior that is impossible at equilibrium, including adaptation, self-healing, and replication.¹ However, the design of analogous abiotic dissipative systems is challenging: whereas systems at equilibrium are controlled by well-understood thermodynamic parameters, dissipative systems require the less-predictable rates of different processes to be balanced. An important step toward the development of nonequilibrium assembly is access to reliable fuel chemistry that can be applied in a wide variety of contexts.

To this end, we are examining the use of *carbodiimides*, common reagents, as chemical fuels as shown in Scheme 1. The treatment of aqueous carboxylic acids with carbodiimides gives anhydrides which subsequently undergo hydrolysis, regenerating the original acids. This system exhibits the formation of a transient covalent bond, a key capability in the design of out-of-equilibrium processes. That is, the unstable anhydride state can be coupled to behavior of interest. Unlike most previous examples of abiotic dissipative assembly,² the fuel is not incorporated into the transient state: an existing equilibrium (acid/anhydride),³ is perturbed through the addition of the fuel. This feature is critically important, as it enables new kinds of behavior including the formation of intramolecular bonds and assembled species of greater complexity. The reaction is straightforward, occurs on convenient timescales (minutes to hours), is readily monitored by NMR/IR spectroscopies or HPLC, and is easily tuned through changes in conditions (solvent, buffer, temperature).

This project has three key goals. First, we are examining fundamental features of carbodiimide-fueled assembly, including structure–property effects to better understand the chemistry, the preparation of complex species connected by multiple transient bonds, and the formation of dynamic libraries. Second, we are designing transient supramolecular hosts, examining templation effects in host assembly and the development of high-affinity hosts for cations for use in, for example, active transport. Third, we are exploring how transient bond formation can be used to drive molecules into unstable geometries.



Scheme 1. Coupling of carboxylic acids to give aqueous anhydrides, fueled by the hydration of carbodiimides.

Recent Progress

Structure–Property Effects. Although carbodiimide-fueled anhydride formation has been applied in several contexts,^{4,5} basic structure–property relationships have not been reported. Characterization of the fundamental chemistry is necessary to guide the design of complex systems. Of course, the two reactions comprising this system, the reactions of carbodiimides with carboxylic acids and anhydride hydrolysis, are textbook reactions that have been studied for decades. However, they have not typically been studied together under conditions that are relevant for nonequilibrium systems chemistry. We have therefore been exploring the basic physical organic chemistry of a series of functionalized benzoic acids (Figure 1).

A representative experiment is shown in Figure 1: the conversion of carbodiimide EDC to urea EDU drives the clean conversion of **Ac2** to anhydride **An2**. The data can be fit to a simple mechanism based on the known mechanisms for the two processes independently (solid lines in Figure 1). The kinetic parameters characterizing each system can then be compared. Figures of merit for these systems, such as the efficiency (fraction of fuel that productively leads to anhydride), lifetime, or maximum/minimum species concentrations, are concentration-dependent but easily calculated from the kinetic model. Thus, these simple experiments provide useful insights into the chemistry underlying carbodiimides as chemical fuels.

Transient Assembly of Complex Architectures. Thermodynamically controlled self-assembly by dynamic covalent chemistry often exploits the formation of many dynamic bonds to access functional macrocycles and cages.⁶ The formation of comparable transient architectures linked by multiple bonds would broaden the usefulness of carbodiimide-fueled assembly. The challenge is to direct polyfunctional non-equilibrium assembly toward well-defined products.

It has long been known that anhydride exchange is faster than anhydride hydrolysis. Thus, as shown in Figure 2(a), a system driven from equilibrium should have time to relax to local free energy minima before reverting to the resting state. To test this hypothesis, we designed and synthesized the rigid diacid **M1**, shown in Figure 2(b). On treatment with EDC, NMR spectroscopy indicates that the **M1** is quickly consumed to give a species exhibiting heavily broadened peaks. Analysis of the reaction mixture by LC/MS shows predominant formation of macrocycle **Mac1**. We conclude that the macrocycle is formed quickly and then undergoes aggregation, presumably via stacking of the hydrophobic cores. Further experiments confirm that labeled macrocycles exchange components faster than hydrolysis occurs, supporting

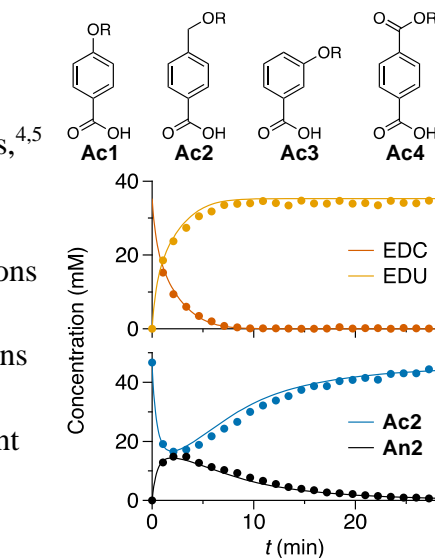


Figure 1. Top: Simple monoacids investigated for structure–property effects on dissipative assembly (**An2** is the anhydride of **Ac2**, R = (CH₂CH₂O)₆CH₃). Bottom: Representative kinetic run monitored by ¹H NMR spectroscopy (0.5 M pyridine/pyridinium buffer in D₂O, pD = 4.5).

the hypothesis that anhydride exchange plays a role in directing self-assembly.

Transient Supramolecular Hosts.

Previously, we showed that carbodiimides could be used to generate crown ether analogues such as **CE1**, as shown in Scheme 2.⁵ These systems undergo an unexpected negative templation effect in response to cations. That is, in the presence of the matched cation (i.e., K^+ for **CE1**), the formation of the crown ether is suppressed. This effect does not have a parallel in self-assembly at equilibrium, and could be important to understanding the behavior of out-of-equilibrium dynamic libraries. Further, minimizing it is important in the design of systems where effective binding is important.

To study the origin of templation effects in these systems, we have prepared model systems designed as mechanistic probes, including diacid **DA2** and a series of monoacids (not shown). Remarkably, initial experiments suggest that **DA2** and related compounds show positive templation; that is, enhanced macrocycle formation in the presence of matched cations. We are presently carrying out kinetics experiments on these systems to extract mechanistic details.

Functional Materials. In order to couple the fuel chemistry to materials properties, we examined the behavior of polymers with pendant acids, as shown in Figure 3. Treatment of aqueous solutions of these polymers with EDC yields hydrogels that dissolve on the timescale of hours, corresponding to the formation of polymer networks crosslinked by transient bonds. The lifetimes of the gels and the mechanical properties (storage and loss moduli) are dependent on the proportion of acid groups in the polymers.

Future Plans. We have several new directions in progress or planned that build on the studies described above: We are preparing analogues of the dianhydride macrocycles (Figure 2(b)) that are capable of binding guests; we are also examining systems with more flexible structures to promote the formation of dynamic libraries, so that we can examine the effect of

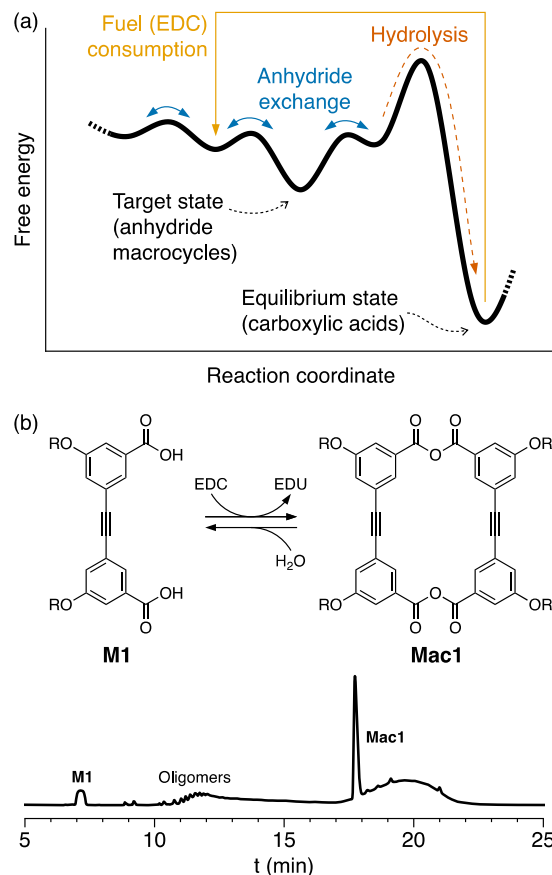
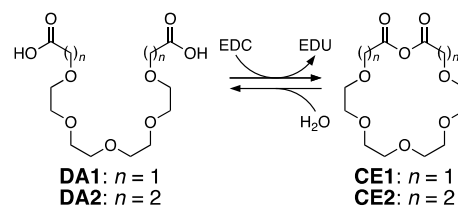


Figure 2. (a) Reaction coordinate diagram for the assembly of complex transient species. (b) Assembly of a **Mac1** comprising two transient bonds ($R = (CH_2CH_2O)_6CH_3$); the HPLC chromatogram was acquired after 56 min.



Scheme 2. Transient formation of crown ether analogues fueled by carbodiimides.

changing parameters on library compositions (e.g., concentrations, fuel input rate, guests). We are preparing precursors to transient hosts (Scheme 2) that are expected to exhibit much higher affinities for cations in water.

Another direction for this project focuses on the use of carbodiimides to drive molecules into unstable geometries, a concept that is commonly exploited in biology. Our model system for this effort is based on diphenic acids, as shown in Figure 4. Intramolecular anhydride formation in these systems is expected to greatly reduce the twist of the biaryl. A series of model compounds has been synthesized and we are beginning experiments to determine the effect of steric resistance on the fuel chemistry.

References

- (1) Fialkowski, M.; Bishop, K. J. M.; Klajn, R.; Smoukov, S. K.; Campbell, C. J.; Grzybowski, B. A. *J. Phys. Chem. B* **2006**, *110*, 2482–2496.
- (2) Boekhoven, J.; Hendriksen, W. E.; Koper, G. J. M.; Eelkema, R.; van Esch, J. H. *Science* **2015**, *349*, 1075–1079.
- (3) Astumian, R. D. *Chem. Commun.* **2018**, *54*, 427–444.
- (4) Tena-Solsona, M.; Rieß, B.; Grötsch, R. K.; Löhrer, F. C.; Wanzke, C.; Käsdorf, B.; Bausch, A. R.; Müller-Buschbaum, P.; Lieleg, O.; Boekhoven, J. *Nat. Commun.* **2017**, *8*, 15895.
- (5) Kariyawasam, L. S.; Hartley, C. S. *J. Am. Chem. Soc.* **2017**, *139*, 11949–11955.
- (6) *Dynamic covalent chemistry*, Zhang, W.; Jin, Y., Eds.; John Wiley & Sons, Ltd: Hoboken, NJ, 2017.

Publications

- (1) Zhang, B.; Jayalath, I. M.; Ke, J.; Sparks, J. L.; Hartley, C. S.; Konkolewicz, D. Chemically fueled covalent crosslinking of polymer materials. *Chem. Commun.* **2019**, *55*, 2086–2089.

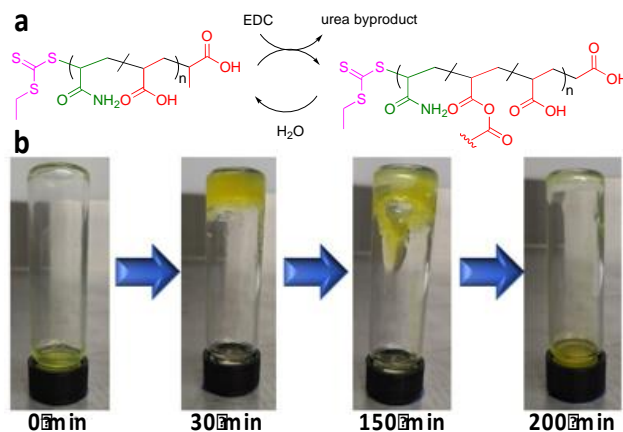


Figure 3. Transient assembly of a polymer network.

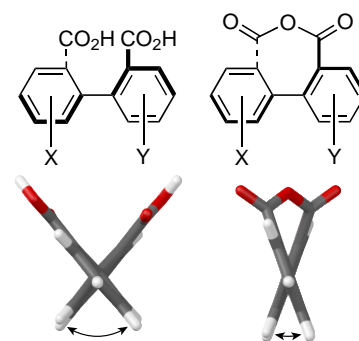


Figure 4. Geometry changes in diphenic acids (about 76° to 35°).

Bioinspired mineralizing microenvironments generated by liquid-liquid phase coexistence

Prof. Christine D Keating
Professor of Chemistry
104 Chemistry Building
University Park, PA 16802

Program Scope

Understanding how Biology uses mineralizing microenvironments to control the process and outcome of materials synthesis is a grand challenge that promises to enable new routes to high-performance materials. This project exploits bioinspired microenvironments formed through liquid-liquid phase coexistence to understand and control mineral formation. Liquid-liquid phase coexistence has only recently been appreciated as a mechanism for subcellular compartmentalization. Intracellular aqueous droplet phases are increasingly appreciated to be key features of intracellular organization, providing distinct biochemical microenvironments where reactions can be controlled by local concentration of reagents and biocatalysts. Liquid-liquid phase separation thus appears to be an important and previously unappreciated tool in Biology's toolbox for materials synthesis.

This project's bioinspired mineralizing microenvironments are expected to: (1) enable gradients of organic and inorganic inclusions within minerals/crystals by tuning their local availability during their synthesis; and (2) produce distinct mineral compositions in adjacent compartments at the microscale, with control over their physical association, from noncontacting through Janus structures to core-shell geometries. These microenvironments further provide exciting opportunities to explore the impact of competing reactions and complex active media on materials synthesis. Although the goal is not to produce specific structures for applications but rather to understand and control the mineralization process in multiphase aqueous solutions, we anticipate that the insight gained will enable future applications.

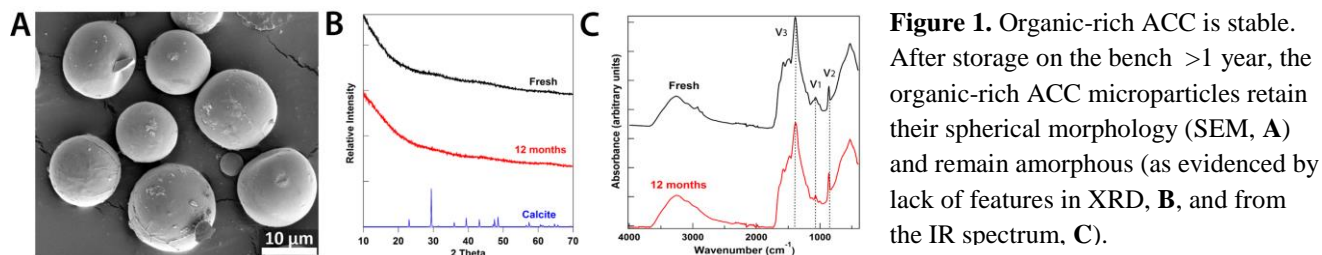
Recent Progress

Previously, we developed biomineralizing all-aqueous emulsion droplets, and incorporated a third phase to form coacervate-containing artificial mineralizing vesicles (AMVs).^{1,2} We recently submitted a manuscript that describes the preparation, characterization, and function of these coacervate-containing AMVs as bioinspired mineralizing microenvironments. Focus areas in the past 2 years include: (1) further characterizing the organic-rich amorphous calcium carbonate microspheres formed in coacervate-containing AMVs, (2) evaluating the potential of this approach to production of other materials, and (3) increasing understanding of the lipid vesicle stabilized all-aqueous emulsion's role in mineralization.

(1) Characterization of material formed in coacervate-containing AMVs.

1.1 Factors impacting mineral particle size. We have quantified the size distributions of coacervate droplets and ACC microparticles under a variety of conditions. Particles form in, and are smaller than, the coacervates. Reducing the average coacervate size shifts the distribution of particle sizes to smaller values, as does increasing the amount of mixing after reaction initiation.

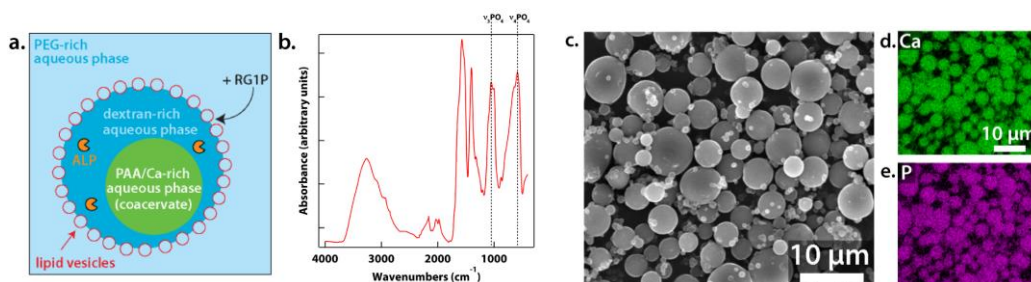
1.2 Stability of hybrid organic-inorganic microspheres. While slow heating results in conversion to porous, polycrystalline calcite that retains the overall spherical shape of the original ACC particles, unheated samples stored in air on the benchtop remain ACC indefinitely (>12 months so far, Figure 1), and those stored in water remained unchanged for at least 3 days. ACC normally converts to more stable forms such as calcite over time particularly when heated or exposed to water, although freeze-drying or additives can slow conversion.^{3,4} We attribute ACC stability in our microparticles to the high organic content (~30 w/w%), which prevents restructuring. Stable organic-rich ACC that can be stored under ambient conditions for long



times and later converted to crystalline form may be of interest for repair of hard materials.

(2) Evaluating the ability of coacervate-containing AMVs to produce other materials. The multiphase reaction environment approach should be generalizable to other reactions to form other materials. Additionally, products may be convertible to other materials after formation.

2.1 Calcium phosphate production in coacervate-containing AMVs. We replaced the urease/urea enzyme/substrate pair with alkaline phosphatase (ALP) and *rac*-glycerol 1-phosphate (RGIP) to adapt the coacervate-containing AMVs for calcium phosphate production (Figure 2a).



XRD of the resulting particulate material showed no features, and ATR-FTIR spectra were consistent with PAA-rich amorphous calcium phosphate (Figure 2b).⁵ Figure 2 shows SEM images and EDS elemental mapping for calcium phosphate particles produced by this process, which were smaller than the ACC particles but otherwise similar in appearance as smooth, round microspheres. Further characterization of this material is ongoing. These results are important because they illustrate the generality of our mineralizing microenvironment platform for production of different materials and will allow us to study the impact of mineralizing microenvironment in a distinct reaction. Replacing the Ca^{2+} with another metal cation should also be possible. Although Mg^{2+} cannot fully replace Ca^{2+} in the coacervates of our standard system, it is possible to produce Mg^{2+} -doped ACC microspheres by replacing a portion of the Ca^{2+} with Mg^{2+} . Interestingly, the resulting particles have lower N content than for Ca^{2+} -only particles. We have also successfully produced adjacent Mg^{2+} -rich and Ca^{2+} -rich coacervates using a phosphate-based polyanion to form the Mg^{2+} -rich⁶ phase.

2.2 Conversion of pre-formed organic-rich ACC microspheres to other materials.

Cation exchange for conversion to lead carbonates. Calcium carbonates can be converted to lead perovskites by first exchanging the Ca^{2+} for Pb^{2+} , followed by exchanging the carbonate with perovskite.⁸ We have taken a step in this direction with our particles by soaking the organic-rich ACC microspheres in Pb^{2+} solution and checking for changes in particle morphology and composition by SEM/EDS. Organic-rich ACC microspheres reacted to form PbCO_3 with retention of overall spherical particle morphology. In contrast, porous calcite microspheres prepared by heat treatment of the organic-rich ACC particles show much slower conversion, while still faster than nonporous calcite. This work continues; we are interested in better understanding the role of the organic component in facilitating transformation and in examining the particle interiors to determine penetration depth of conversion.

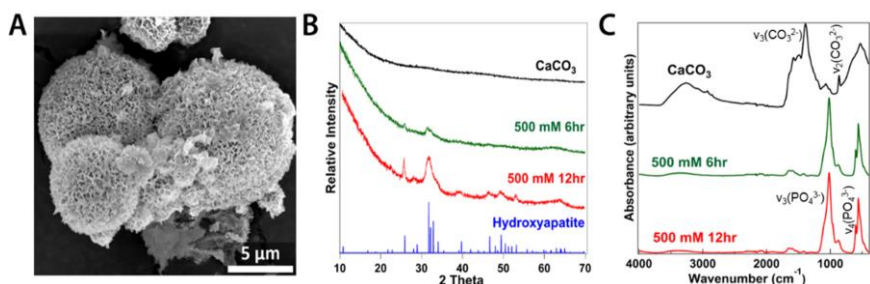


Figure 3. Conversion of organic-rich ACC particles upon exposure to phosphate buffer. A) SEM after soaking in phosphate buffer showing what appears to be hydroxyapatite formation on the surface, B, C) XRD, IR spectra of treated samples.

Conversion to calcium phosphates. CaCO_3 can be converted to calcium phosphates by anion exchange reactions through dissolution/reprecipitation mechanisms.⁷ We found that our ACC microspheres transition to calcium phosphate when placed in pH 7.4 phosphate buffer. Although literature indicated that organic materials should be removed prior to reaction, we found this was unnecessary, another indicator of the reactivity of these particles. The spherical overall morphology of the original ACC microparticles is preserved, however the originally smooth surfaces become rough as a result of the conversion to hydroxyapatite (HA) (Figure 3).

(3) Vesicle stabilized all-aqueous emulsions. The PEG/dextran segregative aqueous two-phase system (ATPS) plays an important role in the coacervate-based mineralizing microenvironments that we use to produce organic-rich stable ACC microspheres. In addition to providing the structure of the all-aqueous emulsion, we find that the polymer-rich media of the ATPS influences coacervation and mineral particle outcomes (structure, morphology, and organic inclusions). Indeed, at our standard Ca^{2+} and PAA concentrations, coacervation does not occur in buffer, it requires the macromolecularly-crowded solution environment of the ATPS. In an effort to better understand the role of the ATPS and vesicle components, and as a means of evaluating the generality of our overall approach, we have tested additional ATPS compositions based on PEG/ficoll and PEG/sulfate. In both cases droplets can be stabilized by interfacial lipid vesicle adsorption. The PEG/sulfate system is relatively less stable than both PEG/polysaccharide systems, which is unsurprising due to its high ionic strength. Additionally, we find that vortexed liposomes, while not as monodispersed as extruded liposomes, are acceptable alternatives for forming all-aqueous emulsions for any of the ATPS compositions tested.

Future Plans

This project is in no-cost extension, so our major emphasis is completion and publication of the work that is already underway. We recently submitted the main manuscript describing mineralization in coacervate-containing AMVs and plan to submit additional manuscripts describing variations on this theme in the coming months. These include effects of different polycarboxylates, expansion to new phase systems, and production of additional material types. Going forward, we are interested in how changes to the microenvironment during reaction impact outcomes, and in how multiple materials can be produced in adjacent compartments.

References

1. Dewey, D. C.; Strulson, C. A.; Cacace, D. N.; Bevilacqua, P. C.; Keating, C. D., Bioreactor droplets from liposome-stabilized all-aqueous emulsions. *Nature Commun.* **2014**, *5*, 4670.
2. Cacace, D. N.; Rowland, A. T.; Stapleton, J. J.; Dewey, D. C.; Keating, C. D., Aqueous emulsion droplets stabilized by lipid vesicles as microcompartments for biomimetic mineralization. *Langmuir* **2015**, *31*, 11329-11338.
3. Ihli, J.; Wong, W. C.; Noel, E. H.; Kim, Y.-Y.; Kulak, A. N.; Christenson, H. K.; Duer, M. J.; Meldrum, F. C., Dehydration and crystallization of amorphous calcium carbonate in solution and in air. *Nature Commun.* **2014**, *5*, 3169.
4. Polyamine/nucleotide coacervates provide strong compartmentalization of Mg^{2+} , nucleotides, and RNA. Frankel, E. A.; Bevilacqua, P. C.; Keating, C. D. *Langmuir* **2016**, *32*, 2041-2049.
5. Rey, C.; Marsan, O.; Combes, C.; Drouet, C.; Grossin, D.; Sarda, S., Characterization of calcium phosphates using vibrational spectroscopies. In *Advances in Calcium Phosphate Biomaterials*, Ben-Nissan, B., Ed. Springer: Berlin, Heidelberg, 2014; pp 229-266.
6. Müller, W.E.G., et al., Nonenzymatic transformation of amorphous CaCO_3 into calcium phosphate mineral after exposure to sodium phosphate in vitro: Implications for in vivo hydroxyapatite bone formation. *ChemBioChem*, **2015**. *16*, 1323-1332.

7. Holtus, T.; Helmbrecht, L.; Hendrikse, H. C.; Baglai, I.; Meuret, S.; Adhyaksa, G. W. P.; Garnett, E. C.; Noorduyn, W. L. Shape-preserving transformation of carbonate minerals into lead halide perovskite semiconductors based on ion exchange/insertion reactions. *Nature Chem.* **2018**, *10*, 740-745.

Publications

1. Liquid-liquid phase separation in artificial cells. Crowe, C. D.; Keating, C. D. *Interface Focus* **2018**, *8*, <https://doi.org/10.1098/rsfs.2018.0032>.
2. Bioinspired mineralizing microenvironments generated by liquid-liquid phase coexistence. Rowland, A. T.; Cacace, D. N.; Pulati, N.; Gulley, M. L.; Keating, C. D. *Submitted*.

Controlling Lattice Organization, Assembly Pathways and Defects in Self-Assembled DNA-Based Nanomaterials

Sanat K. Kumar and Oleg Gang

Columbia University, New York, NY

Program Scope

The major objective of this effort is to devise platform methods for the rational assembly of nanoscale objects into targeted, ordered organizations using DNA-based approaches. We also aim to reveal the key parameters controlling these assembly processes. Our integrated experimental and theoretical efforts were focused on exploring how nanoscale lattice architectures can be formed through “engineering” nanoscale valence and uncovering how molecular factors affect nanoscale assembly. Towards the goal of rationalizing lattice formation, we have established a strategy of encapsulating nanoparticles (NP) into DNA frames.^{2,3} The frame’s shape and bonding architecture controls the effective valence and that consequently leads to formation the crystals whose symmetry is directly correlated with the engineered valence. NP ordering is thus templated by these superstructures apparently independent of the NP details. We also investigated, for the case of cubic NP, how molecularly crowded soft shells can modify the effective valence imposed by shapes leading to the formation of novel phases with broken orientational symmetry.¹ Through a combination of experiment and theory, we have developed approaches for creating, characterizing and understanding several types of these valence-guided self-assembled systems. In the next stage we plan to generalize these methods, to integrate experiment and mean-field liquid-state theory and molecular simulations to develop inverse design strategies for nanomaterial assembly. These should permit for the robust and tailorable assembly of desired NP lattice types using prescribed directional and highly-specific DNA bonds. While this concept is potentially facile for ordering NPs into arbitrarily desired crystal structures, the presence of defects limits the size and the perfection of the crystals that result. Revealing and analyzing these defects in 3D nano-arrays is a significant challenge that will be addressed by our studies. In addition, using a suite of advanced characterization and computational methods, we aim to delineate the pathways for NP crystallization and to establish optimal pathways for minimizing defects and arrested states. In parallel, we are developing novel 3D electron and x-ray-based imaging techniques and the related analysis methods to measure and quantify defects and the local arrangements in 3D NP structures.

Recent Progress

Overview. We have recently developed a new versatile method of assembling three-dimensionally ordered DNA origami arrays, demonstrating control over crystal symmetry, unit cell spacing and nanoparticle (NP) organization, with the added ability to decouple self-assembly processes from the details of NP shells, shapes and interactions.¹⁻³ The development of ideas to achieve structural control over NP arrays and the designability of NP-based 3D materials is a major and unifying objective of this effort. Our approach intellectually merges and expands ideas about controlling 3D periodic architectures through nanoscale valence in an organic way using DNA-based methodology. We use inorganic NPs, DNA shells and complex DNA constructs to control binding energies, shapes of nano-objects, topology of connections, and local orientations, to investigate how the resulting, comprehensive control at the nanoscale can be rationalized for establishing platform strategies for the assembly of targeted periodic NP organizations. We utilize advanced x-ray scattering methods and newly developed methods for 3D imaging, and theoretical and computational methods to gain a quantitative understanding of the assembly process and to rationalize and guide experimental protocols for advancing the assembly methods.

Soft-Shell Cube Assembly.¹ We have investigated the role of the soft shell, formed by grafted chains, on packing of nanoscale cubes. The cube is the most basic polyhedral building block with surface termination of six identical crystallographic facets. The formation of 1D arrays with tunable cube

orientations, i.e., either face-to-face or edge-to-edge, have been revealed in recent experiments of polymer-coated nanocube (NC) assembly, which depends on polymer chain length, rigidity or grafting density. These observations further stimulate interest in assembling NCs into 3D structures. An application of the DNA-driven assembly to the fabrication of 3D ordered arrays revealed that the NCs grafted with relatively rigid DNA motifs form SC and corner-to-corner body-centered tetragonal (BCT) lattices depending on the DNA length, indicating that chain length and chain rigidity are defining contributors to the formation of phases with specific translational and orientational order. Despite the diversity of reported arrangements, characterized by lattice type and cube orientation in unit cell, the previously observed well-defined phases are oriented in the same manner relative to all the three vectors of unit cell.

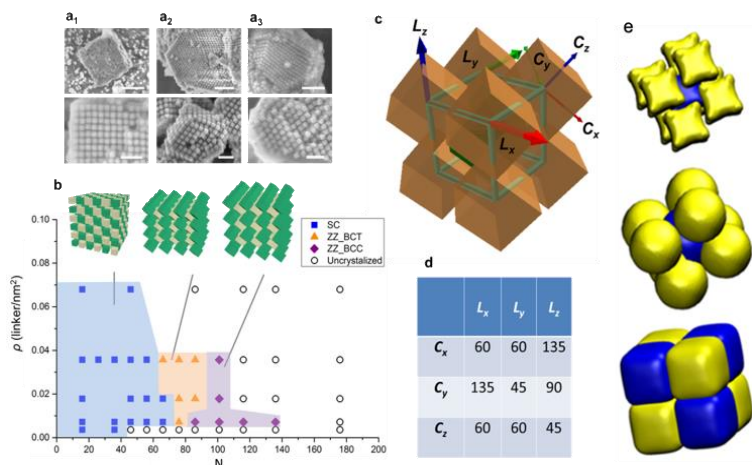


Figure 1. The assembly behavior of cubes as a function of DNA linker length and linker grafting density³⁷. **a₁-a₃**, low (top cell)- and high (bottom cell)-magnification SEM images of silica-encapsulated lattices with DNA linkers of different length. Scale bars: (a₁) 1 μ m (top) and 200nm (bottom), (a₂-a₃) 500nm (top) and 200nm (bottom). (b) Phase diagram for cube-assembled lattices as a function of N (the nucleotides number per linker chain) and ρ (linker grafting density), coded with colors for different structures, *FF*-SC (blue), *ZZ*-BCT (orange), *ZZ*-BCC (purple), and disorder (white). (c) Definition of lattice base vectors (L_x, L_y, L_z) and cube vectors (C_x, C_y, C_z) in a *ZZ*-BCC unit cell. (d), Table summarizes the angle between lattice base vectors and cube vectors; a break of orientational symmetry of cubes in the *ZZ*- BCC and BCT lattices is observed. (e) Theoretically calculated particle packing orientations.

We discovered that soft-shelled cubes, over a range of shells formed by grafted DNA chains on their other surface, form new types of cube packing with *broken orientational symmetry* (Figure 1).¹ In this case, the orientation of cubes is the same with respect to only two vectors of unit cell, while relatively to the third axis the orientation is different. This previously unknown cube packing within a lattice results in a peculiar, *zig-zag (ZZ)*, arrangement. That orientation is adopted in both *flat* BCT and body-centered-cubic (BCC) arrangements of NCs for medium and larger sizes of the soft DNA shells, formed by predominantly single stranded motifs, while for shorter chains a conventional SC packing with trivial symmetric orientation occur. Our detailed theoretical modeling uncovers that the non-trivial NC orientations result from the anisotropic surface distribution of flexible DNA grafts, that allow us to reconcile conflicting requirements on coordination number for attraction (=6)

and repulsion (=8) interactions while still maintaining BCC and BCT crystal symmetry. The observed phenomenon reveals the decisive role played by shell-modulated nano-object anisotropy in nanoscale packing and suggests that a plethora of new types of spatial organization exist for molecularly decorated shaped nanoparticles.

3D-organized nanomaterials through valence-prescribed ‘material voxel’.^{2,3} One of the outstanding challenges in nanoscience is to establish platform approaches for assembly of nanoscale objects of different nature in 3D ordered arrays. We have tackled this challenge by using 3D DNA frameworks formed from polyhedral DNA frames for organizing nano-objects that are contained inside. One of the key difficulties in the realization of this strategy is to reveal the relationship between the design of the frame and inter-frame connectivity, and the formation of the 3D ordered framework. To address this, we proposed to use DNA origami frames of different shapes to both host desired nano-objects and access different lattice symmetries. Although co-assembly of lattices of spherical NPs and DNA frames of

different shapes has been demonstrated by us, lattice formation in such an approach depends on the intricate balance of maximizing a number of particle-to-frame hybridization and minimizing interframe interactions. That issue was addressed in our recent work, where the frame's shapes impose effective valence and allow decoupling the assembly process from the shape/interactions of the NPs placed inside of the frames. Using this idea, we demonstrated that 3D ordered lattice can be fully assembled purely from DNA frames with shapes of Platonic solids, e.g., tetrahedra, octahedra, and cubes, and the NPs assemblies are templated by these solids.

In our approach, polyhedral frames are capable of inter-frame hybridization only via vertex-to-vertex hybridization (Figure 2). Thus, the DNA frame possess a spatially determined valence defined by its shape. Inter-frame hybridization results in assembly with the ability to form an ordered lattice, whose type is determined by the frame valence. This strategy allows us to use the same assembly process for creating arrays of very different types of nano-objects (inorganic nanoparticles and proteins), due to decoupling a formation of a lattice from the nano-objects material identity. Since the DNA frame represents a building block for the formation of 3D lattice, we term such a block as a valence-prescribed material voxel. Material voxel is an elementary block carrying material property and binding characteristics fully determined by frame shape that lead to a rationally prescribed 3D lattice. Using this strategy, we have rationally assembled lattices of different kinds, including diamond, and revealed using the developed theoretical framework the relationship between the frame geometry, valence, bond energies and the lattice symmetry. The developed approach offers a powerful pathway for the rational assembly of 3D ordered nanomaterials from desired nano-objects for a broad range of applications.

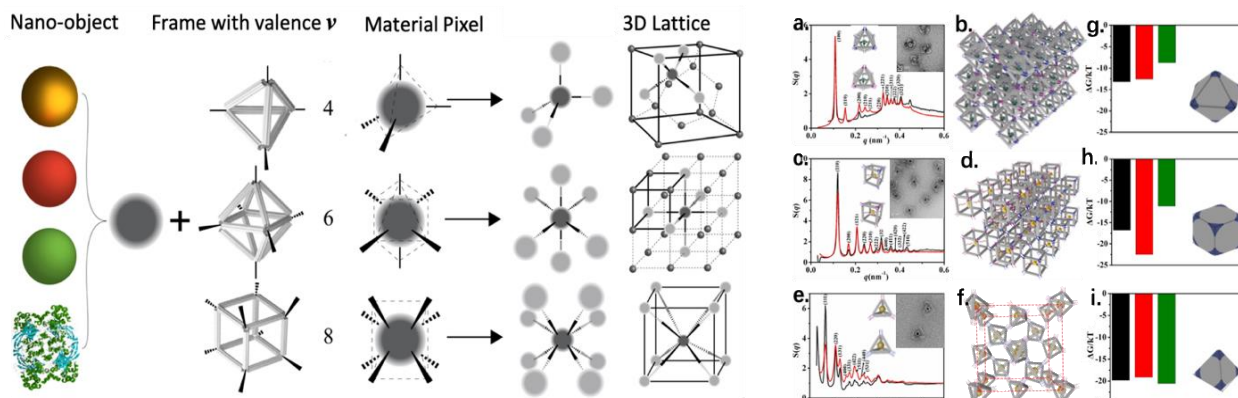


Figure 2. (Left panel). **Schematic of the valence-prescribed material voxel (3D pixel) platform for assembly of 3D lattices from nano-objects with DNA frames.** Tetrahedra, octahedra and cubic DNA frames have correspondingly valence $\nu=4, 6$ and 8 and can incorporate nano-objects of different nature (Right panel). Experimental and computational results for rational assembly of SC, BCC and diamond lattice for NP of different kinds, encaged in DNA frame. (g)-(i) represent results from liquid-state theory.

Future Work

Our future efforts will be focused on developing and optimizing the assembly strategy based on the prescribed valence concept. We will combine this assembly methodology with structure-predictive inverse design strategy. Inverse design, whose goal is to find optimal materials for a particular function/application, goes from the required metrics of product performance to designing the optimal building blocks (BB) and processing protocols (jointly termed as “product formulation”). This approach must be contrasted to the traditional “forward modeling” methodology where one uses well-developed tools, such as analytical theory or computer simulations, to go (typically) from details of the BBs and processing protocols to structure. Two strategies will be followed in this inverse design procedure – both

involving different means of doing “forward” predictions of structure from knowledge of building blocks. In particular, we shall use a liquid-state based method or alternately a machine learning methodology – these represent two extremes of a physics-based model vs. a dominantly data-based approach, and we shall critically examine the role of such more empirically based methods in this context.

In addition, to investigate questions about establishing principles and practical approaches for assembly of equilibrium structures, we aim to explore what assembly pathways can lead to the faster structure formation with minimal defects. *In-situ* probes of structure and assembly, e.g., x-ray scattering, will be utilized. Also, we will establish x-ray- and electron microscopy-based methods for 3D imaging of nanoparticle lattices to obtain information about defects, interfaces and types of imperfections. Finally, we will investigate principles and develop quantitative methods for creating complex designed lattices using systems with distinctive sequence-encoded interactions. Prescribing, creating and understanding designed nanoparticle organizations, the key factors that control their formation and the methods for perfecting the formed lattices are the objectives of future work.

References

1. F. Lu, T. Vo, Y. Zhang, A. Frenkel, K. G. Yager, S. Kumar* and O. Gang*, “Unusual Packing of Soft-Shelled Nanocubes”, *Science Advances* 5, 5, eaaw2399 (2019)
2. Y. Tian, J. R. Lhermitte, L. Bai, T. Vo, H. L. Xin, H. Li, R. Li, M. Fukuto, K. G. Yager, J. S. Kahn, Y. Xiong, B. Minevich, S. K. Kumar, and O. Gang* “3D-Organized Nanomaterials through DNA-programmed Valence-prescribed Material Voxels”, (in revision)
3. Zhiwei Lin, Yan Xiong, Shuting Xiang, and Oleg Gang* “Controllable Covalent-bound Nano-Architectures from DNA Frames” *JACS*, 141, 17, 6797 (2019)

Publications

1. W. Y. Liu, N. A. Mahynski, O. Gang*, A. Z. Panagiotopoulos & S. K. Kumar* “Directionally Interacting Spheres and Rods Form Ordered Phases” *ACS Nano* 11, 4950-4959, doi:10.1021/acsnano.7b01592 (2017).
2. N. C. Seeman* & O. Gang* “Three-dimensional molecular and nanoparticle crystallization by DNA nanotechnology” *MRS Bulletin* 42, 904-912, doi:10.1557/mrs.2017.280 (2017).
3. S. Srivastava, M. Fukuto & O. Gang*. Liquid interfaces with pH-switchable nanoparticle arrays. *Soft Matter* 14, 3929-3934, doi:10.1039/c8sm00583d (2018).
4. G. Chen, K. J. Gibson, D. Liu, H. C. Rees, J. H. Lee, W. W. Xia, R. Q. Lin, H. L. L. Xin, O. Gang and Y. Weizmann* “Regioselective surface encoding of nanoparticles for programmable self-assembly” *Nature Materials* 18, 169-, doi:10.1038/s41563-018-0231-1 (2019).
5. F. Lu, T. Vo, Y. Zhang, A. Frenkel, K. G. Yager, S. Kumar* and O. Gang*, “Unusual Packing of Soft-Shelled Nanocubes”, *Science Advances* 5, 5, eaaw2399 (2019)
6. S. Pal and O. Gang*, “Molecular Amplifier based on Nanoparticle-based Cascade Reaction” (in submission)
7. Y. Tian, J. R. Lhermitte, L. Bai, T. Vo, H. L. Xin, H. Li, R. Li, M. Fukuto, K. G. Yager, J. S. Kahn, Y. Xiong, B. Minevich, S. K. Kumar, and O. Gang* “3D-Organized Nanomaterials through DNA-programmed Valence-prescribed Material Voxels”, (in revision)
8. Zhiwei Lin, Yan Xiong, Shuting Xiang, and Oleg Gang* “Controllable Covalent-bound Nano-Architectures from DNA Frames” *JACS*, 141, 17, 6797 (2019)
9. A. Federica De Fazio, A. H. El-Sagheer, J. S. Kahn, I. Nanhakumar, M. Burton, Tom Brown, O. L. Muskens, O. Gang*, A. G. Kanaras*, “Light-induced reversible DNA ligation of gold nanoparticle superlattices”, *ACS Nano*, 13, 5, 5771 (2019)
10. F. Sciortino*, O. Gang, S.K. Kumar, “Entropy drives the assembly of DNA grafted Nanoparticles”, (submitted)
11. T. Vo, O. Gang, S.K. Kumar*, “A liquid-state model for modeling the assembly of DNA-grafted Nanoparticles”, in preparation

Command of active and responsive elastomers by topological defects and patterns

Oleg D. Lavrentovich, Sergij V. Shiyanovskii, Qi-Huo Wei,

Advanced Materials and Liquid Crystal Institute, Kent State University, Kent, OH 44242

Program Scope

As stated in the description of Biomolecular Materials research area, “biology provides a blueprint for translating atomic and nanoscale phenomena into mesoscale materials that display complex yet well-coordinated collective behavior.” An excellent example of such a blueprint is epithelium formed by cells in constant motion, in which orientational order and activity (such as contraction-dilation) are the key controlling factors. The objective of this project is to use these two key factors to create a synthetic analog of dynamic biological tissues, namely, an artificial “skin” that changes its shape in a preprogrammed fashion when activated by temperature or light.

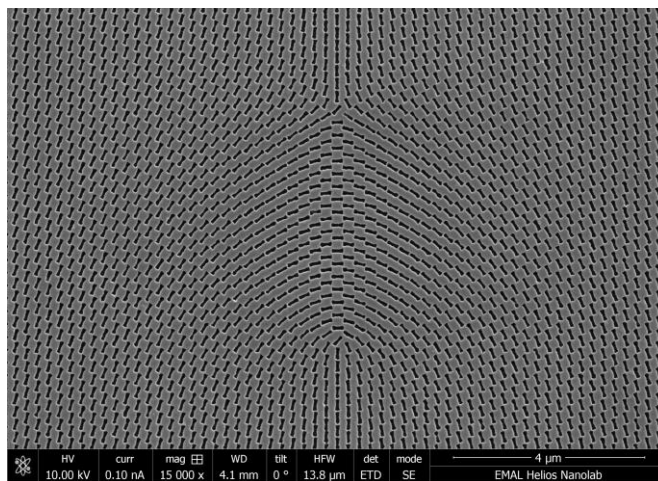


Fig.1. Scanning electron microscopy of a plasmonic metamask with a pattern of elongated slits.

The material under study is a special type of organic rubber, the so-called liquid crystal elastomer (LCE), in which molecules tend to align parallel to each other. The molecular orientation within the elastomer is predesigned to change from point to point by optical plasmonic technique developed by Qi-Huo Wei and Oleg D. Lavrentovich. In this technique, a plasmonic mask is used to create a beam of light in which polarization changes from point to point. To create this modulated pattern of polarized light, one uses a plasmonic metamask in a thin metallic film with thin elongated slits, Fig.1. The light beam transmitted through the mask

becomes locally linearly polarized along the short axis of the slit. The pattern of light polarization is transferred into a pattern of spatially-varying molecular orientation by irradiating a layer of photosensitive molecules of a dye deposited at a substrate that defines the footprint for the layer of liquid crystal (LC) molecules. The elastomer skin is prepared as a flat film with molecular orientation changing from point to point according to the predesigned pattern. Both smooth and singular director patterns are explored. Once the skin is activated by temperature or light, Fig.2, this in-plane two-dimensional pattern is expected to cause three-dimensional changes of shape. Namely, the skin will develop elevations, depressions, in-plane shifts, contractions and expansions in accordance with the pre-inscribed molecular orientation. By using a battery of microscopic techniques, including the polarizing optical microscopy and digital holographic microscopy, the team will establish the relationship between the patterns of in-plane molecular orientation and

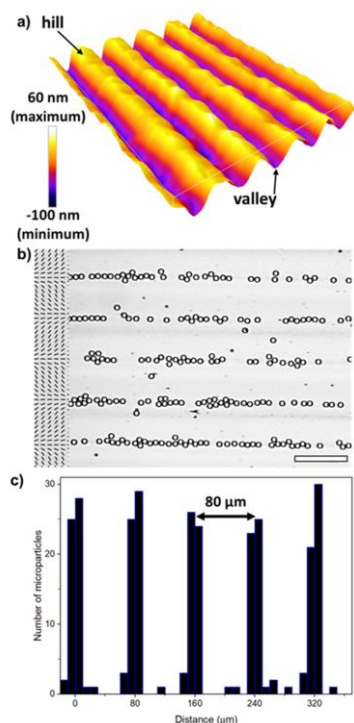


Fig.2. (a) Photoactuated LCE profile with periodic hills and valleys collects (b,c) colloids at the microscale; the process is reversible. Scale 100 microns.

into deterministic topographic change of the LCE coating. The microparticles placed at the interface between the LCE coating and water, guided by gravity, gather at the bottom of photoinduced troughs. The effect is reversible: when the substrates are irradiated with a visible light, the coatings become flat and the microparticle arrays disorganize again, Fig.3. The proposed non-contact manipulation of particles by a photo-activated LCEs may be useful in development of drug delivery or tissue engineering applications.

Dr. Wei and his group succeeded in developing a photopatterning system with the capability to photo-pattern large areas, $750 \times 750 \mu\text{m}^2$, by a step-and-flash approach. The group has also implemented a motorized stage and an optical shutter with computer controls. Programming codes have been developed to control the exposure time and position.

In the second subproject, we explored how the LCE can be used to control the growth of human cells tissues. Our work has been inspired by the

dynamic three-dimensional shape changes and then use the developed approaches to demonstrate control of colloidal particles and to interface the synthetic elastomers with materials of biological origin, such as arrays of cells.

Recent Progress. As a monomer, we use a special class of liquid crystal (LC) molecules with polymerizable acrylate groups. Once the monomer is aligned, the LC order is fixed by photopolymerization, the resulting film with one free surface and one surface clamped at a substrate represents a LCE coating [1]. The LCE material also incorporates azodye derivative that undergoes a trans-to-cis isomerization when illuminated by UV light and reverse transition under visible light. The pre-patterned director which specifies the average orientation of LC molecules, determine the three dimensional profile of an initially flat LCE when the latter is activated by UV light at 365 nm, Fig.2. For theoretical studies of photo-induced modifications of LCE films we have developed an LCE model based on the step tensor concept introduced by Warner and Terentjev, and on vector of the variable length, called nemator, $\mathbf{N} = \sqrt{s} \hat{\mathbf{n}}$, where $\hat{\mathbf{n}}$ is the director, and s is the uniaxial order parameter. The nemator description takes into account spatial inhomogeneity of s and allows one to simulate structures with point defects and disclinations. The dynamic properties of photo-addressable LCEs were demonstrated as a useful tool to control placement of colloidal particles [2], Fig.3. Upon UV illumination, these in-plane director distortions translate

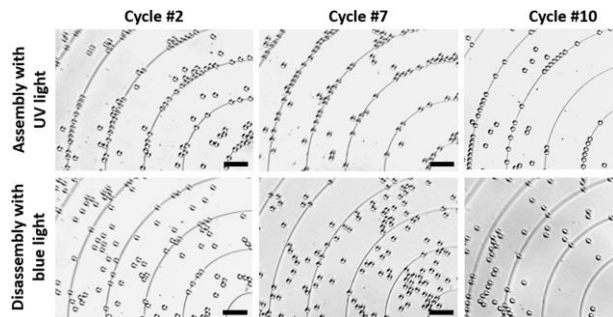


Fig.3. Assembly/disassembly of microparticles at the LCE substrate with dynamic flat-structured topography showing the reversibility and reproducibility of the system. Scale 50 microns.

recent publications in *Nature* [3,4], which demonstrated that biological tissues represent aligned arrays of living cells with spatially varying orientation and topological defects in them, such as $+1/2$ and $-1/2$ disclinations in Fig.4 (a). These defects are prepatterned by a photonic metamask similar to the one in Fig.1. The topological defects play an important role in biological functions, for example, they serve as the sites where dead cells are expelled from the tissue. However, the mechanisms of their formations are not known. In our work, we demonstrate that by growing a tissue of human dermal fibroblasts (HDFs) on a LCE substrate with a predesigned molecular orientation, Fig. 4(b), we can pattern cells' alignment in biological tissues and introduce topological defects such as $+1/2$ and $-1/2$ disclinations, in predetermined locations and

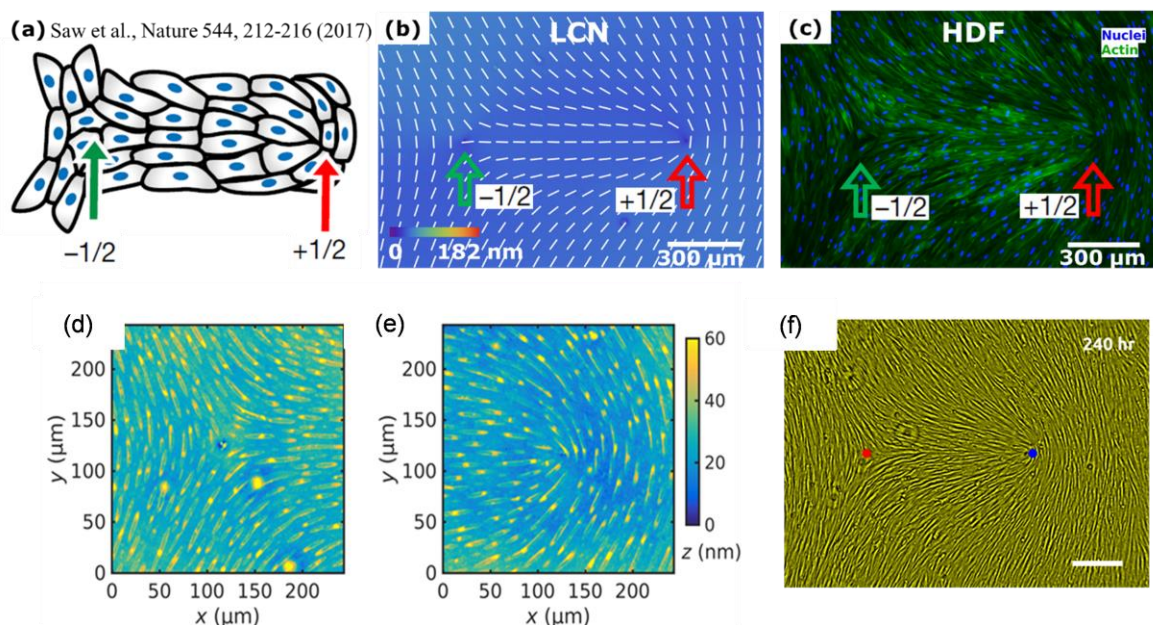


Fig. 4. (a) Live cell tissues demonstrating orientational order with topological defects [3]; (b) director pattern in LCE coating forces the cells to create (c) an orientationally ordered arrays with predesigned topological defects; cells are fluorescently labelled ; (d,e) structured profile of LCE substrate that aligns the cells; (f) cell tissues imaged under the light microscope.

configurations, Fig.4(c). We demonstrate that the mechanism of this alignment and patterning of the tissues is caused by anisotropic swelling of the substrate when in contact with the cell culture medium. Besides alignment, the patterned LCE substrates dramatically influence other important aspects of tissues, such as cells density, fluctuations of density and phenotype of the cells. For example, positive defects accumulate a higher density of cells and make the cells more round, while cells near negative defects are more elongated and less densely packed. The approach opens vast possibilities in designing biological tissues with controllable alignment and properties of the cells, potentially including functions such as cell migration, differentiation and apoptosis. Furthermore, the proposed approach is conceptually very simple and can be further advanced by chemical functionalization of the LCN substrates and by making LCNs with dynamic topographies controlled by chemical or physical cues, which would open another dimension to control the growth of biological tissues.

Future Plans

Because of the fundamentally new mechanism of growing living tissues by interfacing them with a predesigned artificial soft material, we plan to continue the study and see how topological defects of different strength would affect the morphology of the cells, their size distribution and dynamic behavior. In the fundamental physics part, we plan to explore how the director field that contain singular topological defects affect the surface profile development of the LCE coatings. In Fig.2, the director field is smooth and nonsingular, while in Fig.3, it is singular, thanks to complex 3D structure of the prepatterned director. One can clearly see that the sharpness of valleys in the latter case is higher than in the former case. It would be of interest to explore the mechanism in details, by using experiments with a digital holographic microscopy that reveal the profiles of the coatings with great accuracy, and to establish how the profile depends on the director gradients. To understand mechanisms causing the observed patterns, Dr. Shiyakovskii will simulate the profiles of LCE coatings using the developed nemator model. We will also explore a smectic A LCEs, in addition to the standard nematic LCE, since these can be used to produce spontaneous grooves of nanoscale dimension that fits the range of scales needed to manipulate cell tissues. To obtain a better control of the LCE substrate preparation, Dr. Wei will complete development of a new optical imaging system in which photopolymerization and photopatterning can be monitored in-situ.

References

- [1] G. Babakhanova, T. Turiv, Y. B. Guo, M. Hendrikx, Q. H. Wei, A. Schenning, D. J. Broer, and O. D. Lavrentovich, *Liquid crystal elastomer coatings with programmed response of surface profile*, Nature Communications **9**, 456 (2018).
- [2] G. Babakhanova, H. Yu, I. Chaganava, Q. Wei, -H., P. Shiller, and O. D. Lavrentovich, *Controlled Placement of Microparticles at the Water–Liquid Crystal Elastomer Interface*, Acs Applied Materials & Interfaces **11**, 15007-15013 (2019).
- [3] T. B. Saw, A. Doostmohammadi, V. Nier, L. Kocgozlu, S. Thampi, Y. Toyama, P. Marcq, C. T. Lim, J. M. Yeomans, and B. Ladoux, *Topological defects in epithelia govern cell death and extrusion*, Nature **544**, 212-216 (2017).
- [4] K. Kawaguchi, R. Kageyama, and M. Sano, *Topological defects control collective dynamics in neural progenitor cell cultures*, Nature **545**, 327-331 (2017).

Publications

We published the following papers:

1. G. Babakhanova, H. Yu, I. Chaganava, Q.-H. Wei, P. Shiller, O.D. Lavrentovich, *Controlled placement of microparticles at the water-liquid crystal elastomer interface*, ACS Applied Materials & Interfaces **11**, 15007-15013 (2019)
DOI:10.1021/acsami.8b22023 (2019)
2. G. Babakhanova, A. P. H. J. Schenning, D. J. Broer, O.D. Lavrentovich, *Surface structures of hybrid aligned liquid crystal network coatings containing reverse tilt domain*, Proc. of SPIE **10941** Emerging Liquid Crystal Technologies XIV, 109410I (1 March 2019); DOE: 10.1117/12.2515507
3. C. Peng, O.D. Lavrentovich, *Liquid crystal enabled electrokinetics*, Micromachines **10**, 45 (2019).
4. J.-K. Guo, S.-H. Hong, H.-J. Yoon, G. Babakhanova, O.D. Lavrentovich, J.-K. Song, *Laser-induced nanodroplet injection and reconfigurable double emulsions with designed inner structures*, Advanced Science **2019** 1900785 (2019).
5. T. Turiv, Jess Krieger, Greta Babakhanova, Hao Yu, Qi-Huo Wei, Min-Ho Kim, Oleg D. Lavrentovich, *Patterned control of human cells by liquid crystal networks*, submitted to Nature Materials (currently under review).

Biomolecular assembly processes in the design of novel functional materials

Jeetain Mittal

Department of Chemical and Biomolecular Engineering, Lehigh University, Bethlehem, PA 18015.

Email: jeetain@lehigh.edu

Program Scope

The objective of our research program is to develop new computational models calibrated, aided, and validated by experimental measurements to understand and predict biomolecular assembly processes with a special emphasis on these happening in the presence of nanomaterials such as carbon nanotubes, gold, and polymer nanoparticles. The first focus area is the rational design of complex materials mediated by hybridization between DNA-functionalized particles (DFPs). We have developed a multiflavoring approach to demonstrate the usefulness of DFP assembly for the design of binary superlattices which is enthalpically driven as opposed to commonly used entropically driven assembly due to particle size disparity. We also developed a method based on symmetry to predict the structure of such multi-component colloidal mixtures. In addition, we are developing a computational model to understand the self-assembly behavior of intrinsically disordered proteins. We are particularly interested in mapping out the sequence-dependent thermoresponsive phase separation of proteins that can be used as a guide for the design of protein-based materials.

Recent Progress

Size-dependent thermodynamic structural selection in colloidal crystallization. The processes of nucleation and growth of crystalline phases from fluids are critically important for a comprehensive understanding of a myriad of physical systems. One particularly interesting property of such processes, common to many systems, is the appearance of thermodynamically metastable solid polymorphs. Since the proposal of Ostwald's step rule, many investigations have been performed to understand the underlying driving forces behind the crystallization of phases other than the one most thermodynamically stable in the bulk. These explanations have typically relied upon classical nucleation theory (CNT) and ultimately arrived at a kinetic

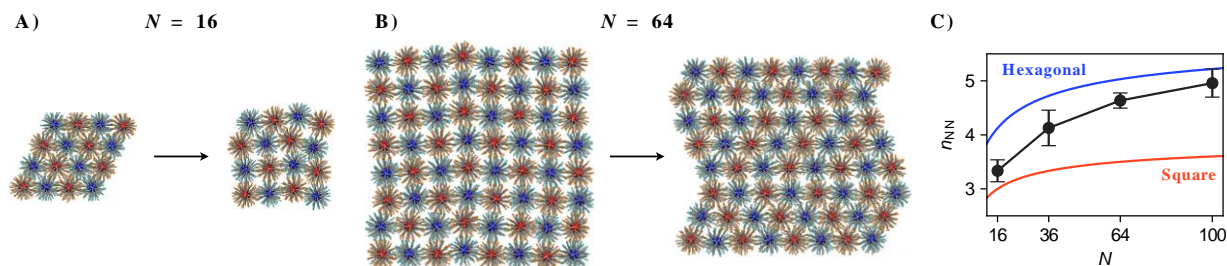


Figure 1. A–B) Snapshots of transformations occurring in a DNA-functionalized nanoparticle system with explicitly modeled DNA chains. C) Average nearest neighbor count for explicit-chain model systems, compared with reference values for pure static square and hexagonal crystallites in the chosen shapes.

explanation for the observed phenomenon.

In this work, we demonstrate explicitly for the first time a system in which the appearance of a solid phase other than the most thermodynamically stable can be explained purely in terms of thermodynamic effects. This represents a complete departure from traditional explanations involving CNT, or even those demonstrating deviations from behavior expected by CNT due to kinetic effects. Specifically, we show using various computational methods a particular system in which the size-dependent thermodynamics of solid phases are responsible for a transformation between phases during crystallization. This is in contrast to all previous studies of polymorphism in nucleation and growth in which such an effect is attributed either to kinetics or to structural ordering in the parent fluid phase. We have provided a demonstration of this purely thermodynamic selection effect in a general system modeled by pairwise interaction potentials, as well as a specific system of DNA-functionalized colloidal particles. This demonstrates the generality of the phenomenon and its potential for observation in a variety of systems, as well as its applicability to a physically realizable system of significant experimental interest. We developed a method based on the modification of the Einstein molecule method for non-periodic crystals as part of this work and showed that the free energy data are also consistent with the MD results. The free energy code was released for public use as well.

We also developed a method based on symmetry to predict the structure of multi-component colloidal mixtures. This method allows one to exhaustively enumerate candidates from all wallpaper groups, guaranteeing all planar symmetries have been explored which can be used to compute ground-state phase diagrams for multicomponent lattices. We used this method to demonstrate that simple potentials can also give rise to complex structures which are thermodynamically stable at moderate to low temperatures. Most importantly, we illustrated that crystalline lattices can be rationally designed from systems by tuning the mixture composition alone, demonstrating that stoichiometric control can be a tool as powerful as directly tuning the interparticle potentials themselves.

Designing Molecular Building Blocks for the Self-assembly of Complex Porous Networks. We used Monte Carlo simulations of patchy vertex-like building blocks to show how the addition of chemical specificity via orthogonally reacting functional sites can allow vertex-like building blocks with even asymmetric geometries to self-assemble into ordered crystallites of various complex structures. In addition to demonstrating the utility of such a strategy in creating ordered, heteroporous structures, we also demonstrated that it can be used as a means for tuning specific features of the crystal structure, accomplishing such aims as the control of relative pore sizes. We also discuss heuristics for properly designing molecules so that they can assemble into target structures. The building blocks used in this work consist of hard spheres with attractive patches which stand as proxies for the reactive ends of covalent organic framework (COF) molecules or DNA-functionalized patches. We showed that building block geometry is a necessary but insufficient condition for self-assembly into target structures, and that this issue is particularly acute for vertex-like building blocks with lower degrees of symmetry because of their tendency

to self-assemble into polymorphous structures. We also found that this polymorphism can be reduced by making the building blocks chemically specific. We also showed that the quality of crystallites could be improved further by using building blocks which conform to the geometry of secondary vertex structures. The use of secondary vertex building blocks is effective because it can reduce the number of molecular components in the system, and it can also add further rigidity to the structure which helps prevent the formation of defects. We plan to extend this model to study three-dimensional assembly of COFs and non-planar building blocks to form 3D porous materials.

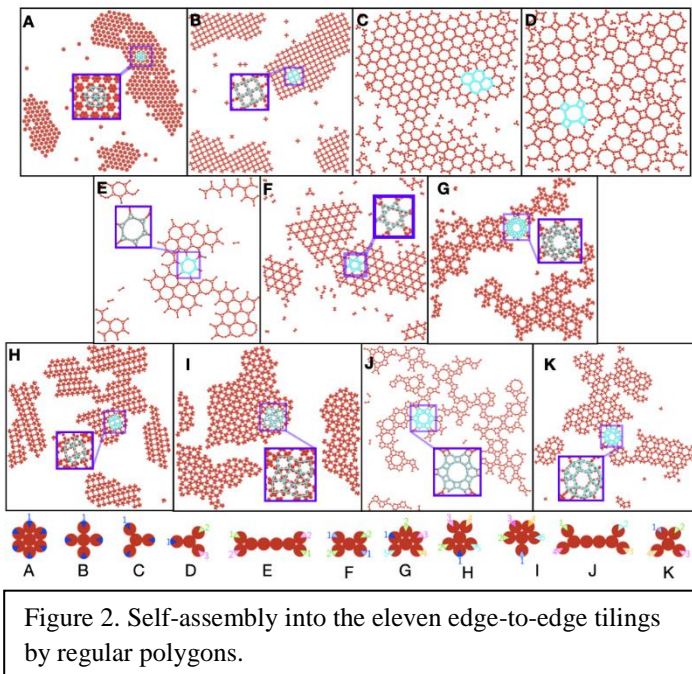


Figure 2. Self-assembly into the eleven edge-to-edge tilings by regular polygons.

Temperature controlled liquid-liquid phase separation of disordered proteins. We have developed a unique knowledge-based amino acid potential that accounts for the temperature-dependent effects on solvent-mediated interactions for each amino acid type. This is accomplished by tuning the model parameters using knowledge from both single molecule Förster Resonance Energy Transfer (smFRET) experiment and all-atom simulations on the dimensions of disordered proteins across a wide range of temperatures. Remarkably, we are able to distinguish between more than thirty five intrinsically disordered proteins with upper or lower critical solution temperatures at experimental conditions, thus providing direct evidence that incorporating the temperature-dependent solvent-mediated interactions to IDP assemblies can capture the difference in the shape of the resulting phase diagrams. Using this newfound knowledge, we apply the new model to propose sequence determinants of the protein LLPS in terms of their UCST or LCST characteristics, which should allow for the design of protein-based materials.

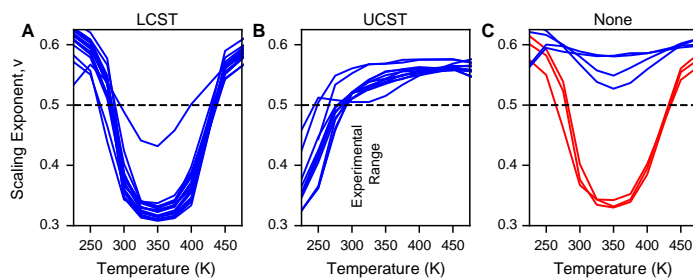


Figure 3. Verification of the temperature-dependent coarse-grained model to study protein liquid-liquid phase separation. The model correctly captures LCST vs. UCST behavior as well as lack of phase separation for 4 sequences. The 3 sequences highlighted in red suggest mismatch with experiment.

Identifying sequence-determinants of protein phase separation. In collaboration with Prof. Dan Hammer's group, we have developed a joint computational and experimental strategy to characterize the phase separation of disordered proteins. We used this to design several variants of Laf-1 RGG sequence which can phase separate at significantly different conditions than the wild-type sequence. These predictions were validated using *in vitro* and *in vivo* experiments. We also identified the role of conserved glycine residues in the phase separation of TDP-43 protein and the contribution of hydrogen bonding interactions in the phase behavior of FUS protein in collaboration with Prof. Nick Fawzi (Brown University). Together these studies pave the way for quantitative characterization of sequence-dependent behavior of protein assembly using accurate computational models that we have developed.

Future Plans

Inverse design of DNA-mediated interactions to stabilize desired superlattices. To go beyond what can be done using a forward design strategy alone, we plan to implement a novel inverse design strategy to design binary superlattices using simple isotropic potentials that can be realized using DFPs. Our preliminary investigations suggest that the major shortcoming of pair potentials obtained using an inverse design strategy, i.e., physically unrealizable nature can be overcome using constraints imposed by pair interactions feasible using DNA-mediated interactions. A central requirement to accomplish this goal is to develop an accurate pair potential model that can account for various design parameters that can be tuned such as DNA grafting density, DNA sequence, types of DNA, etc. As part of previous work, we have already generated sufficient simulation data to accomplish this goal.

Effect of DNA multicoloring on the design of porous materials. For this part of the project, we plan to use Monte Carlo Simulations of patchy spheres in addition to patchy molecules with the shape expanded ensemble technique. We will use either the interaction range or the patch width as order parameters. We plan to start off the project by studying the effect of these parameters on the assembly of simple Kern-Fernkel spheres. Then we will expand the study to patchy molecules. The effect of interaction parameters on the assembled structure can be quantified using the radial angular distribution function or additionally the fast neighborhood graphlet analysis.

Design of protein sequences to control protein co-assembly. The last PI meeting allowed us to connect with Prof. Dan Hammer whose group is working on complementary experimental systems with respect to our ongoing work on liquid-liquid phase separation of disordered proteins. As discussed above, we are working with his group to design protein sequences with controllable protein phase separation. Future work will focus on the co-phase separation of proteins to form orthogonal membraneless organelles which can perform separate function distinct from the ongoing biological processes. We will also extend this particular effort to gain a fundamental understanding of molecular interactions that underlie the ability of proteins to co-localize and how to control it.

Publications (*equal contribution)

1. A. E. Conicella*, G. L. Dignon*, G. H. Zerze, H. B. Schmidt, A. M. D'Ordine, Y. C. Kim, R. Rohatgi, Y. M. Ayala, J. Mittal, and N. L. Fawzi, "TDP-43 α -helical structure tunes liquid-liquid phase separation and function" *Proc. Natl. Acad. Sci.* (under review).
2. E. Pretti, H. Zerze, M. Song, Y. Ding, R. Mao and J. Mittal, "Size-dependent thermodynamic structural selection in colloidal crystallization" *Science Advances* (in press).
3. E. Pretti and J. Mittal, "Extension of the Einstein molecule method for solid free energy calculation to non-periodic and semi-periodic systems" *Journal of Chemical Physics* **DOI:** 10.1063/1.5100960 (2019).
4. E. Pretti, R. Mao, and J. Mittal, "Modeling and simulation of DNA-mediated self-assembly for superlattice design" *Molecular Simulation* **DOI:** 10.1080/08927022.2019.1610951 (2019).
5. G. L. Dignon*, W. Zheng*, Y. C. Kim, and J. Mittal, "Temperature-controlled liquid-liquid phase separation of disordered proteins" *ACS Central Science* **5**, 821 (2019).
6. A. C. Murthy, G. L. Dignon, Y. Kan, G. H. Zerze, S. Parekh, J. Mittal, and N. L. Fawzi, "Molecular interactions underlying liquid phase separation of the FUS low-complexity domain" *Nature Structural and Molecular Biology* **26**, 637 (2019).
7. G. H. Zerze, W. Zheng, R. B. Best, and J. Mittal, "Evolution of all-atom protein force fields to improve local and global properties" *Journal of Physical Chemistry Letters* **10**, 227 (2019).
8. N. A. Mahynski, E. Pretti, V. K. Shen, and J. Mittal, "Using symmetry to elucidate the importance of stoichiometry in colloidal crystal assembly" *Nature Communications* **10**, 2028 (2019).
9. G. L. Dignon, W. Zheng and J. Mittal, "Simulation methods for liquid-liquid phase separation of disordered proteins" *Current Opinion in Chemical Engineering* **23**, 92 (2019).
10. T. A. Maula, H. A. Hatch, V. K. Shen, S. Rangarajan, and J. Mittal, "Designing Molecular Building Blocks for the Self-assembly of Complex Porous Networks" *Molecular Systems Design and Engineering* **4**, 644 (2019).
11. G. L. Dignon*, W. Zheng*, R. B. Best, Y. C. Kim, and J. Mittal, "Relation between single-molecule properties and phase behavior of intrinsically disordered proteins" *Proc. Natl. Acad. Sci.* **115**, 9929 (2018).
12. A.T. V. Galassi, P. V. Jena, J. Shah, G. Ao, E. Molitor, Y. Bram, A. Frankel, J. Park, J. Jessurun, D. S. Ory, A. H.-Friedman, D. Roxbury, J. Mittal, M. Zheng, R. E. Schwartz, D. A. Heller, "In Vivo Reporter of Endolysosomal Lipids Reveals Enduring Effects of Diet on Hepatic Macrophages" *Science Translational Medicine* **10**, eaar2680 (2018).
13. E. Pretti, H. Zerze, M. Song, Y. Ding, N. A. Mahynski, H. A. Hatch, V. K. Shen, and J. Mittal, "Programmable assembly of three-dimensional binary superlattices from multi-flavored DNA-functionalized particles" *Soft Matter* **14**, 6303 (2018).
14. P. Das, S. Matysiak, and J. Mittal, "Looking at the disordered proteins through the computational microscope" *ACS Central Science* **4**, 534 (2018).
15. J. D. Harvey, G. H. Zerze, K. M. Tully, J. Mittal, and D. A. Heller, "Electrostatic screening modulates analyte binding and emission of carbon nanotubes" *J. Phys. Chem. C* **122**, 10592 (2018).

16. G. L. Dignon*, W. Zheng*, Y. C. Kim, R. B. Best, and J. Mittal, “Sequence determinants of protein phase behavior from a coarse-grained model” *PLoS Computational Biology* **14**, e1005941 (2018).
17. M. Song, Y. Ding, H. Zerze, M. A. Snyder, and J. Mittal, “Binary superlattice design by controlling DNA-mediated interactions” *Langmuir* **34**, 991 (2018).
18. V. H. Ryan, C. V. Chabata, A. E. Conicella, J. Amaya, R. Silva, K. A. Burke, G. Zerze, G. L. Dignon, J. Mittal, and N. L. Fawzi, “Mechanistic View of hnRNPA2 Low-Complexity Domain Structure, Interactions, and Phase Separation Altered by Mutation and Arginine Methylation” *Mol. Cell* **69**, 465 (2018).
19. A. M. Janke, D. H. Seo, K. A. Burke, A. E. Conicella, V. Rahmanian, J. Mittal, and N. L. Fawzi, “Lysines in RNA polymerase II C-terminal domain contribute to TAF15 fibril recruitment”, *Biochemistry* **57**, 2549 (2018).
20. N. A. Mahynski, H. Zerze, H. W. Hatch, V. K. Shen, and J. Mittal. “Assembly of multi-flavored two-dimensional colloidal crystals”, *Soft Matter* **13**, 5397 (2017).

Calibration between trigger and color: Electrically driven neutralization of a genetically encoded Coulombic switch precisely tunes reflectin assembly

Daniel E. Morse

Institute for Collaborative Biotechnologies

University of California, Santa Barbara

Santa Barbara, CA 93106-5100

Program Scope

Using the reflectin proteins as a uniquely tractable model, we are elucidating the detailed structure-function relationships and behavior governing tunable biomolecular materials, and the mechanisms by which their signal-activated reconfiguration drive the tunable color and brightness of light reflected from intracellular biophotonic nanostructures. The greatest significance and broadest impact of our research to date is the discovery and deeper understanding of structure-function relationships in biomolecular and polymer-based materials that can enable the cryptic, linear encoding of tunably emergent structures to drive dynamically and cyclably reconfigurable conformational changes and assembly with consequent tunable control of colligative and other physical properties. These efforts thus reveal new paradigms for the design of complex, controllably reconfigurable materials.

Recent Progress

We are learning how the signal-induced assembly of reflectin proteins dynamically tunes the color and brightness of light reflected from membrane-enclosed, photonic nanostructures in skin cells of squids. While the reflectins are widely distributed in such structures in many species of cephalopods, only in the recently evolved Loliginid squids are they and the sub-wavelength photonic structures they control dynamically tunable, driving changes in skin color for camouflage and communication. In our previous BES-supported research, we discovered that: (1) the reflectins are intrinsically disordered block copolymers with repeated canonical domains interspersed with cationic linkers; (2) neurotransmitter-activated signal transduction culminates in catalytic phosphorylation of the tunable reflectins' cationic linkers, with the resulting charge-neutralization overcoming Coulombic repulsion to progressively allow condensation and concomitant assembly to form multimeric spheres of tunable well-defined size and low polydispersity; and (3) the resulting assembly progressively reduces the particle number concentration of reflectins in the membrane-enclosed Bragg reflector lamellae containing them, driving an osmotic efflux of water that simultaneously shrinks the thickness and spacing of the Bragg lamellae while increasing their refractive index contrast, thus simultaneously tuning the wavelength and increasing the brightness of their reflectance.

Now, structural transitions of reflectins A1 and A2 were analyzed by dynamic light scattering, cryo- and conventional TEM, SAXS, circular dichroism, EPR, AFM, fluorimetry and computational modeling^{1,2}. We analyzed the assembly behavior of phospho-mimetic, deletion, and other mutants in conjunction with pH-titration as an *in vitro* surrogate of phosphorylation to discover a previously unsuspected, precisely predictive relationship between the extent of

neutralization of the protein's net charge density and the size of the resulting multimeric protein assemblies (**Figure 1**) with surprisingly narrow polydispersity, stability with time, and rapid reversibility when charge is restored^{1,2}.

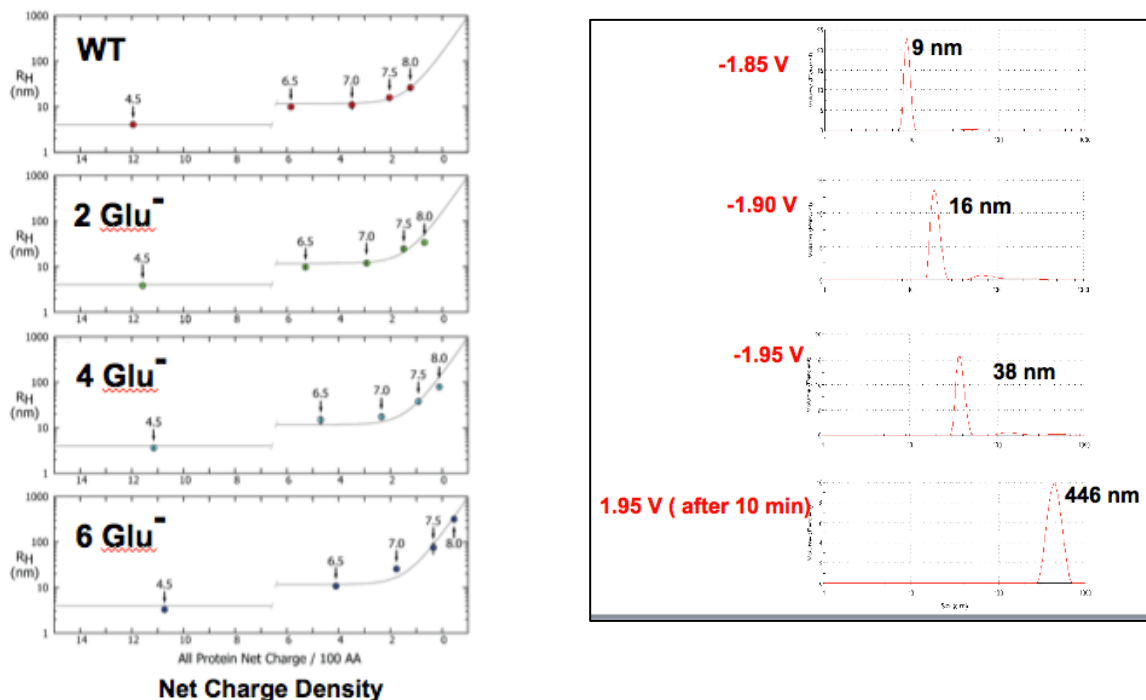


Figure 1 (left): Size of reflectin particles (R_H on the y-axis) measured by DLS vs. calculated net charge density (net charges/100 amino acid residues) for: reflectin A1 WT and phosphomimetic mutants (in which each added Glutamate residue adds a single negative charge, so 2 Glutamates adds the charge equivalent to one physiologically added phosphate). Sizes are measured at values of pH = 4.5, 6.5, 7.0, 7.5 and 8.0.

Figure 2 (right): Size of reflectin particles (R_H on the x-axis; particle numbers on the y-axis) measured continually as voltage is increased to the values shown. R_H of the unassembled monomer = 9 nm.

Analyses of deletion mutants shows this sensitivity to neutralization – a “*Coulombic switch*” – resides in the linkers and is spatially distributed along the protein¹. (In contrast, the conserved domains possess a thermodynamic drive to fold, yielding internally phase-segregated surfaces that subsequently facilitate hierarchical assembly¹; cf. below). Imaging of large particles and analysis of sequence composition suggest that assembly may proceed through a dynamically arrested liquid-liquid phase separated intermediate¹. Intriguingly, it is this dynamic arrest that enables the observed fine-tuning by charge and the resulting calibration between neuronal trigger and color in the squid.

Most recently, we found that we can precisely drive reflectin assembly by application of a weak electrical potential on the order of -1 volt (**Figure 2**)³. This enables us to exquisitely tune the controlling processes, revealing the sequence of their action: neutralization (physiologically by

neurotransmitter-activated phosphorylation; *in vitro* by application of electric potential³, titration with pH^{1,2}, anion-screening², or genetic engineering¹) opposes Coulombic repulsion of the cationic linkers, with the resulting relaxation of strain allowing the interspersed conserved domains to act like *entropic springs*¹, thermodynamically driven to condense and fold, with consequent emergence of their cryptically encoded, amphiphilic beta structures (seen with CD)¹, and the new hydrophobic surfaces then mediating assembly via beta-stacking (seen with EPR). Rapid internal cross-linking via numerous cation-pi bonds quickly arrests this process, stabilizing the newly formed spherical multimers of size limited by the initial extent of charge-neutralization (DLS and TEM, **Figure 3**; SAXS and cryo-TEM, **Figure 4**²). This process is reversible and repeatedly cyclable *in vitro*, as it is *in vivo* (**Figure 5**).

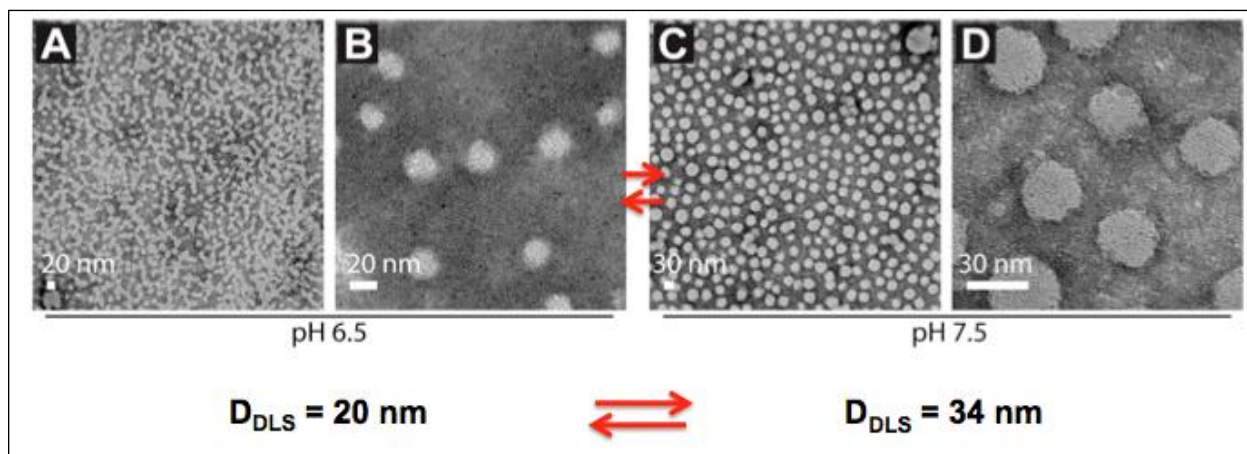


Figure 3. TEM analyses of reflectin A1 (10 micromolar) multimers formed at two stages of neutralization by pH titration, showing close agreement with diameters (D_H) of the same samples determined by DLS. For each of the two samples, TEM views are shown at both low and high magnification, illustrating surprisingly low polydispersity, and apparent sphericity of the assembled particles.

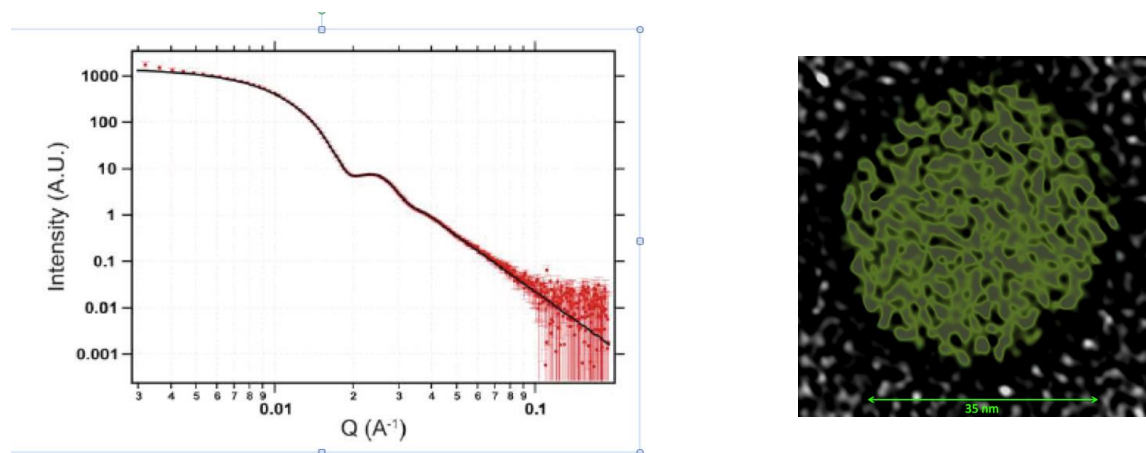


Figure 4. (left): SAXS analysis of reflectin A1 multimers (4 mg/mL) in 15 mM MOPS, pH 7.5, after subtraction of buffer background. The data were fit to a spheroid model using SAXS modeling package IRENA, yielding an average particle radius of $23.2 \text{ nm} \pm \text{s.d.} = 3.0 \text{ nm}$. The same sample was measured by DLS to have $R_H = 20 \text{ nm}$.

(right): Cryo-EM tomographic image of reflectin A1 multimer showing apparent sphericity. Diameter (35 nm) was confirmed by DLS analysis of the same sample.

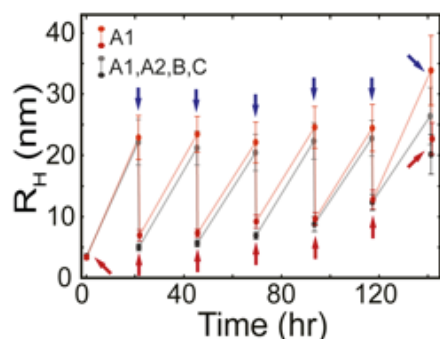


Figure 5. *In vitro* cyclability of reversible assembly (@ pH 7.5, blue arrows) and disassembly (pH 4.5, red arrows) of reflectin A1 and physiological mixture of all 4 reflectins. Results of DLS analyses at 10 micromolar total reflectin concentration.

It is this precise proportionality between charge-neutralization and assembly size, enabled by dynamic arrest of multimer growth and subsequent stability with time, that ensures the reciprocally precise control of the particle number concentration of the reflectin assemblies, thereby **encoding a precise calibration** between the extent of neuronal signaling, osmotic pressure, and the resulting optical changes. Charge regulation of reflectin assembly precisely fine-tunes a colligative property-based biological machine^{1,2}.

These results offer insights into the basis of reflectin-based tunable biophotonics and open new paths for the design of new materials with tunable properties.

Future Plans We plan to continue our high-resolution structural analyses conducted at the DOE-BES user facilities of the Stanford Synchrotron Light Source and LBL National Laboratory’s Molecular Foundry, leveraging their capabilities for time-resolved SAXS and cryo-TEM with our ongoing genetic engineering, biophysical and computational analyses to further identify the structural determinants and mechanisms governing the dynamic behaviors of the reflectins. We will augment these methods with EPR analyses that have revealed for the first time the existence of a *specific pathway* of reflectin assembly culminating in hierarchical assembly mediated by extensive beta-sheet stacking. Using our newly discovered to precisely fine-tune these processes with incremental low voltages, we will use dynamic light scattering and continuously monitored circular dichroism and Raman microscopy to elucidate the progression of structural changes underlying the mechanisms of signal-induced condensation, folding, assembly, liquefaction, dynamic arrest, and their regulation and reversal.

References

1. Levenson, R. C. Bracken, C. Sharma, P. Kohl, Y. Li, J. Santos, C. Arata, and D.E. Morse, 2019. Neutralization of a distributed Coulombic switch precisely tunes reflectin assembly. doi: <https://doi.org/10.1101/456442>. In review at J. Biological Chemistry; preprint available in BioRxiv.
2. Levenson, R. C. B. Malady, T. Lee, P. Kohl, Sharma, P. Kohl, Y. Li, and D.E. Morse, 2019. Charge-Neutralization is the Proximate Trigger and Precise Governor of Reflectin Assembly. In review at Nature Communications.
3. Sepunaru, L., R. Levenson, B. Malady, M. Gordon and D.E. Morse, 2019. Direct electrical reduction of histidine residues in reflectin drives hierarchical assembly. In preparation for Science.

Publications supported by BES (last 2 years)

Levenson, R., D. DeMartini and D.E. Morse (2017). Molecular mechanism of reflectin's tunable biophotonic control: Opportunities and limitations for new optoelectronics. Applied Physics Lett. – Materials 5, 104801: 1-12 [<http://dx.doi.org/10.1063/1.4985758>]

Dearden, S.J., A. Ghoshal, D. G. DeMartini and D. E. Morse, 2018. Sparkling reflective stacks of purine crystals in the nudibranch, *Flabellina iodinea*" Biological Bulletin, 234: 116-129.

Morse, D.E. and S.,Johnsen, (Eds.), 2018. Bioinspiration and Biomimetics, Special Issue on Biophotonics and Biologically Inspired Photonics, 13: [<https://doi.org/10.1088/051001-056006>]

Levenson, R. C. Bracken, C. Sharma, P. Kohl, Y. Li, J. Santos, C. Arata, and Daniel E. Morse, 2019. Neutralization of a distributed Coulombic switch precisely tunes reflectin assembly. doi: <https://doi.org/10.1101/456442>; in review at J. Biological Chemistry; preprint available in BioRxiv.

Levenson, R. C. B. Malady, T. Lee, P. Kohl, Sharma, P. Kohl, Y. Li, and D.E. Morse, 2019. Charge-Neutralization is the Proximate Trigger and Precise Governor of Reflectin Assembly. In review at Nature Communications

Electrostatic Driven Self-Assembly Design of Functional Nanostructures

Monica Olvera de la Cruz (PI) and Michael J. Bedzyk (co-PI)

Department of Materials Science and Engineering, Northwestern University, Evanston, IL 60208

Program Scope

The goal of this project is to understand the role of electrostatics in determining the equilibrium assembly structures composed of charged amphiphilic molecules in a heterogeneous environment. Specifically, we focus on: (1) exploiting the local heterogeneity at protein surfaces to disperse and organize functional proteins in non-biological environments, and (2) designing amphiphilic molecules to drive structural transitions that lead to specific functionalities.

The outcomes of the proposed works are i) to guide the synthesis of protein-based assembly (see Figure 1A), and ii) to investigate the conformational behavior of amphiphilic molecules in confinement (Figure 2B).

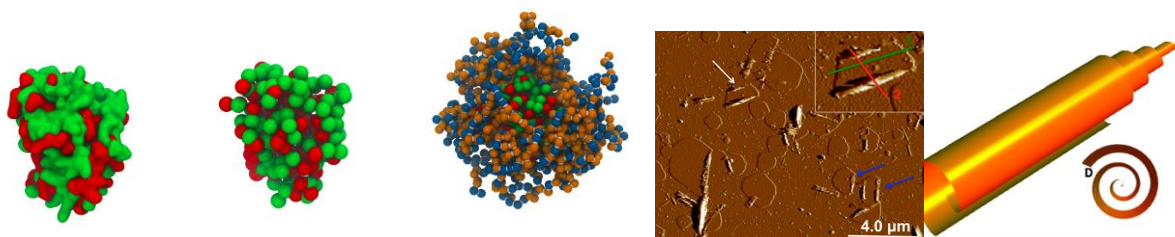


Figure 1. (A) Three snapshots of enzyme of hydrophilic and hydrophobic domains of candida Antarctica lipase B (1TCA) by all-atom computer simulations (left), by coarse grained simulations (middle) and with random copolymer covering the protein. (B) AFM images of drop-cast bilayer membranes; as the NaCl concentration increases, structural transformations are observed from nanoribbon to isotropic sheet and to rolled-up cochleates.

Recent Progress

Proteins and Amphiphilic Molecules Membranes

The local distribution of hydrophilic and hydrophobic protein surface domains enriches the profound functions of proteins and their applications. We are taking advantage of this local heterogeneity at the protein surface to organize them and stabilize them in non-biological conditions. In particular, the need to improve the catalytic activity of enzymes in organic solvents has for the past decade been of interest in waste treatment and biocatalysis. We focus on computationally designing copolymers that are reminiscent of intrinsically disordered proteins (IDPs), which organize enzymes and biomolecules to promote cellular functions in living cells, in a sense that they are composed of random sequences of hydrophobic and hydrophilic segments. The idea is that the random heteropolymers would stabilize and deliver enzymes across non-biological environments, including organic solvents (Science, 2018). We investigated the

interaction between ensembles of random copolymers with widely used proteins, and showed that the diversity in the monomer sequences of the random copolymers enables the proteins to selectively pick the most favorable sequences to protect themselves in any unfavorable medium (*PNAS*, 2018). This is of practical importance, because it means that there is no need to control the precise sequence and composition of individual polymer chains when one wants to stabilize multiple types of proteins, or switch to different solvents. Furthermore, we found the relationship between the average polymer composition and attraction strength between the monomers and the protein surface polar and non-polar domains to the protein surface coverage. Our work provides molecular-level insights into the interaction between proteins and random copolymers and provides insight for the computational design of copolymers for stabilizing and delivering enzymes across multiple media.

Synthetic random heteropolymers were also used to mimic the function of membrane proteins (*Nature* 2019, in revision). Membrane proteins are able to selectively transport protons or metal ions to fine tune the local environment inside cells. Proton-selective membranes assembled with synthetic random heteropolymer exhibited selective proton ion transport at rates similar to those of natural proton channels. The simulations supported that in the presence of the random heteropolymer, the lipid membranes have much higher amount of water in the hydrophobic interior in comparison with those in the absence of the polymers, that may facilitate the transport of proton ions by means of hydrogen bond chains.

Additionally, open crystalline protein assemblies were designed via functionalization of proteins with linkers. Coarse-grained molecular dynamic simulations determine the physical properties of the linker required for assembling protein into 3D crystalline open structures. The optimal linker length was found to depend on the linker to protein concentration ratio and binding energy. Our study demonstrates that grafted linkers length is a better tunable parameter than the length of free linkers to achieve high porosity protein superlattices (*Soft Matter*, 2019).

We furthered the understanding of the influences of protein surface heterogeneity on protein assembly. We analyzed, via all-atom molecular dynamics simulations, the orientation of the water around surface domains in three technically important enzymes: PETase, cytochromes P450s, and organophosphorus hydrolase (*PNAS*, resubmitted 2019). Water is essential for the catalytic reactions of the three enzymes. We found that the water molecules around these domains are oriented within a few Ångstroms from the protein surface domains, regardless of whether the domains are charged or not. Our results suggest that the orientation of the water around the protein domains determines their solubility and the recognition of molecules, drugs, and DNA/RNA.

We also investigated the assembly of P450 and OPH (*J. Phys. Chem. B.* 2019). The calculation of the potential of mean force for the protein dimer-monomer dissociation and protein-protein docking calculations supported that the dimers are more energetically stable, and the native protein-protein orientation observed in the crystal structures are the most stable orientations. Impressively, the active sites of the proteins are still exposed in the dimeric form, increasing the

feasibility in synthesizing protein aggregates for elevated catalytic performance by increasing the concentration of the enzymes.

Phase Diagram of heterogeneous molecules: Steric and Electrostatic Effects.

We analyzed bilayers of amphiphiles that can organize into spherical vesicles, nanotubes, planar, undulating and helical nanoribbons, and scroll-like cochleates. These bilayer-related architectures interconvert under suitable conditions. A charged amphiphile was used to elucidate the pathway for planar nanoribbon to cochleate transition induced by salt (NaCl) concentration. In-situ small- and wide-angle X-ray scattering (SAXS/WAXS), atomic force and cryogenic transmission electron microscopies (AFM and cryo-TEM) tracked these transformations over Å to μm length scales. AFM revealed that the large length (L) to width (W) ratio nanoribbons ($L/W > 10$) convert to sheets ($L/W \rightarrow 1$) before rolling into cochleates. A theoretical model showed that the nanoribbons convert to sheets via a first order transition, at a critical Debye length, with two shallow minima of the order of thermal energy at $W/L \ll 1$ and at $W/L=1$. SAXS showed that the inter-bilayer spacing in the cochleates scales linearly with the Debye length. Theoretical arguments that include electrostatic and elastic energies explain the membrane rolling and the bilayer separation-Debye length relationship. These models suggest that the salt-induced ribbon to cochleate transition should be common to all charged bilayers possessing an intrinsic curvature, which in the present case originates from molecular chirality (*PNAS*, 2019, to be resubmitted).

Future Plans

Protein adsorption to surfaces is ubiquitous in biology and is key for various functions including transmembrane signaling. It is also relevant to the operation of sensor surfaces, protein chips, assay platforms as well as in membranes for water purification. Next funding period we will study the adsorption of proteins on peptide-amphiphile bilayer. We will determine the conditions required to co-assemble protein in the scroll-like or cochleates structure described in the absence of proteins in the last funding period. We will determine the arrangement of proteins on the surface of the bilayer at low and high concentrations.

We will work on understanding how the charge and shape anisotropy of the protein surface affects their 2D assembly. To study protein adsorption and assembly, we will first deposit positively charged lipid layers on solid surfaces, the electrostatics-driven adsorption and assembly of proteins above their isoelectric point on such surfaces will be studied by grazing incidence X-ray diffraction studies. This study will serve as a guide to assemble protein and bilayers in bulk.

Enzymes within membraneless organelles exhibit catalytic activities under spatially confined conditions, where dielectric mismatch occurs and the polarization effects should exhibit nontrivial influences on the confined macromolecules. We are aiming for a better understand of the conformational behavior of proteins and enzymes in the presence of both spatial confinement and dielectric mismatch. To address this goal, we will develop coarse-grained models for the macromolecules and for the confined space that incorporates dielectric mismatch. We will employ

advanced sampling techniques to characterize the thermodynamic stability and conformational flexibility of the macromolecules as functions of their charge fraction, counterion valency, the volume and geometry of the confined space relative to the molecule dimensions and the Coulombic interaction strength. We will also develop and extend the state-of-the-art techniques for evaluating the surface polarization effects that allow us to perform large-scale simulations efficiently

We are planning to extend our works in designing random polymers to assemble proteins. Our previous coarse-grained work has demonstrated that by adjusting the hydrophilicity/hydrophobicity of random copolymers, protein encapsulation could be manipulated. In our ongoing project, we are designing random polymers which are composed of three types of monomers (one positively charged, one polar neutral, and one nonpolar). We are aiming to optimize the polymer composition in fabricating protein assemblies that function at water-oil interfaces. The heteropolymers composition capable of assembling the dimeric form of P450 found last funding period, which are enzymatic active, will be determined.

References

1. Brian Panganiban, Baofu Qiao, Tao Jiang, Christopher DelRe, Mona M. Obadia, Trung Dac Nguyen, Anton A. A. Smith, Aaron Hall, Izaac Sit, Marquise G. Crosby, Patrick B. Dennis, Eric Drockenmuller, Monica Olvera de la Cruz & Ting Xu. "Random heteropolymers preserve protein function in foreign environments". *Science* 359: 1239-1243 (2018); DOI: 10.1126/science.aao0335
2. Trung Dac Nguyen, Baofu Qiao, and Monica Olvera de la Cruz, "Efficient encapsulation of proteins with random copolymers" *PNAS* 26, 6578-6583 (2018); DOI: 10.1073/pnas.1806207115.
3. Tao Jiang, Aaron Hall, Marco Eres, Zahra Hemmatian, Baofu Qiao, Yun Zhou, Zhiyuan Ruan, Andrew D. Couse, William T. Heller, Haiyan Huang, Monica Olvera de la Cruz, Marco Rolandi, Ting Xu, "Unimolecular Proton-selective Channels Based on Segmental Heterogeneity in Random Heteropolymers" *Nature* (2019), to be resubmitted.
4. Baofu Qiao, Luis G. Lopez and Monica Olvera de la Cruz, "'Mirror"-like Protein Dimers Stabilized by Local Heterogeneity at Protein Surfaces" *J. Phys. Chem. B.* 123, 3907-3915 (2019); DOI: 10.1021/acs.jpccb.9b01394
5. Yuba Raj Dahal and Monica Olvera de la Cruz, "Crystallizing protein assemblies via free and grafted linkers" *Soft Matter* 15, 4311 (2019); DOI: 10.1039/c9sm00693a
6. Baofu Qiao, Felipe Jiménez-Ángeles, Trung Dac Nguyen, and Monica Olvera de la Cruz, "Water Follows Polar and Nonpolar Protein Surface Domains" *PNAS*, (2019) under review
7. Changrui Gao, Sumit Kewalramani, Dulce Maria Valencia, Honghao Li, Joseph McCourt, Monica Olvera de la Cruz, and Michael J. Bedzyk, "Electrostatic shape control of a charged molecular membrane from ribbon to scroll" *PNAS*, (2019) to be resubmitted.

Publications

1. Baofu Qiao, Felipe Jiménez-Ángeles, Trung Dac Nguyen, and Monica Olvera de la Cruz, "Water Follows Polar and Nonpolar Protein Surface Domains" PNAS, (2019) under review
2. Changrui Gao, Sumit Kewalramani, Dulce Maria Valencia, Honghao Li, Joseph McCourt, Monica Olvera de la Cruz, and Michael J. Bedzyk, "Electrostatic shape control of a charged molecular membrane from ribbon to scroll" PNAS, (2019) to be resubmitted
3. Tao Jiang, Aaron Hall, Marco Eres, Zahra Hemmatian, Baofu Qiao, Yun Zhou, Zhiyuan Ruan, Andrew D. Couse, William T. Heller, Haiyan Huang, Monica Olvera de la Cruz, Marco Rolandi, Ting Xu, "Unimolecular Proton-selective Channels Based on Segmental Heterogeneity in Random Heteropolymers" Nature (2019), to be resubmitted.
4. Adam Dannenhoffer, Hiroaki Sai, Dongxu Huang, Benjamin Nagasing, Boris Harutyunyan, Daniel J. Fairfield, Taner Aytun, Stacey M. Chin, Michael J. Bedzyk, Monica Olvera de la Cruz and Samuel I. Stupp, "Impact of charge switching stimuli on supramolecular perylene monoimide assemblies" Chem. Sci.10, 5779-5786 (2019); DOI: 10.1039/C8SC05595E
5. Baofu Qiao, Luis Lopez and Monica Olvera de la Cruz, "'Mirror'-Like Protein Dimers Stabilized by Local Heterogeneity at Protein Surfaces" The Journal of Physical Chemistry 123, 3907-3915 (2019); DOI: 10.1021/acs.jpcc.9b01394
6. Yuba Raj Dahal and Monica Olvera de la Cruz, "Crystallizing protein assemblies via free and grafted linkers" Soft Matter 15, 4311 (2019); DOI: 10.1039/c9sm00693a
7. Chao Sun, Meng Shen, Anton D. Chavez, Austin M. Evans, Xiaolong Liu, Boris Harutyunyan, Nathan C. Flanders, Mark C. Hersam, Michael J. Bedzyk, Monica Olvera de la Cruz, and William R. Dichtel, "High aspect ratio nanotubes assembled from macrocyclic iminium salts" PNAS 115, 8883-8888 (2018); DOI: 10.1073/pnas.1809383115
8. Trung Dac Nguyen, Baofu Qiao, and Monica Olvera de la Cruz, "Efficient encapsulation of proteins with random copolymers" PNAS 26, 6578-6583 (2018); DOI: 10.1073/pnas.1806207115
9. Brian Panganiban, Baofu Qiao, Tao Jiang, Christopher DelRe, Mona M. Obadia, Trung Dac Nguyen, Anton A. A. Smith, Aaron Hall, Izaac Sit, Marquise G. Crosby, Patrick B. Dennis, Eric Drockenmuller, Monica Olvera de la Cruz & Ting Xu. "Random heteropolymers preserve protein function in foreign environments". Science 359: 1239-1243 (2018); DOI: 10.1126/science.aao0335

Active Noise to Control and Direct Self-Assembly

J. Palacci, University of California, San Diego (PI)

Program Scope

In the classical picture of Brownian motion, the particles and fluid molecules are passive, driven by thermal fluctuations (1, 2). The incessant motion of particles in a fluid is due to multiple collisions of the particles with the surrounding fluid molecules. In living systems, molecular motors ballistically zoom around and exert forces on the surrounding passive elements, yielding a riotous environment radically different from an equilibrium one. This non-equilibrium dynamics induces additional fluctuations that boost transport (3) or assist assembly in biological systems. Self-propelled colloids and bacteria, that consume energy to move, hold similar potential for the control of man-made assembly of microparticles. Yet, their use to tune the internal activity and control passive colloids remains largely unexplored.

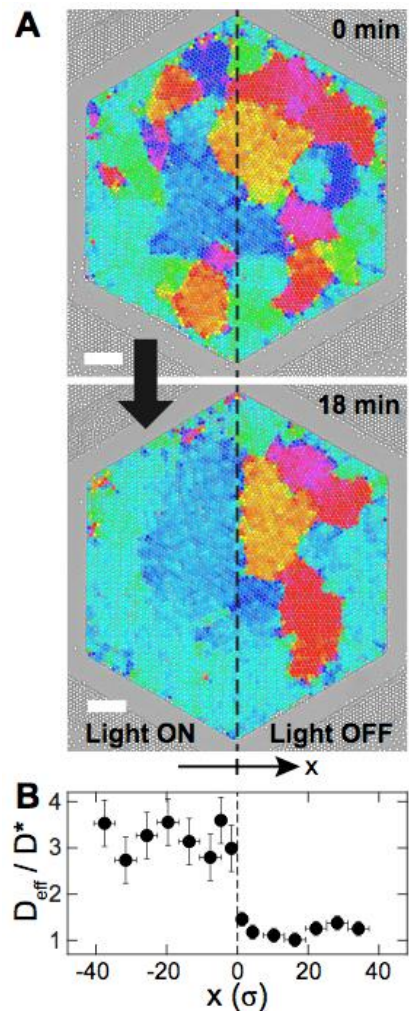
This program addresses the opportunities offered by disseminated active agents to constitute active baths that generate active fluctuations to control and organize surrounding and passive particles. It is an experiment-driven proposal, rooted in basic science that interrogates the role of active noise to organize or destroy order.

Recent Progress

Preliminary results: We showed a massive acceleration of the annealing of a monolayer of passive beads following the moderate addition self-propelled microparticles [Fig.1]. We showed that the active particles collide with the matrix of passive particles constituting the colloidal monolayer, adding large non-equilibrium fluctuations to the system. The effect is dramatic in spite of the reduced number of active particles and active noise boosts the mobility of the grain boundaries to accelerate the recrystallization process, up to 40-fold.

Figure 1. [Preliminary Results] Accelerated annealing of a colloidal monolayer following the moderate addition of active microparticles in the monolayer. A monolayer made of ~ 5000 passive beads contains ~ 50 active colloids, which propulsion is activated by light. Colors indicate the different orientations of the grains in the monolayer.

(A) On the left side, the light is ON and the active colloids self-propel, the monolayer anneals within 18mins. Same system, right side, the light is off: the active colloids are inactive and the system is thermal. It will take hours to anneal and reorganize. (B) The effective diffusivity of the passive beads show that the presence of activated colloids strongly increase the level of noise in the system and accelerate the annealing. Active particles allow the control of active noise in space (and time).



Future Plans

We will study how active fluctuations allow to increase the susceptibility of a medium by avoiding metastable states. Specifically, we will study the potential of active particles to induce active fluctuations that further favor the formation of equilibrium structures from passive particles. We will further study how active fluctuations can lead to enhanced accuracy of sensing thanks to additional fluctuations, a counter-intuitive property, however used by biological systems (4). Finally, we will study the opportunity offered by activity and active fluctuations, in combination with equilibrium interaction, to direct the assembly of 2D structures and enable the design of non-equilibrium interactions. Further we will study the potential of “active bath” (5) to control the phase transitions of passive particles.

References

1. J. Perrin, Mouvement brownien et réalité moléculaire. *Annales de Chimie et de Physique*, (1909).
2. A. Einstein, The motion of elements suspended in static liquids as claimed in the molecular kinetic theory of heat. *Annalen der physik* **17**, 549 (1905).
3. C. P. Brangwynne, G. H. Koenderink, F. C. MacKintosh, D. A. Weitz, Cytoplasmic diffusion: molecular motors mix it up. *The Journal of Cell Biology* **183**, 583 (2008).
4. A. Berut, H. Chauvet, V. Legue, B. Moullia, O. Pouliquen, Y. Forterre, Gravisensors in plant cells behave like an active granular liquid. *Proceedings Of The National Academy Of Sciences Of The United States Of America* **115**, 5123 (2018).
5. X.-L. Wu, A. Libchaber, Particle Diffusion in a Quasi-Two-Dimensional Bacterial Bath. **84**, 3017 (2000).

Publications

None

Self-Assembly and Self-Replication of Novel Materials from Particles with Specific Recognition: Self-Assembly of Colloids with Chemically Heterogeneous Surfaces

David J. Pine, Department of Physics, New York University

Joonsuk Oh, New York University

Gi-Ra Yi, Sungkyunkwan University

Sharon Glotzer, University of Michigan

Program Scope

This project explores the use of DNA-coated colloids to study the self-assembly of colloids with chemically heterogeneous surfaces, which serve as model systems to explore structure formation of surfactants, proteins, and other complex systems. We focus on Janus colloids, which are particles with one attractive patch on an otherwise repulsive particle surface. We have developed a simple scalable method to precisely vary the Janus balance over a wide range, which has not been achieved previously. We produce the attractive patch by functionalize it with DNA. We observe the dynamic formation of a wide variety of superstructures: colloidal micelles, chains, or bilayers, depending on the Janus balance. Flexible dimer chains form through cooperative polymerization while trimer chains form by a two-stage process, first by cooperative polymerization into disordered aggregates followed by condensation into more ordered stiff trimer chains. Introducing substrate binding through depletion catalyzes dimer chains to form nonequilibrium rings that otherwise do not form.

Recent Progress

We have developed a new synthetic approach for making Janus colloids, that is, colloids with one attractive patch on an otherwise repulsive particle surface. The method is versatile and scalable and can produce Janus particles with well-controlled Janus balance χ from 0.01 to 0.86. One face of the Janus particles is selectively functionalized with DNA having self-complementary sticky ends. We use DNA-mediated attraction rather than a hydrophobic attraction¹, which has been used by others for three reasons: (1) the DNA-mediated interaction is thermally-reversible, (2) properly-functionalized DNA-coated colloids can anneal after they bind to each other,² and (3) the strength of the DNA-mediated attraction can be continuously varied from essentially zero to about $10k_B T$ by varying the temperature over a range of about 10°C ^{3,4}

We use micron-sized colloidal particles that can be observed in real time under an optical microscope, which is not possible for surfactants and proteins, and thus we can follow their

assembly in real time. In addition, we conduct molecular dynamics (MD) simulations, which reproduce the formation process. Taken together, our experimental and computational observations reveal the dynamical processes that lead to the formation of colloidal chains at different patch ratios, as well as a new dynamical process of surface-catalyzed ring formation of dimer chains.⁵

In Fig. 1 we show some of the various structures we observe as well as a phase diagram that shows how the structures formed depend on the Janus balance. Various types of chains with different internal structures are observed, including dimer chains, trimer chains, and surface-catalyzed rings.

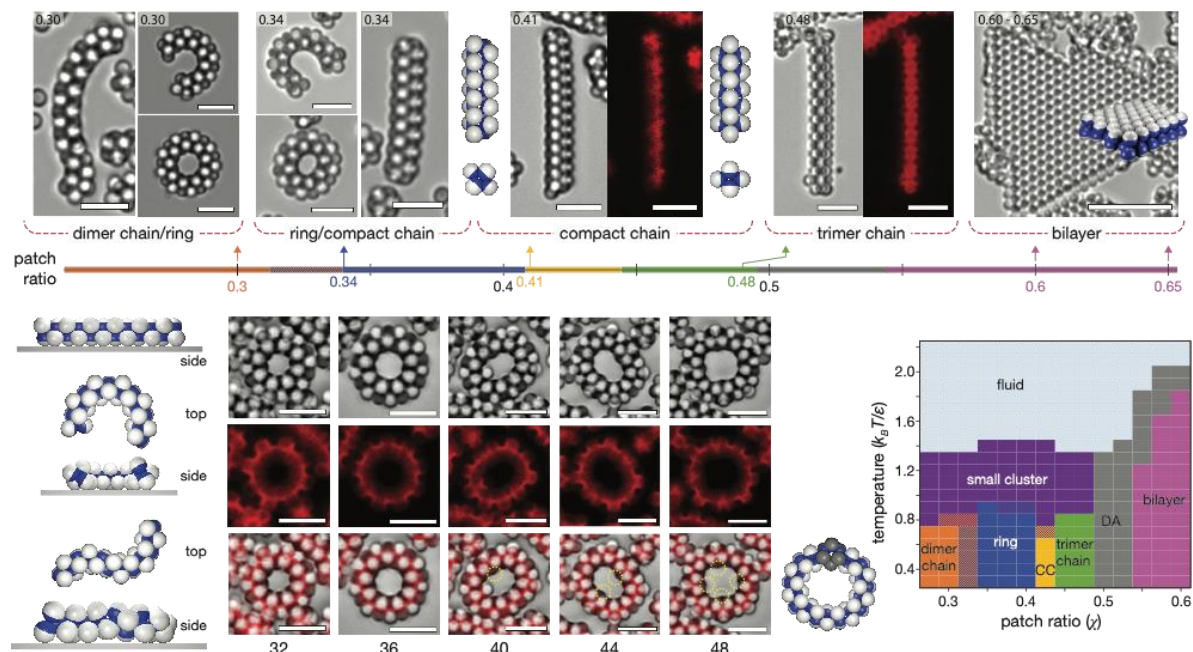


Figure 1. Top panel shows sequence of structures that form for patch ratios from about 0.3 to 0.65. Bottom left and center panels show the formation of surface-catalyzed ring structures. Bottom right panel shows phase diagram from computer simulations, which generally agree with experiments.

Future Plans

- Multi-flavored DNA-coated particles for programmed order-to-order transition
- Measuring and modeling interactions between DNA-coated colloidal particles
- Diffusion and annealing in colloidal crystals of DNA-coated colloidal particles

Publications

Joon Suk Oh, Sangmin Lee, Sharon C. Glotzer, Gi-Ra Yi, David J. Pine, “Colloidal fibers and rings by cooperative assembly” *Nature Communications*, *in press*.

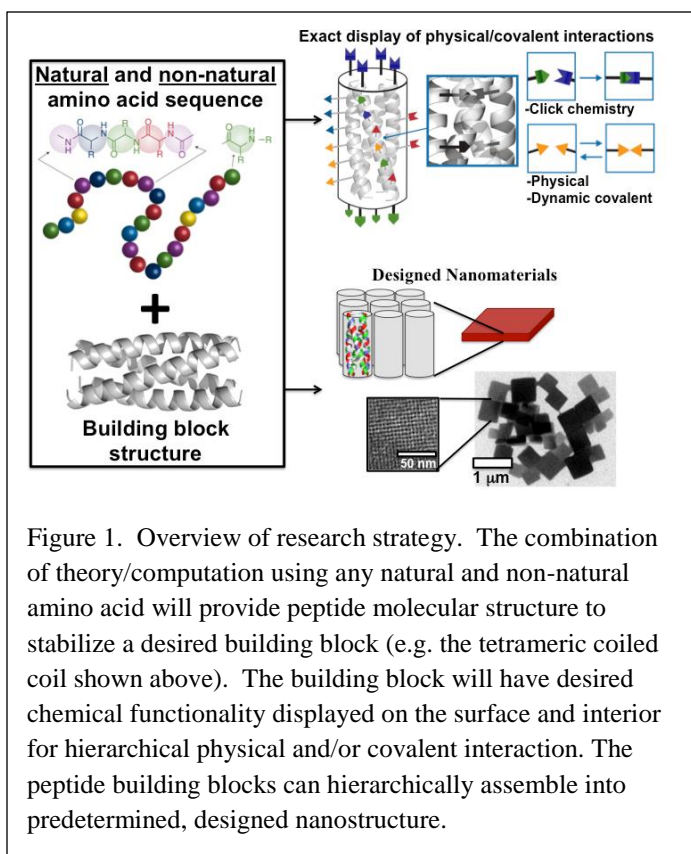
-
- ¹ Chen, Q. *et al.* Supracolloidal reaction kinetics of Janus spheres. *Science* **331**, 199–202 (2011).
- ² Wang, Y. *et al.* Crystallization of DNA-coated colloids. *Nat. Commun.* **6**, 7253 (2015).
- ³ Rogers, W. B. & Crocker, J. C. Direct measurements of DNA-mediated colloidal interactions and their quantitative modeling. *Proc. Natl. Acad. Sci.* **108**, 15687–15692 (2011).
- ⁴ Mladek, B. M., Fornleitner, J., Martinez-Veracoechea, F. J., Dawid, A. & Frenkel, D. Quantitative Prediction of the Phase Diagram of DNA-Functionalized Nanosized Colloids. *Phys. Rev. Lett.* **108**, 1–5 (2012).
- ⁵ Tang, L., Stith, L. & Jaffe, E. K. Substrate-induced interconversion of protein quaternary structure isoforms. *J. Biol. Chem.* **280**, 15786–15793 (2005).

Nanomaterial Construction through Peptide Computational Design and Hierarchical Solution Assembly

Darrin J. Pochan (University of Delaware), Christopher Kloxin (University of Delaware),
Jeffery G. Saven (University of Pennsylvania)

Program Scope

The team is leveraging methods for the computational design of biomolecules to design de novo nanomaterials with covalent crosslinking, noncovalent assembly, and sites-specific functionalization, which are realized and characterized experimentally. Using natural and non-natural amino acid modifications, modular, functional building blocks are being created that will be the basis for materials fabrication. The development of robust building block structural units will provide tools for producing complex nanomaterial structures in a wide variety of applications. Computational design is used to craft peptides containing combinations of natural and non-natural amino acids for assembly of materials with predetermined, customizable nanostructures.



Recent Progress

Peptides have been designed by the team to fold into tetrahelical bundle structures which then undergo self-assembly into lattice systems. Circular dichroic spectroscopy and analytical ultracentrifugation have confirmed that the peptides form helical, tetrameric structures, and transmission electron microscopy studies have been used to characterize lattice formation. (Zhang 2016; Tian 2017; Haider 2018; Tian 2018a; Tian 2018b) In the past year, efforts have been underway to determine atomically resolved structures of some of these peptides using x-ray crystallography. Preliminary structures of the bundles are indeed tetrameric, and the crystallographic structure is in close agreement with the computationally generated model structure.

These structural studies are being used to assess the computational modeling and design approach.

Individual tetrahelical bundles when linked using nonnatural covalent “click” chemistries form a variety of interesting polymeric structures, comprising monomers of helical bundles with nanometer dimensions. One such construct forms polymeric rods (Figure 2). Molecular simulations are being employed to investigate the roles that interbundle interactions and covalent linkages have on the relative orientations of linked bundles. The simulations are being used to suggest testable hypotheses regarding the interactions between amino acid residues within the polymeric assembly.

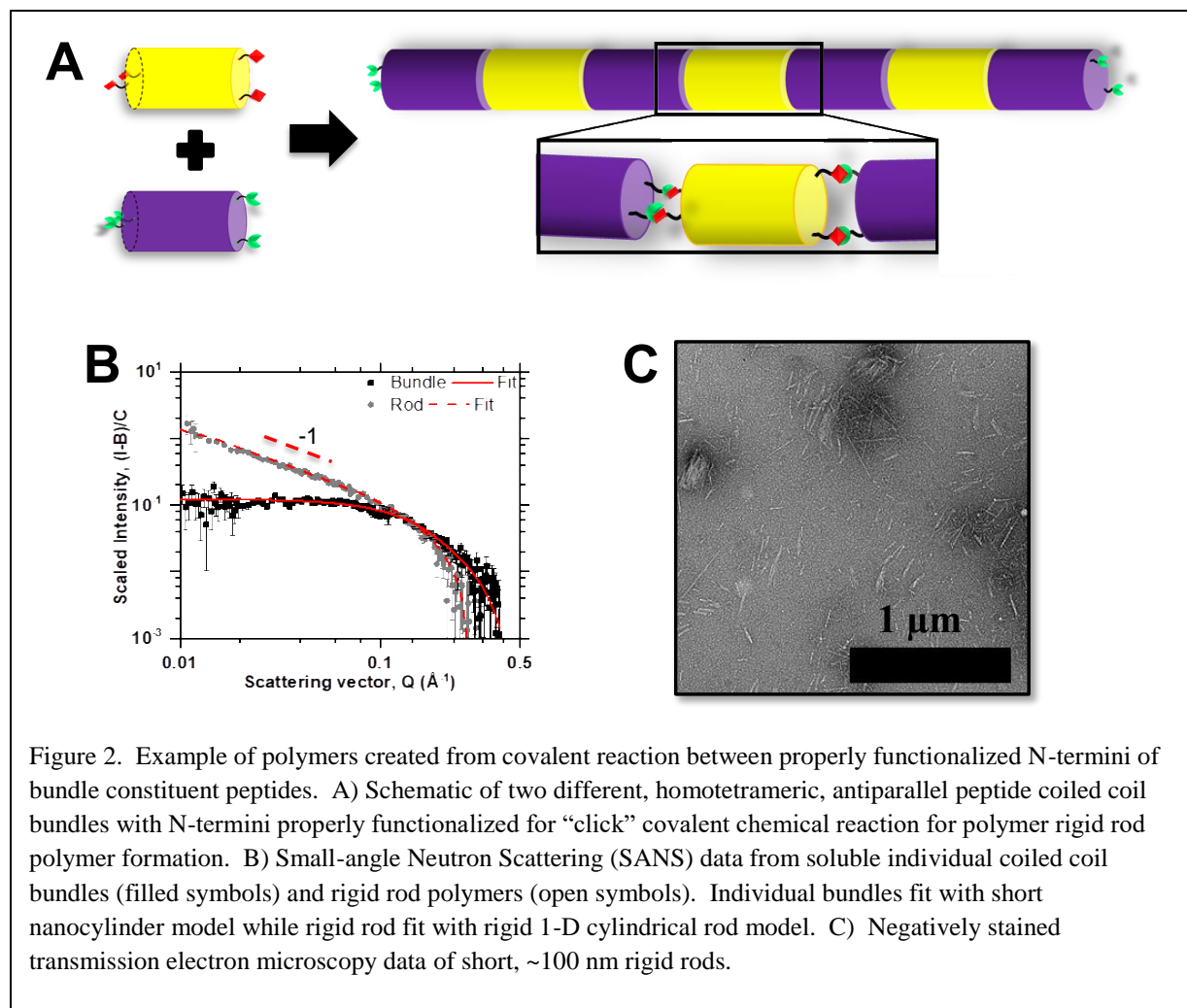


Figure 2. Example of polymers created from covalent reaction between properly functionalized N-termini of bundle constituent peptides. A) Schematic of two different, homotetrameric, antiparallel peptide coiled coil bundles with N-termini properly functionalized for “click” covalent chemical reaction for polymer rigid rod polymer formation. B) Small-angle Neutron Scattering (SANS) data from soluble individual coiled coil bundles (filled symbols) and rigid rod polymers (open symbols). Individual bundles fit with short nanocylinder model while rigid rod fit with rigid 1-D cylindrical rod model. C) Negatively stained transmission electron microscopy data of short, ~100 nm rigid rods.

Future Plans

The assembly of designed helical bundles will continue to be explored. We will build bundle monomers of varying charge in an effort to control association and repulsion between individual bundles in solution via controlled electrostatic interactions. Concentrated solutions of rigid rods will be studied to determine control of liquid crystalline behavior. New computational bundle designs will include variation of bundle structure and composition. Additionally, we will be pushing into one- and two-dimensional nanostructure formation through designed interactions both within and between bundles.

References

Zhang, H. V., Polzer, F., Haider, M. J., Tian, Y., Villegas, J. A., Kiick, K. L., Pochan, D. J., and Saven, J. G. (2016) Computationally designed peptides for self-assembly of nanostructured lattices, *Science Advances* 2, e1600307-e1600307.

Tian, Y., Zhang, H. V., Kiick, K. L., Saven, J. G., and Pochan, D. J. (2017) Transition from disordered aggregates to ordered lattices: kinetic control of the assembly of a computationally designed peptide, *Organic & biomolecular chemistry* 15, 6109-6118.

Haider, M. J., Zhang, H. V., Sinha, N., Fagan, J. A., Kiick, K. L., Saven, J. G., and Pochan, D. J. (2018) Self-assembly and soluble aggregate behavior of computationally designed coiled-coil peptide bundles., *Soft matter*.

Tian, Y., Polzer, F. B., Zhang, H. V., Kiick, K. L., Saven, J. G., and Pochan, D. J. (2018a) Nanotubes, Plates, and Needles: Pathway-Dependent Self-Assembly of Computationally Designed Peptides, *Biomacromolecules* 19, 4286-4298.

Tian, Y., Zhang, H. V., Kiick, K. L., Saven, J. G., and Pochan, D. J. (2018b) Fabrication of One- and Two-Dimensional Gold Nanoparticle Arrays on Computationally Designed Self-Assembled Peptide Templates, *Chemistry of Materials* 30, 8510-8520.

Publications

Dongdong Wu, Nairiti Sinha, Jeeyoung Lee, Bryan Sutherland, Nicole Halaszynski, Jeffrey Caplan, Huixi Violet Zhang, Jeffery G. Saven, Christopher J. Kloxin, and Darrin J. Pochan. (2019) Physical-Covalent Polymers of Designed Peptide Bundles with Programmable Chemical Display and Chain Flexibility. Submitted.

Abstract Title: Metal-ions Impart Self-Assembling Functionality to Intrinsically Disordered Proteins

(Grant Title: Miniaturized Hybrid Materials Inspired by Nature)

Principle Investigator (PI): C. R. Safinya

Co-PIs: Y. Li and K. Ewert

Materials Department, University of California at Santa Barbara

Santa Barbara, CA 93106

E-mail: safinya@mrl.ucsb.edu

Program Scope

The overall goals of our research program are to clarify the nature of assembly of biomolecular materials mediated by a range of poorly understood mechanisms that often mimic complex events in the cellular environment. The building blocks and biopolymers that we study include intrinsically ordered proteins (IDPs) [1-3], tubular and filamentous proteins [4-6], and membranes and nucleic acids [7]. The systems, consisting of novel functional assemblies, include those mediated by the polyampholytic nature of IDPs [2,6], metal-ion stabilized short-range attractions [8], hydrophobic-mediated assembly of water soluble building blocks [9], and membrane directed assembly of nucleic acids organized in a variety of geometries [7]. Novel new assemblies may further result due to controlled shape changes in building blocks [4,5].

In ongoing studies we have discovered a metal-ion-induced reversible transition of microtubule (MT) bundles coated with IDP Tau [8]. We find that linking of the protruding anionic part of Tau's projection domains, by transient metal-ligand bonds, triggers a remarkable transition from MT bundles with small lateral bundle dimensions to strongly enhanced, extended bundle arrays with smaller MT spacing. Thus, the data show that the condensation of metal ions on Tau's projection domain imparts the new self-assembling functionality to IDP Tau. This remarkable discovery is in contrast to the normal function of metal-ligand bonds in biological systems linking residues along a *single* peptide chain in order to achieve a distinct protein shape for shape-dependent interactions between biological macromolecules (e.g. ligand-receptor interactions). In parallel work we sought to harness hydrophobic interactions for mediating the assembly of building blocks beyond the simple self-association of lipophilic molecules [9]. We designed double-end-anchored poly(ethylene glycol)s (DEA-PEGs), i.e., hydrophilic PEG polymer modified with hydrophobic groups on both ends. Multilayer membranes were found to *reversibly* transition from a locked to an unlocked state by variations in the strength of the interlayer attractions due to bridging conformations. The results of the work are expected to open a new direction for *hydrophobic-mediated* assembly of objects with distinct shape and size, at predictable spacing, in aqueous environments. This complements prevalent types of directed assembly of water-soluble building blocks with specific interactions, including, H-bonding of complementary nucleic acid base pairs.

The projects utilize the broad spectrum of expertise of the PI and the two co-PIs in biomolecular self-assembling methods, custom organic/polymer synthesis and purification of biological molecules, synchrotron x-ray scattering, electron and optical microscopy, and SAXS-osmotic pressure techniques for *in-situ* force measurements.

Recent Progress

(I) Metal Ion Condensation and Linking of Tau-Projection Domains by Metal–ligand Bonds Drives the Expanded-to-Collapsed Microtubule Bundle Transition Microtubules (MTs) are hollow cylinders (outer, inner diameters of ≈ 25 nm and 15 nm) (Fig. 1A) and components of the cytoskeleton of eukaryotic cells [1-5]. Our recent experiments have used the protein Tau, which is a polyampholyte and an important IDP controlling MT dynamics in neurons. Tau contains cationic domains, which bind to the anionic MT surface and partially suppress MT dynamic instability. The N-terminal tail consisting of a polyampholytic anionic/cationic dipolar projection domain projects off the MT surface (Fig. 1A). In recent synchrotron SAXS experiments we discovered that the expanded MT bundle state [1,2] undergoes a transition to a collapsed MT bundle state as a function of time if a critical concentration (c_M^*) of divalent metal ions (Mg^{2+} or Ca^{2+}) is exceeded (Fig. 1B) [8]. *The most remarkable difference between the two MT states seen in TEM* (which probes much larger length scales beyond SAXS measurements) is the extended nature of the bundles in the collapsed MT bundle state with significantly increased lateral dimensions of the bundles. The combined SAXS and TEM data suggest collapse and linking of Tau projection domains bound to MTs, by metal–ligand bonds, in the collapsed bundle state (Fig. 1B). In one conformation, Mg^{2+} ions mediate intra-chain ion bridges, tightly stitching local sections of the PD^- together. Mg^{2+} ions also induce inter-digitation of the opposing anionic PD^- s linking neighboring MTs (Fig. 1B) consistent with TEM images of extensive arrays of MTs in the collapsed MT bundle state.

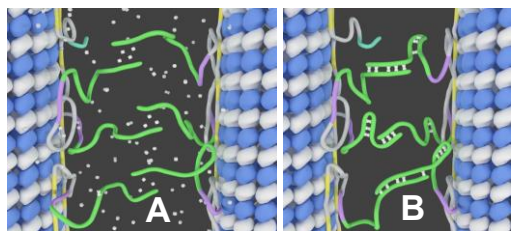


Figure 1. Metal-ion-induced expanded-to-collapsed transition in microtubule (MT) bundle arrays. (A) Sketch of the stretched conformation of the anionic segment of Tau's projection domain (PD^- , green), in the expanded MT bundle state revealed in SAXS, due to the osmotic pressure of uniformly distributed univalent counterions (short cylinders) within the charged Tau sheath coating MTs. The expanded state occurs for divalent metal ion concentrations below a critical concentration c_M^* . The attraction

between PD^- s near the midplane-layer between the MT surfaces is provided by correlated counterion fluctuations near the distal end of weakly penetrating opposing Tau PD^- s. (B) Cartoon of interacting Tau chains on neighboring microtubules (MTs) in the collapsed MT bundle state after condensation of oppositely charged divalent metals (paired short cylinders) on PD^- (green chain). Condensation of metal ions significantly reduces the osmotic pressure on the PD^- , facilitating chain collapse. Metal ions may stitch sections along individual PD^- , or link opposing PD^- sections of Tau chains bound to neighboring MTs. Adapted from 8.

Significance. To date, the focus of metal–ligand bonds in biological systems has often been on metal ions linking distinct residues along a *single* peptide chain through metal–ligand bonds for the purpose of catalysis or fine-tuning of protein shape; e.g., in metalloproteins containing Zn-finger motifs, the local coordination sphere of the metal–ligand bonds leads to shape-dependent interactions with the major grooves of DNA in gene regulation. In contrast, our discovery has shown that metal–ligand bonds linking *two* IDPs attached to neighboring MTs (i.e. building blocks) may drive a reversible linking of the protruding projection domains of Tau, by Mg^{2+} - and Ca^{2+} -ligand bonds, thus imparting new self-assembling functionality to an IDP.

(II) Controlled Assembly of Charged Nanosheet Clays by DNA: Phosphate Groups on the DNA Backbone are Ligands for Mg^{2+} on the Clay Rim The goal of this study was to investigate the interactions between DNA and anionic solid nanosheets [10]. The systems studied consisted of anionic clays (i.e. solid nanosheets of montmorillonite or beidellite ≈ 1.0 nm thick plate-like clays with diameters around 2 μm and 0.2 μm , respectively)) and double-stranded DNA.

Isomorphous substitutions in either the octahedral sheet (montmorillonite clay) or the tetrahedral sheets (beidellite clay) render them anionic with hydrated cations (Na^+) concentrated near the sheets. A spectroscopic study shows that, upon DNA addition, the first DNA molecules adsorb onto the clay particles in spite of the DNA and clay being both negatively charged. This suggests that phosphate groups on the DNA backbone acts as ligands for Mg^{2+} on the clay rim.

Significance. Remarkably, synchrotron scattering experiments reveal that the average distance between the clay sheets decreases with increasing DNA concentration and that the inhibition of swelling by DNA becomes *independent of clay concentration*. This is consistent with a model where the inter-clay spacing, due to the balance between repulsions (due to DNA looping conformations between two sections adsorbed on the same clay rim) and attractions (DNA bridging conformations where a single DNA links neighboring clay sheets by adsorbing to sections of their respective rims), both originate from the conformations of DNA and are thus independent of the clay concentration, in agreement with experiments.

(III) Hydrophobically Mediated Tethering with Symmetric and Asymmetric Double-End-Anchored PEGs: Reversible Control of Spacing in Charged Multilayer Membranes Complex materials often achieve remarkable functional properties by hierarchical assembly of building blocks via competing and/or synergistic interactions. We investigated the properties of new double-end-anchored poly (ethylene glycol)s (DEA-PEGs) macromolecules designed to impart hydrophobically mediated tethering attractions between charged lipid membranes. We synthesized DEA-PEGs with two double-tail (symmetric) or a double-tail and a single-tail (asymmetric) hydrophobic end anchors. Control multilayer membranes with and without simple PEG-lipid (i.e. single-end-anchored PEG) swelled continuously due to electrostatic as well as, in the case of PEG-lipid, steric repulsion. In contrast, interlayer spacings in multilayer membranes containing DEA-PEGs expanded over a limited water dilution range and reached a “locked” state, which displayed a near-constant membrane wall-to-wall spacing with further increases in water content (Fig. 2). The multilayers may be designed to *reversibly* transition from a locked to an unlocked (Fig. 2) state by controlling the strength of the interlayer attractions due to bridging conformations.

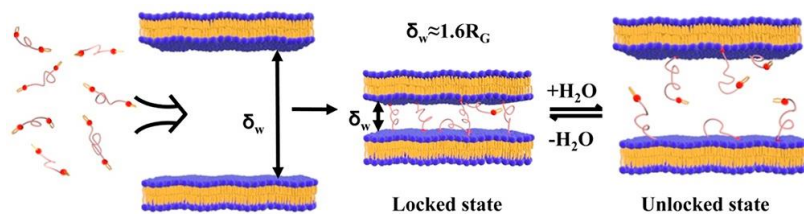


Figure 2. Cartoon depicting how custom-synthesized double-end-anchored PEG tethers are able to lock interlayer spacings in the nanometer range with few angstrom precision. Remarkably, the transition from the locked state to the unlocked state is reversible.

Significance. The locked state displays a simple relation to the PEG radius of gyration $\delta_w \approx 1.6 R_G$ for both 2K and 4.6K PEG. The fact that the “locked” δ_w is considerably less than the physical size of PEG ($2(5/3)^{1/2}R_G$) is highly unexpected and implies that, compared to free PEG, anchoring of the PEG tether at both ends leads to a considerable distortion of the PEG conformation confined between layers.

Future Plans

Our current ongoing studies have led to the discovery of a metal-ion-induced reversible transition of microtubule (MT) bundles coated with protein Tau. The transition is a result of linking of interpenetrating Tau projection domains, attached to neighboring MTs, by metal–ligand bonds. We further made the discovery that when DNA chains are added to an isotropic

suspension of anionic clays, the nanosheets spontaneously crowd and align due to the tethering of the clay sheets by DNA's phosphate groups that act as ligands to the Mg^{2+} metal ions on the clay rim [10]. The future plans include experiments to develop and characterize a new class of metal-ion-stabilized functional biomolecular materials consisting of soft building blocks labeled by custom peptides with amino acid sequences encoding assembly by metal–ligand bonds. Key experiments will also focus on demonstrating the reversibility properties of the new metal-ion-stabilized hydrogels, and developing and characterizing dynamical metal-ion-stabilized assemblies with stimuli-responsive, shape-changing building blocks on the nanometer scale.

References

1. Chung, P. J.; Song, C.; Deek, J.; Miller, H. P.; Li, Y.; Choi, M. C.; Wilson, L.; Feinstein, S. C.; Safinya, C. R.: Comparison between 102k and 20k Poly(ethylene oxide) Depletants in Osmotic Pressure Measurements of Interfilament Forces in Cytoskeletal Systems. *ACS Macro Lett.* **2018**, *7*, 228-232.
2. Chung, P. J.; Song, C.; Miller, H. P.; Li, Y.; Choi, M. C.; Wilson, L.; Feinstein, S. C.; Safinya, C. R.: Tau mediates microtubule bundle architectures mimicking fascicles of microtubules found in the axon initial segment. *Nature Communications* **2016**, *7*, 12278.
3. Chung, P. J.; Choi, M. C.; Miller, H. P.; Feinstein, H. E.; Raviv, U.; Li, Y.; Wilson, L.; Feinstein, S. L.; Safinya, C. R.: Direct force measurements reveal that protein Tau confers short-range attractions and isoform-dependent steric stabilization to microtubules. *Proc. Natl. Acad. Sci. U. S. A. (PNAS Plus)* **2015**, *112*, E6416-E6425.
4. Lee, J.; Song, C.; Lee, J.; Miller, H. P.; Cho, H.; Gim, B.; Li, Y.; Feinstein, S. C.; Wilson, L.; Safinya, C. R.; Choi, M. C.: Tubulin Double Helix: Polycation-Induced Protofilament Lateral & Longitudinal Curvature Changes. (*under review*, **2019**).
5. Ojeda-Lopez, M. A.; Needleman, D. J.; Song, C.; Ginsburg, A.; Kohl, P.; Li, Y.; Miller, H. P.; Wilson, L.; Raviv, U.; Choi, M. C.; Safinya, C. R.: Transformation of taxol-stabilized microtubules into inverted tubulin tubules triggered by a tubulin conformation switch. *Nature Materials* **2014**, *13*, 195-203.
6. Deek, J.; Chung, P. J.; Kayser, J.; Bausch, A. R.; Safinya, C. R.: Neurofilament sidearms modulate parallel and crossed-filament orientations inducing nematic to isotropic and re-entrant birefringent hydrogels. *Nature Communications* **2013**, *4*, 2224.
7. Bouxsein, N. F.; Leal, C.; McAllister, C. S., Li, Y.; Ewert, K. K.; Samuel, C. E.; Safinya, C. R.: A 3D columnar phase of stacked short DNA organized by coherent membrane undulations. (**2019**, *under review*).
8. Song, C.; Kohl, P.; Fletcher, B.; Chung, P. J.; Miller, H. P.; Li, Y.; Choi, M. C.; Wilson, L.; Feinstein, S. C.; Safinya, C. R.: Metal-ions Impart Self-Assembling Functionality to Intrinsically Disordered Protein Tau (manuscript in preparation).
9. Liu, C.; Ewert, K. K.; Wonder, E.; Kohl, P.; Li, Y.; Qiao, W.; Safinya, C. R.: Reversible Control of Spacing in Charged Lamellar Membrane Hydrogels by Hydrophobically Mediated Tethering with Symmetric and Asymmetric Double-End-Anchored Poly(ethylene glycol)s. *ACS Appl. Mater. Interfaces* **2018**, *10*, 44152–44162.
10. Yamaguchi, N.; Anraku, S.; Paineau, E.; Safinya, C. R.; Davidson, P.; Laurent J. Michot, L. J.; Miyamoto, N.: Swelling Inhibition of Liquid Crystalline Colloidal Montmorillonite and Beidellite Clays by DNA. *Scientific Reports* **2018**, *8*, 4367.

Publications (BES-supported, last 24 months)

11. Choi, M. C.; Chung, P. J.; Song, C.; Miller, H. P.; Kiris, E.; Li, Y.; Wilson, L.; Feinstein, S. C.; Safinya, C. R.: Paclitaxel suppresses Tau-mediated microtubule bundling in a concentration-dependent manner. *Biochim. Biophys. Acta - General Subjects* **2017**, *1861*, 3456-3463. DOI: [10.1016/j.bbagen.2016.09.011](https://doi.org/10.1016/j.bbagen.2016.09.011).
12. Chung, P. J.; Song, C.; Miller, H. P.; Li, Y.; Raviv, U.; Choi, M. C.; Wilson, L.; Feinstein, S. C.; Safinya, C. R.: Synchrotron small-angle X-ray scattering and electron microscopy characterization of structures and forces in microtubule/Tau mixtures. *Meth. Cell Biol.* **2017**, *141*, 155-178. DOI: [10.1016/bs.mcb.2017.06.002](https://doi.org/10.1016/bs.mcb.2017.06.002).
13. Case, R.; Schollmeyer, H.; Kohl, P.; Sirota, E. B.; Pynn, R.; Ewert, K. K.; Safinya, C. R.; Li, Y.: Hydration forces between aligned DNA helices undergoing B to A conformational change: in-situ x-ray fiber diffraction studies in a humidity and temperature controlled environment. *J. Struct. Biol.*, **2017**, *200*, 283-292. DOI: [10.1016/j.jsb.2017.07.003](https://doi.org/10.1016/j.jsb.2017.07.003).
14. Chung, P. J.; Song, C.; Deek, J.; Miller, H. P.; Li, Y.; Choi, M. C.; Wilson, L.; Feinstein, S. C.; Safinya, C. R.: Comparison between 102k and 20k Poly(ethylene oxide) Depletants in Osmotic Pressure Measurements of Interfilament Forces in Cytoskeletal Systems. *ACS Macro Lett.* **2018**, *7*, 228-232. DOI: [10.1021/acsmacrolett.7b00937](https://doi.org/10.1021/acsmacrolett.7b00937).
15. Yamaguchi, N.; Anraku, S.; Paineau, E.; Safinya, C. R.; Davidson, P.; Laurent J. Michot, L. J.; Miyamoto, N.: Swelling Inhibition of Liquid Crystalline Colloidal Montmorillonite and Beidellite Clays by DNA. *Scientific Reports* **2018**, *8*, 4367. DOI: [10.1038/s41598-018-22386-7](https://doi.org/10.1038/s41598-018-22386-7).
16. Liu, C.; Ewert, K. K.; Wonder, E.; Kohl, P.; Li, Y.; Qiao, W.; Safinya, C. R.: Reversible Control of Spacing in Charged Lamellar Membrane Hydrogels by Hydrophobically Mediated Tethering with Symmetric and Asymmetric Double-End-Anchored Poly(ethylene glycol)s. *ACS Appl. Mater. Interfaces* **2018**, *10*, 44152–44162. DOI: [10.1021/acsmi.8b16456](https://doi.org/10.1021/acsmi.8b16456).
17. Bouxsein, N. F.; Leal, C.; McAllister, C. S., Li, Y.; Ewert, K. K.; Samuel, C. E.; Safinya, C. R.: A 3D columnar phase of stacked short DNA organized by coherent membrane undulations. (*under review*).
18. Lee, J.; Song, C.; Lee, J.; Miller, H. P.; Cho, H.; Gim, B.; Li, Y.; Feinstein, S. C.; Wilson, L.; Safinya, C. R.; Choi, M. C.: Tubulin Double Helix: Polycation-Induced Protofilament Lateral & Longitudinal Curvature Changes. (*under review*).
19. Song, C.; Kohl, P.; Fletcher, B.; Chung, P. J.; Miller, H. P.; Li, Y.; Choi, M. C.; Wilson, L.; Feinstein, S. C.; Safinya, C. R.: Metal-ions Impart Self-Assembling Functionality to Intrinsically Disordered Protein Tau (*manuscript in preparation*).

Tension- and Curvature- Controlled Fluid-Solid Domain Patterning in Single Lamellae

Maria M. Santore and Gregory M. Grason

Department of Polymer Science and Engineering

University of Massachusetts, Amherst, MA 01003

Program Scope

Using giant unilamellar phospholipid vesicles as a model 2-D material, this program explores the impact of tension and curvature on the morphology and patterns of coexisting solid and fluid domains. The work is motivated by recent demonstrations of the impact of curvature-related geometrical frustration on material structure, for instance colloidal crystallization on spherical forms¹ or ice crystals on soap bubbles.² In the case of vesicles with coexisting fluid domains, line tension can stabilize round domains; however, the solid domains of the current program possess additional features, including multiple polymorphs, a finite shear modulus that prevents solid domains from assuming the shape of a spherical cap (as occurs for fluid domains), and, sometimes, kinetic trapping. This program explores how the solid mechanics, membrane fluid properties and factors produce intricate morphologies and patterned arrangements. The current scope combines experiment and modeling to 1) develop a new assessment method of solid domain mechanics based on the overall vesicle shape and 2) to identify classes of patterns and morphological behaviors, mapping mechanism-based regimes of morphologies in terms of curvature, thermodynamic, and processing variables.

Recent Progress

Overview. Previous studies of two-component (DOPC/DPPC) giant unilamellar vesicles mapped thermodynamic membrane phase diagrams (composition-temperature-tension space), including the boundaries between different classes of solid-fluid membrane morphologies (patchy domains or stripes) and demonstrated the presence of different solid polymorphs.³ Current activities target the impact of tension and curvature on domain morphology and interactions. In experiments, consideration of vesicles of different sizes along with systematic variation of processing variables (osmotic pressure differences, incubation times, and cooling rate histories) produced tension- and temperature- histories that altered curvature and affected domain morphology and interactions more dramatically than anticipated, but still consistent with the previous thermodynamic phase space. In addition to the influence of tension and curvature on domain growth and arrangement within a given

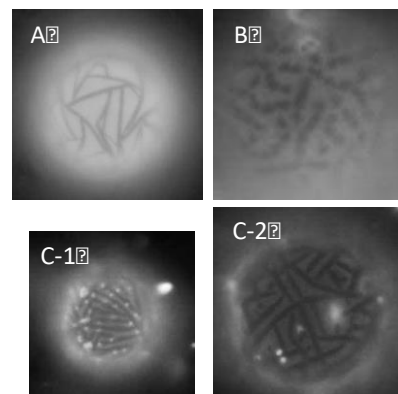


Fig. 1. A) L_{β} intersecting stripe pattern formed at high tension. B) Alignment of low tension P_{β} patches. C) Possible fusion of aligned patches into nearly parallel stripes. Solid is dark regions.

morphology class, for instance in Figure 1, we also find evidence of tension- curvature driven domain fracture, domain yielding, and domain agglomeration, two dimensional versions of solid material behavior.

Interactions between patchy domains. In recent experiments, two component (DPPC/DOPC) vesicles, initially comprising a single fluid phase at elevated temperatures, underwent phase separation during controlled cooling to produce patterns of monodisperse patchy (mostly radially symmetric) solid domains.

Appropriate choice of the osmotic pressure of sucrose and glucose solutions inside and outside the vesicles, respectively, produced vesicles that were mostly spherical (inflated, tense) or which had curved membrane fluid regions between mostly flat patchy solid domains (slightly deflated).

When the ratio of patch to approximate vesicle diameter was within the range 0.1-0.25, the arrangement of the domains was sensitive to the membrane tension and curvature. Modest deflation of vesicles, with fluctuating curvature in the membrane fluid produced long-range inter-domain repulsions, evident in patterned arrays of many domains for tens of microns.

Long-range repulsions were also evident in the pair-wise encounters within multi-patch domain vesicles, as domains underwent Brownian motion within the membrane fluid. Conversely with fuller osmotic inflation of the vesicles, such that the local curvature

in the fluid phase approached the overall vesicle curvature (which may have additionally produced a finite membrane tension), inter-domain repulsion was found to be shorter range and inter-domain attractions were evident: multi-domain vesicles exhibited disordered arrangements and in other cases patchy domains arrange in lines. The pairwise interaction between patchy domains appears to depend on several variables: the domain size relative to the vesicle, membrane tension, and fluid curvature (vesicle inflation). Current experiments target measurements of pairwise interactions in vesicles engineered to contain only 2 domains, using image stacks to generate statistics, or documenting the irreversible approach domain pairs.

Modeling Domain Interactions. The effect of 2-D shear rigidity qualitatively alters the shape and mechanics of solid domains relative to the well-studied case of fluid domain elasticity⁴. This fact derives from the geometric incompatibility of planar crystals and Gaussian curvature. Unlike the case of bending mechanics, forcing a 2-D solid to conform to a spherical curvature leads to strains that grow with area. This effect amounts to a *geometric rigidification* of solid domains leading those domains to expel Gaussian curvature, notwithstanding the global spherical geometry of vesicle. The geometric rigidity of solid domains leads to a novel perspective that patch domains behave effective like “2-D, plate-like colloids” embedded within the fluid vesicle.

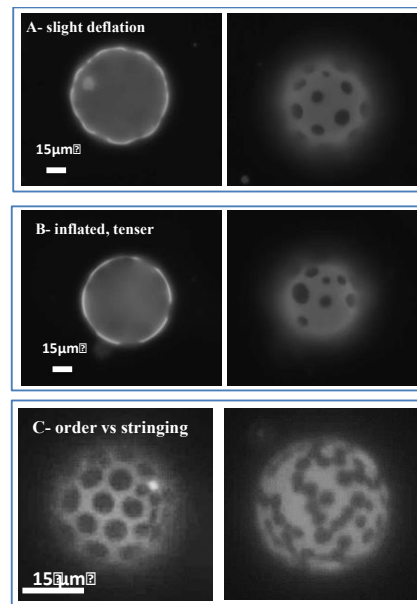


Fig. 2. A) order and B) disorder of similarly sized domains on similar vesicles, with different tensions. C) long range order at low tension versus domain chaining at higher tension.

The question then becomes, how does the mechanics of the fluid membrane phase shape the energetics of inter-domain configurations of plate-like inclusions?

To address this we have developed 2-D and 3-D vesicle models based on the Helfrich model of fluid domain elasticity in vesicles with fixed enclosed volume, surface area, solid domain fraction, and size. The full shape phase diagram for a single-domain 2-D vesicle (computed via exact shape equilibria) is shown in Fig. 3A, revealing that the increase of pressure leads to the formation of high-bending “hinges” in the fluid domain that compatibilize the globally rounded shape with the rigid, plate shape of the solid. These same qualitative behaviors are exhibited by a 3-D fluid-solid composite model. The high-curvature “hinges” play a critical role in mediating non-trivial domain-

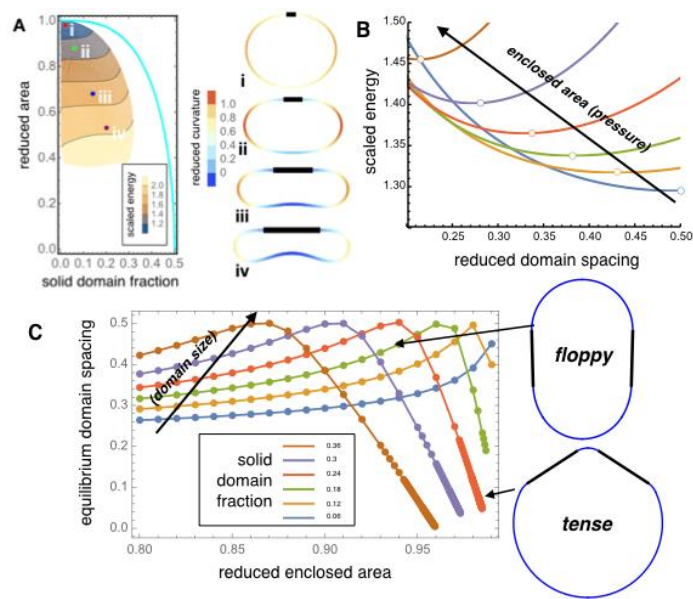


Fig 3. (A) Shape phase diagram of (2-D) single solid-domain model; (B) Vesicle energy vs. inter-domain separation (25% solid); and (C) Equilibrium solid separation vs. enclosed area.

domain interactions, as shown in Fig. 3B for a vesicle containing two identical solid domains. For relatively floppy vesicles, elastic energy leads to long-range repulsion that drives solid domains to antipodal points of the vesicle. Whereas for large domains on sufficiently tense vesicles, the equilibrium domain spacing rapidly drops to value that *decreases* with increased pressure. Analysis of this minimal model reveals that this effective domain-domain attraction derives from a novel “depletion-like” mechanism, whereby the highly-bent hinges that flank solid domains are driven to overlap to consolidate their high elastic energy. A phase diagram of repulsive/attractive inter-domain forces, shown in Fig. 3C, predicts that the large-scale interdomain morphology can be regulated by tailoring both the size of solid domains (relative to vesicle radius) and the vesicle tension, predictions that will be tested experimentally.

Ongoing efforts include the implementation of coarse-grained simulations of fluid-solid vesicle composites to i) test the basic predictions of the 2-domain theory; ii) explore the effect of non-pairwise additive mechanics in multi-domain interactions; and iii) explore effect of solid domain number on their ground state arrangements in tensed and floppy fluid-solid composites.

Individual Domain Morphology. As patchy domains nucleate and grow upon cooling from the one phase fluid membrane region, the entire membrane contracts thermally and fluid area is replaced by solid, both of which increase membrane tension. At the same time there is a tension dependent diffusion of water out across the membrane. Thus the tension history is cooling rate –

dependent, and in our studies is further manipulated osmotically, providing a preliminary ranking of tensions during domain formation and growth. Strong curvature in the membrane fluid and initial evidence for flat hexagonal domains at low tensions suggests that hexagonal patches may be the preferred flat morphology of the ripple, P_{β} solid.

Deviations from hexagonal patches have been discovered for vesicles with more nearly round shape, where curvature may be imposed on the solid during growth by tension in the fluid. Varying degrees of edge roughness on the hexagons or nucleation of strings of patchy domains from the hexagons suggest that domain growth has been altered by curvature in these cases, producing flower shaped domains in the extreme. Also at high tension, we find evidence of monodisperse hexagons each bearing a single uniform notch, suggesting uniform domain fracture or yielding at high tension and curvature.

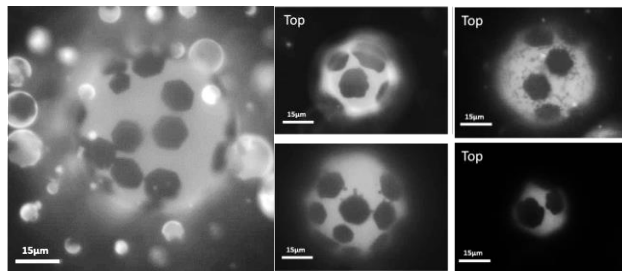


Fig. 4. Clean hexagonal (low tension) and rough-edged domains (higher tension) seen during cooling.

Future Plans

Current work has established a large variable space for domain shape and interactions. For the case of two interacting solid patch domains in a single vesicle, the impact of vesicle and domain size, tension, and vesicle inflation will be addressed thoroughly through modeling, to determine pairwise interactions and a state space map to broadly address multiple variables. Targeted experimental studies will probe pairwise interactions for select vesicle and domain sizes, probing a broad range of membrane tensions. (Related experiments with a single domain will probe the solid mechanics themselves.) Experiments will also probe the impact of tension on ordering in multi-domain vesicles, aiming to determine conditions of long range order versus chaining. More difficult experiments addressing the impact of curvature and tension on the morphology of growing domains during cooling will target the impact of domain to vesicle size ratio at elevated tensions.

References

- 1) Meng, G.; Paulose, J.; Nelson, D. R.; Manoharan, V. Elastic Instability of a Crystal on a Curved Surface. *Science*. **2014**, *343*, 634-637.
- 2) Ahmadi, F.; Nath, S.; Kingett, C.M.; Yue, P.; Boreyko, J. How Soap Bubbles Freeze. *Nature Comm.* **2019**, *10*, 2531.
- 3) Chen, D.; Santore, M. M. Large Effect of Membrane Tension on the Fluid-Solid Phase Transitions of Two-Component Phosphatidylcholine Vesicles. *Proc. Natl. Acad. Sci. U. S. A.* **2014**, *111*, 179-184.
- 4) Schneider, S.; Gompper, G. Shapes of Crystalline Domains on Spherical Fluid Vesicles. *Europhys. Lett.* **2005**, *70*, 136-142.

Publications

- 1) Li, S.; Zandi, R.; Traveset, A.; Grason, G. M. Ground States of Crystalline Caps: Generalized Jellium on Curved Space, *submitted*, arxiv:1906.03301 (2019)

Controlling exciton dynamics with DNA origami for quantum information science

Gabriela S. Schlau-Cohen (PI), Department of Chemistry
Mark Bathe (co-PI), Department of Bioengineering
Adam Willard (co-PI), Department of Chemistry
Massachusetts Institute of Technology

Project Scope

The goal of this research project is to design, synthesize, and characterize DNA-dye constructs with rationally programmed excited-state (*i.e.*, excitonic) properties. We aim to construct “excitonic circuits” that encode specific spatiotemporal dynamics upon illumination. We will use scaffolded DNA origami to embed dyes with molecular precision within arbitrary 2D and 3D nanoscale, self-assembled structural scaffolds as illustrated in Figure 1. These constructs uniquely enable local, individual, and systematic tuning of the numerous molecular parameters that govern exciton dynamics. Previous attempts to develop complex excitonic circuits have been limited by an inability to precisely control molecular positions. Our use of scaffolded DNA origami overcomes this limitation by offering:

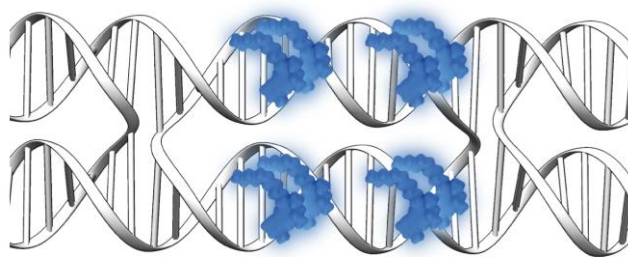


Figure 1. Schematic of DNA-dye construct. The position of dyes (blue) is precisely controlled by the DNA scaffold (gray). The position and energetics of the dyes determine the spatiotemporal dynamics of excitons.

(1) nanoscale control over spatial positioning of dyes, and thus their electronic coupling, with sub-nanometer precision; and (2) control over the mechanical properties of the scaffold itself. This control, in combination with high-resolution spectroscopy and advanced theoretical modeling techniques, will provide a new understanding of, and rational control over, nanoscale materials for applications such as quantum information processing.

Future plans

Our interdisciplinary team spans synthesis, spectroscopy, and simulation. Theory and simulation will guide excitonic and scaffold design. Designed circuits will be fabricated using bottom-up self-assembly of scaffolded DNA origami with covalently positioned dye molecules, and subsequently characterized using single-molecule and ultrafast spectroscopies. Throughout this project, we will leverage our expertise in condensed phase dynamics of biological and materials systems to create a robust platform for programmable exciton dynamics.

Development of DNA nanostructures.

We successfully incorporate dyes into DNA structures using phosphoramidite chemistry. We covalently link Cy3 (Figure 2A) into the DNA backbone. Cy3 dimers and trimers (Figure 2B) are formed by adding consecutive Cy3 on single-stranded DNA (ssDNA). Cy3-modified DNA structures are formed by hybridizing Cy3-mutated ssDNA with canonical complementary strands. Electronic coupling between dyes causes a redistribution of oscillator strength, and so the creation of a coupled network is confirmed through changes in relative peak intensity in absorption and fluorescence spectra and a change in quantum yield (Figure 2C,D).

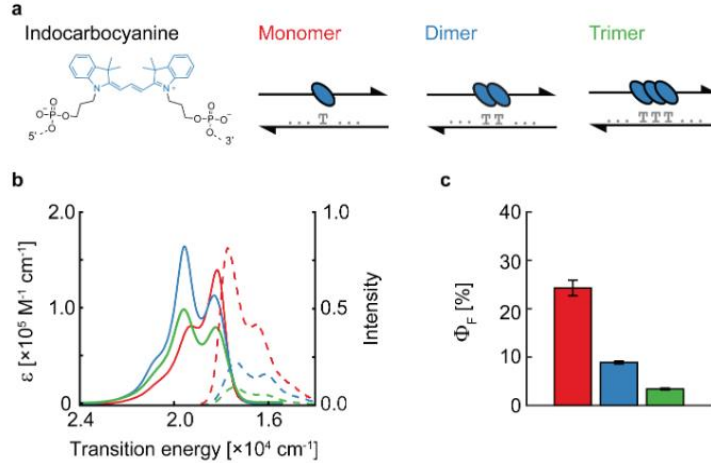


Figure 2. A chemical approach to form exciton-coupled Cy3 constructs using DNA scaffolds. a, Cy3 covalently links to the deoxyribose-phosphate backbone of single-stranded DNA (left). Exciton-coupled Cy3 dimers and trimers are formed by adding consecutive Cy3 on single-stranded DNA and hybridizing with canonical complementary strands. b, Absorbance (solid lines) and fluorescence spectra (dashed lines) of Cy3 monomer (red), dimer (blue), and trimer (green). c, Fluorescence quantum yields of Cy3 monomer, dimer, and trimer on DNA duplexes.

We have also performed advanced spectroscopic characterization of our DNA-dye constructs via single-molecule and ultrafast spectroscopy. For example, to characterize the impact of the DNA on the excitons, specifically the short-timescale effects, we use two-dimensional electronic spectroscopy (2DES). 2DES is an ultrafast transient absorption technique that correlates electronic excitation and emission frequencies as a function of a delay time between excitation and emission events, which gives insight into excitonic dynamics and energy landscapes. The center line slope (CLS) of a diagonal peak in a 2DES

spectrum is proportional to the frequency-fluctuation correlation function, which decays due to short-timescale bath fluctuations. Using CLS

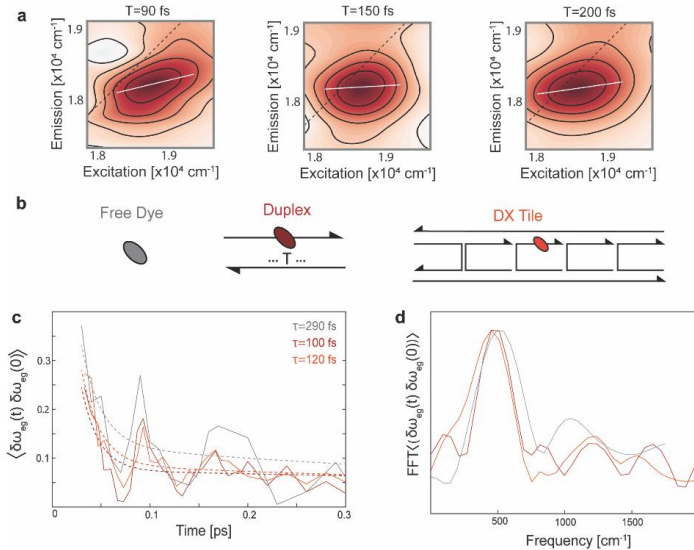


Figure 3. Spectral density in monomer constructs. (A) Selected 2D spectra at varying waiting times from free dye CLS analysis showing oscillatory features. (B) Relevant structures of dye and DNA constructs. (C) Frequency-fluctuation correlation function derived from CLS analysis for free dye (Cy3) and dye-DNA duplexes and double-cross over (DX) tiles. (D) Power spectrum of frequency-fluctuation correlation function (50-200 fs) showing an underdamped mode at 450 cm^{-1} .

analysis, the decay of the frequency-fluctuation correlation function $\langle \delta\omega(T)\delta\omega(0) \rangle$ was measured for our DNA environment and the free dye. The decay was found to be 100 fs for free dye and 55 fs for DNA duplex-scaffolded dye (Figure 3).

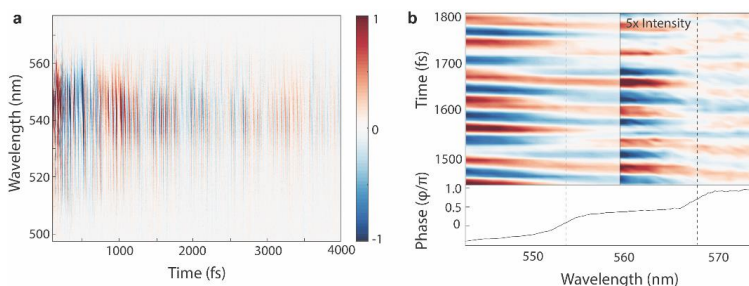


Figure 4. Coherent vibrational dynamics. (A) Cy3 free dye residual oscillations extracted from homodyne transient grating experiments showing ground and excited state vibrations. (B) Time domain nodes and phase shifts of the long-lived 615 cm^{-1} node likely corresponding to two states on the excited state potential energy surface.

homodyne transient grating experiments (Figure 4). By examining long-lived oscillatory features primarily at 615 cm^{-1} , we identify two states on the excited-state potential energy surface giving rise to nodes in the transient oscillations. One of these nodes corresponds to an emissive excited state following structural reorganization, and the second likely corresponds to a low energy stationary point that is separated from a conical intersection to the ground state by a bond activation barrier.

We will extend our DNA-dye constructs by varying the transition energy through incorporation of a range of dyes compatible with phosphoramidite chemistry. We will use our DNA synthesizer to incorporate these dyes into oligonucleotides, which will be screened using an optical plate reader to measure steady-state absorption and fluorescence spectra. These spectra already report on exciton delocalization and electronic structure. We will also investigate the exciton dynamics through increasingly complex and DNA structures via the following series of constructs: individual DNA duplexes; higher order DX-tiles; and six-helix bundle honeycomb structures.

Application to quantum computing. In our approach to quantum computing, the state of the qubits involved in the computation are encoded into the state of the excitonic wavefunction in an excitonic circuit. The encoding is specified by,

$$\hat{H}_{\text{comp}} = \frac{i}{\hbar} \ln \hat{U}_{\text{comp}},$$

where \hat{U}_{comp} specifies the desired computation and \hat{H}_{comp} specifies an excitonic Hamiltonian. In dye-based circuits, this Hamiltonian can be generated by representing each qubit as a pair of dye molecules. In this way, the state of each qubit is reflected by the excitation state of its dye-molecule pair. In simple systems, such as the gates we

describe below, these states can be directly measured with experiment. However, in more complex systems, such as those we hope to build toward, these states will have to be determined with a combination of experiment and theory.



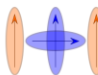
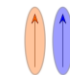
Gate	NOT	Hadamard	CNOT	$\pi/8$
Operator (\hat{U})	$\begin{pmatrix} 0 & 1 \\ 1 & 0 \end{pmatrix}$	$\frac{1}{\sqrt{2}} \begin{pmatrix} 1 & 1 \\ 1 & -1 \end{pmatrix}$	$\begin{pmatrix} 1 & 0 & 0 & 0 \\ 0 & 1 & 0 & 0 \\ 0 & 0 & 0 & 1 \\ 0 & 0 & 1 & 0 \end{pmatrix}$	$\begin{pmatrix} 1 & 0 \\ 0 & e^{i\pi/4} \end{pmatrix}$
System Hamiltonian (\hat{H}_{comp})	$\frac{\pi}{2\tau} \begin{pmatrix} -1 & 1 \\ 1 & -1 \end{pmatrix}$	$\frac{\pi}{2\sqrt{2}\tau} \begin{pmatrix} (1-\sqrt{2}) & 1 \\ 1 & (-1-\sqrt{2}) \end{pmatrix}$	$\frac{\pi}{2\tau} \begin{pmatrix} 0 & 0 & 0 & 0 \\ 0 & 0 & 0 & 0 \\ 0 & 0 & -1 & 1 \\ 0 & 0 & 1 & -1 \end{pmatrix}$	$\frac{\pi}{4\tau} \begin{pmatrix} -1 & 0 \\ 0 & 0 \end{pmatrix}$
Excitonic circuit				

Figure 5. Representing quantum gate operations as excitonic circuits. The unitary operator and corresponding system Hamiltonian for the four universal quantum gates. The systems that encode these gates are also shown as: NOT, a coupled pair of identical molecules; Hadamard, a coupled pair of different molecules; CNOT, two uncoupled molecules and a coupled pair of identical molecules; $\pi/8$, a pair of uncoupled different molecules.

The quantum gates that we propose to study are simple one- or two-qubit operations. For one-qubit gates (*i.e.*, NOT, Hadamard, and $\pi/8$) the circuits include two dye molecules and for the two-qubit gate (*i.e.*, CNOT), the circuit includes four dye molecules. Candidate circuits for each of these gates are shown in Figure 5. After designing excitonic circuits that perform elementary quantum gate operations, we will attempt to couple the unitary gates together by developing a generalizable method for representing a sequence of gate operations.

Resilient Hydrogels from the Nanoscale to the Macroscale

Rebecca Schulman, Johns Hopkins University

Program Scope

Biological systems illustrate how a material composed of fragile molecular components can collectively be highly resilient. While the average protein, cell or even many tissues may not last more than a few weeks, many animals and plants have lifetimes of a century or more. Continual component regeneration and multiple systems to resist mechanical and chemical damage together make this capacity possible. The goal of this project is to develop biomimetic methods to enable a material, specifically a DNA-crosslinked hydrogel, to resist multiple types of damage across multiple scales using distinct, modular damage protection mechanisms.

Our current work focuses on two questions. First, how can a hydrogel sense mechanical forces that could indicate the onset of a yield stress and resist them by becoming stronger? This question is inspired by the observation that living tissues can not only repair themselves if damaged, but can also adapt to stress by reconfiguring in order to avoid damage in the first place. Such a mechanism could make materials lightweight and flexible but still resistant to damage and enable them to dynamically use limited resources to maximize their functionality. Second, how can a material with a particular spatial structure recover that structure autonomously if the pattern is damaged? The response to damage within skin or other organs can not only return a material's microscopic properties to their original form, it can also repair mesoscale organization. Such a feature is required if we are to not only build self-healing materials with homogeneous organization, but self-healing material devices with multiple layers or regions that each contribute to the functionality of the whole.

We address these questions using simple materials with dynamic chemistries, specifically DNA hybridization, where the mechanical, physical and chemical properties are well understood and tools exist for designing synthetic signal transduction cascades to mediate response.

Recent Progress

Force-triggered DNA chemistry. To design materials that can resist mechanical force by dynamic material reorganization, we have been developing a new class of mechano-responsive hydrogels which can respond to mechanical stress via chemical activation of molecular complexes. Critically, these force sensor complexes are present at a low enough concentration within a hydrogel that their presence does not change the mechanical properties of the hydrogel they are integrated within, suggesting how these sensors might be used within a variety of materials. In our experiments, DNA duplex force sensors are integrated into polyethylene-glycol diacrylate (PEGDA) hydrogels. A DNA force sensor is activated or triggered, when it dehybridizes, exposing a single-stranded domain that can react with free species within the hydrogel.

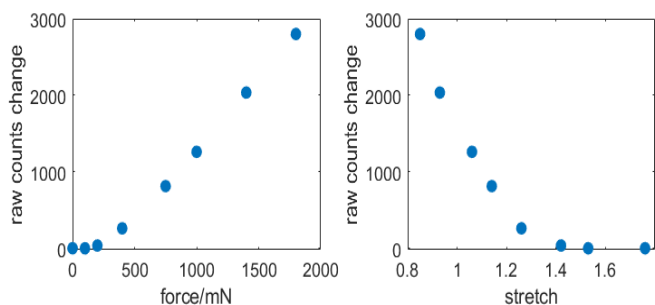


Figure 1. The raw fluorescence counts change (raw counts – initial raw counts) increases as a function of the applied force and stretch during uniaxial compression. Stretch is measured where 1 is the size of the gel after synthesis; hydrogel swelling to equilibrate solvent increases the value. A uniaxial compressive force decreases stretch.

to precisely control the degree of uniaxial compression while imaging a hydrogel. Our current experimental results suggest that DNA force sensors are activated at a critical level of compressive force (Figure 1), consistent with the predictions of our model.

Self-healing reaction diffusion patterns in hydrogels. To develop materials in which micron-scale

structure can be restored after being partially damaged, we have developed self-healing architectures.

These architectures are formed using DNA reaction-diffusion networks in hydrogels, so that their architected structure consists of chemical gradients.

We have shown that these patterns can resist changes to their spatial profile, such as those caused by chemical agents that react with and degrade the components that make up the chemical gradient, by actively reforming their original shapes.

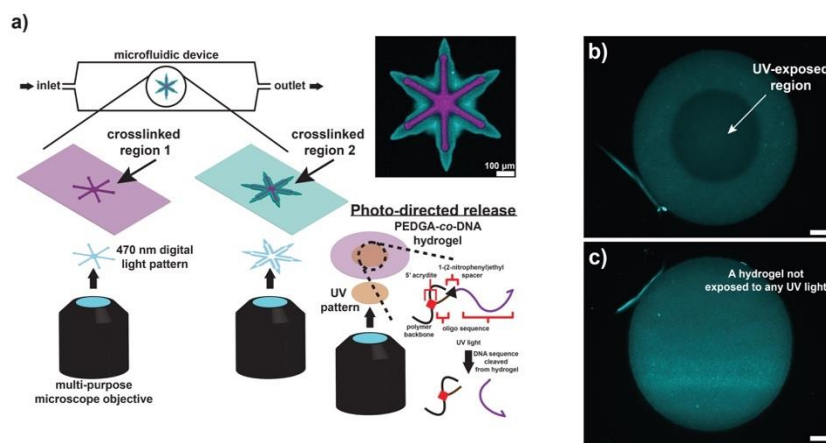


Figure 2. Digital maskless photopatterning of PEGDA hydrogels enabling UV-directed DNA release. a) Photopatterning of structured hydrogels with different DNA species conjugated to the polymer network in different locations. b) Fluorescent image of a hydrogel containing conjugated DNA possessing a photocleavable 1-(2-nitrophenyl)ethyl spacer after UV exposure. Cleaved fluorescent probes diffuse out of the gel, leaving a region with reduced fluorescence intensity. c) A control hydrogel not exposed to UV light.

We have used the Arruda-Boyce constitutive polymer model^{Ref1} to predict how force sensors should respond to the extent of compression in terms of hydrogel strain. To test these predictions experimentally, we use PEGDA-co-DNA hydrogels containing DNA reporter complexes that can react with active force sensors, separating fluorophore-quencher pairs within the reporters. To test how a gel with integrated force sensors responds to force, we use multi-mode force microscopy^{Ref2}

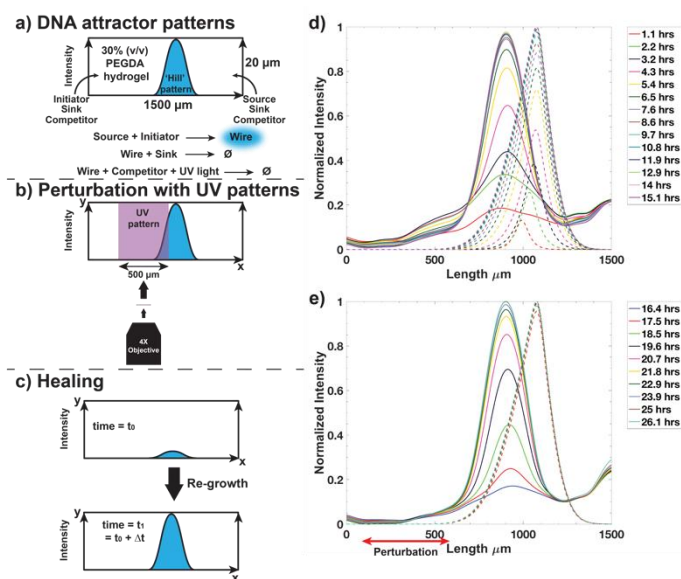


Figure 3. Formation and perturbation of linear and hill-shaped DNA patterns within a microfluidic diffusion cell. a) Reactants diffuse into the cell from the boundaries at either end where input concentration is kept constant. DNA strand displacement reactions within network generate a pattern visualized via fluorescence. b) Patterns are perturbed in specific regions by exposing them to a pattern of UV light. c) Perturbed patterns eventually return to their original steady state (the attractor). d) Formation and e) healing of a hill-shaped pattern perturbation after UV perturbation (shown with red arrow)

conditions, which sustains the patterns over time¹. The patterns are damaged at specific sites by controlling what regions of the hydrogel are exposed to UV-light, which activates a competitor species that reacts with the species that forms the gradient. We show that after regions of the chemical gradients are damaged by competitor, the gradients can reform their original shapes. thus acting as “attractor patterns”. PDE-based reaction-diffusion models of the process quantitatively recapitulate both the formation of the gradients and their recovery after damage (Figure 3, manuscript in preparation).

Future Plans

Our current work suggests how nucleic acid sensors within hydrogels can respond chemically to force via the exposure of a new DNA binding site that could serve as an initiation site for a chemical cascade. Our next task will be to use the exposure of this binding site as a trigger to direct the synthesis and dissemination of new nucleic acid strands at the site of damage. Such strands will be used to direct chemical processes that adaptively reorganize the hydrogel.

To repeatably form these gradients within materials and study their response to different types of damage, we have developed a toolkit for forming hydrogels and their constituent gradients involving digital maskless photolithography, microfluidic assembly and a visible light photoinitiator system compatible with DNA (Figure 2, manuscript in revision). This platform can be used to pattern gels with DNA in prescribed domains and to photo-direct release of short DNA oligos from specific regions of a hydrogel.

We have used this toolkit to pattern hydrogels in which well-defined gradients of specific DNA species hundreds of microns form because of reactions driven by DNA hybridization and diffusion of the different DNA species and anisotropic boundary conditions. Energy is provided to the system by maintaining these boundary

The ability to program the shape of self-stabilizing chemical patterns in soft materials using DNA reaction diffusion-networks enables the design of more sophisticated systems that store chemical and molecular information within materials. Specifically, we are developing a primitive chemical associative memory consisting a distributed network of nodes where specific chemical species, such as DNA strands, are immobilized within a hydrogel. Communication between nodes occurs via chemical release and uptake. One mechanism of operating this network would be to use *in vitro* transcriptional networks or genelets^{Ref3} localized in space. We will program this network of nodes to communicate via excitatory and inhibitory reactions to emulate a Hopfield network, which contains multiple stable states, or “patterns”. When the network is perturbed and enters a non-stable state, it will converge to the closest stable state, thus allowing a given pattern of the network to “heal”. We will explore how such systems of reactions can use diffusion and convection to remember patterns and measure the healing capacity of a spatial array of networks. Finally, we will show that by coupling this network to a downstream reaction process, the associative memory can direct a given set of reactions arrayed across space. This demonstration will show how networks of chemical reactions in space can display complex, programmable emergent behavior that drive spatial coordination of chemical process and complex structural repair.

References

1. E. M. Arruda, and M. C. Boyce (1993). A three-dimensional constitutive model for the large stretch behavior of rubber elastic materials. *Journal of the Mechanics and Physics of Solids*, 41(2), 389-412.
2. Roberts, P., Pilkington, G. A., Wang, Y., & Frechette, J. (2018). A multifunctional force microscope for soft matter with in situ imaging. *Review of Scientific Instruments*, 89(4), 043902.
3. S. W. Schaffter and R. Schulman. Building *in vitro* transcriptional regulatory networks by successively integrating multiple functional modules. *Nature Chemistry*. Accepted for publication.

Publications

1. J. Zenk, D. Scalise, K. Wang, P. Dorsey, J. Fern, A. Cruz and R. Schulman. “Stable DNA-based Reaction-Diffusion Patterns”, *RSC Advances* 7 18032-18040, 2017.
2. A. Cangialosi*, C. Yoon*, J. Liu, Q. Huang, J. Guo, T. Nguyen, D. Gracias and R. Schulman. “DNA Sequence Directed Shape Change of Photopatterned Hydrogels via High-Degree Swelling.” *Science*. 357: 1126-1130, 2017.
3. J. Fern and R. Schulman. “Modular DNA Strand-Displacement Controllers that Direct Material Expansion.” *Nature Communications* 9, Article 3766, 2018.

*These authors contributed equally to this work.

What are the principles controlling biomimetic heteropolymer secondary structure?

PI: Michael Shirts

Department of Biological and Chemical Engineering, University of Colorado Boulder

Program Scope

The term “foldamers” describe heteropolymers with stable low-entropy, low-energy structures. Proteins and folding RNAs are examples of foldamers, but new classes of biomimetic foldamers, such as peptoids, β - and γ -peptides have been investigated more recently, with a number of other completely abiotic foldamers emerging as well. The ultimate goal of this research program is to understand the physics of foldamers with sufficient detail to directly guide experimental efforts to create functional heteropolymer materials. This understanding would greatly aid the design of materials ranging from single molecule switches, to larger heteropolymers with angstrom-scale precision in structure, to self-assembled materials constructed of oligomeric building blocks. To make progress on this larger aim, we are first developing a better understanding of the basic building blocks underlying most molecular architectures: local secondary structural elements. Once these local structural elements are better understood and can be designed more easily, they can then be assembled hierarchically into larger structures, either covalently, creating protein analogs, or through self-assembly.

Biology suggests that secondary structure elements serve as an ideal foundation to build both stable and responsive materials. In all known heteropolymers with defined three-dimensional structure, we observe secondary structure, such as the well-known α -helices and β -sheets in proteins, or stem-loops and pseudoknots in RNA. This bioinspiration suggests that the simplest and most controllable way to achieve larger-scale three-dimensional structure is to create local structural units and then to connect them as described above. Therefore, **the overarching objective of the current research is to identify and classify the short-scale structural elements that heteropolymers can form, show how chemical interactions can stabilize them, and understand how these interactions create cooperative transitions between alternative conformational states.**

The initial activities of this work therefore focus on understanding fundamental physical principles about heteropolymer secondary structure in small oligomeric units, independent of specific chemical identities, which will then guide later investigation on specific molecular compositions. We define secondary structure here as significant restriction of the backbone conformational ensemble from what would be expected in a random coil polymer, leading to stable structural units. Such units are also likely to be periodic, which leads to additional stability through cooperativity, but other particularly stable arrangements may be possible, such as pseudoknots in RNA.

During the current phase of this research, we are working to answer the specific questions:

1. What monomer geometries and interactions can *energetically* stabilize secondary structure?
2. What energetically favored secondary structural elements are *entropically* favored?
3. How can we manipulate these favored secondary structural elements to create highly cooperative transitions between alternative secondary structures of similar stability?
4. How well do these general heteropolymer theories match atomistic models and experimental data for oligomers?

Our primary current theoretical tool for the initial work is coarse-grained modeling. The main purpose of using coarse-grained potentials is not primarily about computational efficiency—instead, the primary purpose of using coarse-grained models is to reduce the dimensionality of the design parameter space. By studying the properties of models with a relatively small number of parameters, we drastically simplify the process of generating and testing overarching hypotheses about the nature of foldamers. An important longer-term goal of the work is to develop reasonable methods for back-constructing potential atomistically detailed models given a coarse-grained model ensemble with desired thermodynamic behavior.

We are using two parallel and complementary theoretical approaches to attack this problem: high-throughput conformational energy searches using Rosetta, and exhaustive parameter searches through a combination of molecular dynamics with OpenMM and reweighting to compute thermodynamic properties including indicators of stability and cooperativity.

Recent Progress

We have successfully ‘hijacked’ Rosetta/PyRosetta to accept CG residues, both for energy Rosetta scoring functions and configuration ‘movers’, with maximal modularity and minimal perturbation of existing Rosetta code. Using PyRosetta functionality, we have created and streamlined CG model building process, and can build sequences of arbitrarily constructed models with general N bead-per-backbone / M bead-per-sidechain models custom residues (abbreviated as N-M models) read from a PDB file. We have also created custom PyRosetta

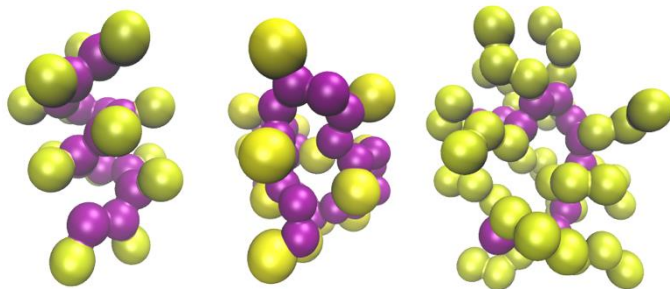


Figure 1: (left) 1 backbone – 1 sidechain (1-1), (center) 2-backbone – 1 sidechain (2-1) and (right) 1 backbone – 3 sidechain (1-3) coarse-grained models of heteropolymers sampled with PyRosetta-based tools developed during this

movers for our specific CG models. For example, we have adapted PyRosetta/Rosetta mover algorithms to create a backbone small mover (random angle perturbation), shear mover (random angle perturbation with downstream adjustment) and minimization movers. Typical Rosetta simulations only sample dihedral phase space, however as these CG beads do not represent full atoms, the bond angles, rather than being fixed, have a

significant overall contribution to the overall movement of the polymer while folding. We have been able to use our new PyRosetta optimization and search algorithms to rapidly and consistently fold small (10-20 CG residues) model systems to their potential energy minima in less than an hour on a single node. At this point we have found parameters that result in consistent folding to helices and beta sheets in 1-1 models. We have also converged on various 2-1, 3-1, 1-2 and 1-3 minimum energy structures, with less obvious secondary structure for the initial parameters tested.

We have also built the infrastructure for molecular dynamics and property reweighting of protein ensembles using OpenMM. Using the OpenMM simulation API approach allows us substantial flexibility to define both building block geometry and arbitrary functional form energy functions, including CG models required to test the hypotheses of interest. We have implemented temperature replica exchange in order to effectively sample the folding transitions of small oligomers. The current models allow us to build equivalent N-M models as in Rosetta, with specified bonded and nonbonded force parameters, along with the infrastructure to carry our reweighting to predict properties at new other parameters sets. The infrastructure has been benchmarked for timing on XSEDE for a request in the next cycle.

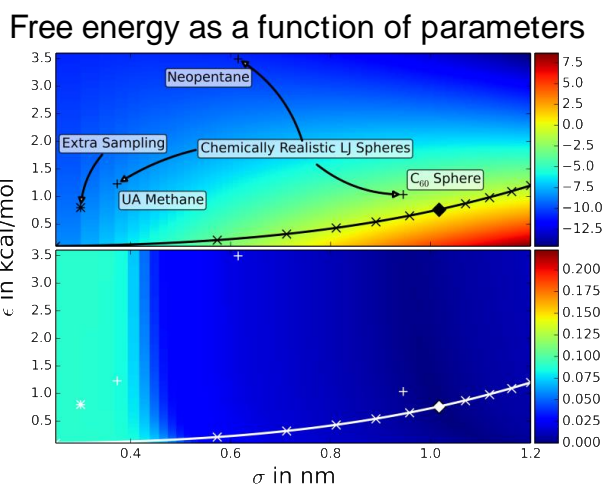


Figure 2: Example of reweighting techniques developed in the Shirts lab to allow physical properties to be extrapolated in parameters space (above) with uncertainties (below). Figure shows estimated solvation energies predicted over a larger range of Lennard-Jones σ , ϵ using data from only 12 equilibrium simulations.

Future Plans

In the near future (in 2019), we will publish our work on coarse-grained modeling in the Rosetta framework, demonstrating the capability to fold CG models of varying complexity, and showing how perform parameter scans identifying various types of minimum energy folded structures as a function of model parameter. Although the initial implementation uses the Rosetta wrapper PyRosetta, we actively working with Rosetta developers (one week hackathon carried out with them in July) to have some of this functionality implemented natively in the C++ source code of Rosetta and in a public release of the software. Also in 2019, we will also publish our implementation of the molecular simulation sampling infrastructure in the generalizable OpenMM infrastructure and demonstrate how reweighting allows rapid parameter searching and optimization using target thermodynamic observables.

With these completed tools, we will carry the core of our research, tests to examine a range of physical questions about individual foldamers as well as parameter sensitivity analysis of the

proposed foldamer models, with initial focus on simpler CG model geometries to form a baseline for phase diagrams of more complex monomers. These questions include:

- How does chain stiffness affect the stability and cooperativity of secondary structure elements?
- To what extent can excluded volume interactions stabilize folded structures? Do such folding structures have different energetic characteristics than ones stabilized by energetic interactions?
- How does the length and flexibility of side chains affect stability and cooperativity of foldamers?
- How important are anisotropic interactions in the stability and cooperativity of secondary structure?
- How do changes in effective solvation modulate the folding ability?

After examining these questions to the extent possible using simpler intermolecular energy functions, we will add more complicated energy models, including an embedded atom model for solvation, anisotropic interaction potentials, effective entropy terms and increasingly diverse side-chain geometries and heterogeneities. With experimental collaborators in the Kaar group at CU Boulder we will also select canonical and noncanonical peptide sequences to test the hypotheses developed in the initial stages of research, using CD, FTIR, scans of temperature and solvents, and in some cases determining secondary structure contacts using NMR for identification of structural ensembles.

Switchable functional materials operating must have alternate configurational ensembles that are metastable and requiring only small environmental perturbations to change their relative stability. We will therefore also investigate the utility of different foldamer architectures and classes, with different determinants of stability, as potential responsive materials. After identifying patterns in metastability in model foldamers, we will test how these patterns change in response to a range of methods of perturbation of the environment.

Overall, this plan will allow us to develop basic theories of how nonbiological heteropolymers assemble locally into three-dimensional structures and to generate and test specific design principles for molecular materials built from such oligomers. A complete elucidation of the principles involved in heteropolymer folding, especially routine design of foldamers from first principles, is larger than any three-year effort. The work described here will allow us to develop basic theories of how nonbiological heteropolymers assemble locally into three-dimensional structures and to generate and test specific design principles for molecular materials built from such oligomers.

Publications

No published papers in first year.

Bio-inspired Polymer Membranes for Resilience of Electrochemical Energy Devices

Meredith N. Silberstein, Sibley School of Mechanical and Aerospace Engineering, Cornell University

Program Scope

Like biological cell membranes, polymer membranes for electrochemical energy storage and conversion devices must control ion transport and be mechanically robust. Biological membranes are constantly assessing evolving “operating” conditions such as electric field and optimizing their function by dynamically adjusting their material state; the current generation of synthetic polymer membranes are static. *Synthetic membrane performance and durability can be dramatically improved by imbuing the membrane with the ability to sense and adapt to the local electrochemical environment.* One key enabler of biological self-regulation is ionic interactions. We are applying this biological concept to modulating ionic crosslinking within synthetic polymers, considering two classes of approaches – (1) polymers with dual charged sidechains that ionically bond directly with each other; (2) polymers with like-charged sidechains that ionically bond through either multivalent ions or nanoparticles of the opposite charge.

The scope of this program is to discover the fundamental physical mechanisms for self-regulation of polymers and gels under electric fields by focusing on the following three aspects: (I) The influence of an external electric field on the strength of ionic bonds between polymer chains and how this interaction depends on concentration of ionic bonds, any solvent, free ions, polymer backbone rigidity, chemical details of the polymer; (II) How ionic bond strength and concentration among linear polymer chains influences polymer mechanical properties and self-healing for different polymer backbone rigidities and chain lengths; (III) Complete mechanical property dependence on electric fields by adding to I and II, key coupled aspects such as polymer reconfiguration guided by locally high electric field gradient. We are approaching this unexplored concept computationally, utilizing molecular dynamics (MD) simulations and constitutive modeling and validating our findings using synthesis, solution-based experiments, spectroscopy, and mechanical testing.

Recent Progress

Over the first year of this grant, progress has been made on the concept of polymer networks formed from combining two sets of polymer chains with matched charge of opposite sign (Figure 1). This

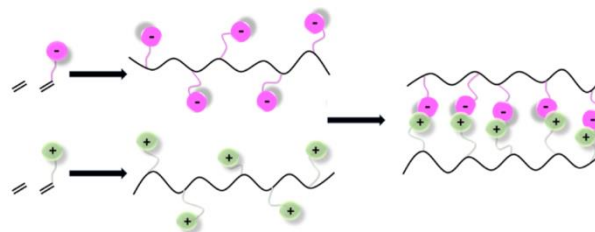


Figure 1. Schematic of ionically interacting polymer composed of oppositely charged chains.

progress has been both in synthesis/experimental characterization and molecular dynamics simulations.

We performed synthesis of an initial pair of ionic polymers. The ionic polymers were synthesized by radical co-polymerization of 2-Hydroxyethyl acrylate with either an anionic monomer (potassium sulfopropyl-acrylate) or a cationic monomer (ethyl-trimethylammonium chloride acrylate) with 4,4'-Azobis(4-cyanovaleric acid) as the radical initiator in water (Figure 2). Each polymer was tagged with a distinct dye functionality so that their separation could be readily visualized. The polymers were purified in dialysis bags to remove low molecular weight impurities (monomers and oligomers). The fractions of functional monomers were determined by comparing the integration values for each of the methylene protons in the $^1\text{H-NMR}$ spectrum of the polymer. The main challenge in synthesizing these polymers is that ionic monomers are not soluble in organic solvents. Since the polymerization needs to be performed in water, a water-soluble neutral monomer is needed, thereby limiting monomer choice and ability to fine tune the mechanical properties with that choice.

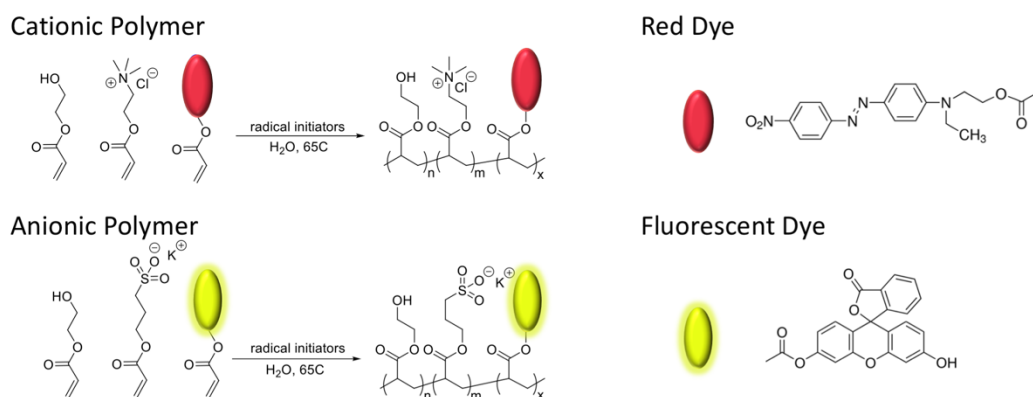


Figure 2. Synthetic scheme for cationic and anionic polymers with acrylic dye functionalities.

Preliminary experimental characterization was conducted on the gelation of the two oppositely charged polymers when mixed and on electric field driven separation of the combined gel network into the separate polymers. When a current is applied across the gel via immersion of oppositely charged electrodes, there is a visually apparent separation of two polymers. When instead, an electric field is applied across the gel by non-immersed parallel plates, there is no visually apparent separation.

In terms of molecular dynamics, we have established both coarse grained (CG) and fully atomistic (FA) simulations. The purpose of the CG simulation is to enable rapid exploration of the parameter space. The purpose of the FA simulation is (1) to verify that the CG results are reasonable and (2) to allow direct comparison with our future experimental results. A python script was implemented to create initial configurations for the CG model. The chain generation step uses a random walk to build a polymer of desired degree of polymerization and number of

chains with set percentage of the beads in each chain assigned charged. For the simulations to date we have created a model of twenty chains, degree of polymerization of 100, with 10% charged beads (+/- 1), in which half the chains are cationic and the other half are anionic. The bonded potential is represented by a harmonic bond stretching potential. All beads interact according to a 12-6 Lennard Jones potential and a Coulombic potential. The initial configuration was equilibrated into a representative polymer using five different steps similar to those used in many polymer MD simulations, with an electric field applied in the final step. For the FA model, a model building tool called Amorphous Cell from BIOVIA Materials Studio was used to build the ionic polymer shown in Figure 1. The chemical structure of this polymer matches that of our first synthetic polymer described above. Within Amorphous Cell, the Theodorou and Suter method was used to build the polymer, and the Gasteiger method was used for computing charges. For the simulations to date we have created a model of twenty chains and one hundred repeating units in each chain. Similar to the CG model, half of the chains are anionic, and the other half are cationic, with ten percent of the repeat units in each type of chain possessing charge. Parameters from CVFF forcefield were used to compute local interactions between atoms [1]. The initial configuration was equilibrated similarly to the procedure for the CG simulations.

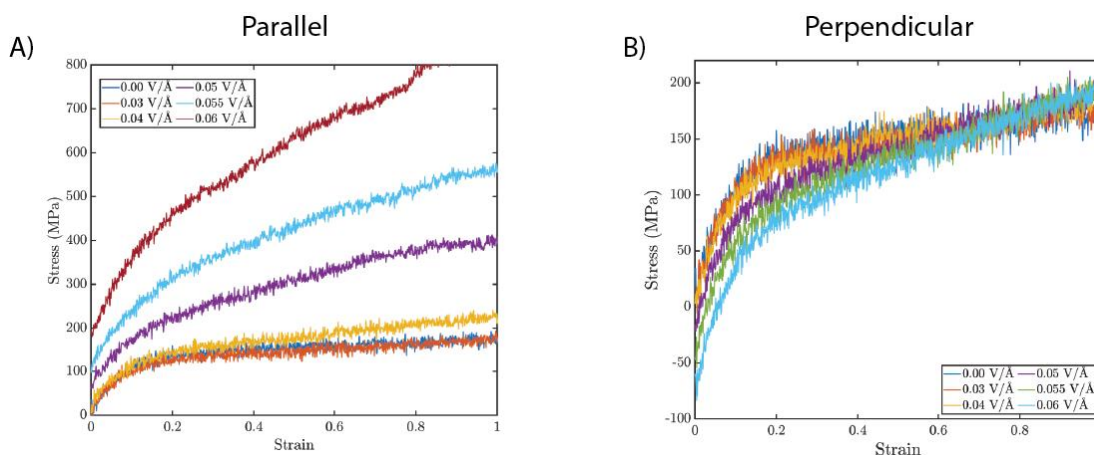


Figure 3. Stress-strain results from preliminary coarse-grained molecular dynamics simulations of an ionically functionalized polymer assembly under electric field: (A) field parallel to the pulling direction. (B) field perpendicular to the pulling direction.

Preliminary deformation simulations have been run with each of these equilibrated models at 100 K. The CG models exhibit an essentially bilinear behavior with a gradual transition between the two linear regions (Figure 3). With the application of a field parallel to the pulling direction, the elastic slope increases slightly with increasing field strength and the yield stress and post-yield hardening increase significantly with increasing field strength. Opposite trends are seen for a perpendicular field. Changes in the stress-strain response are apparent starting at a field strength of 4×10^8 V/m, we expect this required value will reduce significantly in the rubbery state. Further, under reasonable equilibrations times, the systems under high

electric field are not able to rearrange to a zero-stress configuration. Most likely this is an artifact of the short simulation times. In the future, we will modify our equilibration with electric field step to occur at higher temperatures. The fully atomistic models exhibit minimal changes with applied electric field prior to failure for both perpendicular and parallel field directions (not shown), but to date, only field strengths of up to 3×10^8 V/m were applied.

Future Plans

Experimentally, we will perform extensive characterization on the recently synthesized pair of ionically charged polymers. A series of separation experiments will be conducted in the gel state both under applied current and applied electric field. Rheological and chemical characterization will be conducted on the initial separate polymers, the combined gel, and the separated products. We will also perform uniaxial mechanical testing on the combined gel with an electric field applied across the specimen, perpendicular to the direction of applied tension.

In terms of MD simulations, we will be focusing on the CG model. We will modify the equilibration procedure so that the electric field is applied at elevated temperature so that an equilibrium state can be achieved. We will then run deformation simulations above and below the glass transition temperature and at different electric field strengths. We will focus on two key parameters: the charge on the ionic beads and the fraction of ionic beads. Another key aspect over the next year will be to improve our analysis codes for these simulations. For example, we will extract an evolving count of ionic pairs that are acting as crosslinks and their associated current bond distance.

Finally, we will work on establishing a continuum modeling framework and implementing it within a finite element software. This first round of the framework will focus on capturing behavior with no free particle transport – this correlates with our initial synthetic system. We will augment a previously implemented crosslinked elastomer constitutive model with crosslink strength parameters that depend on the electric field strength. Relations for bond weakening and bond reforming will be extracted from the CG MD simulations as well as physics-based relations.

References

[1] Dauber-Osguthorpe et. al., *Proteins: Structure, Function, and Bioinformatics*, 1988: 4(1), 31-47

Publications

None

Synthesis of Novel Hybrid Nanostructures Employing Advanced Structural Characterization Techniques

Sunil K Sinha, Dept. of Physics, UC San Diego (P.I.)

Atul N. Parikh, Materials Science & Engineering and Biomedical Engineering,

UC Davis (Subcontract)

Program Scope

Hybrid nanostructures composed of nanoparticles integrated with organic and polymeric host templates can give rise to novel functional materials depending on the types of nanoparticles and how they are geometrically embedded in the templates. These new composite materials have potential applications for energy harvesting, sensing, advanced optical devices, sensors, displays, and magneto-optic devices, to name a few. We are studying the self-assembly of such hierarchical hybrid nanostructures consisting of nanoparticles of Au (and in the future, of Ag, Fe₃O₄, or TiO₂) interacting with the host multilamellar films of amphiphilic lipids, surfactants, and triblock copolymers in geometrically defined and spatially compartmentalized manners. In our first system, the nanoparticles are functionalized with surfactants (or ligands) in order to geometrically localize their distributions within the host templates. We are studying the systematics (structure and dynamics) of their cooperative self-assembly as a function of several variables such as nanoparticle size, charge, functionality and host template parameters and we plan to monitor the self-assembly with multiple characterization techniques using X-Rays and neutrons and various imaging techniques. In particular, we plan to study the assembly of 1D, 2D, and possibly 3D ordered nanocrystal arrays and their properties as tunable photonic crystals.

We will also explore how elastically, optically, and electrically powered non-random dynamics of nanoparticles within the interlamellar confinement of smectically-ordered, amphiphilic mesophases generate cooperative dynamics of the composite matter. Addressing this basic goal should produce a novel class of structured liquids, which are hierarchically ordered, dynamically assembled, and actively propelled to produce far-from-equilibrium (as well as active) order and organization. Such structured liquids, we envisage, will provide fundamental design principles for dynamic control of structure and organization – a major challenge at the frontier of matter and energy, a transformative opportunity identified by the BESAC Report dated Nov. 2015.

Recent Progress

Previously, we have shown a counter-intuitive phenomenon of stacking of domains in multi-component, multilamellar lyotropic phases of *equilibrated* phases (so-called liquid-ordered (L_o) and liquid-disordered (L_d) phases) of stacked lipid bilayers with intercalated water channels between the constituent units, i.e., amphiphilic bilayers ((Tayebi, et al. Nat. Mater. 2012) [1]. Here, the origin of the one-dimensional positional order is purely entropic. Thermally excited out-of-plane fluctuations – suppressed by the spatial confinement within the stacked multilayer due to

neighboring bilayers – produce interlamellar repulsive interactions stabilizing the long-range smectic order. During the current funding period, we have shown that compositionally differentiated domains of differing elastic and hydration properties in turn are hierarchically composed of multilamellar subdomains which furthermore exhibit a hierarchical columnar lateral structure, organized in distorted face centered square 2D lattices. (see Fig. 1). We are currently exploring how the introduction of cholesterol-functionalized Au nanoparticles with diameters roughly equal to the bilayer thickness into the bilayer regions provides a way to modulate these entropic forces and generate organized phases through non-specific interactions between the membranes and the colloidal nanoparticles. We have demonstrated with X-ray

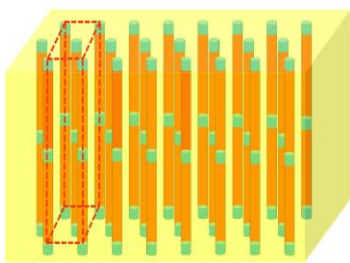


Fig. 1: Schematic shows the face centered oblique structure of crystalline sub-domains of the L_o phase consisting primarily of DPPC & Cholesterol. The lipid bilayers of the L_o phase are indicated in orange, and the inter-bilayer water layers are indicated in blue. The unit cell of the ordered sub-domains with twice the bilayer periodicity along the z-axis is denoted by the red dashed lines. The surrounding L_d phase is indicated in yellow and its bilayer periodicity is not shown in the figure for reasons of clarity.

reflectivity and with X-ray Small Angle Scattering (SAXS) measurements that these nanoparticles intercalate within the bilayers of the multilamellar structure and incorporate into the laterally ordered columnar hexagonal subdomains of the phase-separated multicomponent systems. (Fig. 2).

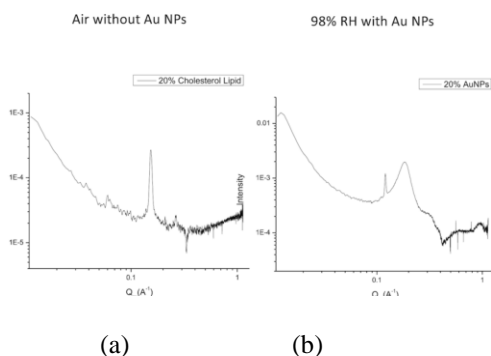


Fig. 2: SAXS data taken on phase separated mixed lipid multilayers. Peak in (a) is due to in-plane ordering of L_o domains. (b) SAXS data taken after 20% by volume of functionalized Au NPs inserted in above system showing considerable intensity enhancement of domain-ordering peak (note change in vertical scale) plus intense broad peak due to short-range ordering of Au NPs.

In order to study how nanocomposites form, it is important to understand the dynamics of nanoparticles inserted into our lipid or polymeric multilamellar phases. We have been studying

this with the technique of X-ray Photon Correlation Spectroscopy (XPCS). We have introduced cholesterol-functionalized Au nanoparticles into a single-component multilamellar lipid system and studied the 2-dimensional lateral diffusion of the Au nanoparticles within the bilayer using XPCS. This diffusion turns out to be relatively fast and ballistic, as opposed to Brownian, diffusion. We have carried out similar studies of the diffusion of Au nanoparticles of various diameters functionalized with polystyrene ligand chains dispersed in bulk polystyrene matrices of various molecular weights, and shown that for host PS matrices of higher molecular weight, the diffusion is both ballistic and one-dimensional, which can be qualitatively explained as due to avalanche-like releases of strain energy from polymer chains of the host matrix aligned by the anisotropic motion of the nanoparticles in a thermal gradient during the annealing process. A detailed theoretical explanation for this type of dynamics does not exist, but we have shown that molecular dynamics simulations reproduce our results very well. [2]

Structural Color: In collaboration with Prof. Dhinojwala's group at U. Akron, we have been utilizing high-resolution SAXS and SANS techniques to investigate the structure factor of melanin nanoparticles and melanin/silica nanoparticle (diameters ~ 120 nm) mixtures assembled hierarchically into supraball spherical structures in order to be able to calculate quantitatively the Mie scattering of light from these objects which give them various colors, depending on the arrangement of the nanoparticles [3].

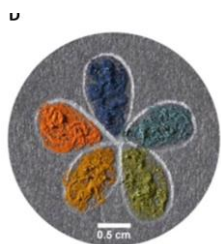


Fig.3: An image of rainbow-like flower, painted with supraball inks made of five different sizes of mixed NPs: navy blue (126/36 nm), blue-green (124/43 nm), olive (160/36 nm), orange (160/50 nm) and red (160/66 nm)

Future Plans

Our observations of the incorporation of cholesterol-derivatized nanoparticles and their ballistic mobilities within the host lamellae raises a number of fundamental questions, e.g. how does the placement of nanoparticles, significantly larger than the width of the aqueous channels separating neighboring lamellae, alter the smectic order? Do they pave the way for stabilization of hyperswollen lamellae? Can the swelling be extended to optical lengthscales such as needed for generating photonic effects? Do the nanoparticles distribute uniformly within single lamellae? and by analogy to our earlier findings (Tayebi et al., Nat. Mater. 2012), can nanoparticles be arrayed in 3D across multiple lamellae of the multilamellar hosts? Our observations of super-diffusive nanoparticle mobilities within the multilamellar host raises intriguing questions regarding the possibility that they exert an “osmotic pressure” on the host thereby providing mechanisms for producing hyperswollen states. We plan to pursue these questions in parallel

during the next phase of the current funding period. Moving forward, the recent involvement of our partner laboratory at UC Davis (Parikh lab) will further allow us to both introduce chemical complexities in our host configurations (e.g. using long chain amphiphilic diblock copolymers as the host matrix, and complement our x-ray and neutron based characterization with larger length scale, optical and fluorescence microscopy based characterization in time-resolved manner.

Additionally, we plan to extend our activities to include multilamellar cylindrical hosts, also referred to as myelin figures, to design hybrid nanostructures. First reported by Virchow more than 150 years ago, myelin figures form spontaneously during the hydration of a dry, concentrated mass of amphiphiles above their gel-fluid transition temperatures. Appearing at the lipid-water boundary, myelin figures are tens of micrometers wide and extend in lengths of tens to hundreds of micrometers. They represent a class of lyotropic smectic mesophases consisting of hundreds of cylindrically stacked lipid bilayers wrapping the central aqueous core. Their 1D smectic order is stabilized by the inter-membrane repulsive interactions inhibiting molecular exchange between the layers and the fluid character of the amphiphilic bilayers allow for in-plane 2D lateral diffusion in cylindrical coordinates. In preliminary recent work, we have discovered that myelin figures produced by mixtures of phase-separating lipids (e.g., cholesterol, sphingomyelin, and phospholipid) develop a striking compositional gradient in which cholesterol and sphingomyelin concentration decays continuously from the outermost to the innermost lamellae comprising myelin figures (Fig. 4).

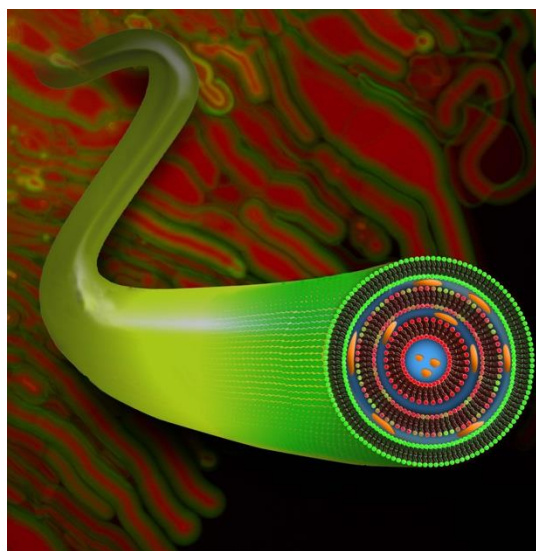


Fig. 4: Epifluorescence image of a dense array of cylindrical multilamellae formed during the hydration of a dry, concentrated lipid mass consisting of of equimolar concentration of POPC, sphingomyelin, and cholesterol. NBD-PE (1 mol %, green) labels the cholesterol-rich membrane phase and Rhodamine-PE (1 mol%, red) dopes the fluid POPC.

Based on our findings that the cholesterol-derivatized nanoparticles readily embed in lipid multilayers, we now plan to explore if the spontaneous generation of the cholesterol concentration gradient can be translated into a corresponding gradient of nanoparticle occupancy in cylindrical lipid multilamellae. As above, we plan to develop these novel hybrids and characterize them using the full

suite of x-ray, neutron, optical, fluorescence, and electron microscopies.

References

- [1] Tayebi, L. et al., *Nature Materials* **11**, 1074-1080 (2012)
- [2] Jing-Jin Song et al., *Phys. Rev. Lett.* **122**, 107802 (2019)
- [3] Xiao, M., et al., *Sci. Adv.* **3** :e1701151. (2017)

Publications

[1] Song, Jing-Jin; Bhattacharya, Rupak; Kim, Hyunki; et al., “One-Dimensional Anomalous Diffusion of Gold Nanoparticles in a Polymer Melt”, *Phys. Rev. Lett.* **122**, 107802 (2019)

[2] Bhattacharya, Ahanjit; Brea, Roberto J.; Song, Jing-Jin; et al., “Single-Chain beta-D-Glycopyranosylamides of Unsaturated Fatty Acids: Self-Assembly Properties and Applications to Artificial Cell Development”, *J. Phys. Chem. B* **123**, 3711-3720 (2019)

[3] Bhattacharya, Ahanjit, Brea Roberto J.; Niederholtmeyer, Henrike; et al., “A minimal biochemical route towards de novo formation of synthetic phospholipid membranes”,
Nature Communications **10**, 300 (2019)

[4] Brea, Roberto J.; Bhattacharya, Ahanjit; Bhattacharya, Rupak; et al.,” Highly Stable Artificial Cells from Galactopyranose-Derived Single-Chain Amphiphiles”, *J. Am. Chem. Soc.* **140**, 17356-17360 (2018)

Self-assembly, crystal quality, and the biomimetic reconfiguration of colloidal structure

Michael J. Solomon and Sharon C. Glotzer, University of Michigan Ann Arbor

Program Scope

The purpose of this project is to establish fundamental relationships that connect the properties of building blocks used in the self-assembly of colloidal crystals; the quality of the resulting self-assembled crystals; and, the intensity of structural color. The use of colloids, self-assembly, and structural color serves as a specific platform to address fundamental questions about the inverse design of materials, when the targeted material property is sensitive to the quality of self-assembly. The project draws its rationale from the observation that proteinaceous building blocks in a number of living organisms, including cephalopods, self-organize at the colloidal scale so as to generate coloration that is brilliant, reconfigurable, and resilient. This intense coloration is remarkable because it arises from structures that histology shows to be quite defect rich. The objectives of our work are to: (1) quantify the abundance and type of local defect structures as well as the extent of long-range ordering, as quantified by global order parameters, in self-assembled colloidal crystals, so as to understand how these two measures of crystal quality combine to determine the brilliance of structural color; (2) change the shape and interactions of the building blocks to understand how anisotropic colloidal properties affect the quality of crystals that can be self-assembled from them; and, (3) incorporate reconfigurability into the self-assembly process to probe how kinetic pathways such as time-dependent cycling

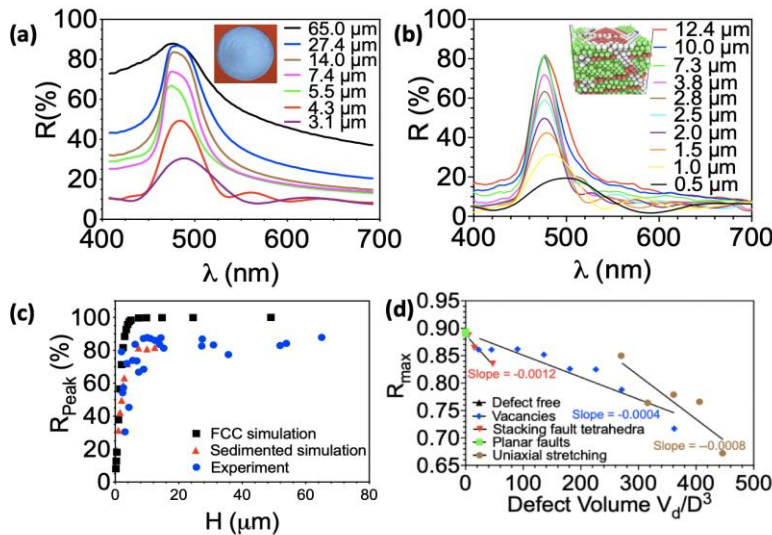


Figure 1. (a) Experimentally measured and (b) simulated reflection spectra of colloidal crystal films of different thickness; (c) relationship between peak reflection and film thickness for experimental, simulated and fcc theoretic assembly; (d) Peak reflectance as a function of defect volume added to the system for different defect types. (Results by Tianyu Liu and Bryan VanSaders)

affect crystal quality and structural color brilliance.

Recent Progress

In the recent period, we have: (i) identified the relationship between structural color intensity and crystal quality described through thickness and defect microstructures (objective 1); (ii) reported the effect of colloidal shape anisotropy on kinetics of reconfigurable assembly (objective 2); (iii) deployed time-dependent cycling (annealing) of alternating current (AC) electric fields to study the effect of kinetic pathways on

crystal quality and light diffraction (objective 3).

Relationship between crystal quality and brilliance of structural color. Fig. 1 reports the relationship between the intensity of structural color in colloidal assemblies and their microstructural properties. The peak in reflection spectra of assemblies of microspheres of different film thickness self-assembled by solvent evaporation is reported in Fig. 1a. Comparative structures resulting from simulations of sedimentation driven crystal growth, as performed using HOOMD-blue [1], are reported in Fig. 1b inset. Finite-difference time-domain calculations of the reflection spectra of these simulated structures are also reported in Fig. 1b. Experimentally, we find that the maximum structural color reflection increases linearly as a function of the crystal thickness; it ultimately reaches a saturation of 87% for colloidal crystals of thickness greater than about 8 μm (Fig. 1c). The wavelength of structural color response follows a consistent trend, saturating at a particular wavelength for crystals thicker than 8 μm . The saturation in reflectance as stack thickness is increased to be due to diffraction that progressively increases layer by layer. The reflectance achieves a plateau at a value less than the theoretical value of 100% for the perfect fcc crystal due to polydispersity in stacking as well as crystal distortions caused by the presence of defects such as vacancies, stacking faults,

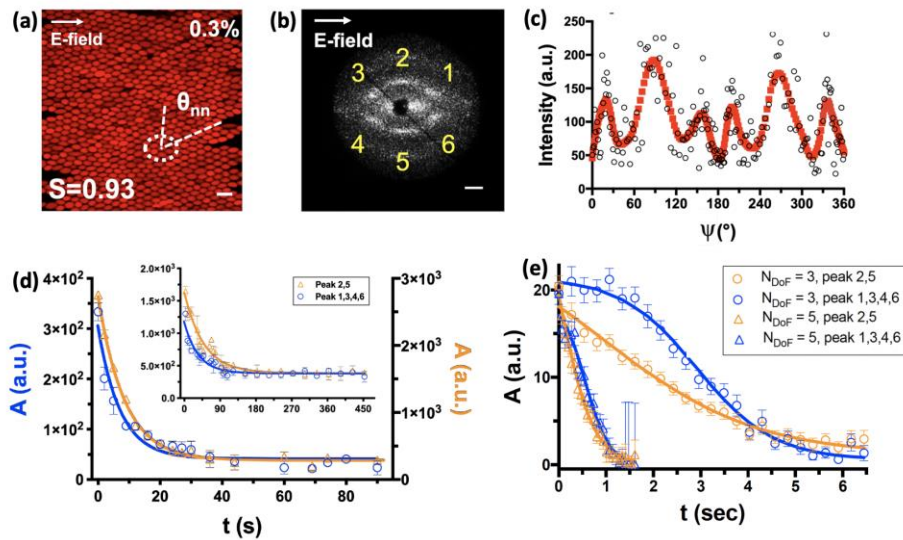


Figure 2. CLSM micrograph (a), SALS image (b) and diffraction peak intensity along azimuthal angle (c) of AC field assisted 2D ellipsoid assembly; (d) measured time evolution of diffraction peak area during melting for ellipsoids and spheres (inset); (e) simulated time evolution of diffraction peak area for ellipsoids with ($N_{\text{DOF}} = 5$) and without ($N_{\text{DOF}} = 3$) rotational degree of freedom during melting. (Results by Peng-Kai Kao and Bryan VanSaders.)

dislocations and grain boundaries. Simulations of such defect structures show that the reduction in peak reflection intensity scales with increased defect volume (Fig. 1d); clusters of vacancies have a particularly strong effect. Defects that do not significantly decrease crystal density – such as planar stacking faults – have much

more modest impact on the structural color reflection. The measurements here are directly connected to color quality, as applied for example in the use of chroma diagrams. This study therefore provides fundamental insight into optical quality in ways that can be applied to the design of optical materials with specified reflection and chroma. It in particular provides constraints on the performance of any self-assembly method used to generate a reflective film.

Effect of shape anisotropy on reconfigurable assembly kinetics. We use AC electric field assisted self-assembly to produce two-dimensional arrays of ellipsoidal colloids (Fig. 2a) and find that the ellipsoids of aspect ratio 2.0 exhibit striking differences in their assembly kinetics when compared to spheres. The simple geometry of ellipsoidal building blocks offers an ideal platform to study the role of shape anisotropy in self-assembly kinetics. Self-assembly kinetics set the time scales upon which self-assembly kinetics can reconfigure their form and function. Confocal laser scanning microscopy (CLSM) imaging and angularly-dependent diffraction peak intensities with small-angle light scattering (SALS) are reported in Fig. 2 a,b,c. These measurements identify local and ensemble-averaged global crystal quality, respectively. Field conditions were optimized to generate high quality crystals for kinetic studies. By comparing the time evolution of the area under the diffraction peaks for spheres and ellipsoids during melting (Fig. 2c), differences in assembly kinetics as a function of shape anisotropy are revealed. Modeling the data using a growth equation indicates that the ellipsoids melt into disordered structures 5.7 times faster than spheres (Fig. 2c). On the other hand, no differences in the self-assembly kinetics of crystallization were observed. The anisotropy effects on melting, but not crystallization, are unexpected; the mechanistic origin of the difference was explored. Computer simulation of the crystallization kinetics using HOOMD-blue [1] shows that the difference in melting kinetics for spheres and ellipsoids is due to the rotational degrees of freedom present in the ellipsoids system but not in the sphere system. This difference was identified by noting that ellipsoids in which rotational degrees of were blocked had a reduced rate of change in the peak area during melting (Fig. 2e); the kinetics in this case were similar to that of spheres. Studies have shown that shape anisotropy can create dense structures with complex symmetries [2–4] and our current study contributes to the understanding of how the kinetics of orientational and positional ordering can analogously be manipulated by changing the particle’s shape anisotropy.

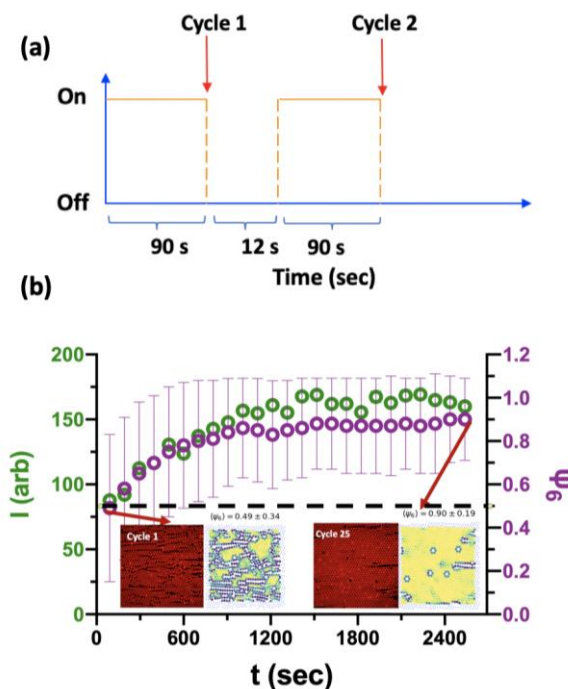


Figure 3. (a) AC field on-off cycle pattern; (b) Time evolution of SALS average peak intensity and the $\langle \Psi_6 \rangle$. The dashed black line is the corresponding values for particles assembling under a constantly ON field. (Results by Peng-Kai Kao and Bryan VanSaders.)

Manipulation of assembly defect structures. The above studies describe the effect of shape anisotropy and assembly microstructure on measures of crystal quality. We are currently studying how modulating the time dependence of applied electric field can contribute to the annealing of crystal microstructure. The hypothesis is that field and shape can be synergistically

deployed to improve crystal quality in ways that can directly improve functional properties such as structural color and light diffraction. As a first step in this direction, we self-assemble particles using an AC electric field that is switched on and off (Fig. 3a) in a systemic fashion. Modulating the switching time results in a steady increase in crystal quality, which is quantified by means of the measured $\langle\Psi_6\rangle$ parameter from CLSM images and average SALS peak intensity (Fig. 3b). In comparison, particles assembling under a constantly applied AC field achieve a significantly lower crystal quality (Fig. 3b).

Future Plans

Our future plans will take us in three new directions. First, we will continue to understand the role of defects on structural color reflection by incorporating controlled levels of impurities into the self-assembled crystals. These impurities can interact with the base crystal structure in self-correlated ways which we will study with a combination of local microstructure measurement, computer simulation, and optical property measurement. Second, we will extend our work to directly measure structural color of colloidal crystals self-assembled from anisotropic building blocks, so as to understand how measures of orientational crystal quality impact the magnitude of structural color reflection. Third, we will pursue self-assembly measurements with discoid colloids, to explore the possibility of self-assembling complex motifs with this building block.

References

1. Anderson JA, Glotzer SC (2013) The development and expansion of HOOMD-blue through six years of GPU proliferation. *arXiv preprint arXiv:1308.5587*,
2. Glotzer SC, Solomon MJ (2007) Anisotropy of building blocks and their assembly into complex structures. *Nature materials*, 6(8):557–562. <https://doi.org/10.1038/nmat1949>
3. Ganesan M, Solomon MJ (2017) High-density equilibrium phases of colloidal ellipsoids by application of optically enhanced, direct current electric fields. *Soft Matter*, 13(20):3768–3776.
4. Shah AA, Kang H, Kohlstedt KL, Ahn KH, Glotzer SC, Monroe CW, Solomon MJ (2012) Liquid crystal order in colloidal suspensions of spheroidal particles by direct current electric field assembly. *Small*, 8(10):1551–1562. <https://doi.org/10.1002/sml.201102265>
5. Tianyu Liu, Peng-Kai Kao, Bryan Vanders and Mahesh Ganesan contributed to the authorship of this extended abstract.

Publications supported by BES in last two years

1. Kao, P.K., VanSaders, B.J., Durkin, M.D., Glotzer, S.C. and Solomon, M.J. “Reconfigurable light diffraction of colloidal ellipsoids by electric field assisted self-assembly” under review (2019).
2. Solomon, M. J. “Tools and Functions of Reconfigurable Colloidal Assembly” *Langmuir* 34 11205-11219 (2018).
3. Ganesan, M. and Solomon, M. J. “High-Density Equilibrium Phases of Colloidal Ellipsoids by Application of Optically Enhanced, Direct Current Electric Fields” *Soft Matter* 6 (2017): 557.
4. Silvera Batista, C. A., Rezvantlab, H., Larson, R. G., and Solomon, M. J. “Controlled Levitation of Colloids through Direct Current Electric Fields” *Langmuir* (2017): doi:10.1021/acs.langmuir.7b00835.

Materials Exhibiting Biomimetic Carbon Fixation and Self Repair: Theory and Experiment

Michael S. Strano, Carbon P. Dubbs Professor of Chemical Engineering

Department of Chemical Engineering, Massachusetts Institute of Technology
77 Massachusetts Avenue, Cambridge, MA 02139-4307

Program Scope

Our laboratory at MIT has been interested in learning from the mechanisms of self-assembly and self-repair displayed particularly in living plant systems to create human-synthesized analogs that benefit from these higher functions operating under non-biological conditions. Here, we highlight our recent efforts in engineering biomimetic systems that exploit ambient solar energy harvesting and carbon dioxide conversion to create a new class of regenerative, densifying materials – a class that literally grow in CO₂ and sunlight. This proposed class of materials point to several fundamental questions relating to carbon fixation and its incorporation into functional materials. By performing these reactions compartmentally, we assert that it is possible to create materials that grow and self-repair using carbon dioxide as a carbon source. Such materials would significantly benefit transportation and construct costs, as well as exhibit self-healing and densification over time. We have made significant progress to date on two systems:

System I: Materials with embedded, functional plant chloroplasts as photocatalysts for glucose to monomer to polymer matrix production from ambient solar energy and CO₂

In this system, we establish the prospective application of chloroplasts as photocatalysts, which only rely on atmospheric carbon dioxide and ambient solar energy to produce high-energy molecules consisting of carbon, oxygen and hydrogen, needed to build self-growing materials as a proof-of-concept. This approach involves the extraction of functional plant chloroplasts from biomass and using them as embedded, functional photocatalysts for the production of glucose and starches from ambient solar energy and atmospheric carbon dioxide. Glucose can be converted to gluconolactone by glucose oxidase, which can then readily react with nucleophiles, such as the primary amine group (-NH₂) to generate a growing polymer matrix.

System II: Self assembled semiconducting photocatalysts (replacing the chloroplasts) for the direct CO₂ reduction to formaldehyde and then to stable polyoxymethylene

As a next generation material system, we replace the function of the chloroplast with a semiconducting photocatalyst. Coupling the photocatalytic compartment with the secondary polymerization compartment can extend the life time of the system, avoiding concerns such as chloroplast short life span. This system includes two catalytic units for (i) photocatalytic conversion of atmospheric CO₂ to formaldehyde and (ii) polymerization of formaldehyde into a polyoxymethylene (POM). Devising a thermodynamically feasible pathway from CO₂ to POM and assessing the kinetics of the overall pathway is our first step toward realizing this novel class of the materials. In addition, synthetic efforts going forward will examine hierarchical integration and self-healing of both systems, coupled to a theoretical framework within which we explore the design and function of these fundamentally new types of materials.

Recent Progress

System I:

Among the three major sugars exported from chloroplasts (glucose, maltose, and triose phosphate), glucose is often used for glycopolymer synthesis since it is easily converted to gluconolactone by glucose oxidase. We demonstrate that these sugars can form hydrogels, which are lightly cross-linked polymer networks that self-assemble, swell in water and show a self-healing ability. Several strategies are systemically investigated to improve glucose export from the isolated chloroplasts. The exported glucose is converted by glucose oxidase to gluconolactone (GL), which subsequently reacts to primary amine-functionalized acrylamide monomers, 3-aminopropyl methacrylamide (MAA), to form a polymer matrix. This synthetic pathway thus utilizes isolated chloroplasts as functional photocatalysts for the formation of self-growing materials from glucose (**Figure 1A and 1B**).

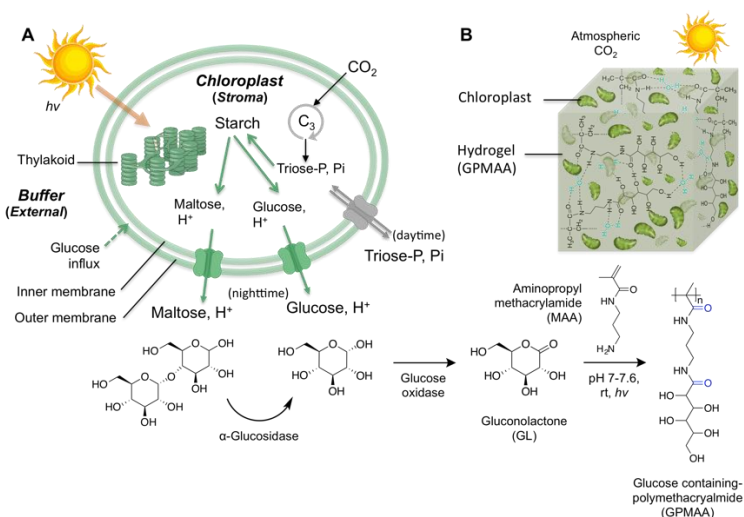


Figure 1. A schematic illustration of a synthetic material that grows, densifies and self-repairs with embedded plant chloroplasts. (A) Chloroplasts transform solar energy and carbon dioxide into the chemical energy and export the newly fixed carbon in form of triose phosphate during the day. Exported glucose and glucose from enzymatic hydrolysis of maltose are converted to gluconolactone (GL) by glucose oxidase, subsequently react to primary amine functionalized methacrylamide (MAA) and polymerize to glucose-containing polymethacrylamide (GPMAA) in the medium. **(B)** GPMAA forms hydrogel as lightly cross-linked by hydrogen bonding in water. The hydrogel continuously grows, densifies and self-repairs as long as chloroplasts carry out carbon fixation and export glucose.

We have investigated the importance of inorganic phosphate (Pi) concentration, glucose equilibrium across the chloroplast membrane, and the concentration of photo-generated reactive oxygen species (ROS) towards glucose export efficiency. We have enhanced glucose export from the isolated chloroplasts to gain quantifiable molecules for building of a self-growing material. In the presence of light and exposure to atmospheric carbon dioxide for 18 hours at room temperature, the formation of hydrogel-like material was observed around the chloroplast membrane as confirmed by Raman spectroscopy 3D mapping (**Figure 2**). This system achieves an average growth rate of 60 $\mu\text{m}^3 \text{h}^{-1}$ per chloroplast under ambient CO₂ and illumination over 18 h, thickening with a shear modulus of 3 kPa. This material can demonstrate self-repair using the exported glucose from chloroplasts and chemical crosslinking. These efforts have benefited from a new technique, Lipid Exchange Envelope Penetration (LEEP) developed at MIT for the incorporation of nanoparticles into living plants, protoplasts and chloroplasts *in vivo*. This work highlights how the photosynthetic hydrogel composite systems can be optimized by achieving higher productivity and stability of extracted chloroplasts via controlling the illumination period, delivering antioxidant nanoceria inside of chloroplasts, and increasing chloroplast glucose export rate.

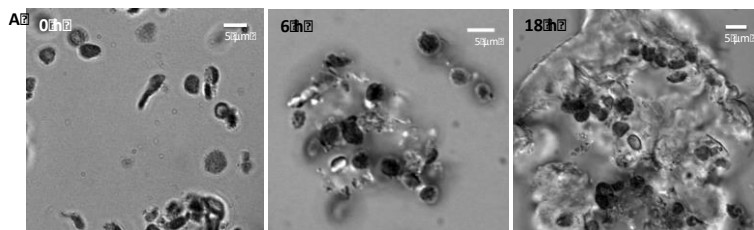


Figure 2. Hydrogel growth over time from ambient carbon dioxide and light around isolated chloroplasts. Microscope images of growing hydrogel near the isolated chloroplasts in the medium containing glucose oxidase (20 U mL^{-1}) and 0.1% w/v MAA. Exposure conditions are ambient CO_2 and 18 h ambient illumination with 1 h dark period.

System II:

We proposed and evaluated a thermodynamically feasible pathway from CO_2 to polyoxymethylene (POM). The full chemical pathway consists of three main compartments: (A) photocatalytic reduction of atmospheric CO_2 to formaldehyde, (B) formaldehyde conversion to 1,3,5-trioxane, and (C) trioxane polymerization to POM (**Figure 3**). For each compartment, we proposed a reaction mechanism and fitted the mechanism to the previously reported kinetic data in the literature. This kinetic modeling led to estimated/calculated reaction rate constants for all three compartments and determining the main rate-limiting steps in each compartment.

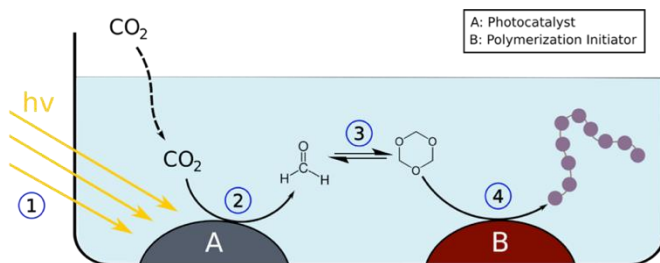


Figure 3. Schematic Illustration of System II: (1&2) CO_2 reduction to formaldehyde using solar energy over photocatalyst A, (3) Formaldehyde trimerization to trioxane, and (4) Trioxane polymerization to polyoxymethylene (POM) in presence of initiator B.

For *Compartment A*, we found that a reaction pathway consisted of a series of irreversible reactions in which two electron and protons are transferred to the reactants explains the kinetic data with minimal error (**Figure 4A**). The competing pathways from CO_2 to formaldehyde and CO lead to the formation of formaldehyde as an intermediate toward methanol, which is subsequently reduced to methane. To capture the complicated pathway to trioxane formation in *Compartment B*, we used a reaction pathway consisted of reversible reactions of formaldehyde hydration, dimerization, trimerization, and finally a cyclization reaction to produce trioxane from the linear methyl glycol trimer (**Figure 4B**). In *Compartment C*, POM is mainly produced through cationic polymerization of trioxane in presence of an initiator. In our proposed pathway and corresponding kinetic model the chain propagation phase follows a second-order reaction with respect to the trioxane monomer and a first order reaction with respect to initiator concentration (**Figure 4C**).

Next, we integrated the reactions from each compartment into an overall reaction pathway from CO_2 to POM. The main pathway from formaldehyde toward POM competes with a pathway from formaldehyde to methane and both are limited by the low photocatalyst activity. Also, another rate-limiting step in the polymerization of formaldehyde to POM restricts the yield and growth rate of POM. Assuming increased activity for both photocatalyst and the polymerization catalyst/media and combining this compartmental catalytic unit with CO_2 capture technologies, we determine the catalytic activity space in which the POM production dominates the competing

methane production pathway and results in higher yields and growth rates of the POM (**Figure 5A and B**).

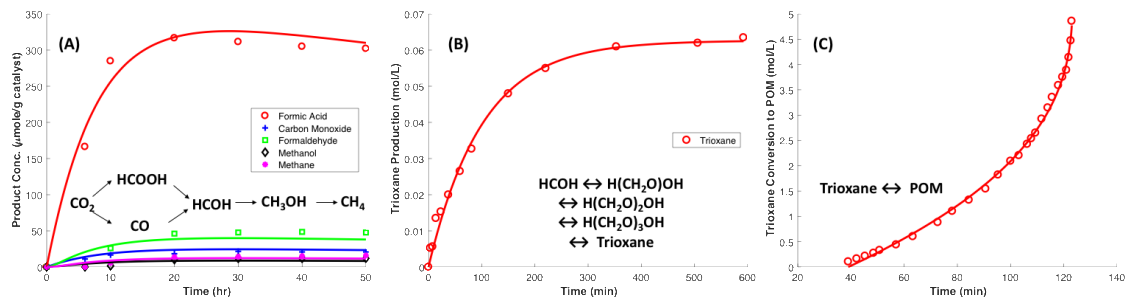


Figure 4. Kinetic models proposed and fitted for all three compartments: (A) CO₂ reduction to formaldehyde intermediate occurs through competing pathways that produce formic acid and carbon monoxide and it proceeds to methanol and methane formation, **(B)** Trioxane formation pathway includes formaldehyde hydration, dimerization, trimerization and ring formation from linear methyl glycol trimer, **(C)** trioxane polymerization proceeds through cationic chain growth polymerization and depends on square of trioxane as well as catalytic initiation concentrations. The experimental kinetic data was obtained from literature.

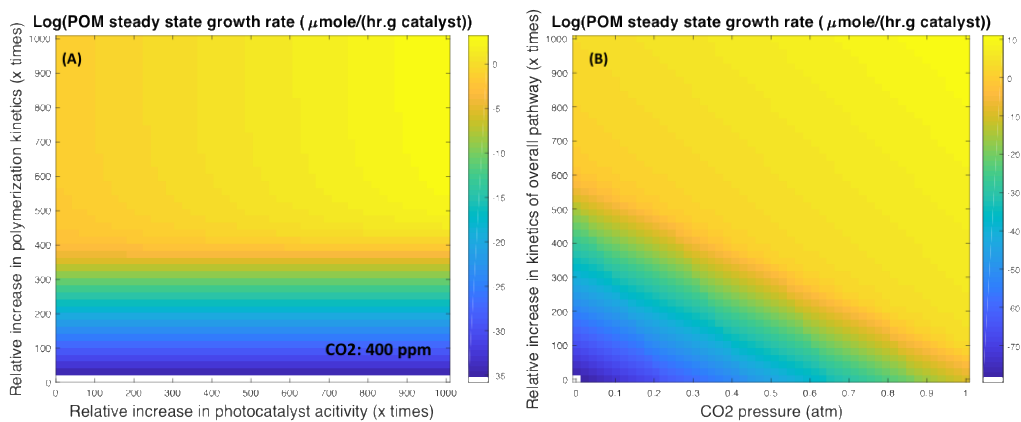


Figure 5. dependence of the POM growth rate to the photocatalyst activity, polymerization kinetics, and CO₂ pressure. (A) at 400 ppm CO₂ pressure, the photocatalyst activity and the polymerization kinetics of conventional systems must be enhanced to achieve higher growth rates, 200 times improvement in overall kinetics of a baseline conventional polymerization unit is the minimum requirement for the photocatalytic kinetics to become effective, **(B)** higher CO₂ pressures, achievable through interfacing this catalytic unit with CO₂ adsorbents, increases the polymer production drastically and requires less improvement in catalytic units.

Future Plans

We intend to screen the formation of POM from CO₂ at room temperature through a series of photocatalytic and polymerization reaction and maximize the POM growth rate. To achieve this goal, we first study three sets of reactions (photocatalytic reduction of CO₂, formaldehyde trimerization, and trioxane polymerization) in separate units over time. Then we will vary catalyst type and structure as well as experimental conditions for optimization of the yield of the products of each unit. Finally, we will connect three reaction units in an engineered, compartmental catalytic system and will screen the overall process. Comparison against the overall kinetic model enables us to determine the rate limiting steps of each unit, and optimize the experimental parameters for higher POM growth rates.

Publications

- (1) Seon-Yeong Kwak, Juan Pablo Giraldo, Tedrick Thomas Salim Lew, Min Hao Wong, Pingwei Liu, Yun Jung Yang, Volodymyr B. Koman, Melissa K. McGee, Bradley D. Olsen, Michael S. Strano, “Polymethacrylamide and Carbon Composites that Grow, Strengthen, and Self-Repair using Ambient Carbon Dioxide Fixation”, *Advanced Materials* 2018, 30, 1804037.
- (2) Dorsa Parviz, Daniel J. Lundberg, Seon-Yeong Kwak, Michael S. Strano, “From Atmospheric CO₂ to Polyoxymethylene: Kinetic Study of an Artificial Photosynthetic Pathway toward Polymeric Products”, *in preparation*

Protein Self-Assembly by Rational Chemical Design

F. Akif Tezcan, University of California, San Diego

A) Program Scope: Our research aims to develop design strategies to control protein self-assembly and to construct protein-based materials with emergent chemical and physical properties. Proteins represent the most versatile building blocks available to living organisms for constructing functional materials and molecular devices. Underlying this versatility is an immense structural and chemical heterogeneity that renders the programmable self-assembly of protein an extremely challenging design task. To circumvent the challenge of designing extensive non-covalent interfaces for controlling protein self-assembly, we have endeavored to develop a toolkit of interactions (metal coordination, disulfide linkages, computationally prescribed non-covalent bonds, etc.) to control protein self-assembly. This toolkit has been further supplemented through the use of synthetic molecules, DNA and polymer frameworks to guide the structures and dynamics of protein assemblies. The initial focus of our DOE/BES-funded program was to establish design strategies for obtaining desired structures such as discrete (*i.e.*, closed) or 0-, 1-, 2- and 3D (*i.e.*, infinite) protein assemblies with crystalline order. While we still pursue such methodology development, our efforts now also focus on obtaining functional, dynamic, reconfigurable and far-from-equilibrium protein materials with new and unusual functional/physical properties (e.g., negative thermal expansion, negative Poisson's ratios, hyperexpandability, self-healing) and developing an experimental/computational/theoretical framework to obtain structure-property relationships in these materials.

B) Recent Progress

Dynamic, reconfigurable protein assemblies: A distinguishing characteristic of many natural protein assemblies is the fact that they are structurally well-ordered yet highly adaptive and can undergo distinct conformational changes in response to external cues. One way to construct such assemblies from scratch is to individually design each of the target structures that correspond to energetic minima along a reaction coordinate. However, this route represents a highly labor- and computation-intensive process, which has, at best, yielded bi-stable systems with limited dynamic range. To guide protein self-assembly, we have instead chosen to use distinct chemical bonding interactions/networks that are (can be) inherently flexible and externally tunable, thus giving rise to dynamic protein materials.

Dynamic 2D lattices: In one case, we engineered a C_4 symmetric protein, RhuA, with Cys residues in its corners (C^{98} RhuA) such that it arranged into μm -sized 2D crystals through disulfide bonding. While the reversibility of disulfide bonds enabled defect-free assembly, their flexibility allowed C^{98} RhuA crystals to be dynamic and auxetic, with a corresponding Poisson's ratio of -1 . In this reporting period, we mapped the free-energy landscape of C^{98} RhuA crystals through extensive experimental characterization and all-atom molecular dynamics (MD) simulations and established that their dynamics were driven primarily by solvent reorganization entropy. Importantly, we could perturb the free-energy landscape via rational mutations to obtain second-generation 2D lattices (C^{EE} RhuA) whose dynamics could be both mechanically and chemically actuated. This example represented the first example of a synthetic protein assembly whose free energy landscape was fully delineated and could be modified to predictably obtain desired structural/dynamic outcomes. Another interesting attribute of the C^{98} RhuA crystals is that the neighboring protein molecules adopt a perfect antiparallel (up-down) registry with respect to the 2D normal ($p4_212$ plane group symmetry). Given that the only connection between the proteins are disulfide bonds which provide no energetic bias with respect to the relative orientation of neighboring molecules, the non-random registry of C^{98} RhuA molecules implies the presence of indirect, long-distance

inter-protein interactions. This realization prompted us to examine the involvement of molecular dipole-dipole interactions. Indeed, our calculations revealed that C^{98} RhuA have a sizeable macrodipole moment (*ca.* 1200 D) and that the antiparallel arrangement of $p42_12$ crystals are favored by *ca.* 1.4 kcal/mol ($2.4 k_B T$) per C^{98} RhuA monomer. These results indicate that weak, long-distance interactions (stemming from the anisotropy of protein building blocks) can control the precise patterning of extended protein assemblies, opening a new perspective in biomolecular design.

We are now seeking to exploit the coherent dynamics of 2D C^{98} RhuA lattices to generate functional materials. In particular, our aim is to build the complexity of this system further such that conformational changes are tied to functional outcomes (e.g., changes in optical signals and capture/release of molecular targets in the pores). To this end, C^{98} RhuA was genetically modified with various peptide and protein tags, to enable binding to plasmonic nanoparticles, fluorescent reporters and protein guests. In general, we have found that C^{98} RhuA lattices can form robustly despite substantial modifications and can be functionalized with Au and Ag nanoparticles through electrostatic interactions (Fig. 1) as well as fluorescent tags by enzymatic labeling while retaining crystalline order.

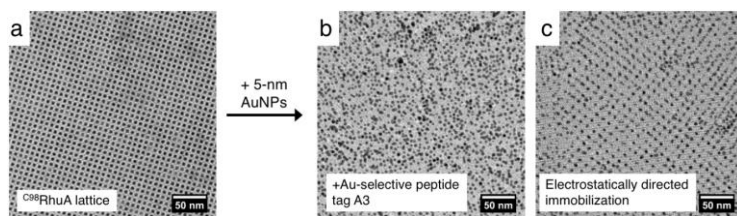


Figure 1. C^{98} RhuA lattices (a) are used as templates for patterning Au nanoparticles. More efficient patterning is achieved through electrostatic interactions with unmodified C^{98} RhuA (c) compared to when C^{98} RhuA is genetically modified with Au-specific peptide A3 (b).

Protein-Metal-Organic Frameworks: In a second case, we tailored O (432) symmetric ferritin molecules with metal coordination motifs in their C_3 symmetric vertices such that they could be assembled into 3D lattices upon binding ditopic linkers bearing hydroxamate functional groups. The structures and symmetries of the resulting protein-metal-organic frameworks (protein-MOFs) could then be controlled in a modular fashion by changing the length and geometry of the dihydroxamate linkers as well as the coordination preferences of the metal ions anchored in the C_3 symmetric vertices. A consideration of the structure of ferritin-MOFs reveals a striking picture: in terms of ferritin-to-linker mass ratios, ferritin-MOFs (*ca.* 2500/1) are akin to a lattice of regulation-size soccer balls held together by wooden toothpicks, suggesting that the structure of the 3D framework could be responsive to external stimuli. In initial studies, we examined the thermal response of ferritin-MOFs. We observed that in most cases the lattices cooperatively lose their crystalline order and that the transition midpoints are highly dependent on the metal ion used, suggesting that bulk properties of the crystals can be finely tuned by metal-linker interaction strengths. Interestingly, Ni-ferritin-MOFs mediated by a furan-based linker showed a markedly different behavior (Fig. 2). Instead of decomposition, the body-centered cubic

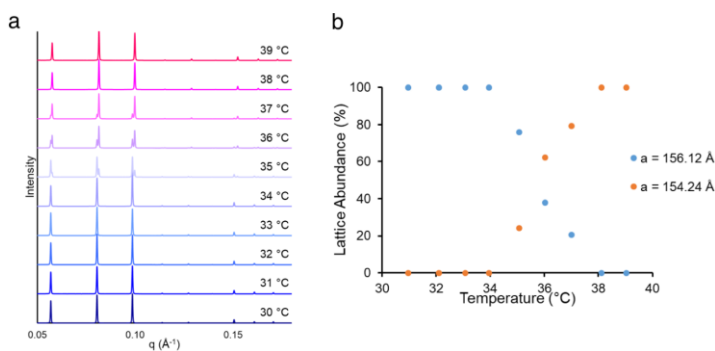


Figure 2. (a) Temperature-dependent contraction of the *bcc* Ni-furan-dihydroxamate-ferritin lattice as measured by SAXS. (b) Temperature dependence of the unit cell parameter *a*.

lattice contracted from $a=156.1 \text{ \AA}$ to $a=154.2 \text{ \AA}$ (i.e., by 3.6%) within a window of $4 \text{ }^\circ\text{C}$, indicating a highly cooperative phase transition with associated negative thermal expansion (NTE). Our crystallographic studies suggest that this transition is not associated with changes in the linker geometry (as is the case in most NTE-materials), but rather with the expansion/contraction of the ferritin molecules themselves. In turn, this finding suggests that inherent dynamics of proteins (at the \AA -nm scale) can be coupled to the entire 3D lattice framework (at μm -mm scale) when properly interconnected.

Dynamic protein crystals with integrated polymer networks:

As the aforementioned examples of 2D RhuA and 3D ferritin-MOF lattices show, structural order and flexibility need not necessarily be mutually exclusive. However, even in such cases, the extent of structural changes and elasticity are constrained by the necessity to maintain a continuous network of bonding interactions between the constituents of the lattice. Consequently, even the most dynamic porous materials tend to be brittle and isolated as microcrystalline powders, and flexible organic/inorganic molecular crystals cannot expand without fracturing. To

overcome these fundamental limitations, we asked whether we could create an integrated hybrid of molecular crystals and hydrogel polymers which would be simultaneously ordered and highly flexible. To this end, mesoporous, face-centered cubic crystals of ferritin were infused with acrylate and acrylamide monomers, which were then polymerized *in crystallo* via free radical initiators to fully integrated the protein lattice with a hydrogel networks. These hybrid materials displayed exciting properties (Fig. 3): a) they can isotropically expand to 570% of their original volume while retaining crystalline periodicity and faceted polyhedral morphologies; b) after substantial expansion (i.e., separation of the ferritin molecules in the lattice by more than 50 \AA), they can contract back to their original state (upon increase in ionic strength) whereby they fully regain atomic-level periodicity; c) owing to the dynamic bonding interactions between the hydrogel network and ferritin molecules, the crystals are toughened and display self-healing behavior; d) the chemical tailorability of the protein components can be used to create chemically and mechanically differentiated domains within single crystals.

New chemical strategies for protein self-assembly: While metal-coordination and disulfide bonding interactions provide distinct advantages for controlling protein self-assembly such as stability, reversibility, chemical tunability, they either do not offer considerable specificity or are limited to homotopic protein-protein interactions. To overcome these limitations, we devised a new chemical strategy that enable selective interactions between proteins.

Constructing protein polyhedra from asymmetric monomers via chemically orthogonal interactions: In protein design, cage-like protein assemblies have featured prominently due to their aesthetically appealing structures and their isolated interiors that enable them to encapsulate molecular cargo and to perform selective chemical transformations. Yet, some of the key structural features of natural protein cages (e.g., viruses, ferritin) have been difficult to emulate in these design efforts: a) each cage is invariably composed of asymmetric protomers, which possess multiple self-associative patches to simultaneously satisfy the symmetry requirements necessary

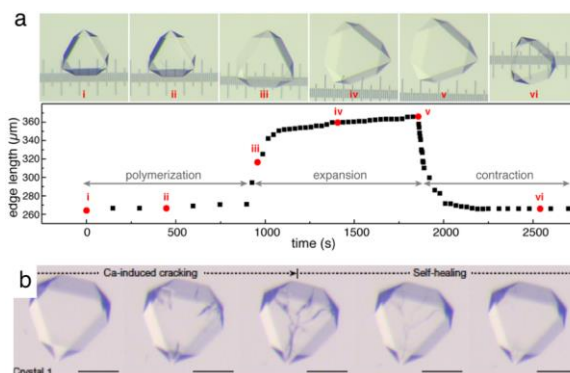


Figure 3. (a) Reversible expansion/contraction of ferritin crystals with an integrated polyacrylate network. (b) Self-healing behavior of the same material.

to build polyhedral assemblies; b) their shells are typically tightly packed to enable influx and efflux of select species – sometimes as small as a solvated ion; c) they are often conformationally flexible and chemically tunable, allowing them to undergo cooperative motions or disassembly in response to external cues.

Inspired by previous work on bimetallic supramolecular coordination cages, we sought to achieve these properties using an inorganic chemical approach, wherein a protein building block is equipped with chemically orthogonal coordination motifs to self-assemble into polyhedral architectures. To this end, we first developed a hydroxamate-bearing reagent, iodo-hydroxamic acid (IHA), which specifically reacts with Cys residues to give a sidechain functionality with the ability to selectively bind Fe^{3+} ions and induce C_3 symmetric oligomerization on a

single-residue footprint (Fig. 4). A monomeric protein, cytochrome cb_{562} , was then modified in appropriate surface locations with these IHA groups (which are “hard” ligands) and Zn^{2+} -binding His/Asp/Glu motifs (which are “soft” ligands to induce C_2 symmetrization). Solution-phase and crystallographic studies established that the resulting cytochrome cb_{562} variants efficiently self-assembled into dodecameric, tetrahedral cages only when both Fe^{3+} and Zn^{2+} were present. High resolution crystal (up to 1.4 Å) and cryoEM (up to 2.6 Å) structures revealed a compact structure with the shape of a truncated tetrahedron, outer dimensions of 80 x 90 Å and an interior cavity volume of 32,700 Å³ (Fig. 4). Like natural protein cages, the shell is tightly packed whereby the largest opening measures less than 4 Å across. Anomalous X-ray diffraction data collected at and below Fe and Zn K-edges indicated that the designed Fe- and Zn-coordination sites exclusively bound their cognate ions with no evidence of crosstalk, establishing that the metal-dependent self-assembly of the cages occurs with absolute chemical selectivity. Owing to their heterobimetallic construction on minimal interprotein-bonding footprints, the cytochrome cages could assemble and disassemble in response to diverse stimuli including temperature, metal chelators, reductants, which makes them highly analogous to natural protein cages and unique among designed systems.

C) Future Plans: Our continuing goal is to fabricate increasingly more complex, functional protein materials that not only emulate but also extend what natural evolution has produced. Our immediate objectives are: 1) to investigate through combined EM/AFM imaging and MD simulations the effects of various osmolytes and crowding agents (which modulate water activity) on the dynamics of $^{C98}\text{RhuA}$ lattices, 2) to optimize the modification of $^{C98}\text{RhuA}$ lattices with inorganic nanoparticles, fluorophores and extrinsic protein guests for engineering optically active lattices and selective “catch-and-release” systems, 3) to elucidate the molecular basis of NTE in ferritin-MOFs and to develop optically active linkers for the construction of light-tunable protein-MOFs, 4) to develop functional protein crystal-hydrogel hybrids in which the reversible expansion/contraction process is exploited to trap and release large biomacromolecules and to produce co-catalytic systems, and 5) to use the Fe^{3+} -IHA system for the modular construction of alternate polyhedral, 2D and 3D protein assemblies using monomeric protein building blocks.

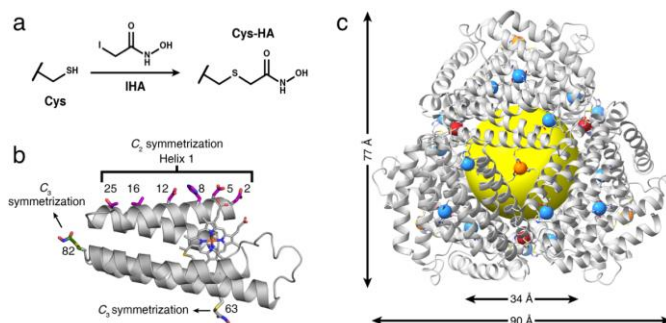


Figure 4. (a) Modification of Cys with iodo-hydroxamate (IHA). (b) Cytochrome cb_{562} building block surface-modified with Zn and Fe-coordination motifs. (c) A tetrahedral dodecameric cage with the composition [12 proteins:8 Fe: 18 Zn]. Blue spheres are Zn and red/orange spheres are Fe.

D) Publications:

- 1) L. Zhang, J. B. Bailey, R. H. Subramanian, F. A. Tezcan, “Hyperexpandable, Self-Healing Macromolecular Crystals with Integrated Polymer Networks”, **Nature**, 557, 86–91 (2018) (Highlighted by DOE-BES).
- 2) R. G. Alberstein, Y. Suzuki, F. Paesani, F. A. Tezcan, “Engineering the entropy-driven free-energy landscape of a dynamic nanoporous protein assembly”, **Nat. Chem.**, 10, 732–739 (2018) (Highlighted by DOE-BES).
- 3) R. H. Subramanian, S. J. Smith, R. G. Alberstein, J. B. Bailey, L. Zhang, G. Cardone, L. Suominen, M. Chami, H. Stahlberg, T. S. Baker, F. A. Tezcan, “Self-Assembly of an Artificial Nucleoprotein Architecture Through Multimodal Interactions”, **ACS Central Sci.**, 4, 1578-1586 (2018).
- 4) E. Golub, R. H. Subramanian, J. Esselborn, R. G. Alberstein, J. B. Bailey, J. A. Chiong, X. Yan, T. Booth, T. S. Baker, F. A. Tezcan, “Constructing Protein Polyhedra from Asymmetric Monomers via Chemically Orthogonal Interactions”, **Nature**, *in revision*.
- 5) S. Zhang, R. G. Alberstein, J. De Yoreo, F. A. Tezcan, “Assembly of a patchy protein into variable 2D lattices via tunable, multiscale interactions”, **Science**, *under review*.

Designing adaptive information processing materials using non-equilibrium forcing

Suriyanarayanan Vaikuntanathan, Department of Chemistry, University of Chicago.

Program Scope

Non-equilibrium forces can drive specific and novel pathways to modulate control and information processing. The benefits of using non-equilibrium forces for information processing and control are particularly apparent in biological mechanisms like those responsible for sensory adaptation, error correction in molecular recognition in immunology and DNA replication, accurate sensing of morphogen gradients during development, and accurate timing of cell cycle events. Motivated by these examples, the main goal of this proposal is to develop theoretical design principles for the construction of bio-inspired adaptive materials. We will specifically focus on uncovering theoretical design principles that will enable bio-inspired materials to respond to external forcing in an adaptive manner and respond accurately to spatio-temporal molecular cues and self-assemble or reorganize. Each of these goals is inspired by particular functionality seen in biological materials - actin polymerization networks and actomyosin networks.

Future Plans

As a first aim, we will develop design principles for the construction of materials that can change their compositions and morphologies in a required adaptive manner as external conditions are modified. The work in this aim is inspired by adaptive phenomenology observed in polymerizing actin networks [1]. Using and extending a recently developed non-equilibrium variational theory [2] in combination with non-linear dimensional reduction techniques, we propose to uncover thermodynamic design principles for how material properties can be modulated precisely even far from equilibrium. Our second aim is motivated by phenomenology exhibited by actomyosin networks as they respond to the non-equilibrium forcing due to the action of myosin motors. Adapting a recently discovered connection between energy dissipation and fluctuations [4,5], we plan to study how the local structure and dynamics of bioinspired materials can be modified by energy dissipation.

References

[1] Bieling, P., Li, T.-D., Weichsel, J., McGorty, R., Jreij, P., Huang, B., Fletcher, D. A., and Mullins, R. D. “**Force Feedback Controls Motor Activity and Mechanical Properties of Self-Assembling Branched Actin Networks**” *Cell* 164, no. 1–2 (2016): 115–127.
doi:10.1016/J.CELL.2015.11.057

[2] Nguyen, M. and Vaikuntanathan, S. “**Design Principles for Nonequilibrium Self-Assembly.**” *Proceedings of the National Academy of Sciences of the United States of America* 113, no. 50 (2016)

[3] Ross, T. D. and Lee, H. J. and Qu, Z. and Banks, R. A and Phillips, R. and Thomson, M. “**Controlling Organization and Forces in Active Matter Through Optically-Defined Boundaries**”, arXiv preprint arXiv:1812.09418

[4] Tociu, L., Fodor, É., Nemoto, T., and Vaikuntanathan, S. “**How Dissipation Constrains Fluctuations in Driven Liquids: Diffusion, Structure and Biased Interactions**”. arXiv preprint arXiv:1808.07838

[5] Junco, C. del, Tociu, L., and Vaikuntanathan, S. “**Energy Dissipation and Fluctuations in a Driven Liquid**” *Proceedings of the National Academy of Sciences of the United States of America* 115, no. 14 (2018): 3569–3574.

Self-Assembly and Self-Replication of Novel Materials from Particles with Specific Recognition: The Depletion Interaction Approach

Paul M. Chaikin, Dept. of Physics, New York University
David Pine, Dept. of Physics, New York University
Nadrian C. Seeman, Dept. of Chemistry, New York University
Marcus Weck, Dept. of Chemistry, New York University

Program Scope

This program seeks to extend the use of DNA recognition and other noncovalent interactions from the nanoscale to the micro scale. Assembling colloidal particles using site-selective directional interactions into pre-determined colloidal superlattices with desired properties is broadly sought-after but challenging to achieve. A current goal is the exploitation of regioselective depletion interactions to engineer the directional bonding and assembly of non-spherical colloidal hybrid microparticles.

Recent Progress

Colloidal particles featuring site-selective directional bonding¹⁻³ have long been proposed as building blocks to achieve desirable colloidal superstructures with unique properties such as photonic badgaps^{4,5} via hierarchical and programmable assembly.^{6,7} Strategies to achieve bonding directionality often rely on emulating the structures and bonding principles of simple molecules on the colloidal scale, and thus include the use of molecular recognition⁸⁻¹¹ in conjunction with shape anisotropy.¹²⁻¹⁵ Various building blocks have been reported such as DNA functionalized patchy particles,¹⁶ triblock Janus spheres,¹⁷ particles of non-spherical geometry¹⁴ and others.^{1-3,15,18} Colloidal superstructures based on such building blocks have been proposed from simulation,^{13,19-22} though, the experimental verification of ordered structures and crystals^{17,23,24} are rare due to limited control over site-selective particle surface modification or the difficult synthesis of specific shapes in combination with poor control and tunability of noncovalent interactions. A general and robust method to directionally fabricate non-spherical colloids into ordered structures or crystals that omits complex surface functionalization has not been reported.

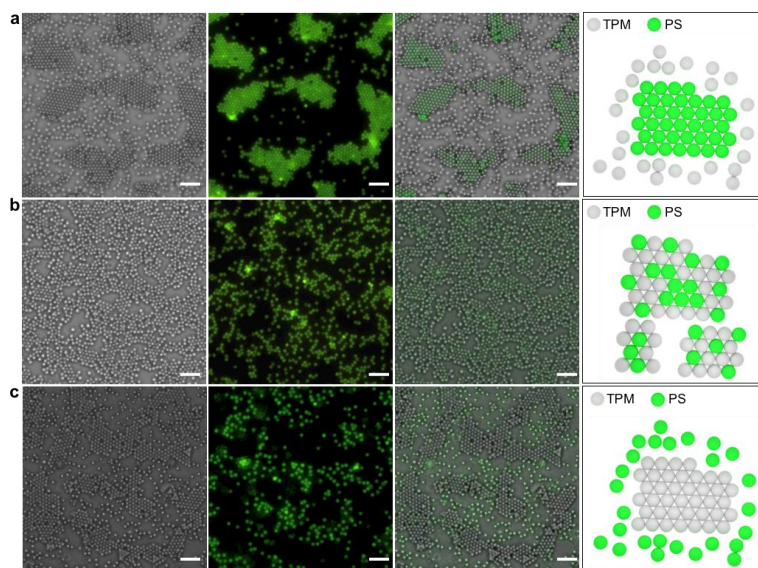


Figure 1. Bright-field images (1st column), confocal fluorescent images (2nd column), overlay of both images (3rd column) and schematic representation (4th column) of selective crystallization behavior of PS, labeled with GFP dye, and TPM spheres under the following conditions: **a)** PBS buffer solution with 2.0 % wt. Pluronic F127, **b)** PBS buffer solution with 3.5 % wt. Synperonic F108, and **c)** DI water with 6 % wt. silica nanoparticles (Ludox HS-40) and 0.5 % wt. Synperonic F108. Scale bars, 5 μm .

We are exploiting regioselective depletion interactions to engineer the directional bonding and assembly of non-spherical colloidal hybrid microparticles. In particular, we demonstrate the selective and tunable depletion crystallization of polymerized 3-(trimethoxysilyl)propyl methacrylate (TPM) and poly(styrene) (PS) spheres. Close-packed 2D crystals consisting of only PS, only TPM, or a random mixture of both spheres are assembled under different depletion conditions at room temperature (21.5 ± 0.5 °C) (Figure 1).

Using a cluster encapsulation method, we are fabricating biphasic triblock PS-TPM-PS particles and show that selective depletion interactions can induce pole-to-pole directional assembly of these particles into a variety of different structures varying from one-dimensional (1D) cross-chains (Figure 2), ladder-like chains and tilted ladder-like chains to two-dimensional (2D) structures simply by tuning the ratio of the two materials on the surface of the particles. Interestingly, we observe polymorphs in 2D structures where particles of a specific aspect ratio form crystals with different symmetries simultaneously (Figure 3). Although polymorphism has profound implications for materials stability and properties,²⁵ there are few examples of polymorphism reported on the colloidal scale.²⁶⁻²⁹

In-situ assembly videos allow for identification of the generation of the polymorphs. Two kinds of seeds are observed during the nucleation process. One is the “three-particle seed” derived from chain-like intermediate structures. The other is a larger “super seed” consisting of more than three particles formed from a metastable colloidal intermediate. The formation of this metastable intermediate, where particles align with each other in a state that is similar to but not as ordered as in crystals, can be attributed to the increased translational and rotational freedom of

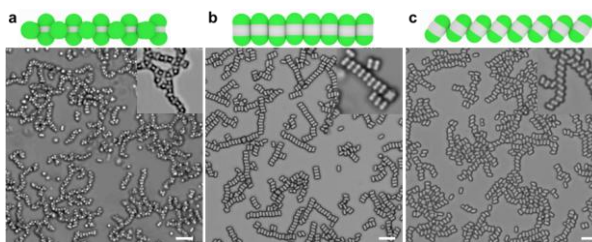


Figure 2. Bright-field images (bottom) and schematic illustration (top) of **a)** cross chains assembled from particles with R_A (aspect ratio defined as the ratio of length (L) and width (W) of particles, $R_A = L/W$) = 2.33, **b)** colloidal ladder chains assembled from particles with $R_A = 1.89$, and **c)** tilted ladder chains assembled from particles with $R_A = 1.67$. Insets show the enlarged images of each assembly. Scale bars, 5 μm .

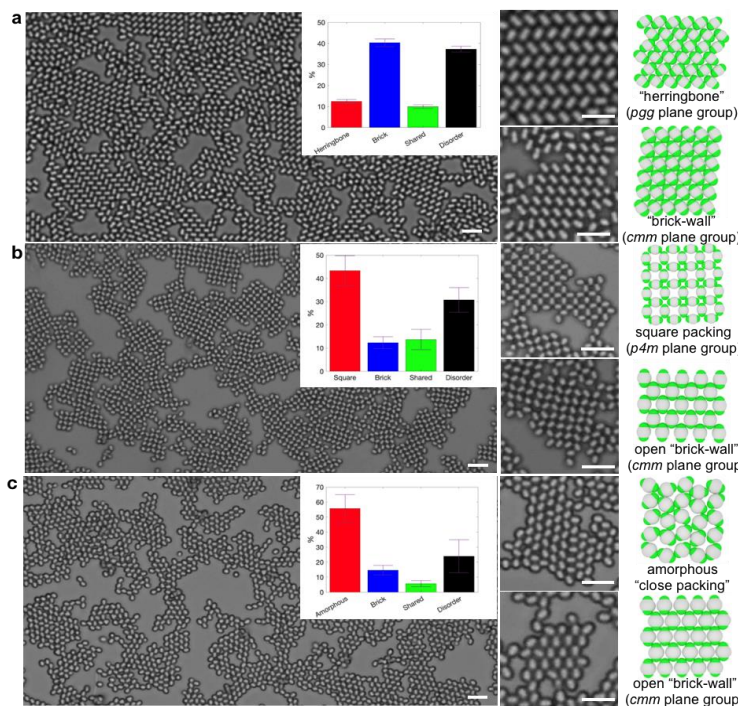


Figure 3. Bright-field images of large area (left), abundances of each form (inset), enlarged areas of representative forms (middle) and schematic illustration (right) of **a)** assemblies of “herringbone” pattern and “brick-wall” like pattern with particles $R_A = 1.49$, **b)** assemblies of open square structures together with open “brick-wall” like pattern with particles $R_A = 1.35$, and **c)** assemblies of amorphous close packing and open “brick-wall” like pattern with particles $R_A = 1.23$. Insets show the distribution of each structure based on ten images. Scale bars, 5 μm .

the colloids. After the formation of those seeds, the crystals grow as other free particles approach until the suspension reaches equilibrium. Crystalline boundaries can be formed when the newly joined particles violate the orientation of the “mother” crystal. The final structures depend on the initial seed structure and the growth process.

The interaction between these particles can be regulated by changing the depletant, yielding new series of colloidal chains and membranes featuring center-to-center interactions. The presented science opens the possibility to achieve directional and specific bonding of colloidal particles towards open-packed superlattice with rational particle design rather than complex functional group synthesis and surface modification. Fabrication of template-free 1D chains and 2D membranes with tunable flexibility sheds new light in processing colloidal materials. For example, a membrane with a heterogeneous “sandwich” structure can be realized with designable triblock particles. Reconfigurable assemblies are within reach given switchable depletion interactions achieved by using stimuli-responsive depletants.

Future Plans

- Introduction of DNA hybridization to the system thereby creating a two-step assembly strategy
- Fabrication of chiral colloids

References

- 1 Ravaine, S. & Duguet, E. Synthesis and assembly of patchy particles: Recent progress and future prospects. *Curr. Opin. Colloid Interface Sci.* **30**, 45-53 (2017).
- 2 Zhang, J., Luijten, E. & Granick, S. Toward design rules of directional janus colloidal assembly. *Annu. Rev. Phys. Chem.* **66**, 581-600 (2015).
- 3 Yi, G. R., Pine, D. J. & Sacanna, S. Recent progress on patchy colloids and their self-assembly. *J. Phys. Condens. Matter* **25**, 193101 (2013).
- 4 Hynninen, A. P., Thijssen, J. H., Vermolen, E. C., Dijkstra, M. & van Blaaderen, A. Self-assembly route for photonic crystals with a bandgap in the visible region. *Nat. Mater.* **6**, 202-205 (2007).
- 5 Maldovan, M. & Thomas, E. L. Diamond-structured photonic crystals. *Nat. Mater.* **3**, 593-600 (2004).
- 6 Duguet, E., Hubert, C., Chomette, C., Perro, A. & Ravaine, S. Patchy colloidal particles for programmed self-assembly. *C. R. Chim.* **19**, 173-182 (2016).
- 7 Cademartiri, L. & Bishop, K. J. Programmable self-assembly. *Nat. Mater.* **14**, 2-9 (2015).
- 8 Elacqua, E., Zheng, X., Shillingford, C., Liu, M. & Weck, M. Molecular Recognition in the Colloidal World. *Acc. Chem. Res.* **50**, 2756-2766 (2017).
- 9 Gerth, M. & Voets, I. K. Molecular control over colloidal assembly. *Chem. Commun.* **53**, 4414-4428 (2017).
- 10 Nguyen, T. A., Newton, A., Kraft, D. J., Bolhuis, P. G. & Schall, P. Tuning Patchy Bonds Induced by Critical Casimir Forces. *Materials* **10**, 1265 (2017).
- 11 Chen, G. *et al.* Regioselective surface encoding of nanoparticles for programmable self-assembly. *Nat. Mater.* **18**, 169-174 (2019).

- 12 Petukhov, A. V., Tuinier, R. & Vroege, G. J. Entropic patchiness: Effects of colloid shape and depletion. *Curr. Opin. Colloid Interface Sci.* **30**, 54-61 (2017).
- 13 van Anders, G., Ahmed, N. K., Smith, R., Engel, M. & Glotzer, S. C. Entropically patchy particles: engineering valence through shape entropy. *ACS Nano* **8**, 931-940 (2014).
- 14 Sacanna, S., Pine, D. J. & Yi, G.-R. Engineering shape: the novel geometries of colloidal self-assembly. *Soft Matter* **9**, 8096-8106 (2013).
- 15 Sacanna, S. & Pine, D. J. Shape-anisotropic colloids: Building blocks for complex assemblies. *Curr. Opin. Colloid Interface Sci.* **16**, 96-105 (2011).
- 16 Wang, Y. F. *et al.* Colloids with valence and specific directional bonding. *Nature* **491**, 51-55 (2012).
- 17 Chen, Q., Bae, S. C. & Granick, S. Directed self-assembly of a colloidal kagome lattice. *Nature* **469**, 381-384 (2011).
- 18 Gong, Z., Hueckel, T., Yi, G. R. & Sacanna, S. Patchy particles made by colloidal fusion. *Nature* **550**, 234-238 (2017).
- 19 Li, Z. W., Zhu, Y. L., Lu, Z. Y. & Sun, Z. Y. General patchy ellipsoidal particle model for the aggregation behaviors of shape- and/or surface-anisotropic building blocks. *Soft Matter*, **14**, 7625-7633 (2018).
- 20 Morphew, D., Shaw, J., Avins, C. & Chakrabarti, D. Programming Hierarchical Self-Assembly of Patchy Particles into Colloidal Crystals via Colloidal Molecules. *ACS Nano* **12**, 2355-2364 (2018).
- 21 Du, C. X., van Anders, G., Newman, R. S. & Glotzer, S. C. Shape-driven solid-solid transitions in colloids. *Proc. Natl. Acad. Sci. USA* **114**, E3892-E3899 (2017).
- 22 Wang, Y., Jenkins, I. C., McGinley, J. T., Sinno, T. & Crocker, J. C. Colloidal crystals with diamond symmetry at optical lengthscales. *Nat. Commun.* **8**, 14173 (2017).
- 23 Ducrot, E., He, M., Yi, G. R. & Pine, D. J. Colloidal alloys with preassembled clusters and spheres. *Nat. Mater.* **16**, 652-657 (2017).
- 24 Rossi, L. *et al.* Cubic crystals from cubic colloids. *Soft Matter* **7**, 4139-4142 (2011).
- 25 Liu, G. R., Gou, R. J., Li, H. Z. & Zhang, C. Y. Polymorphism of Energetic Materials: A Comprehensive Study of Molecular Conformers, Crystal Packing, and the Dominance of Their Energetics in Governing the Most Stable Polymorph. *Cryst. Growth Des.* **18**, 4174-4186 (2018).
- 26 Patra, N. & Tkachenko, A. V. Programmable self-assembly of diamond polymorphs from chromatic patchy particles. *Phys. Rev. E* **98**, 032611 (2018).
- 27 Zhao, K. & Mason, T. G. Shape-designed frustration by local polymorphism in a near-equilibrium colloidal glass. *Proc. Natl. Acad. Sci. USA* **112**, 12063-12068 (2015).
- 28 Reinhart, W. F. & Panagiotopoulos, A. Z. Equilibrium crystal phases of triblock Janus colloids. *J. Chem. Phys.* **145**, 094505 (2016).
- 29 Kim, J. *et al.* Polymorphic Assembly from Beveled Gold Triangular Nanoprisms. *Nano Lett.* **17**, 3270-3275 (2017).

Publications

1. Wang, Xiao, Ruojie Sha, Martin Kristiansen, Carina Hernandez, Yudong Hao, Chengde Mao, James W. Canary, and Nadrian C. Seeman. "An Organic Semiconductor Organized into 3D DNA Arrays by "Bottom-up" Rational Design." *Angew. Chem. Int. Ed.* **56** (2017): 6445-6448.
2. Zion, Matan Yah Ben, Xiaojin He, Corinna C. Maass, Ruojie Sha, Nadrian C. Seeman, and Paul M. Chaikin. "Self-assembled three-dimensional chiral colloidal architecture." *Science* **358** (2017): 633-636.
3. Xiaolong Zheng, Mingzhu Liu, Mingxin He, David J. Pine, and Marcus Weck. "Shape-Shifting Patchy Particles." *Angew. Chem. Int. Ed.* **56** (2017): 5599-5603.
4. Yudong Hao, Martin Kristiansen, Ruojie Sha, Jens J. Birktoft, Carina Hernandez, Chengde Mao, and Nadrian C. Seeman. "A device that operates within a self-assembled 3D DNA crystal." *Nature Chem.* **9** (2017): 824.
5. Xiaojin He, Ruojie Sha, Rebecca Zhuo, Yongli Mi, Paul M. Chaikin, and Nadrian C. Seeman. "Exponential growth and selection in self-replicating materials from DNA origami rafts." *Nature Mater.* **16** (2017): 993.
6. Yin Zhang, Angus McMullen, Lea-Laetitia Pontani, Xiaojin He, Ruojie Sha, Nadrian C. Seeman, Jasna Brujic, and Paul M. Chaikin. "Sequential self-assembly of DNA functionalized droplets." *Nature Commun.* **8** (2017): 21.
7. Nadrian C. Seeman, Ruojie Sha, Jens Birktoft, Jens, Jianping Zheng, Wenyan Liu, Tong Wang, and Chengde Mao. "Designed 3D DNA crystals." In *3D DNA Nanostructure*, pp. 3-10. Humana Press, New York, NY, 2017.
8. Carina Hernandez, Jens J. Birktoft, Yoel P. Ohayon, Arun Richard Chandrasekaran, Hatem Abdallah, Ruojie Sha, Vivian Stojanoff, Chengde Mao, and Nadrian C. Seeman. "Self-assembly of 3D DNA crystals containing a torsionally stressed component." *Cell Chem. Biol.* **24** (2017): 1401-1406.
9. Fiona W. Conn, Michael Alexander Jong, Andre Tan, Robert Tseng, Eunice Park, Yoel P. Ohayon, Ruojie Sha, Chengde Mao, and Nadrian C. Seeman. "Time lapse microscopy of temperature control during self-assembly of 3D DNA crystals." *J. Cryst. Growth* **476** (2017): 1-5.
10. Joanna A. Ellis-Monaghan, Greta Pangborn, Nadrian C. Seeman, Sam Blakeley, Conor Disher, Mary Falcigno, Brianna Healy, Ada Morse, Bharti Singh, and Melissa Westland. "Design tools for reporter strands and DNA origami scaffold strands." *Theor. Comp. Science* **671** (2017): 69-78.
11. Elizabeth Elacqua, Xiaolong Zheng, Cicely Shillingford, Mingzhu Liu, and Marcus Weck. "Molecular Recognition in the Colloidal World." *Acc. Chem. Res.* **50** (2017): 2756-2766.
12. Yue Zhao, Ruojie Sha, Yudong Hao, Carina Hernandez, Xinshuai Zhao, David Rusling, Jens J. Birktoft et al. "Self-Assembled Three-Dimensional Deoxyribonucleic Acid (DNA) Crystals." *Found. Crystal.* **74** (2018): a253.
13. Yin Zhang, Xiaojin He, Rebecca Zhuo, Ruojie Sha, Jasna Brujic, Nadrian C. Seeman, and Paul M. Chaikin. "Multivalent, multiflavored droplets by design." *Proc. Nat. Acad. Sci. USA* **115** (2018): 9086-9091.

14. Xiao Wang, Chen Li, Dong Niu, Ruojie Sha, Nadrian C. Seeman, and James W. Canary. "Construction of a DNA Origami Based Molecular Electro-optical Modulator." *Nano Lett.* **18** (2018): 2112-2115.
15. Jiemin Zhao, Yue Zhao, Zhe Li, Yong Wang, Ruojie Sha, Nadrian C. Seeman, and Chengde Mao. "Modulating Self-Assembly of DNA Crystals with Rationally Designed Agents." *Angew. Chem. Int. Ed.* **57** (2018): 16529-16532.
16. Mingzhu Liu, Xiaolong Zheng, Fangyuan Dong, Michael D. Ward, and Marcus Weck. "Reversible Morphology Switching of Colloidal Particles." *Chem. Mater.* **30** (2018): 6903-6907.
17. Xing Wang, Arun Richard Chandrasekaran, Zhiyong Shen, Yoel P. Ohayon, Tong Wang, Megan E. Kizer, Ruojie Sha et al. "Paranemic crossover DNA: There and back again." *Chem. Rev.* **119** (2018): 6273-6289.
18. Saerom Lee, Jeong Hoon Yoon, In-Seong Jo, Joon Suk Oh, David J. Pine, Tae Soup Shim, and Gi-Ra Yi. "DNA-functionalized 100 nm polymer nanoparticles from block copolymer micelles." *Langmuir* **34** (2018): 11042-11048.
19. Jeongbin Moon, In-Seong Jo, Etienne Ducrot, Joon Suk Oh, David J. Pine, and Gi-Ra Yi. "DNA-Coated Microspheres and Their Colloidal Superstructures." *Macromol. Res.* **26** (2018): 1085-1094.
20. Xiang Gao, Matthew Gethers, Si-ping Han, William A. Goddard III, Ruojie Sha, Richard P. Cunningham, and Nadrian C. Seeman. "The PX motif of DNA binds specifically to Escherichia coli DNA polymerase I." *Biochemistry* **58** (2018): 575-581.
21. Rebecca Zhuo, Feng Zhou, Xiaojin He, Ruojie Sha, Nadrian C. Seeman, and Paul M. Chaikin. "Litters of self-replicating origami cross-tiles." *Proc. Nat. Acad. Sci. USA* **116**, (2019): 1952-1957.
22. Hao Pei, Ruojie Sha, Xiwei Wang, Ming Zheng, Chunhai Fan, James W. Canary, and Nadrian C. Seeman. "Organizing End-Site-Specific SWCNTs in Specific Loci Using DNA." *J. Am. Chem. Soc.* DOI: 10.1021/jacs.9b03432 (2019).
23. Yoel P. Ohayon, Carina Hernandez, Arun Richard Chandrasekaran, Xinyu Wang, Hatem O. Abdallah, Michael Alexander Jong, Michael G. Mohsen, Ruojie Sha, Jens J. Birktoft, Philip S. Lukeman, Paul M. Chaikin, Stephen L. Ginell, Chengde Mao, and Nadrian C. Seeman "Designing Higher Resolution Self-Assembled 3D DNA Crystals via Strand Terminus Modifications." *ACS Nano*. DOI: 10.1021/acsnano.9b02430 (2019).

Dynamic, Adaptive, Systems and Materials: Complex, Simple, and Emergent Behaviors

Applicant: President and Fellows of Harvard College

Principal Investigator: George M. Whitesides

Program Scope

In the past year, the research program focused on two subjects, all related to functional, dissipative, adaptive systems, and soft-matter science:

- a. **Soft Actuators.** We fabricated pneumatically actuated “intelligent” devices using organic elastomers. We demonstrated prototypes of a pneumatically actuated soft “transistor”, which was used to fabricate grippers, walkers as well as soft objects that respond to an external stimulus. The key scientific component of the program was the exploitation of mechanical instabilities, such as buckling and pop-through, to achieve useful work.
- b. **Magnetically Levitated Ensembles of Organic Objects.** In this part of the program, we explored the behavior of diamagnetic polymeric materials suspended in a paramagnetic fluid (an aqueous solution of manganese(II) dichloride), in the presence of competing gravitational, magnetic, centrifugal, and shear forces. This easily assembled experiment provides a tractable model for a dissipative, complex (or complicated) system. We also developed new uses of the techniques of magnetic levitation to study polymerizing, viscous liquids. We also extended magnetic levitation for dynamic, continuous flow systems using axial magnets.

Recent Progress

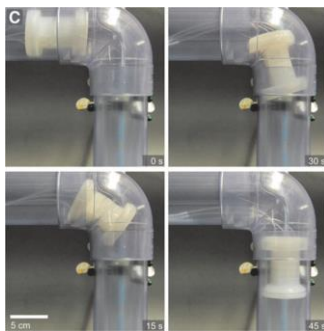


Figure 1. Demonstrations of the tube-climbing robot turning in a dry tube.

Soft Actuators: In this program, we developed several pneumatically actuated soft devices that introduce new functionalities in soft robotics (e.g. negative pressure actuated soft robots, a soft tube climbing robot, etc.).

We also explored integration of simple control and logic functions directly into soft actuators and robots using a soft, elastomeric valve that contains a bistable membrane, which acts as a mechanical “switch” to control air flow. The structural instability enables rapid transition between two stable states of the membrane. When integrated in a feedback pneumatic circuit, the valve functions as a pneumatic oscillator, generating periodic motion using air from a

single source of constant pressure. The valve was used to demonstrate (i) a gripper to grasp a ball autonomously (ii) autonomous earthworm-like locomotion using an air source of constant pressure (iii) soft logic gates (iv) soft ring oscillator.

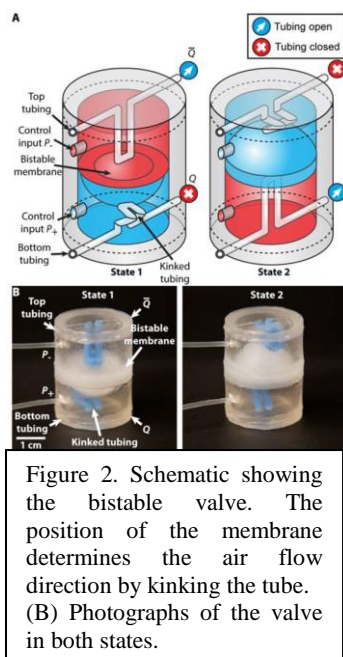


Figure 2. Schematic showing the bistable valve. The position of the membrane determines the air flow direction by kinking the tube. (B) Photographs of the valve in both states.

In this program, we also demonstrated the fabrication of elastomeric three-dimensional (3D) structures starting from two-dimensional (2D) sheets using a combination of direct-ink printing and relaxation of strain. This strategy of using initially 2D materials to fabricate 3D structures offers new features that complement existing fabrication techniques - (i) It provides a simple route to create shapes with complex curves, suspended features, and internal cavities. (ii) It is a faster method of fabricating some types of shapes than “conventional” 3D printing, because the features are printed in 2D. (iii) It forms surfaces that can be both smoother, and structured in a way that is not compatible with layer-by-layer processing. (iv) It forms structures that can be deformed reversibly after fabrication by reapplying strain.

Magnetic Levitation: In this part of the program, we used magnetic levitation to to characterize the kinetics of free-radical

polymerization of water-insoluble, low-molecular-weight monomers that show a large change in density upon polymerization. We demonstrated the online characterization of thermal polymerization of methacrylate-based monomers and the photopolymerization of methyl

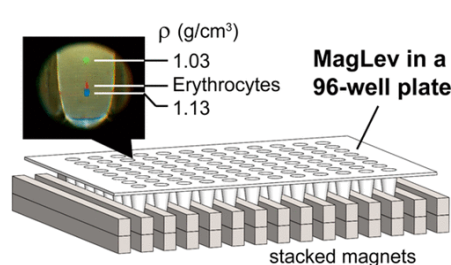


Figure 3. Schematic representation of the MagLev technique used for high-throughput density measurements of diamagnetic particles. The inset picture shows the levitation of erythrocytes in between beads of known densities.

methacrylate. MagLev enabled the determination of the orders of reaction and the Arrhenius activation energy of polymerization. We also demonstrated that MagLev can monitor polymerization in the presence of solids (aramid fibers, and carbon fibers, and glass fibers).

To make the MagLev technique adaptable to the workflow of biochemists and biologists, we adapted the MagLev setup to enable high-throughput density measurements of diamagnetic particles (including cells) using 96-well plates and a flatbed scanner.

We also demonstrated MagLev using ring

magnets (“axial MagLev”) to simplify sampling of objects after a density based separation using the MagLev technique. It significantly simplifies the procedures used to carry out density-based analyses, separations, and manipulations. This “axial” configuration enables (i) simple procedures to add samples and paramagnetic medium from an open end and to retrieve samples while levitating in the magnetic field (e.g., a subpopulation of a cluster of small particles); (ii) simple accesses and the abilities to view the samples 360° around the sample container and from the top

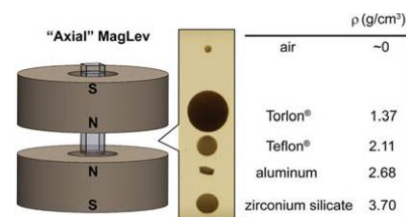


Figure 4. Schematic representation of the axial MagLev. The picture on the right shows an actual density-based separation of materials using the axial MagLev.

and bottom; and (iii) convenient density measurements of small quantities (as small as a single submillimeter particle as demonstrated) of samples. The compact design, portability, affordability, and simplicity in use of the “axial MagLev” device will broaden the uses of magnetic methods in analyzing, separating, and manipulating different types of samples (solids, liquids, powders, pastes, gels, and also biological entities) in areas such as materials sciences, chemistry, and biochemistry.

Future Plans

Soft actuators: In this part of the program, we will focus on imparting “logic” to materials using instabilities in the materials. For example, we will use the buckling of a two dimensional sheet in combination with our demonstrated idea of using kinked tubes to fabricate robots that perform complex functions using a single pressure input. The program will emphasize simplification of the fabrication process of these material logic elements and cascading them to obtain a complex output from a single pneumatic input.

Magnetic Levitation: In this part, we will further develop our MagLev technique to analyse biomolecular binding events (e.g. antibody-antigen binding). We have previously shown that MagLev can detect binding events of biomolecules with molecular weights < 60kDa. We will use new materials to extend this molecular weight range to encompass antibodies. This will provide a simple, label-free and potentially cheap method for antibody / antigen detection. Furthermore, we will explore the application of the MagLev technique to analyse powered mixtures (e.g. narcotic drugs, pharmaceutical drugs). The MagLev technique, when combined with image analysis and machine learning algorithms, would allow the tracing of origin of mixtures as well as easy detection of counterfeit drugs.

References

1. "Negative-Pressure Soft Linear Actuator with a Mechanical Advantage", Yang, D., Verma, M. S., Lossner, E., Stothers, D. and Whitesides, G. M. *Adv. Mater. Technol.*, 2016.
2. "Coated and Uncoated Cellophane as Materials for Microplates and Open-Channel Microfluidics Devices", Hamedi, M. M., Unal, B., Kerr, E., Glavan, A., Fernandez-Abedul, M. T. and Whitesides, G. M. *Lab on a Chip*, 2016.
3. "A Soft Tube-Climbing Robot", Verma, M. S., Yang, D., Harburg, D. V. and Whitesides, G. M. *Soft Robotics*, 2018.
4. "Soft, Rotating Pneumatic Actuator", Ainla, A., Verma, M. S., Yang, D. and Whitesides, G. M. *Soft Robotics* 2017.
5. "Slit Tubes for Semi-Soft Pneumatic Actuators", Belding, L., Baytekin, B., Baytekin, H. T., Rothmund, P., Verma, M. S., Nemiroski, A., Sameoto, D., Grzybowski, B. A. and Whitesides, G. M. *Advanced Materials*, 2018.

6. "Magnetic Levitation to Characterize the Kinetics of Free-Radical Polymerization", Ge, S., Semenov, S. N., Nagarkar, A. A., Milete, J., Christodouleas, D. C., Li, Y. and Whitesides, G. M. JACS, 2017.
7. "A Soft, Bistable Valve for Autonomous Control of Soft Actuators", Rothmund, P., Ainla, A., Belding, L., Preston, D. J., Kurihara, S., Suo, Z. and Whitesides, G. M. Science Robotics, 2018.
8. "High-Throughput Density Measurement Using Magnetic Levitation", Ge, S., Wang, Y., Deshler, N., Preston, D. J. and Whitesides, G. M. JACS, 2018.
9. "Soft Robotics ", Whitesides, G. M. Angewandte Chemie, 2018.
10. "Fabricating 3D Structures by Combining 2D Printing and Relaxation of Strain", Cafferty, B. J., Campbell, V. E., Rothmund, P., Ainla, A., Fulleringer, N., Preston, D. J., Diaz, A. C., Sameoto, D., Lewis, J. A. and Whitesides, G. M. Advanced Materials Tech, 2019.
11. ""Axial" Magnetic Levitation Using Ring Magnets Enables Simple Density-Based Analysis Separation, and Manipulation", Ge, S. and Whitesides, G. M. Analytical Chemistry, 2018.
12. "Fabricating 3D Structures by Combining 2D Printing and Relaxation of Strain", Cafferty, B. J., Campbell, V. E., Rothmund, P., Ainla, A., Fulleringer, N., Preston, D. J., Diaz, A. C., Sameoto, D., Lewis, J. A. and Whitesides, G. M. Advanced Materials Tech, 2019, 4, 1800299 (1-9).
13. "Digital Logic for Soft Devices", Preston, D. J., Rothmund, P., Jiang, H. J., Nemitz, M. P., Rawson, J., Suo, Z. and Whitesides, G. M. PNAS, 2019, 116, 7750-7759.
14. "A Soft Ring Oscillator", Preston, D. J., Jiang, H. J., Sanchez, V., Rothmund, P., Rawson, J., Nemitz, M. P., Lee, W.-K., Suo, Z., Walsh, C. J. and Whitesides, G. M. Science Robotics, 2019, 4, 1-9.

SUBMITTED/IN PRESS:

s/555 "Magnetic Levitation in Chemistry, Materials Science, and Biochemistry", Ge, S., Nemiroski, A., Mirica, K. A., Mace, C. R., Hennek, J. W., Kumar, A. A. and Whitesides, G. M. Angewandte Chemie Intl. Ed., in press 2019

Exploring Fundamental Properties of Dynamic DNA Origami –Nanoparticle Composites

Jessica Winter, Chemical and Biomolecular Engineering, Biomedical Engineering; Carlos Castro, Mechanical and Aerospace Engineering; Michael Poirier, Ezekiel Johnston-Halperin, Department of Physics, The Ohio State University

Program Scope

This research addresses fundamental needs for the development of deoxyribonucleic acid (DNA)-based energy materials by increasing understanding of: (1) the role of nanomaterial sterics and binding interactions on the equilibrium and kinetic properties of dynamic DNA origami structures, (2) mechanical potential energy storage via NP and DNA origami interactions, (3) energy exchange between the bulk solution and DNA-NP composite materials, and (4) nanoscale heat transfer on DNA de/hybridization kinetics in heterogeneous nanoscale environments. This research involves 3 objectives investigating energy harvesting by gold nanoparticles (AuNPs) or magnetic superparamagnetic iron oxide nanoparticles (SPIONs) and transfer of that energy with DNA origami “hinge” and NP-hinge array templates (**Figure 1**). DNA nanostructures are ideal materials for these studies since their geometry, stiffness, and motion can be precisely designed and controlled [1-3].

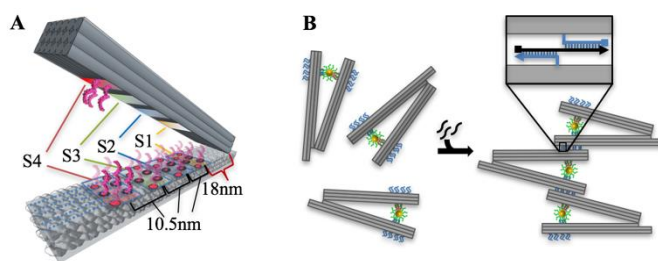


Figure 1. DNA Origami Structures. Hinges (A) can polymerize to form hinge microscale arrays (B). S1-4 in A indicate NP binding sites. Hinge arms are ~ 70 nm long.

Recent Progress

This reporting period led to the completion of free energy landscape distribution studies for DNA origami-AuNP hinge composites and demonstration of NP-hinge arrays. These results show reciprocal tunability between NP and DNA origami conformations at micron scales for the first time. Thermal actuation thermodynamics and kinetics were studied extensively in single hinges and demonstrated for hinge arrays, with time scales of ~seconds achieved. These results were submitted for publication, with additional publications anticipated in the next few months on the role of sterics in: DNA conjugation to QDs, NP-templated DNA tile assembly, combination with DNA base-pairing on thermal actuation of NP-hinges, DNA-AuNP binding with characterization via force microscopy, and also use of single molecule methods to understand kinetics and free energy storage of hinges. Finally, we developed several foundational technologies that will enable future investigations of emergent properties, including schemes for SPION and semiconductor quantum dot (QD) attachment to hinges and composite characterization methods including single molecule microscopy and force spectroscopy (both dual optical tweezers and magnetic tweezers).

Objective 1: Evaluate the ability of DNA-nanoparticle composites to store mechanical energy.

The main goals of Objective 1 are to: (1) understand the influence of nanoparticles (NP) on the free energy landscapes of DNA origami nanodevices; (2) quantify how stored energy alters kinetics and thermodynamics of DNA binding; and (3) explore whether stored energy and sterics designed into DNA devices can generate emergent behaviors in DNA origami–NP composites.

(Obj. 1.1: Free Energy Landscapes) We completed free energy landscape analysis of hinges occluded by 5 nm and 15 nm AuNPs at four locations (**Figure 2**). Advancing on prior work using DNA origami for NP templating [4], these results show that NPs can be used as design elements to tune DNA origami conformations through their size, placement, and attachment constraints (e.g., steric occlusion).

(Obj. 1.2 Actuation Kinetics) Next, we studied composite thermal actuation thermodynamics and kinetics as a function of DNA hybridization length (6, 7, 8, or 9 base pairs, bp.; 9 bp not shown). Equilibrium thermal actuation curves of composites with AuNPs bound at site 4, which exhibit the largest actuated conformation (**Figure 2A**, top left), revealed that the length of NP-binding, single-stranded (ss) DNA on the hinge altered actuation temperature by $\sim 10^\circ\text{C}$ per base (**Figure 3A**). Bulk heating or cooling yielded rapid actuation in \sim seconds (**Figure 3B**), compared to \sim minutes in previous reports [5], with actuation limited by bulk heating time.

(obj. 1.3 Emergent behaviors) To investigate emergent NP behaviors, we constructed micro-scale materials from individual hinge units with AuNPs at site 4 (**Figure 4**). Orientation was altered by adjusting overlap between units, yielding

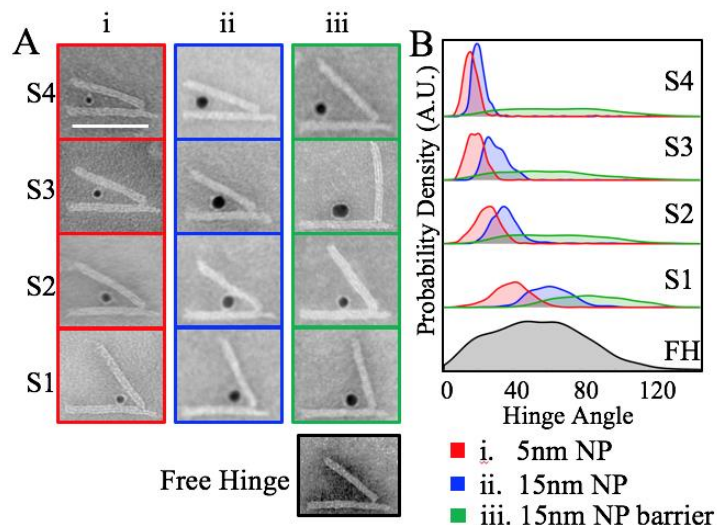


Figure 2. Hinge-NP composite free energy landscapes. (A) Attaching NPs at different hinge sites constrains free energy landscapes relative to the free hinge (FH). (B) Angular distributions of corresponding composites. Scale bar = 50nm.

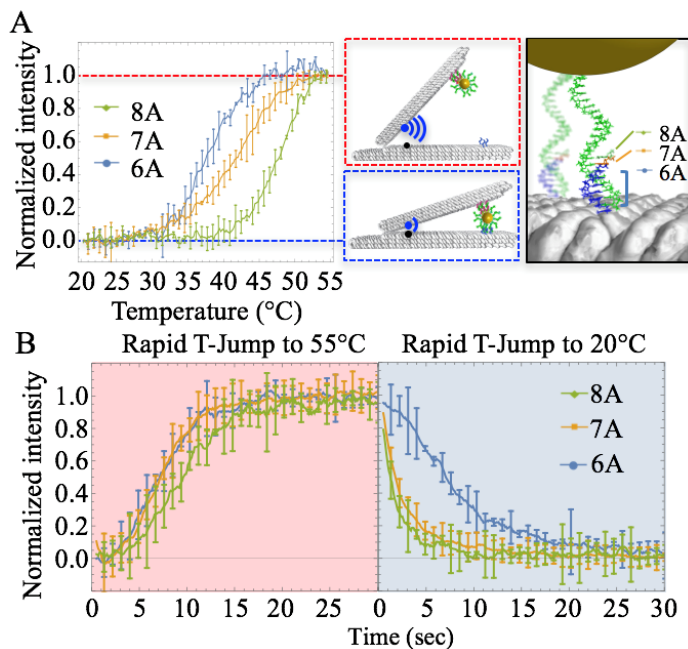


Figure 3. (A) Composite equilibrium thermal actuation curves vs. NP-binding ssDNA lengths (6-8A bps.) measured via reversible quenching between Alexa488 fluorophore (blue) and Black Hole Quencher 1 (black), and (B) rapid, thermal actuation kinetics.

e.g., arrays with linearly-aligned AuNPs (**Figure 4B**) that could be actuated via rapid temperature change to increase AuNP separation (**Figure 4C, D**) or individual hinges (**Figure 4E**). This is the first report of rapid actuation, and thus mechanical energy storage and release, in microscale DNA origami-NP assemblies.

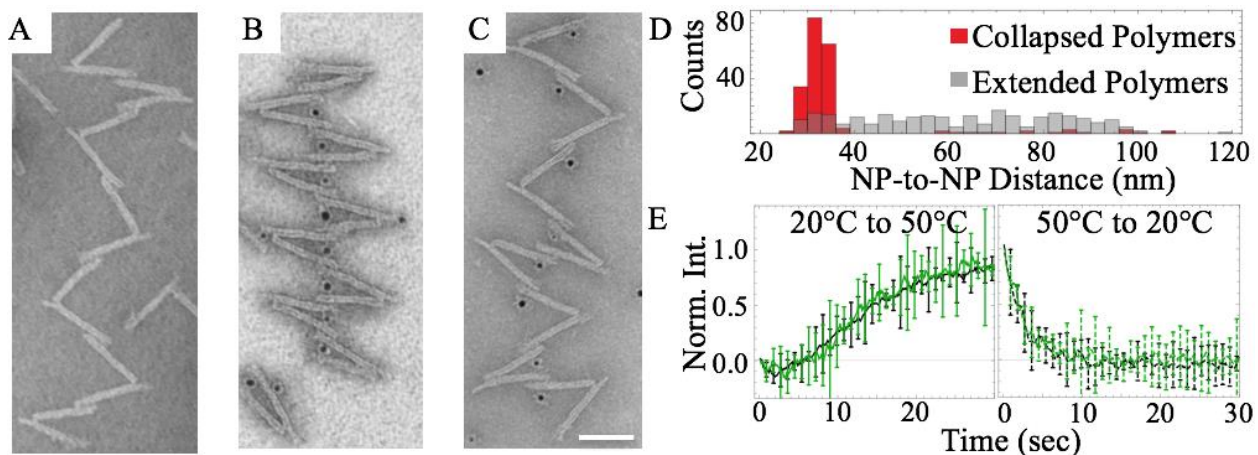


Figure 4. Higher-order NP-hinge Assemblies. (A) Arrays with 33% overlap between hinges. (B) Collapsed NP-hinge arrays with 33% overlap and NPs bound at site 4. (C) Extended NP-hinge arrays. (D) Comparison of NP-to-NP distances between collapsed and extended NP-hinge arrays. (E) Comparison between non-polymerized hinges (black) and NP-hinge arrays (green) during rapid heating (solid) and cooling (dashed).

Objective 2: Explore localized delivery and transfer of heat to DNA origami-NP composites

The main goals of objective 2 are to: (1) evaluate how mechanical potential energy and sterics influence DNA duplex actuation thermodynamics and kinetics, (2) determine the heat transport properties of DNA origami structures, and (3) discover whether local heat transfer in a heterogeneous nanoscale environment follows bulk heating models. [See below]

Objective 3: Explore localized delivery of mechanical work to DNA origami-NP composites

The main goals of objective 3 are to determine the impact of (1) DNA origami structures and (2) bulky NP cargoes on dsDNA interactions, and to (3) evaluate ability of DNA-NP composites to store and release energy from external fields.

(Obj. 3.1, 3.2 Steric Influences on dsDNA Binding Strength) Magnetic tweezer-enabled single molecule force spectroscopy was used to

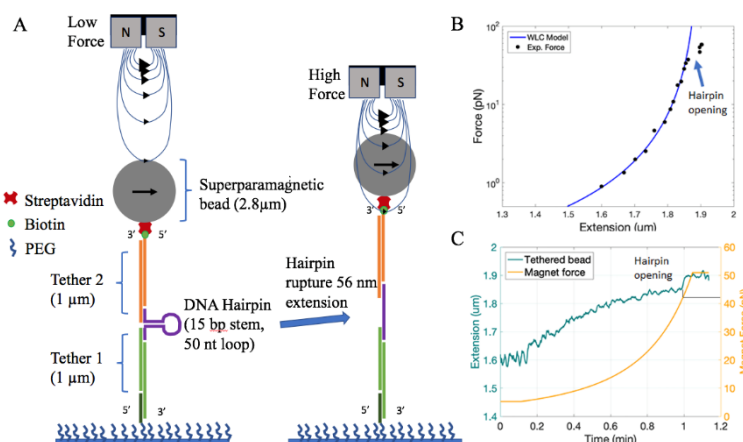


Figure 5. Magnetic tweezers studies of DNA hairpins. (A) DNA construct for pulling experiments. (B) Force-extensions response of the DNA construct and is fit to the worm-like chain model. (C) DNA tether extension for increasing force. The hairpin opening results in 60 nm increase in extension at 40 pN of force.

measure double-stranded (ds)DNA binding strength in DNA hairpins (**Figure 5**), with rupture indicated by a sudden change in bead position (**Figure 5C**); these methods enable the role of sterics in localized mechanical work delivery to be evaluated.

Future Plans

(Obj. 1.3 Emergent Properties) To enable study of NP emergent properties, we have generated composites: (1) with AuNPs bound to each hinge arm (**Figure 6A**) for dynamic surface plasmon resonance (SPR) studies and (2) with quantum dots (QDs) bound to hinge arms (**Figure 6B**) for optical studies. These studies will utilize advanced single molecule assays incorporating Förster Resonance Energy Transfer (FRET) reporters to measure DNA hinge actuation kinetics (**Figure 7**) recently developed by us.

(Obj. 2.1 Thermal Actuation Kinetics) To augment our previous studies of thermoplasmonic heating in bulk solution, we are studying local heat delivery via single molecule experiments using magnetic tweezers and dual trap optical tweezers. This approach has been used to generate DNA force-extension curves, setting the stage for experiments with composites.

(Obj. 2.2 DNA Origami Thermal Properties, 2.3 Nanoscale Heat Transport). Bulk studies will be augmented with single molecule studies using the dual optical trap described above.

(Obj. 3.3 Magnetic Actuation) To enable energy harvesting and storage through magnetic fields, NP-hinge composites were modified magnetic SPIONs (**Figure 8**). Sterics limited attachment of 15 nm SPIONs to only one hinge arm, thus future work will investigate 5 nm hinge-SPION composites.

References

1. Castro, C.E., et al., *Nanoscale*, 2015: 7, 5913-21.
2. Marras, A.E., et al., *Proc. Nat. Acad. Sci.*, 2015: 112, 713-8.
3. Zhou, L., et al., *ACS nano*, 2014: 8, 27-34.
4. Tan, L.H., et al., *Accounts of Chemical Research*, 2014: 47, 1881-1890.
5. Liu, X.Q., et al., *Accounts of Chemical Research*, 2014: 47, 1673-1680.

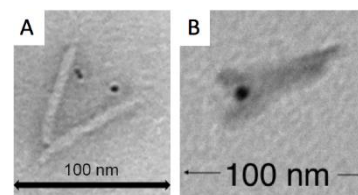


Figure 6. NP-hinge composites with (A) AuNP pairs and (B) QDs.

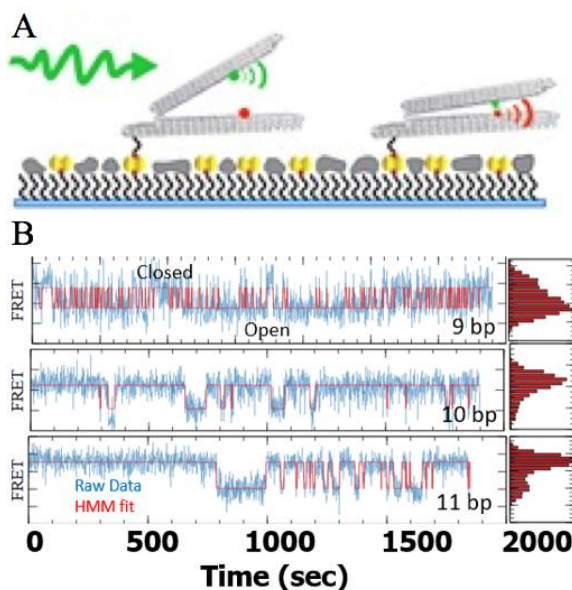


Figure 7. Single molecule FRET of hinges. (A) Schematic of biotinylated hinges attached to a polyethylene glycol surface via streptavidin. (B) Hinge traces for connections of 9, 10, or 11 bp.

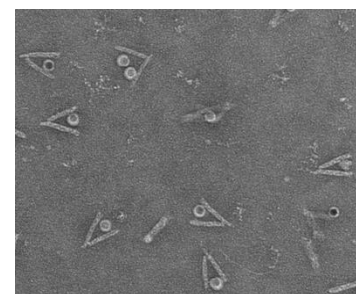


Figure 8. SPION-hinge composites

Publications

J. Johnson, A. Dehankar, J. Winter and C. Castro. “Reciprocal control of hierarchical DNA origami-nanoparticle composites.” *Nano Letters*, *submitted*.

See also description above. Several publications are in progress.

DNA nanostructure directed designer excitonic networks

Hao Yan, Arizona State University (Principal Investigator), Neal Woodbury, Arizona State University (Co-Investigator), Yan Liu, Arizona State University (Co-Investigator), Mark Bathe, Massachusetts Institute of Technology (Co-investigator), David Whitten, University of New Mexico (Co-investigator), Su Lin, Arizona State University (Co-Investigator)

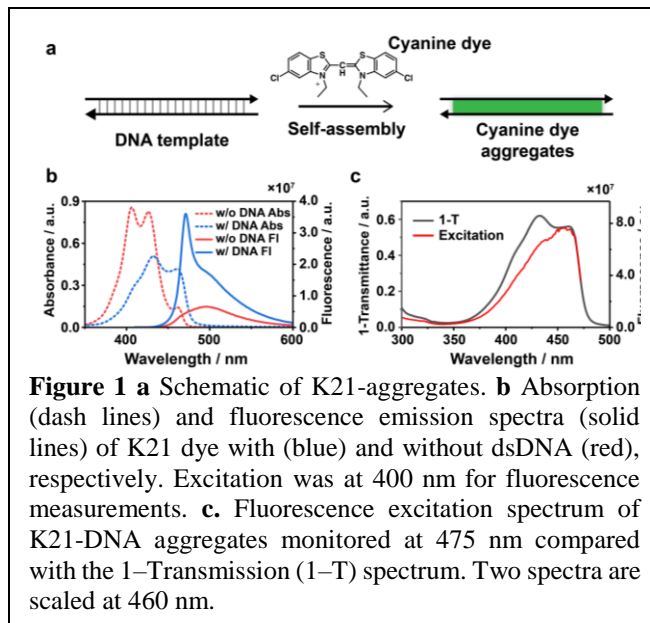
Program Scope

The main scope of this research is to use DNA nanostructures as a template for the self-assembly of dye aggregates in specific and programmable arrangements. The goal is to create a new class of photonic materials that mimic biological light harvesting systems with more robust and scalable components. Towards this goal, we have focused on the self-assembly of J- or J-like dye aggregates on DNA nanostructures, starting with pseudoisocyanine (PIC) dyes based on our previous experimental results and theoretical simulations. We then explored new dyes that bound more tightly to DNA to enhance J-aggregate formation. We found that the dye (K21) results in a markedly increased local density of dye on dsDNA, resulting in an enhanced J-aggregate formation at a much lower concentration than PIC. Furthermore, the K21 aggregate formation on dsDNA is only weakly sequence dependent, providing a flexible approach that is adaptable to many different DNA nanostructures. We have used the DNA-templated K21-aggregates and an energy transfer bridge in a Donor (D)–bridge (B)–Acceptor (A) complex. Energy transfer over a 100 bp (32 nm) long bridge resulted in an overall donor-to-acceptor energy transfer efficiency of 60%, with the loss of excitation energy being almost exclusively at the donor-bridge junction (63%). There was almost no excitation energy loss due to transfer through the aggregate bridge and the transfer efficiency from the aggregate to the acceptor was about 96%. Based on this low-loss transfer, we have now designed an exciton wire that is 400 nm long and have demonstrated energy transfer over that distance. The weakly sequence dependent aspect of the K21/DNA association has also allowed us to develop branched DNA components and construct 2D photonic networks.

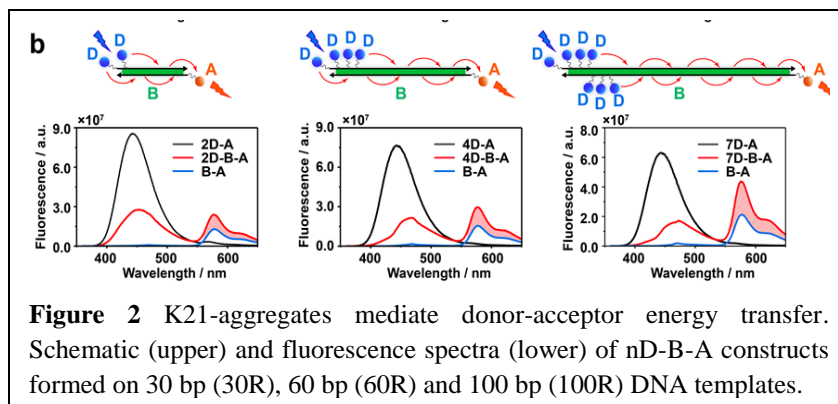
Recent Progress

Robust aggregates formed with K21 dye mediate high efficiency energy transfer. To improve the excitonic properties of the J-aggregate, we experimented with several dyes synthesized by the Whitten lab including the K21 and K28 dyes. The cyan dye, K21, formed aggregates that bind more strongly than the previously studied PIC dye [1], thus requiring much lower dye concentrations for aggregate formation (**Figure 1**). This minimized the competition between direct excitation of the J-aggregate and background excitation of dye in solution, allowing us to more extensively characterize energy transfer processes in various donor-bridge-acceptor (D-B-A) constructs. K21 aggregate formation was also less DNA-sequence dependent, allowing us to build

stable, long aggregates more easily (**Figure 2**). We then explored the use of K21 aggregates as a molecular energy transfer bridge (B) that spectroscopically and geometrically fills the gap between a donor (Alexa Fluor 350) and an acceptor (Alexa Fluor 555) on the DNA. We investigated several D-B-A constructs of different lengths and systematically characterized excitation energy transfer through the aggregate in the D-B-A construct using bridges templated by 30, 60, and 100 base pairs (9.7, 19.4, and 32.4 nm). Multiple donors were used in these constructs to ensure that the donor absorbance cross section remained high



relative to the aggregate. Analysis of the stepwise energy transfer in these constructs showed that there was very little loss during energy transfer through the aggregate as a function its length. Once the exciton enters the aggregate, the efficiency of transfer from the aggregate to the acceptor is uniformly high (92%, 86%, 88% for 30, 60 and 100 base pairs, respectively). This implies that DNA-templated K21 dye aggregates should serve as versatile building blocks for creating larger, more complex structures and for providing an effective means of incorporating energy transfer “wires” into photonic systems based on DNA nanostructures.



DNA nanofibers. The study described above suggests that energy transfer should be feasible over much longer distances. Taken at face value, there was a 4% decrease in energy transfer efficiency upon lengthening the aggregate from about 10 nm to about 30 nm. If that loss is an accurate representation, one would expect about 20% energy transfer efficiency over a micron long distance. We have constructed a six-helix bundle DNA origami (6HB, ~400 nm in length, AFM image shown in **Figure 3b**) and bound the K21 dye to it in order to test this hypothesis. This 6HB construct can be connected in a head-to-tail manner to form micron-scale fibers as well. To characterize the energy transfer function of these photonic fibers, we have designed the 400-nm fibers with acceptors arranged in 2 different ways (**Figure 3a**). Eighteen AF555 were added in each fiber in order to distinguish the spectral contributions of AF555 from K21 (**Figure 3c**). In one case, the acceptors are attached towards the end of the fiber bundle (upper), while in the other

case three groups of 6 AF555 dyes were evenly spaced along the bundle. Using 400 nm excitation, photons are exclusively absorbed by the K21 molecules and evenly distributed along the bundle. The emission at 470 nm from K21 decreases dramatically in the presence of AF555 acceptors, relative to without them. In addition, there is a significant increase in the 580 nm emission from AF555. This implies efficient energy transfer from K21 aggregates to AF555 (**Figure 3d**). The calculated excitation transfer efficiencies with different AF555 arrangements on the 6-helix bundle are both close to 50%. Most of the loss is due to the aggregate-to-AF555 transfer efficiency, which is 63%. The fact that the AF555 placement does not greatly change the energy transfer suggests that excitation energy rapidly explores the entire fiber, regardless of where it started. The loss of excitation during the migration through the 400-nm fiber is very low (estimated to be $\sim 0.1\%$ per nm).

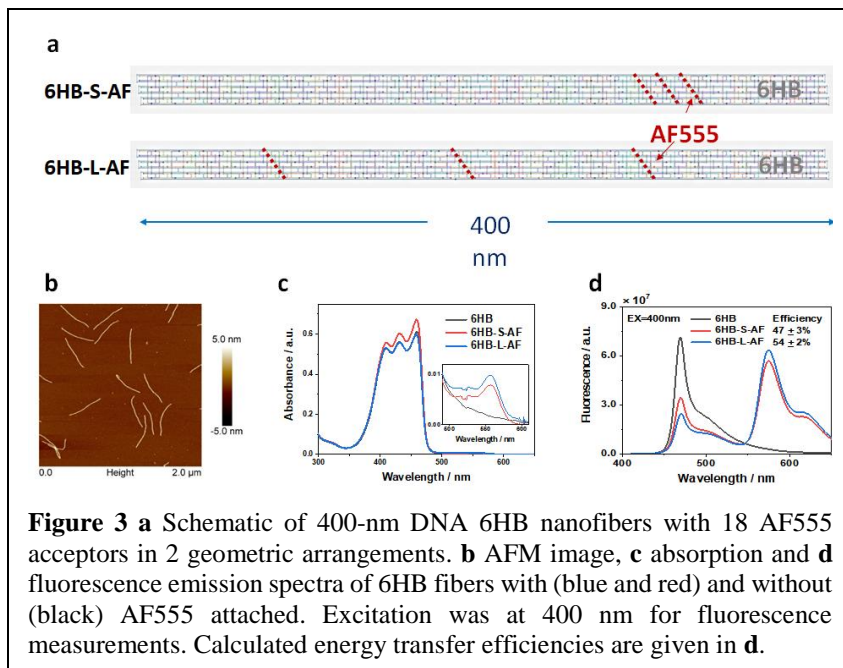


Figure 3 **a** Schematic of 400-nm DNA 6HB nanofibers with 18 AF555 acceptors in 2 geometric arrangements. **b** AFM image, **c** absorption and **d** fluorescence emission spectra of 6HB fibers with (blue and red) and without (black) AF555 attached. Excitation was at 400 nm for fluorescence measurements. Calculated energy transfer efficiencies are given in **d**.

2D Energy Transfer Networks. To expand to large-scale photonic materials, we have developed a set of DNA tiles as building blocks for constructing 2D excitonic networks based on DNA-templated dye aggregates. One 4-arm DNA tile structure with AF555 attached has been designed and characterized in detail (**Figure 4**). We have evaluated the energy transfer properties through different pathways within the structure by incorporating acceptors on different arms and analyzing the efficiency and kinetics of the energy transfer. Based on this study, it appears that the spectral properties of the dye aggregates, as well as the

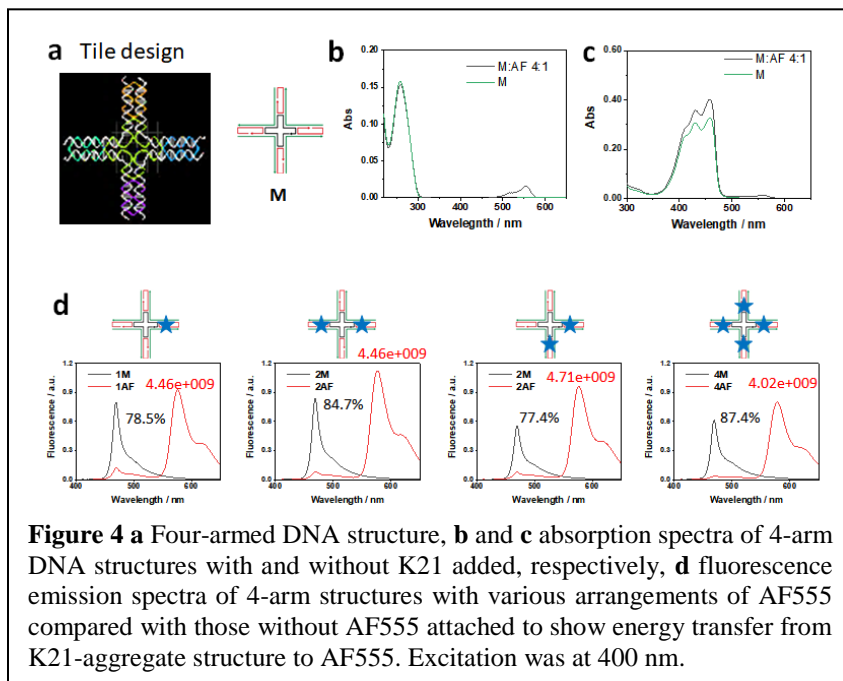


Figure 4 **a** Four-armed DNA structure, **b** and **c** absorption spectra of 4-arm DNA structures with and without K21 added, respectively, **d** fluorescence emission spectra of 4-arm structures with various arrangements of AF555 compared with those without AF555 attached to show energy transfer from K21-aggregate structure to AF555. Excitation was at 400 nm.

energy transfer efficiency observed in the 1D structure are not affected by the multi-arm junction design. The spectral changes due to junction designs and the local alignment of dye molecules near DNA crossover junction sites do not significantly impact the exciton properties characterized in the absorption and fluorescence emission spectra (**Figure 4c, d**). We have systematically studied the excitonic properties of the dye aggregates templated on these more complex structures and their ability to mediate energy transfer. The energy transfer efficiency of each building block has been determined using steady-state and time-resolved spectroscopic approaches. This study has built the foundation for further development of 2D excitonic networks absorbing light and delivering the energy to acceptors in specified patterns. Mostly importantly, it allows us to specifically arrange acceptor molecules at specific locations in a programmable manner to mimic the excitation networks found in natural photosynthetic light-harvesting antenna networks in which a large field of light harvesting complexes are linked to multiple photosynthetic reaction centers.

Future Plans

We plan to (1) optimize energy transfer building blocks and develop DNA nanofibers that enable very long distance 1-dimensional energy transfer by jointing 2 or 3 6HB together to extend to micrometer scales. (2) Build resilient 2-dimensional energy transfer networks of absorbers and capture elements that adapt to the environment, and (3) develop DNA-dye crystals with high absorbance cross section for low-light applications and interface them with 2-D energy capture elements.

References

1. **Programmed coherent coupling in a synthetic DNA-based excitonic circuit** Etienne Boulais, Nicolas Sawaya, Rémi Veneziano, Alessio Andreoni, James Banal, Toru Kondo, Sarthak Mandal, Su Lin, Gabriela Schlau-Cohen, Neal Woodbury, Hao Yan, Alán Aspuru-Guzik, and Mark Bathe, *Nature Materials* 17:159-166 (2018)

Publications

1. **Molecular model of J-aggregated pseudoisocyanine fibers** William P. Bricker, James L. Banal, Matthew B. Stone, Mark Bathe, *J. Chem. Phys.* 149:24905 (2018)
2. **Antimicrobial Activity of Differentially Functionalized Polythiophene Derivatives Under Light and Dark Conditions**, Dylan Brown, Jianzhong Yang, Edward Strach, Mohammed Ismael Khalil, David G. Whitten, *Photochem Photobiol*, 94:1116-1123 (2018)
3. **Automated Sequence Design of 3D Polyhedral Wireframe DNA Origami with Honeycomb Edges** Hyungmin Jun, Tyson R. Shepherd, Kaiming Zhang, William P. Bricker, Shanshan Li, Wah Chiu, Mark Bathe, *ACS Nano*13:2083-2093 (2019)
4. **Directed Energy Transfer through DNA-templated J- aggregates** Sarthak Mandal, Xu Zhou, Su Lin, Hao Yan, Neal Woodbury, *Bioconjugate Chemistry*, published online (2019)
5. **Efficient Long-range, Directional Energy Transfer through DNA-Templated Dye Aggregates** Xu Zhou, Sarthak Mandal, Shuoxing Jiang, Su Lin, Jianzhong Yang, Yan Liu, David G. Whitten, Neal W. Woodbury and Hao Yan, *JACS* 141:8473-8481 (2019)
6. **Programming Structured DNA Assemblies to Probe Biophysical Processes** Eike-Christian Wamhoff, James L. Banal, William P. Bricker, Tyson R. Shepherd, Molly F. Parsons, Rémi Veneziano, Matthew B. Stone, Hyungmin Jun, Xiao Wang, Mark Bathe, *Annual Review of Biophysics*, 48:395-419 (2019)

***AUTHOR
INDEX***

Abbott, Nicholas L.....	35
Aizenberg, Joanna.....	41
Ashby, Paul D.	21
Baer, Marcel.....	17
Baker, David.....	47
Balazs, Anna C.....	41, 52, 57
Bathe, Mark.....	167, 220
Bedzyk, Michael J.....	62, 144
Bevan, Michael A.....	67
Castro, Carlos.....	215
Chaikin, Paul M.	72, 205
Chen, Chun-Long.....	17
Chen, Wei.....	3
de Pablo, Juan J.....	3, 35
De Yoreo, James J.....	17
Dogic, Zvonimir.....	79
Douglas, Trevor.....	83
Dukovic, Gordana.....	85
Emrick, Todd.....	90
Estroff, Lara A.	94
Ewert, K.	157
Franco, Elisa.....	99
Frechette, Joelle.....	67
Gang, Oleg.....	123
Geissler, Phillip.....	21
Glatz, Andreas.....	27
Glotzer, Sharon C.	151, 188
Good, Matthew C.....	109
Grason, Gregory M.	162
Guan, Zhibin.....	104
Hammer, Daniel A.	109
Hartley, C. Scott.....	114
Helms, Brett A.	21
Hillier, Andrew.....	11
Johnston-Halperin, Ezekiel.....	215
Keating, Christine D.....	118
Kewalramani, Sumit.....	62
Kloxin, Christopher.....	154
Kowalewski, Tomasz.....	52
Kumar, Sanat K.....	123
Lavrentovich, Oleg D.....	128
Lee, Daeyeon.....	109
Li, Y.	157
Lin, Su.....	220
Liu, Yan.....	220
Mallapragada, Surya.....	11
Matyjaszewski, Krzysztof.....	52
Mittal, Jeetain.....	133
Morse, Daniel E.	139
Nealey, Paul F.	3
Nilsen-Hamilton, Marit.....	11
Noy, Aleksandr.....	17
Oh, Joonsuk.....	151
Olvera de la Cruz, Monica.....	144
Palacci, J.....	149
Parikh, Atul N.	183
Pine, David J.	72, 151, 205
Pochan, Darrin J.....	154
Poirier, Michael.....	215
Prozorov, Tanya.....	11
Russell, Thomas P.....	21
Safinya, C. R.	157
Santore, Maria M.	162
Saven, Jeffery G.....	154
Schlau-Cohen, Gabriela S.....	167
Schulman, Rebecca.....	99, 171
Seeman, Nadrian C.....	72, 205
Shirts, Michael.....	175
Shiyanovskii, Sergij V.	128
Silberstein, Meredith N.....	179
Sinha, Sunil K.	183
Snezhko, Alexey.....	27
Sokolov, Andrey.....	27
Solomon, Michael J.....	188
Strano, Michael S.....	193
Tezcan, F. Akif.....	198
Tirrell, Matthew.....	3
Travesset, Alex.....	11
Uchida, Masaki.....	83
Vaikuntanathan, Suriyanarayanan.....	203
Vaknin, David.....	11
van Burren, Anthony.....	17
Wang, Wenjie.....	11
Weck, Marcus.....	72, 205
Wei, Qi-Huo.....	128
Whitesides, George M.....	211
Whitten, David.....	220
Wiesner, Ulrich.....	94
Willard, Adam.....	167
Winter, Jessica.....	215
Woodbury, Neal.....	220
Yan, Hao.....	220

Yi, Gi-Ra.....151
Zettl, Alex21

PARTICIPANT LIST

Abbott, Nicholas	Cornell University	nabbott@cornell.edu
Aizenberg, Joanna	Harvard University	jaiz@seas.harvard.edu
Aizenberg, Michael	Harvard University	michael.aizenberg@wyss.harvard.edu
Baker, David	University of Washington	ipdadmin@uw.edu
Balazs, Anna	University of Pittsburgh	jdc9@pitt.edu
Bedzyk, Michael	Northwestern University	bedzyk@northwestern.edu
Bevan, Michael	Johns Hopkins University	mabevan@jhu.edu
Castro, Carlos	The Ohio State University	castro.39@osu.edu
Chaikin, Paul	New York University	chaikin@nyu.edu
De Yoreo, Jim	Pacific Northwest National Lab	james.deyoreo@pnnl.gov
Dogic, Zvonimir	Univ. of California, Santa Barbara	zdogic@ucsb.edu
Douglas, Trevor	Indiana University	trevdoug@indiana.edu
Dukovic, Gordana	University of Colorado, Boulder	gordana.dukovic@colorado.edu
Emrick, Todd	University of Massachusetts	todd.emrick@gmail.com
Estroff, Lara	Cornell University	lae37@cornell.edu
Franco, Elisa	University of California, Los Angeles	efranco@seas.ucla.edu
Frechette, Joelle	Johns Hopkins University	jfrechette@jhu.edu
Ganesan, Mahesh	University of Michigan, Ann Arbor	maheshg@umich.edu
Gang, Oleg	Columbia Univ./ Brookhaven National Lab	og2226@columbia.edu
Gersten, Bonnie	US Department of Energy	bonnie.gersten@science.doe.gov
Grason, Gregory	Univ. of Massachusetts, Amherst	grason@mail.pse.umass.edu
Guan, Zhibin	University of California, Irvine	zguan@uci.edu
Hammer, Daniel	University of Pennsylvania	hammer@seas.upenn.edu
Hartley, Christopher	Miami University	scott.hartley@miamioh.edu
Johnston-Halperin, Ezekiel	The Ohio State University	johnston-halperin.1@osu.edu
Keating, Christine	Pennsylvania State University	keating@chem.psu.edu
Kewalramani, Sumit	Northwestern University	s-kewalramani@northwestern.edu
Kloxin, Chris	University of Delaware	cjk@udel.edu
Kumar, Sanat	Columbia University	sk2794@columbia.edu

Lavrentovich, Oleg	Kent State University	olavrent@kent.edu
Lin, Su	Arizona State University	slin@asu.edu
Mallapragada, Surya	Ames Laboratory	suryakm@iastate.edu
Markowitz, Michael	US Department of Energy	mike.markowitz@science.doe.gov
Matyjaszewski, Krzysztof	Carnegie Mellon University	km3b@andrew.cmu.edu
Mittal, Jeetain	Lehigh University	jem309@lehigh.edu
Morse, Daniel	Univ. of California, Santa Barbara	d_morse@lifesci.ucsb.edu
Nagarkar, Amit	Harvard University	anagarkar@gmwhgroup.harvard.edu
Nealey, Paul	Argonne National Laboratory	pnealey@anl.gov
Noy, Aleksandr	Lawrence Livermore National Lab	noy1@llnl.gov
Olvera de la Cruz, Monica	Northwestern University	m-olvera@northwestern.edu
Parikh, Atul	University of California, Davis	anparikh@ucdavis.edu
Pine, David	New York University	pine@nyu.edu
Pochan, Darrin	University of Delaware	pochan@udel.edu
Russell, Thomas	Univ. of Massachusetts, Amherst Lawrence Berkeley National Lab	russell@mail.pse.umass.edu
Safinya, Cyrus	Univ. of California, Santa Barbara	safinya@mrl.ucsb.edu
Santore, Maria	Univ. of Massachusetts, Amherst	santore@mail.pse.umass.edu
Saven, Jeffery	University of Pennsylvania	saven@sas.upenn.edu
Schaffter, Samuel	Johns Hopkins University	sschaff6@jhu.edu
Schulman, Rebecca	Johns Hopkins University	rschulm3@jhu.edu
Seeman, Nadrian	New York University	ned.seeman@nyu.edu
Sennett, Michael	US Department of Energy	michael.sennett@science.doe.gov
Shirts, Michael	University of Colorado, Boulder	michael.shirts@colorado.edu
Silberstein, Meredith	Cornell University	meredith.silberstein@cornell.edu
Sinha, Sunil	University of California, San Diego	ssinha@physics.ucsd.edu
Snezhko, Alexey	Argonne National Laboratory	snezhko@anl.gov
Solomon, Michael	University of Michigan	mjsolo@umich.edu
Strano, Michael	Massachusetts Institute of Technology	srgoffice@mit.edu
Tezcan, F. Akif	University of California, San Diego	tezcan@ucsd.edu

Tirrell, Matthew	University of Chicago	mtirrell@uchicago.edu
Vaikuntanathan, Suriyanarayanan	University of Chicago	svaikunt@uchicago.edu
Waltmann, Curt	Northwestern University	curtwaltmann2023@u.northwestern.edu
Weck, Marcus	New York University	mw125@nyu.edu
Whitesides, George	Harvard University	gwhitesides@gmwgroup.harvard.edu
Winter, Jessica	The Ohio State University	winter.63@osu.edu
Woodbury, Neal	Arizona State University	NWoodbury@asu.edu
Yan, Hao	Arizona State University	Hao.Yan@asu.edu
Zhang, Ling	University of California, San Diego	liz123@ucsd.edu